Aston University
Birmingham

DOCTORAL THESIS

Comparison of the effect of pre-treatment and catalysts on liquid quality from fast pyrolysis of biomass

Antzela Fivga

COMPARISON OF THE EFFECT OF PRE-TREATMENT AND CATALYSTS ON LIQUID QUALITY FROM FAST PYROLYSIS OF BIOMASS

ANTZELA FIVGA

Doctor of Philosophy

ASTON UNIVERSITY

September 2011

COMPARISON OF THE EFFECT OF PRE-TREATMENT AND CATALYSTS ON LIQUID QUALITY FROM FAST PYROLYSIS OF BIOMASS

ANTZELA FIVGA

Doctor of Philosophy, 2011

THESIS SUMMARY

The overall objective of this work was to compare the effect of pre-treatment and catalysts on the quality of liquid products from fast pyrolysis of biomass. This study investigated the upgrading of bio-oil in terms of its quality as a bio-fuel and/or source of chemicals. Bio-oil used directly as a biofuel for heat or power needs to be improved particularly in terms of temperature sensitivity, oxygen content, chemical instability, solid content, and heating values. Chemicals produced from bio-oil need to be able to meet product specifications for market acceptability.

There were two main objectives in this research. The first was to examine the influence of pre-treatment of biomass on the fast pyrolysis process and liquid quality. The relationship between the method of pre-treatment of biomass feedstock to fast pyrolysis oil quality was studied. The thermal decomposition behaviour of untreated and pretreated feedstocks was studied by using a TGA (thermogravimetric analysis) and a Py-GC/MS (pyroprobe-gas chromatography/mass spectrometry). Laboratory scale reactors (100g/h, 300g/h, 1kg/h) were used to process untreated and pretreated feedstocks by fast pyrolysis.

The second objective was to study the influence of numerous catalysts on fast pyrolysis liquids from wheat straw. The first step applied analytical pyrolysis (Py-GC/MS) to determine which catalysts had an effect on fast pyrolysis liquid, in order to select catalysts for further laboratory fast pyrolysis. The effect of activation, temperature, and biomass pre-treatment on catalysts were also investigated. Laboratory experiments were also conducted using the existing 300g/h fluidised bed reactor system with a secondary catalytic fixed bed reactor.

The screening of catalysts showed that CoMo was a highly active catalyst, which particularly reduced the higher molecular weight products of fast pyrolysis. From these screening tests, CoMo catalyst was selected for larger scale laboratory experiments.

With reference to the effect of pre-treatment work on fast pyrolysis process, a significant effect occurred on the thermal decomposition of biomass, as well as the pyrolysis products composition, and the proportion of key components in bio-oil. Torrefaction proved to have a mild influence on pyrolysis products, when compared to aquathermolysis and steam pre-treatment.

Keywords: pyrolysis-oil, pre-treatment, biomass, catalysts.

ACKNOWLEDGEMENTS

Firstly, I wish to express my gratitude to my supervisor, Professor Tony Bridgwater, for giving me the opportunity to conduct this study. His guidance, patience and help in dealing with the many challenges of this research, have been invaluable.

I would will to acknowledge the EU-FP6 integrated project BIOSYNERGY (EC contract 038994-SES6) for the financial support provided. I would especially like to thank Allan Harms, Tom Drew and Dr Harry Goldingay for their scientific help.

I would also like to extend my gratitude to my friends, Panos Doss, Antonio Oliveira, Charles Greenhalf, Dr. Anna Topakas, Dr. George Lychnos, Dr. Dan Harvey for their friendship and support during this challenging adventure; thanks for providing the beer!

My dearest thanks go to Sofia Topakas for her valuable help and support in this Thesis. She was added to my life relatively recently, but her friendship is so valuable for me already.

I would especially like to thank Ioanna Dimitriou for being next to me all these past years in Birmingham. For listening to my moaning and not letting me quit. She is one of the main reasons that these years were so special. We both shared the same adventure, καπετάνιος and μούτσος together. Thanks also to my second μούτσο, Konstantina Stamouli, that she was able to support me emotionally, even from far away.

I am also very grateful to my parents Georgios and Anastasia, who have supported my education, both financially and emotionally.

Last, but not least, I am deeply grateful to James Bowley. He was next to me, when I needed him the most. I owe him more than can be expressed in words.

ABBREVIATIONS

ECN: Energy Centre of Netherlands

DME: Dimethylether

PAH: Polycyclic Aromatic Hydrocarbons

TGA: Thermogravimetric Analysis

Py-GC/MS: Pyroprobe –Gas Chromatograph/Mass Spectrometry

Aqua' wheat straw: Aquathermolised wheat straw

Tor. poplar: Torrefied poplar

Tor. spruce: Torrefied spruce

270110H: Heavy fraction of wheat straw derived oil from pot 1, run with reference number 270110

270110A: Aqueous fraction of wheat straw derived oil from pot 1, run with reference number 270110

RPM: Revolutions per minute

DDGS: Dried Distillers Grains with Solubles

WOB_TI: Temperature measurements in the reactor unit of ECN

WOB_CO and WOB_CO_2: the volume measurements of CO and CO_2 that were produced during the experiment, respectively.

CONTENTS

LIST OF TABLES

LIST OF FIGURES

1 INTRODUCTION

1.1 Biosynergy project

The work carried out in this thesis was performed within the EC sponsored Biosynergy project which evaluated bio-refineries for transport fuels and high value chemical intermediates. The project examined a variety of methods for deriving valuable fuel and chemical products, one of which was thermochemical processing by fast pyrolysis. The emphasis of this work is on primary and secondary thermal processing by fast pyrolysis and upgrading of pyrolysis products which is a major part of Work Package 2 of the Biosynergy project.

1.2 Background to fast pyrolysis and biofuels

Pyrolysis is the thermal degradation of biomass with rapid heating in the absence of oxygen. The process of fast pyrolysis at temperatures of around 500^{o}C with rapid cooling and quenching of the product vapours, produces bio-oil with by-products of char and gas. Bio-oil is defined as a miscible mixture of polar organics (75-80 wt%) and water (20-25 wt%).

Pyrolysis is interesting because it produces a liquid as the main product, in contrast with other thermochemical processes where the liquid is considered to be a by-product, such as combustion and gasification. A liquid product such as bio-oil has many advantages such as ease of transport and storage. The main use of bio-oil is to produce higher value fuels including biofuels and chemicals. Figure 1-1 illustrates an overview of bio-oil applications [1].

Figure 1-1: Applications of bio-oil [1]

Before bio-oil can effectively be used as a fuel and/or chemical source there are several inherent properties of bio-oil that require consideration before use in any application. An extensive review of these characteristics, as well as the cause, effect and solution, was published by Bridgwater [2]. Bio-oil used directly as a biofuel for heat or power needs to be improved particularly in terms of temperature sensitivity, oxygen content, chemical instability, solid content, and heating values. Chemicals produced from bio-oil need to be able to meet product specification requirements for market acceptability. These may be oxygenated (such as acetic acid or phenol), where the requirement is less on de-oxygenation and more on delivering a product that is of a sufficiently high concentration to justify separation and refining into a marketable chemical.

An approach to improve bio-oil quality in this thesis is the modification of pyrolysis process by adding catalysts. Another approach is to upgrade the quality of bio-oil by pre-treatment of the biomass feedstock. This work focus on processing pre-treated biomass by fast pyrolysis and study the effect on bio-oil products distribution.

1.3 Objectives

The BioSynergy Consortium selected several biomass types and a bio-ethanol refinery residue as the raw materials for this study. The initial stage of the BioSynergy project was to compare various biomass types, by assessing the fast pyrolysis liquid products distribution. The raw materials included woods, wheat straw, and their pre-treatment version. The pre-treatment processes that were applied to the feedstocks were torrefaction, aquathermolysis, and steam treatment. The latter stage of the project focused only on wheat straw, as it was the main feedstock of the evaluated biorefinery.

The two main objectives in this study are as follows:

1. Examine the influence of pre-treatment of biomass on the fast pyrolysis process and liquid quality.
2. Study the influence of catalysts on fast pyrolysis liquids for wheat straw.

The three sub-objectives concerning this thesis include:

1. Compare biomass types in terms of fast pyrolysis liquid quality.
2. Understand and define the concept of bio-oil quality.

3. Determine the optimum pyrolysis reaction temperature for wheat straw to obtain the highest organics yield.

1.4 Thesis structure

The remaining chapters of this thesis are organised as follows:

Chapter 2 provides a general introduction to the key themes of the thesis, which are biomass, fast pyrolysis, the main liquid product bio-oil and the relationship between these three themes. It discusses the criteria by which "quality of bio-oil" is assessed, evaluates the most important for the objectives and then examines methods used to upgrade the quality.

Chapter 3 encompasses a literature review of the various catalysts for bio-oil upgrading. This includes basic introduction of the structure of each catalyst type and the various types of catalysts used by previous researchers. Based on the review of previous research on catalysts, a selection of the appropriate catalysts for further experimental work and the rationale for the specific selection is discussed in Chapter 8.

Chapter 4 includes a description of the pyrolysis reactor systems employed, ranging from analytical equipment, bench scale reactors to laboratory reactors. It includes an overview of thermogravimetric analyser (TGA), pyroprobe gas chromatographic/ mass spectrometric (Py-GC/MS), 100g/h and 300g/h bench scale fluidised reactor units, 1kg/h fluidised reactor unit and the 1kg/h bubbling fluidised reactor unit of ECN. The mass balance methodology is also discussed. Additionally, the methodology used for the analysis of the pyrolysis products is presented in this chapter.

Chapter 5 discusses the analytical characterisation of a variety of raw and pre-treated biomass that was conducted using a thermogravimetric analyser (TGA) and pyrolysis-gas chromatography/mass spectrometry (Py-GC/MS). Proximate, ultimate and heating value analyses were also carried out on the samples.

Chapter 6 describes the fast pyrolysis experiments with wheat straw in terms of pyrolysis products yields and chemical distribution on bio-oil. Optimum temperature is investigated to maximise the liquid yields for further catalytic experiments. In addition, limitations of the equipment and recommendations for improvement are discussed.

Chapter 7 includes the comparison of the fast pyrolysis results obtained from untreated and pre-treated biomass, in terms of pyrolysis products yields and chemical distribution on bio-oil. The influence of pre-treatment methods on bio-oil quality is also examined. Further, limitations of the equipment and recommendations are discussed.

Chapter 8 encompasses the evaluation of various catalysts for upgrading of pyrolysis vapours of untreated and pre-treated wheat straw. The evaluation of catalysts was conducted by analytical and laboratory equipment, including a Py-GC/MS, and a 300g/h fluidised bed reactor coupled with a secondary catalytic fixed bed reactor, respectively. The initial step was to apply analytical pyrolysis (Py-GC/MS) to determine whether catalysts have an effect on fast pyrolysis products. This was done in order to select certain catalysts for further laboratory fast pyrolysis processing. The effect of activation, temperature, and biomass pre-treatment on catalysts were also investigated.

Chapter 9 summarises the main results of this study, and discusses the results in relation to the objectives of the present thesis.

Chapter 10 discusses the recommendations for future work.

2 INTRODUCTION TO PYROLYSIS, PRODUCTS AND UPGRADING

This chapter provides a general introduction to the key themes of the thesis, which are biomass, fast pyrolysis, the main liquid product bio-oil and the relationship between these three themes. It discusses the criteria by which "quality of bio-oil" is assessed, evaluates the most important for the objectives and then examines methods used to upgrade the quality.

2.1 Structure of lignocellulosic biomass

The structure of biomass is important (chemically and biologically) since it affects its decomposition behaviour during pyrolysis. Biomass is defined as any organic matter; in the context of the present thesis, the term biomass refers to a particular type of biomass, namely woody biomass (lignocellulosic biomass) [3].

The three main components of lignocellulosic biomass are hemicellulose, cellulose, lignin; additionally, it contains small amounts of organic extractives, and inorganic materials [4]. The proportion of these components varies depending on the biomass type [5]. Table 2-1 gives analyses of the major feed materials used in this research [6].

Table 2-1: Analysis of Biosynergy lignocellulosic feedstocks on wt% [6]

Hemicellulose, cellulose and lignin are strongly interconnected by physico-chemical bonds, and pyrolysis oils are a complex combination of the thermal degradation products of each biomass constituent. In addition, the primary pyrolysis products react with the original biomass components, as well as inter-reactions of the primary products, resulting in the production of secondary products [7]. To add to this complexity, studies have found that metal compounds in biomass, both as ash and contaminants, behave as catalysts and influence the decomposition behaviour of biomass [8, 9]. The main components of wood, as well as its composition, are shown in Figure 2-1 [10]. This illustrates the complexity of the bio-polymers that make up

biomass and the resulting complexity of random thermal scission of these polymers under thermal degradation.

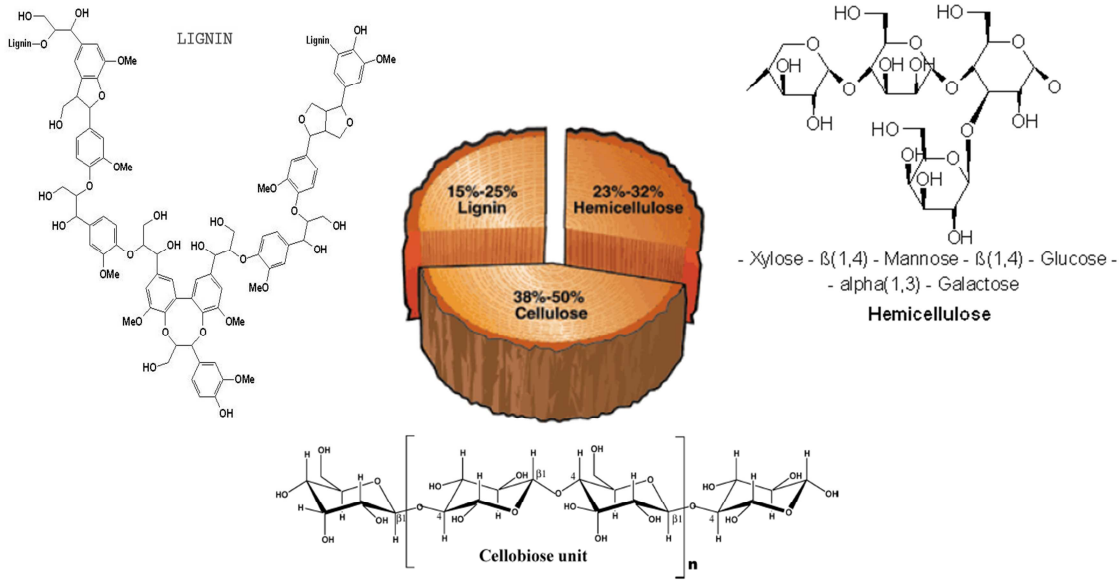

Figure 2-1: The main components of wood [5,10]

Cellulose is a linear homopolysaccharide (sugar) with the elemental formula of $(C_6H_{10}O_5)_n$. A cellobiose unit consists of two cellulose monomers called anhydroglucose units [11]. The possible number of monomer combinations (degree of polymerisation) varies between 700 – 2000 [5]. Compared to cellulose, the degree of polymerisation for hemicelluloses is much smaller, with approximately 200 degrees of polymerisation. Figure 2-1 above depicts cellulose as a long linear chain of molecules, whereas hemicelluloses as a short branched chain. Hemicelluloses is a branched inhomogenous glycan (heteropolysaccharide) composed of two or more monomer units (five different sugars), namely hexoses (D-glucose, D-mannose and D-galactose) and pentoses (D-xylose and L-arabinose) [5]. Furthermore, the thermochemical decomposition of cellulose occurs in the temperature range of 275-350℃, while that of hemicellulose is in the range of 150-350℃ [12]. The long linear chain of cellulose is responsible for its resistance to hydrolysis, solvents, chemicals, and temperature. The short branched structure causes hemicellulose to be more soluble, less resistant to chemicals and easily hydrolysed by weak acids [13].

The chemical structure of lignin is very complicated and it is made up of a high molecular three dimensional, cross-linked, alkylated phenolic polymer [14]. There are three types of phenolics polymers: hydroxyl, guaiacyl and syringyl. The standard structure of lignin is not known, due to its complexity and variety of different species of

plants. The thermochemical decomposition of lignin occurs in the temperature range of 250-500℃, which is wider than that of hemicellulos es and cellulose [12].

Extant studies identify the primary and secondary pyrolysis decomposition products of cellulose, hemicelluloses, and lignin [15, 16]. Specifically, Alen et al. divide the pyrolysis decomposition products of cellulose, hemicellulose and lignin into categories as outlined in Table 2-2 [15].

Table 2-2: Pyrolysis decomposition products of lignocellulosic biomass [15, 12]

Lignocellulosic biomass components	**Degradation temperature**	**Pyrolysis decomposition products Important and/or major products are underlined**
Hemicellulose	150-350°C	Volatiles: carbon dioxide, formic acid. **acetic acid**, hydroxyacetaldehyde, 1-hydroxy-2-propanone Anhydroglucopyranose: (1,6-anhydro-p-D-glucopyranose (**levoglucosan**)); other anhydroglucoses: (1,6-anhydro-β-D-glucofuranose); other anhydrohexoses: (1,6-anhydro-β-D-mannopyranose); levoglucosenone: Furans: (2H)-furan-3-one, 2-furaldehyde, 5-methyl-2-furaldehyde **furfural**
Cellulose	275-350°C	Volatiles: carbon monoxide, carbon dioxide, methanol, acetaldehyde. acetic acid, hydroxyacetaldehyde (glycolaldehyde), I-hydroxy-2-propanone (acetol), and certain < C,-hydrocarbons and/or their derivatives); Anhydroglucopyranose (1,6-anhydro-p-D-glucopyranose (**levoglucosan**)); Anhydroglucofuranose (1,6-anhydro-p-D-glucofuranose); Dianhydroglucopyranose (1,4;3,6-dianhydro-a-D-gludopyranose); Furans: (mainly (2H)-furan-3-one, methyl-(3H)-furan-2-one (or-angelicalactone), 2-furaldehyde (furfural), 5-methyl-2-furaldehyde, and 5-hydroxymethyl-3-furaldehyde); Others (5-hydroxy-2-(hydroxymethyl)- 2,3-dihydro-(4H)-pyran-4-one (1,5-anhydro-4-deoxy-D-glJ>cero-hex-I-en-3-ulose) and 3-hydroxy-5,6-dihydro-(2H)-pyran4-one (1.5anhydro-bdeoxypent-1-en-3-ulose)).
Lignin	250-500°C	Volatiles: carbon monoxide, carbon dioxide, diethyl ether, acetic acid, Catechols: **catechol** Vanillins: **vanillin**, homovanillin, vanillic acid; Other guaiacols: guaiacol Propyl guaiacols: coniferyl alcohol Other phenols: phenol, 2-methyl phenol, Aromatic hydrocarbons: benzene

Biomass also contains organic extractives and inorganic material, commonly referred to as ash. Organic extractives can be extracted from biomass by subjecting them to

various solvents (ethanol, water, acetone). Examples of such extractives are terpenes, resins, fatty acids, tannins, waxes, phenolics, simple sugars, and proteins.

Inorganic materials in wood include alkali metals, such as potassium, sodium, and calcium. Table 2-3 shows a typical analysis of ash in woody biomass and straw. It is evident that straw contains significantly higher amounts of Cl, Ca and K than woody biomass. Alkali metals are very important since they behave as catalysts and influence the decomposition behaviour of biomass during pyrolysis [8, 9].

Table 2-3: Typical analysis of ash in woody biomass and straw [6]

2.2 Fast pyrolysis process

2.2.1 Definition of fast pyrolysis

Fast pyrolysis is the decomposition of biomass when rapid heating occurs in the absence of oxygen. Fragmentation and polymerization of biomass occur to produce pyrolysis vapours and char (solid residue). Pyrolysis vapours include aerosols, non condensable gases, and condensable vapours. The condensation of the condensable vapours form the bio-oil, which is the main product of pyrolysis. Bio-oil is a miscible mixture of polar organics typically 75wt% on dry biomass and water (20-25wt%). Char and gas are both by-products of the pyrolysis process.

2.2.2 Operating conditions

Yields of bio-oils can be maximised with high heating rates of 1000^{o}C/min, a reaction temperature of around 500^{o}C, short vapour residence times of typically 1 second, and rapid cooling of pyrolysis vapours [17]. A typical mass balance of wood during the process of fast pyrolysis is illustrated in Figure 2-2.

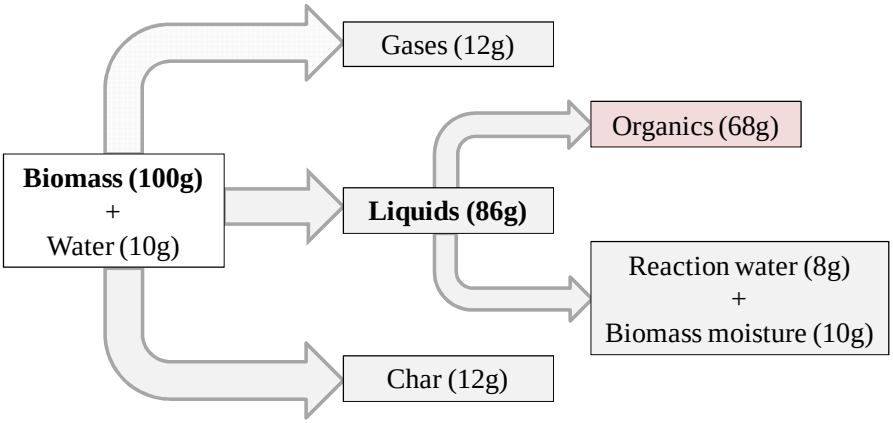

Figure 2-2: Typical mass balance of wood fast pyrolysis

The operation conditions of fast pyrolysis play an important role in maximising the liquid yields. To signify their influence on the liquid yields, the different categories of pyrolysis, conditions, and products are listed in Table 2-4 [18, 19, 20, 21]. It is interesting to note that the operation conditions (vapour residence time, reactor temperature and heating rate) change the proportion of the pyrolysis products. It can be seen from Table 2-4 that the mode of fast pyrolysis produces the highest liquid yield.

Table 2-4: Pyrolysis categories, operating conditions, and products

Pyrolysis categories	**Operating conditions**	**Pyrolysis products**
Fast pyrolysis	• short volatiles residence time (< 1sec.) • reactor temperatures of 500℃ • high heating rates (>1000℃/s)	liquid: 86% char: 12% gas: 12%
Intermediate pyrolysis	• volatiles residence time (< 5sec.) • reactor temperatures (400- 500℃) • very low heating rates of 1-1000℃/s	liquid: 50%-phase separate char: 25% gas: 25%
Slow pyrolysis	• long solids residence time (hours to days) • long volatiles residence time (> 5sec.) • low reactor temperatures (200-400℃) • very low heating rates up to 2℃/s	liquid: 30% char: 33 % gas: 35%

An overview of past research reveals that a variety of reactor configurations can be used to optimise the fast pyrolysis process [22, 23, 24]. The present research uses a fluidised bed reactor, due to its high heat transfer rates; heat supply to fluidising gas or directly to bed; low char yield; very good solids mixing; and simple reactor configuration [17].

2.2.3 Key factors on fast pyrolysis process

2.2.3.1 Temperature

Pyrolysis temperature can be referred as reactor temperature or reaction temperature. The difference between these two terms lies in the former being the temperature of the reactor, while the latter the temperature in which the biomass particles are pyrolised. The reactor temperature needs to be set higher than the desirable reaction temperature, due to the heat transfer phenomenon and the temperature gradient. Additionally, the fact that fast pyrolysis is an endothermic process is yet another reason for the need for a higher reactor temperature .

Pyrolysis temperature has a significant influence on pyrolysis products yield, including liquid, gas, and char [25]. The liquid yields can be divided into organic and reaction water yields. The organic yields reach a maximum at approximately 500^{o}C and further temperature increase results in a reduction of liquid yields [26, 27, 28]. In contrast, reaction water yields rise with an increase in temperature. In the case of gas yields, an increase is observed with rising temperature. The opposite trend is observed with char yields. The increase in temperature enhances secondary cracking of pyrolysis vapours; thus the gas yields increase while the char decreases.

2.2.3.2 Residence time

Vapour residence time is defined as the time required for the pyrolysis vapours to exit the reactor and reach the condensation stage. As discussed in Sub-section 2.2, in order to avoid secondary reactions, including thermal cracking, recondensation, repolymerisation, it is necessary to have a short vapour residence time of less than 1 second. This results in the optimisation of the liquid yields, which are the main product of pyrolysis.

The formula used to calculate the pyrolysis vapour residence time in a fluidised bed reactor is:

$$ResidenceTime_{TotalHotSpace}\ (\text{seconds}) = \frac{(Volume_{TotalHotSpace} - \frac{W_{Sand}}{\rho_{Sand}}) \times T_{Measurement} \times Time}{1000 \times T_{Reactor} \times Volume_{TotalThru-Put}}$$

$Volume_{TotalHotSpace}$= Volume of reactor, cyclone and exit tube in cm^3 [377.86 cm^3]

W_{Sand}= Weight of sand used in trial in grams [150g]

ρ_{Sand}= Particle density of sand in g/ cm^3 [2.67 g/ cm^3]

$T_{Measurement}$= Ambient temperature in Kelvin [273 K]

$T_{Reactor}$= The average temperature of the reactor in K [873 K]

$Time$= The total run time of experiment in seconds [3600 s]

$Volume_{TotalThru-Put}$= Total volumetric output of trial in litres [300 l]

2.2.3.3 Inorganic compounds or ash

Inorganic compounds and specific alkali metals are very important during the process of fast pyrolysis, since they behave as catalysts and influence the decomposition behaviour of biomass [8, 9]. The alkali metals responsible for the catalytic decomposition of biomass and therefore the formation of char, are K and Na [8]. Alkaline earth metal such as Mg, Ca, and inorganic compounds such as Cl, and S have also an influence [29, 30]. The catalytic behaviour of the alkali metals also causes an increase in water and gas formation, and consequently a decrease in the organic yields of biomass [31, 32, 33].

In addition to their effect on product yields, the inorganic compounds have an effect on the chemical distribution of pyrolysis vapours. High yields of both levoglucosan and hydroxyacetaldehyde can be achieved through the removal in case of the former, or the enhancement in case of the latter, of the innate catalysts, such as alkali metals. The “Waterloo model” includes the two major alternative routes for cellulose degradation and is dependent upon the amount of alkali metals present [34]. Lower alkali metal content promotes a de-polymerisation mechanism resulting in higher molecular weight compounds such as levoglucosan and beta-D-fructose, while higher levers of alkali metals present in the degradation mechanism favour fragmentation thus producing lower molecular weight compounds such as hydroxyacetaldehyde.

2.3 Bio-oil

2.3.1 Bio-oil characteristics

Bio-oil is the main product of the process of fast pyrolysis. It is a multi-component mixture of different size molecules obtained from the depolymerization and fragmentation of cellulose, hemicelluloses, and lignin. Comprehensive reviews of bio-oil properties were published in a number of studies [26, 35, 36]. There are several chemical groups in bio-oil, including aldehydes, ketones, acids, alcohols, esters,

sugars, phenolics, furans, and multifunctional compounds [37]. The main bio-oil characteristics are summarised in Table 2-5.

Table 2-5: Bio-oil characteristics – typical data [26]

2.3.1.1 Water

The water in bio-oil derived from the original moisture in the feedstock and from pyrolysis as a product from dehydration reactions. Bio-oil water content ranges from typically 15 to 35 % and the variation of the water content depends on the feedstock water content and the process severity in terms of secondary reactions [38]

2.3.1.2 Oxygen

The oxygen is distributed in more than 300 compounds that were identified in bio-oils. The oxygen content is approximately 45-50 wt.% and depends on the biomass feedstock and the severity of the process. The presence of oxygen is the main reason for immiscibility with hydrocarbon fuels [38].

2.3.1.3 Viscosity

The viscosities of bio-oils vary over a wide range (35 – 1000 cP at 40^{o}C) and depend on the biomass feedstock, the conditions of pyrolysis process, and the efficiency of collection of low boiling components.

2.3.1.4 Acidity

Bio-oils comprise of significant amounts of acids, such as acetic and formic acid, resulting in a low pH of 2-3.

2.3.1.5 Ash

The ash of bio-oils is directly related to the char content of the oils. After the removal of fine char particles by hot-gas filtration, the ash content can be below 0.01% [40].

2.3.1.6 Chemical instability

The formation of bio-oil occurs due the 'freezing' (condensation) of the intermediate pyrolysis products of hemicellulose, cellulose, and lignin. This is the reason for the instability of bio-oil, due to the need of those chemicals to reach chemical equilibrium.

2.3.2 Applications of bio-oil

Potential applications of bio-oil are to produce higher value fuels**,** including biofuels and chemicals. Bio-oil can be used directly in boilers, furnaces, engines and gas turbines as a fuel, but modifications of the existing systems are required. Applications of bio-oils have been the focus of a number of reviews [39, 40, 41]. An extensive review of bio-oil characteristics and the problems that were reported with the use of bio-oil for heat and power, and for biofuels, was published by Bridgwater [2].

Another potential application of fast pyrolysis and consequently of bio-oil could be within a biorefinery. Figure 2-3 below shows a scheme of a biorefinery concept, whereby wheat straw is used as a raw material to produce value added chemicals, such as phenolics, furfural and ethanol [42].

Chemicals need to be able to meet product specification requirements for market acceptability. These may be oxygenated (such as acetic acid or phenol), whereby the requirement is less on de-oxygenation and more on delivering a product that is of a sufficiently high concentration, to justify separation and refining into a marketable chemical. Examples include precursors for phenol substitution in wood panel resin production; these may be whole bio-oil or extracts from bio-oil. Hydrocarbon chemicals are also of interest and may be produced along with biofuels from de-oxygenation.

Figure 2-3: An example of a Biorefinery concept [42]

2.3.3 Definition of quality of bio-oil

Before bio-oil can effectively be used in any application as a fuel and/or chemical source, there are several inherent properties that require consideration.

Biofuels require well defined and carefully specified products. These are either completely compatible with conventional fuels, such as synthetic diesel or gasoline (i.e. hydrocarbons that will require complete de-oxygenation of bio-oil), or can be sufficiently carefully controlled in quality to be blendable in some proportions, such as ethanol or a partially de-oxygenated product that is miscible with conventional fuels. Production of unique or dedicated biofuels such as ethanol, methanol or DME is also possible, but only through gasification to syngas and synthesis of the required product. This route is not considered further for the purpose of the present thesis.

The most important general quality requirements are:

1. All direct uses of bio-oil require a consistent and homogenous product, which homogeneity is the most important for storage, handling and processing.
2. Low solids are important to avoid potential blockage of injectors, filters and catalyst beds.
3. Low alkali metals and other impurities such as traces of sulphur and chlorine are important in catalytic systems.

The most important quality requirements for production of transport fuels and chemicals by any method in addition to the points 1-3 above are:

- Water content.
- Acidity.
- Oxygen content.

2.4 Improvement of bio-oil quality in this study

The present study investigates two different ways of improving the quality of bio-oil:

- Improvement of biomass feedstock by the process of pre-treatment, and consequently improvement of bio-oil quality. The process of pre-treatment is used mainly to improve bio-oil in terms of chemical distribution. The effect of pre-treatment on the initial biomass components affects the bio-oil composition

and it is possible to increase the concentration of a specific chemical. Once this is achieved, the separation of the chemical becomes economically attractive.

- Upgrading of pyrolysis vapours by catalysts. The process of catalytic pyrolysis is used in this study to improve bio-oil in terms of heating value, de-oxygenation, pH, chemical distribution.

Further details regarding the two processes will be discussed in the next subsection.

2.4.1 Pre-treatment processes explored by ECN

The pre-treatment processes that were applied to the feedstocks were torrefaction, aquathermolysis, and steam treatment. The pre-treatment was carried out at ECN as part of their contribution to the project [6, 43].

The present work involved only the processing of the pre-treated samples by fast pyrolysis. The main result of pre-treatment on biomass constituent is the removal of hemicellulose. This is desirable, since it is the component of biomass responsible for the instability and smell of bio-oil [2]. Basic analysis of the fresh and pre-treated feedstocks can be found in Chapter 5.

An illustration of the combinations of pre-treatment process, fast pyrolysis and catalytic pyrolysis for product production can be found in Figure 2-4. The pathways used in the current work are depicted in Figure 2-4 for wheat straw, poplar and spruce.

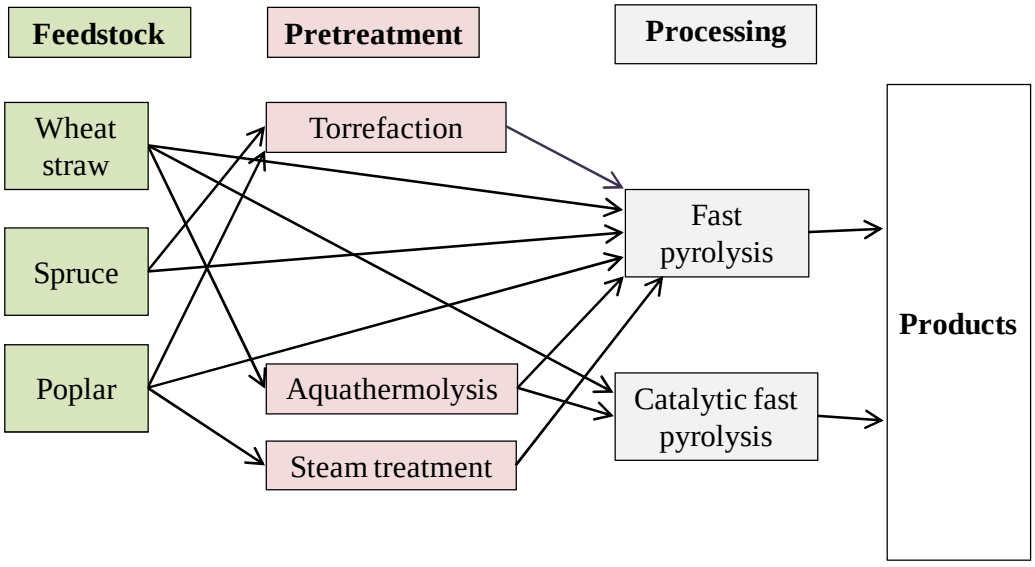

Figure 2-4: Combinations for product production by pre-treatment and thermochemical processes

2.4.1.1 Torrefaction

Torrefaction is a thermal treatment process that occurs in the absence of oxygen at 200^{o}C-300^{o}C, typically involving slow heating rates (10–100^{o}C/min) and long solids residence time [44]. Both heating rate and residence time depend on the biomass particle size and the amount due to heat transfer phenomena. A careful control of temperature, residence time and heating rate is important to avoid whole or partial decomposition of cellulose. During the process of torrefaction, biomass partly decomposes, resulting in a change on biomass components and consequently on bio-oil. Specifically, hemicellulose decomposes into volatiles and char-like solid products, whereas limited devolatilisation and carbonisation occur in the lignin and cellulose structure [45, 46].

The basic biomass components, hemicellulose, cellulose and lignin, decompose thermochemically in the following temperature ranges: 150-350^{o}C, 275-350^{o}C and 250-500^{o}C, respectively [12]. An illustration of the thermal degradation mechanisms during pyrolysis of lignocellulosic biomass can be found in Figure 2-5 [47].

Figure 2-5: Degradation temperatures of each lignocellulosic biomass component during the process of pyrolysis [47]

The decomposition mechanism of the main components of biomass during the pyrolysis process is divided into five main stages (see Table 2-5 for key) [48]:

A: Physical drying of biomass

B: Lignin softening

C:Depolymerisation and recondensation

D: Limited devolatilisation and carbonisation

E: Extensive devolatilisation and carbonisation

The objective of torrefaction is to produce a better quality fuel (biomass) by the removal of hemicellulose. Furthermore, light volatiles (acetic acid) and gaseous products are also produced from the process of torrefaction. This is interesting, since a marketable chemical product can be formed in high concentration that is worth separating. The gases can be used for heat and power purposes. Particularly, when torrefaction was applied for poplar and spruce at ECN, mainly acetic acid was produced in minor quantities (<2wt%).

2.4.1.2 Steam treatment

Steam treatment is a hot pressurised treatment of biomass in a steam atmosphere. The steam treatment of the poplar chips used in the experimentation was conducted in an industrial autoclave of PLATO, in Arnhem, The Netherlands. The poplar was slowly heated up to approximately 185℃ in an autoclave in the presence of steam at approximately 13 bar for 2 hours. After this treatment, it was slowly cooled down to room temperature. The liquids produced were not quantified but low quantities of methanol, furfural, formic acid and acetic acid were detected.

2.4.1.3 Aquathermolysis

Aquathermolysis is similar to steam treatment except that the process begins by heating up a mixture of water and biomass in an autoclave. Work at ECN showed that significant yields of value-added condensables such as furfural can be achieved [6]. The operating conditions are a reaction temperature of 200℃ under a pressure of 16 bar, in a 0.5L reactor autoclave with a heating rate of 6℃/min. Further details for aquathermolysis can be found in the literature [6]. It is interesting to note that the water treatment was more effective to produce high yields of furfural than the steam treatment.

2.4.2 Fast pyrolysis vapour upgrading by catalysts

The upgrading of bio-oil to higher quality and higher value fuels and chemicals can be achieved by a catalytic process. As previously mentioned (section 2.3.3), by using catalysts it is possible to overcome the problems associated with bio-oil properties, since the catalytic process is expected to enhance deoxygenation, cracking, and reforming reactions. The deoxygenation of pyrolysis vapours involves three reactions, namely decarboxylation, decarbonylation, and dehydration and all of them remove oxygen, in the form of carbon dioxide, carbon monoxide and water, respectively.

The Top 10 chemicals in terms of maximum reported yields that can be produced from bio-oil are mentioned in Table 2-6 [40]. The chemicals that can be produced from bio-oil are subdivided to desirable and undesirable. This division is not absolute and should only be used as an indicator. For example acetic acid is categorized in the undesirable category, but if it is produced in high yields it could be an economical attractive chemical. In the desirable category belong economically attractive chemicals, as phenols, alcohols and hydrocarbons. On the other hand, the group of undesirable chemicals is characterized by carbonyls, aldehydes and heavy compounds yield, since they are responsible for many reactions in the aging procedure. This category also includes acids, since low pH causes corrosion problems and polycyclic aromatic hydrocarbon *(*PAH) are considered as hazardous for the environment.

Table 2-6: Top 10 chemicals obtained from bio-oil [40]

This thesis investigated the upgrading of bio-oil by cracking the primary pyrolysis vapours by catalysts. Several researchers re-vaporized the bio-oil and then applied catalysts to crack the vapours [49, 50]. This process is not further considered in this study due to its thermal inefficiency. The condensation of pyrolysis vapours to produce bio-oil and then the evaporation of them for upgrading is not thermally efficient. For this

reason the most promising route to upgrade bio-oil seems to be the use of catalysts before condensation of pyrolysis vapours.

There are several possible ways to modify the production of chemicals and fuels by the catalytic fast pyrolysis process. The catalytic reactor configurations are shown in Figure 2-6.

- Biomass modification [A]: Removal or enhancement of the physical (innate) catalysts. Catalysts are added to the biomass prior to pyrolysis, such as sodium chloride, zinc chloride, cobalt chloride.
- The catalysts are added inside the biomass prior to pyrolysis [B].
- Another modification is the catalysts as part of the fluidising bed [C].
- In-situ catalysis of vapours [D]. This configuration involves a catalyst which is place as fixed or fluidized bed at the reactor freeboard and as a result the pyrolysis vapour and the char particles pass over the catalyst bed.
- Close coupled catalysts of vapours [E] = zeolite cracking. The configuration of close coupled secondary catalysis is similar to the in situ catalysis, but the difference consists that the catalysis takes place in a secondary reactor.

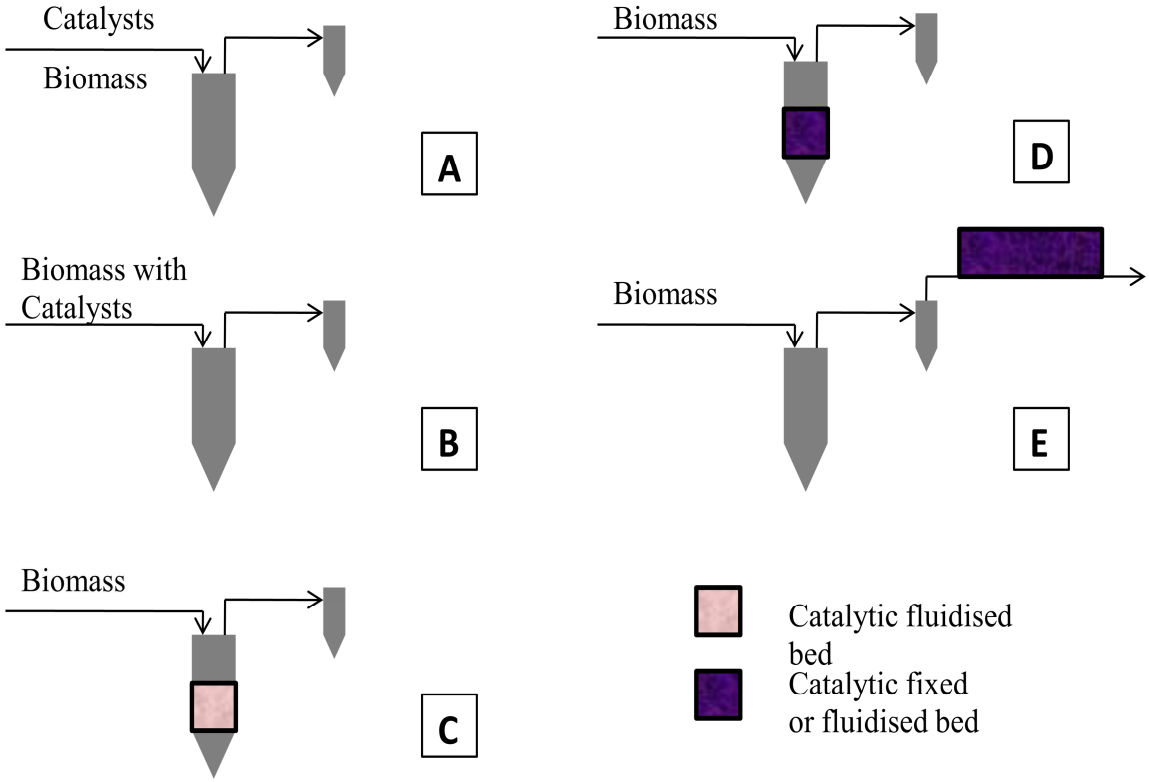

Figure 2-6: Catalytic modifications of reactors

The reactor configuration that was chose in this research to perform the catalytic work was a secondary close coupled catalytic fixed bed reactor. The advantages of this mode is that the char particles have been separated from the pyrolysis vapour by a cyclone before passing over the catalyst bed and that the secondary reactor can be operated under different severity from the primary pyrolysis reactor.

3 LITERATURE REVIEW

This literature review encompasses the various catalysts for bio-oil upgrading. This includes basic introduction of the structure of each catalyst type and the various types of catalysts used by previous researchers. Based on the review of previous research on catalysts, a selection of the appropriate catalysts is made for further experimental work and the rationale for the specific selection is discussed.

3.1 Zeolites

3.1.1 Zeolite structure

Zeolites are microporous crystalline solids with very well defined structures (frameworks or pores of uniform diameter). Silicon, aluminium and oxygen are the main components of the zeolites framework, with cations and water enclosed within their pores [51]. The zeolites framework contains SiO_4^- and AiO_4^- tetrahedral. These tetrahedral can interlink by sharing an oxygen atom to form a three-dimensional structure.

The main properties responsible for the catalytic activities of zeolites are their shape selectivity and acidity. Hence, a short explanation concerning the above properties is necessary for a basic understanding of zeolites catalytic activity. There are three forms of shape selectivity including reactant shape selectivity, product shape selectivity and transition state selectivity, which are analysed below [52, 53].

Reactant selectivity: The size and shape of the reactants are required to be less or equal to the size and shape of the zeolite pores. This will allow the reactants to enter into the pores. After the entrance of the reactants, reaction could occurred at the catalytically active sites.

Product selectivity: The products that were formed in the zeolite pores should be of a certain size and shape to exit zeolite pores. A negative aspect of this selectivity is that the molecules that cannot leave the pores could cause deactivation of the catalyst. This could happen by the conversion of the trap products to undesired by-products or coking.

Transition state shape selectivity: The production of a specific product during catalysis can be formed via intermediates. Each zeolite pore system can produced specific intermediates that are suitable to fit into their pores, resulting to limit the formation of products.

Acidity of zeolites: The main components of the zeolite framework including silicon and aluminium are negatively charged. This attracts the positive cations and encloses them. The acidity though it is not only related to the number of the acid sites, but to the nature of the sites. The acid sites are divided into acid and base sites. They are also named as Brönsted or Lewis sites [54].

"A Brönsted acid is any substance that donates a proton; a Brönsted base is any substance that accepts a proton".
"A Lewis acid is any substance that accepts an electron pair; a Lewis base is any substance that donates an electron pair in forming a covalent bond".

3.1.2 Studies using ZSM-5

The use of ZSM-5 zeolite catalyst to upgrade the pyrolysis vapours and consequently improve the quality of bio-oil was investigated by a number of researchers [55, 56, 57, 58, 59].

Comprehensive work using ZSM-5 was performed by Williams and Horne [55, 56]. Their research focused on the effect of ZSM-5 on pyrolysis product yields and chemical distribution; influence of the regeneration of the former zeolite; influence of de-activation of ZSM-5 on pyrolysis vapours; catalyst dilution. The biomass used was a mixture of wood types. The equipment employed for this research involved a fluidised bed reactor with a series of condensers to trap the pyrolysis vapours. The construction of the reactor was stainless steel with diameter of 7.5 cm and height of 100 cm. The catalyst was placed at the reactor freeboard as a fixed bed (in-situ configuration). The pyrolysis system used, enabled independent control of the temperature of the fluidised and fixed bed and it was set at 550^{o}C and 500^{o}C respectively. Experimental operating conditions were a feed rate between 0.216 and 0.228 kg h $^{-l}$, 200g of catalyst, weight hour space velocity (WHSV) between of 1.05 and 1.14 h^{-1}.

Important results were the influence of H-ZSM-5 in terms of pyrolysis products yields. The oil yields were reduced from 40.4 to 5.5wt% of biomass when ZSM-5 was applied,

whereas a small increase from 14.7 to 19.3wt% of biomass was observed for the aqueous yields. Additionally, reduction was observed for the molecular weight (from 30-1300u to 50-600u). The introduction of ZSM-5 affected the chemical distribution in bio-oil, focusing on the formation of monocyclic aromatic hydrocarbons and polycyclic aromatic hydrocarbons (PAH).

The overall effect of continued regeneration of the zeolite catalyst caused a reduction in its effectiveness. Concerning the pyrolysis product yields, the repetition of regeneration increased the oil yields and reduced the aqueous yields. The significant reduction of molecular weight that was observed by the use of fresh H-ZSM-5 was becoming greater with the continued regeneration. In summary, the effect of the repeated catalyst regeneration lowered the concentration of aromatic hydrocarbons and PAH in bio-oil. This indicates that the effectiveness of the catalyst in converting biomass pyrolysis oils to an aromatic product was reduced after each regeneration.

Another aspect of their work was to investigate the influence of zeolite ZSM-5 catalyst deactivation on pyrolysis vapours [57]. The experimental unit and the operating conditions were the same as described above. The difference in the study described here from the one discussed above lies in the catalytic process. The total run time was 3 hours, however it was not continuous. The run was stopped at 10, 20, 30, 60, 120 and 180 minutes to enable the sampling of catalyst. This was used to observe the coke development over time. Also, a separate catalysis run was performed with a duration of 30 minutes for the purpose of comparison with the non-continuous runs. It was observed that coke formation was greater during the primary stages of catalytic pyrolysis. The elemental analysis of coke showed noteworthy quantities of oxygen, indicating that large molecular weight pyrolysis material was decomposed on the catalyst surface. The effectiveness of the catalyst was reduced with a time increase. This was noticed from the reduction on hydrocarbon levels, as well as an increase in the oxygenated components and molecular weight range in the oil.

Further research on H-ZSM-5 involved the dilution of the catalytic bed with stainless steel balls bearings; catalyst to steel ratios of 1:0, l:l, 1:2, 1:3 and 0:3v/v [58]. The dilution of the catalytic bed increased the residence time and the hot area for thermal cracking of the pyrolysis vapours in the bed. In this study the amount of catalyst used was 100g and consequently the WHSV was 2, with a total run duration of 30 minutes. The presence of steel in the catalyst bed gave a further increase in the production of

aromatic hydrocarbons, though it also increased the polycyclic hydrocarbons (PAH). The optimum catalyst to steel ratio for molecular weight reduction was 1:2v/v. In addition, it was noticed that ZSM-5 was responsible for the production of CO_2, CH_4 and alkene hydrocarbon, while thermal reactions for the formation of CO, H_2 and alkane hydrocarbons.

Williams and Nugranad performed pyrolysis of rice husks with the same reactor unit configuration as described above using a ZSM-5 catalyst [59]. The aim of their work was to investigate the influence of catalyst temperature on pyrolysis vapours. Catalytic experiments were performed in a range of temperatures of 400^{o}C – 600^{o}C. The temperature of the pyrolysis fluidised reactor was held at 550^{o}C. ZSM-5 de-oxygenerated the bio-oil. The oxygen removed from the bio-oil was in the form of water at low catalytic temperatures. At higher temperatures the oxygen was removed in the form of CO and CO_2. Catalytic pyrolysis reduced total liquid yields, molecular weight and oxygenated compounds (phenols, benzenediol etc). On the contrary, it increased the concentration of aromatic hydrocarbons and PAH in bio-oil. Another interesting finding was that the biomass type affected the chemical composition of the oils. In contrast to woods, the concentration of PAH was higher when rice husks were used as feedstock. Regarding the temperature effect, a combination of ZSM-5 and temperature increase led to an increase of aromatic compounds in oils. It should be noted that even though the aromatics increased with temperature increase, the organic yields were in fact reduced.

The effect of catalytic reaction temperature (390, 410, 450, 470, 500, or 550^{o}C) and WHSV (1 to 5 h^{-1}) on ZSM-5 was investigated by Li et al. [60]. The configuration applied for the catalytic runs was a fluidized bed reactor for pyrolysis coupled with a secondary fixed bed reactor for upgrading. Pyrolysis conditions include a temperature of 500℃ and a gas flow rate of 4m^3/h. Sawdust biomass was fed in the reactor with a feeding rate of 3kg/h. The main conclusions regarding the optimum conditions for maximum liquid yields were a temperature of 500^{o}C and a WHSV of 3h^{-1}. The effect of ZSM-5 on chemical distribution using the latter optimum conditions showed that the acid and ketones were reduced, whereas hydroxybenzene and monocyclic or dicyclic aromatic hydrocarbons were increased.

Batch experiments with corncob were conducted by Zhang et al. using H-ZSM-5 catalyst at a fluidised bed reactor [61]. The catalytic configuration used was a mixture

of the catalyst with the bed material. The dimensions of the fluidised bed reactor were 30mm diameter and 400mm height. The experiments were non-continuous. 30g of catalysts were mixed with the bed material, whereas 6 g of biomass was fed in one shot in the reactor. The first part of this work involved pyrolysis of corncob to determine the optimum operational conditions for maximising liquid yields. Parameters tested included pyrolysis temperature, static bed heights, N_2 flow rates and particle size of feedstock. After the assessment of the parameters, pyrolysis temperature of 550^oC (56.8wt% liquid yield) and N_2 flow rate of 3.4 L/min were selected for further catalytic runs. The results showed that H-ZSM-5 selectively increased the amount of aromatic hydrocarbons in oil fraction and de-oxygenated the oil.

3.1.3 Studies with various zeolite structures

The limitations of the pore size (5A) of H-ZSM-5 in the case of large molecules justified the further investigation on zeolite materials with larger pore size. A growing interest in research over mesoporous zeolite catalysts occurred as a result of a need for an upgrade of pyrolysis vapours.

Williams and Horne [62] conducted further research in this area, by using different zeolite structures and by incorporating a metal into the ZSM-5 structure. Different zeolites (Na-ZSM-5, H-ZSM-5 and Y) and activated alumina were used to upgrade bio-oil. The experimental unit and operating conditions used were described previously in section 3.1.2. Results showed indifferences between Na-ZSM-5and H-ZSM-5 catalysts in the products yield and chemical distribution in bio-oil. It should be mentioned that the Na-ZSM-5 catalyst was in a hydrogen exchange form with 0.03% Na. Regarding the products yields, stainless steel balls, Na-ZSM-5, H-ZSM-5, Y and activated alumina showed a reduction on organic liquid yields (blank run-40.41%) of 11.80, 6.01, 5.47, 1.13 and 3.12 respectively, expressed on wt% of biomass feed. The coke formation was higher for the case of Y-zeolite and activated alumina (19.1 and 18.4 wt% respectively), while for the other zeolites it was approximately 12wt%. The overall conclusions were that all the zeolites produced hydrocarbons (aromatic and PAHs); Y-zeolite formed higher PAHs levels compared to the other catalysts; ZSM-5 was the most effective catalyst; hydrocarbon yields were low, when expressed on wt% of biomass feed.

Aho et al. [63, 64, 65] carried out a comprehensive study involving different zeolite structures. Their research focused on the investigation of different proton forms of

Beta, Y, ZSM-5 and Mordenite zeolites on upgrading pyrolysis vapours; different acidities of the H-Beta zeolite; comparison of the proton forms of beta, Y, and ferrierite zeolites with their iron modifications. The feedstock used was pine wood. The experimental apparatus included a fluidised bed reactor, condensers, a char removal system and a screw feeder. The catalyst was placed as the bed material inside the reactor. The reactor dimensions were 45 mm diameter and 590 mm height, of which 210 mm of the lower part of the reactor were used for pre-heating the fluidisation gas. The mass of each dry zeolite was 12 g. The feeder was loaded with approximately 30 g of dry pine biomass. The rate of the feeding was approximately 20 g/h. The pyrolysis reaction temperature was 450^{o}C. Quartz sand was used as a reference material in the non-catalytic pyrolysis experiments.

The initial work focused on investigating the influence of different proton forms of Beta, Y, ZSM-5 and Mordenite zeolites on upgrading pyrolysis vapours [63]. The coke formation on H-Beta-25, H-Y-12, H-ZSM5-23 and H-MOR-20 was 11.2, 16.7, 5.2 and 7.2 wt% of dry biomass respectively. The numbers after the name of the catalysts represent the Si:Al ratio. Y-zeolite formed the highest amount of coke and this is with agreement with the previous study [62]. Regarding the chemical distribution on bio-oil, ketones and phenols were the dominating chemical groups. It is important to mention that the yield of each chemical compound was calculated by multiplication of the percentage of the GC/MS peak area and the liquid yield. H-ZSM-5 produced high level of ketones and phenols; H-Y also formed high amount of ketones. The maximum PAH's concentration was 3.09 wt% of liquid yield for H-ZSM-5.

Further research was conducted using different acidities of the H-Beta zeolite. The acidity of zeolite catalysts depends on the variation of silica to alumina ratio; different acid strengths affect pyrolysis products [64]. Fast pyrolysis experiments were performed to investigate the effect of different zeolite acidities on bio-oil and pyrolysis products. H-beta zeolites influenced the yields of the obtained products and decreased the yield of the organic oil. During catalytic pyrolysis, zeolites with stronger acidity (H-beta-25> H-beta-25 regenerated> H-beta-150> H-beta-300) produced less organic oil, increased water and char yields, while gas yields were constant. The formation of PAHs was possible only at the presence of the zeolites, when compared with the blank run. Higher zeolite acidity increased the yields of PAHs, while lowering the aldehydes yields. The highest yield of PAHs observed was 0.92 wt % of the organic oil for H-beta-25. The chemicals identified in bio-oil were grouped as aldehydes, acids, alcohols,

ketones, phenols and PAHs. The introduction of catalysts as bed material in the process of pyrolysis reduced the production of ketones and phenols, when compared with the use of only sand in the bed.

Another approach was to compare the proton forms of beta, Y, and ferrierite zeolites with their iron modification [65]. The experimental unit used was an in-situ configuration; the catalyst was placed as bed material to form a second fluidised reactor in the freeboard of the main pyrolysis fluidised reactor. De-oxygenation reactions were observed as higher water yield content and greater CO/CO_2 ratio. It was noticeable for both the proton and iron modified zeolites. The most active was Beta zeolite, followed by Y and ferrierite. The iron modifications of the zeolites formed higher levels of coke than the proton ones, with an exception in the case of ferrierite (low iron level). The formation of coke during the catalytic runs could be due to the different pore size of the zeolites. The narrow pores of ferrierite did not allow the majority of the pyrolysis vapours to enter; thus a low amount of coke was formed. On the contrary, the cavities on the structure of Y allowed larger molecules to enter and the coke production was high. Regarding the chemical distribution in bio-oils, levoglucosan levels decreased for all the catalytic runs compared to the non-catalytic. Concerning the iron modified zeolites, it was noticed that the methyl substituted phenol levels increased, while methoxy substituted phenols decreased.

Further work related to the acidity and the metal incorporation of the catalysts was conducted by Antonakou et al. [66]. Pyrolysis experiments using Al -MCM-41 catalysts with various acidities (Si:Al ratios of 20, 40, 60) and metal containing Al -MCM-41catalysts (Cu-Al-MCM-41, Fe-Al-MCM-41 and Zn-Al- MCM-41) were performed using a bench scale fixed bed reactor. The reactor has a height of 12.1 cm and a diameter of 1.25 cm. The liquid products were collected in a liquid bath. The amount of catalysts used in the bed was 0.7 g (or glass beads for the non-catalytic runs) and the biomass was 1.5 g. Commercial wood and Miscanthus used as feedstocks and the pyrolysis reaction temperature was 500^{o}C. The use of Al-MCM-41 influenced the chemical distribution in bio-oil. An increase was observed on the amount of phenols and hydrocarbons in bio-oil, while the opposite effect occurred for the oxygenated compounds. Moreover, a reduction in acids, carbonyls and heavy compounds was noted. The organic yields, though, decreased by about 9 wt% (on biomass base) when catalysts were applied. Higher acidity (lower Si:Al ratio) of Al-MCM-41 caused an increase in the water levels in bio-oil, while the organic yields remained almost

constant. The gases yields seemed to remain unaffected from the catalysts acidity. Acidity also influenced the chemical distribution in bio-oil. The catalyst with the highest acidity (MCM-1, Si/Al=20) favoured the production of phenols, whereas an intermediate acidity (MCM-2, Si/Al=40) reduced the undesirable fractions. With regards to the incorporation of metals in the structure of Al-MCM-41, the greatest metal was Zn. It is an interesting finding, since it has produced less coke and gases and more liquid, without any influence on the aromatisation reactions. The biomass type also seemed to affect the product yields, since the catalytic runs with the Miscanthus showed higher liquid yields and less coke, when compared to the wood.

Further work on various Al-MCM-41 materials was carried out, using the same equipment described above [67]. Tests were conducted with Al-MCM-41 (Si/Al=30 or 50), siliceous MCM-41, and moderate steamed Al-MCM-41 samples (at 550 and 750 ◦C, 20% steam partial pressure). The feedstock used was wood (Lignocel HBS 150-500). Total liquids in bio-oil were increased using both MCM-41 and Al-MCM-41(50) with values of 55.68wt% (on biomass) and 48.38 wt% (on biomass) respectively. Moreover, organic yields for the former catalysts were almost stable (19.81 wt% on biomass) and increased (22.55wt% on biomass), respectively. Total liquids and organics showed a reduction for the rest of the catalysts. Another interesting finding was that the siliceous MCM-41 was the only catalyst that reduced coke levels. Steaming affected the structure of the catalysts and consequently the catalysts' influence on pyrolysis products. A reduction on the surface area and the number of acid sites was observed for all steamed catalysts. Al-MCM-41(30) at 550^{o}C and 20% steam did not result to significant changes in pyrolysis product yields in comparison to the parent calcined catalyst. On the contrary, Al-MCM-41(50) at 750^{o}C and 20% steam, reduced the total liquid yields and specifically the organic part. Regarding the chemical distribution in bio-oil, all the catalysts favoured the production of phenols, carbonyls and alcohols, compared to the non-catalytic tests. Unlike the other catalysts used, the siliceous MCM-41 decreased the former chemical compounds. To summarise, moderate acidity and surface area favoured phenols production (e.g. Al-MCM-41(50) with the steamed Al-MCM-41(30) at 550 ◦C); MCM-41 increased heavy compound yields (except for Al-MCM-41(50)); PAHs were significantly greater when the siliceous MCM-41 was used as catalyst.

The in situ upgrading of biomass pyrolysis vapours with two mesoporous aluminosilicate materials (MSU-SBEA) assembled from zeolite Beta (BEA) seeds was

tested in the present study, in comparison to conventional Al-MCM-41 (Si/Al = 50) and to non-catalytic biomass pyrolysis [68]. MSU-S/H_{BEA} and MSU-S/W_{BEA} catalysts had different structures. Both catalysts caused a reduction of the total liquid products, without affecting the water production. The gases were higher with the wormhole-like MSU-S/WBEA sample, while they were reduced with the hexagonal MSU-S/HBEA sample. Coke was significantly increased with both MSU-S catalysts.

The MSU-S catalytic materials were very selective towards polycyclic aromatic hydrocarbons (PAHs) and heavy fractions, while they produced negligible amounts of acids, alcohols and carbonyls, and very few phenols. The MSU-S materials appeared to possess stronger acid sites than Al-MCM-41, resulting in enhanced yields of aromatics, PAHs and coke, as well as propylene in the pyrolysis gases.

Analytical equipment was used by several researchers to evaluate various catalysts. An on-line pyrolysis-gas chromatography/mass spectrometry (Py-GC/MS) system has been used previously to investigate the effect of various catalysts on the thermal degradation products of biomass.

Micro-scale pyrolysis experiments were carried out by Azzez [69] using five basic and acidic catalysts, namely SN-27, MSN-15, MSM-15, H-ZSM-5-28 and H-ZSM-5-80 zeolites. There were two main objectives of Azzez research; to study the effect of the five basic and acidic catalysts on the thermal degradation products; to evaluate the role of zeolites concentration on the pyrolysis products. The feedstock used was beech. The equipment employed for the catalyst screening was a Py-GC/MS/FID. The pyrolysis temperature was 500^{o}C. The beech sample was held in the former temperature for 12 seconds. The sample preparation was an equal mixture of catalysts and biomass.

The main conclusion of the study was that acidic catalysts have the most important influence on pyrolysis products in comparison to the basic catalysts. Comparison of the basic catalysts showed that SN-27 enhanced the yields of furfural, while MSN-15 improved the yields of anhydrosugars. The effect of the acidic catalysts can be observed on the thermal degradation products of beech, specifically on 1.6-anhydro-β-d-glucopyranose (Levoglucosan), 1.5- anhydro-β-d-xylofuranose, furfural and an unknown carbohydrate. In particular, the initial percentage peak areas of furfural and levoglucosan (1.4% and 3.3% respectively) in untreated beech sample increased when

treated with HZSM-5-80 and MSM-15 catalysts (4.6% and 20% respectively). The lower acidity of MSM-15 could be an explanation for the higher amount of levoglucosan produced in treated beech samples. Regarding the effect of different catalyst concentrations (10% and 40% of MSM-15 and HZSM-5-80) on degradation products, levoglucosan was influenced.

A mesoporous MFI catalyst (Si:Al=20) was used to observe the effect on pyrolysis product distribution and chemical composition of bio-oil [70]. Conventional HZSM-5 and mesoporous material from HZSM-5 (MMZ_{ZSM-5}) were also studied for comparison of the catalytic effect of MFI. The configuration of a bench, g-scale fixed bed reactor coupled with a secondary catalytic fixed bed reactor was used for catalytic pyrolysis of Radiata pine sawdust. The experimental set-up provided an easy way of screening catalysts. The amount of feedstock used was 5 grams, whereas the catalyst placed was 0.5 grams. A series of batch experiments were undertaken at 500^{o}C and the resident time of pyrolysis vapours was 5 seconds. The experiments' configuration required a small amount of feedstock and catalysts, prevented feeding problems and was able to provide a liquid sample for further analysis. The mesoporous MFI showed the best activity in de-oxygenation and aromatization, when compared with the other zeolites in this study. The only disadvantage of MFI was the reduction of the organic yields of bio-oil. It was found that this problem can be improved by introduction of gallium into the MFI structure. 1 wt% and 5wt% of gallium were incorporated into the MFI structure.

Uzun et al. carried out experiments with synthetic zeolite catalysts, namely ZSM-5, H–Y and USY (10wt.% of raw material) [71]. Non-catalytic pyrolysis of corn stalks was also studied in a tubular fixed-bed reactor to determine the optimum operating conditions that maximised liquid yields. The amount of biomass used was 5g, whereas 0.5g was the catalyst. Catalytic pyrolysis was performed using the optimum conditions from the non-catalytic runs; pyrolysis temperature of 500 ℃, sweeping gas flow rate of 400 cm^3 min^{-1}, and heating rate of 500 ℃ min^{-1}. Two different methods were used for the catalytic runs; mixing of the catalyst with biomass in the bed, and catalyst packed to form a fixed bed on top of the biomass. Catalytic pyrolysis reduced the liquid yield when compared with non-catalytic runs. With both methods ZSM-5 produced the maximum liquid yields (from 33.3wt% to 27.55wt%), whereas USU the lowest (from 33.3wt% to 22.5wt%). Furthermore, the USU and ZSM-5 catalysts selectively increased the aromatic compounds in bio-oil, while H–Y increased the aliphatics.

Pattiya tested four catalysts for their activity in changing pyrolysis products [72]. The most active catalyst was ZSM-5, which significantly increased the formation of aromatic hydrocarbons and phenols, decreased considerable amounts of the oxygenated lignin-derived compounds and reduced the yields of carbonyl compounds.

3.2 Metal oxides

Metal oxides were used conventionally as a selective oxidation catalyst to synthesise intermediate chemicals. Currently, they are being used as catalysts in various applications, including the petroleum, chemical and environmental industries [73].

Analytical and bench scale studies were also conducted for metal oxide catalysts. Comprehensive work by Nokkosmäki was performed for three different types of zinc oxide [74]. The research can be divided into micro-scale and bench scale experiments. Bark-free sawdust of Scots pine (Pinus sylTestris) and pine sawdust (Finnmehl) were used as raw material. The micro-scale studies involved a combination of a Pyroprobe with a GC, using the injection port of the GC as a fixed-bed catalytic converter. The reaction temperature used for the experiments was 600^{o}C. The bench scale experiments used a fluidised bed reactor with capacity of 1 kgh^{-1}, with the pyrolysis vapours condensing into a glass bundle. The catalytic fixed bed reactor (10cm long) was connected into the side stream of the reactor system. Pyrolysis reaction temperature was 525^{o}C, while the catalytic reaction temperature was 400^{o}C. The catalyst used was a commercial zinc oxide ZnO(1). Silicon carbide had been used as the reference for the catalyst reactor. The results showed that ZnO was a mild catalyst and this was observed from the unaffected yields of liquid. It did not influence the water-insoluble fraction (lignin-derived compounds), but it decomposed the diethyl ether-insoluble fraction (water-soluble anhydrosugars and polysaccharides). The increase in viscosity was significantly lower for the ZnO-treated oil (55%) than for the reference oil, without any catalyst (129%) thus indicating an improvement in the stability.

Another study was performed using three commercial meso- or macroporous catalysts (TiO_2 (Rutile), TiO_2 (Anatase) and ZrO_2&TiO_2) and their modified ones with incorporation of Ce, Ru or Pd into their structure [75]. Poplar wood was used as a reference feedstock. Pyrolysis was conducted using a CDS Pyroprobe 5250 pyrolyser. The catalytic configuration inside the tube involved poplar wood in the middle, while the

catalyst was placed at both sides of poplar. The mass of the poplar wood and the catalyst (each layer) was 0.50 and 1.00 mg respectively. The methodology used held for 10 seconds the pyrolysis temperature at 600 ^{o}C, with the heating rate of 20 ^{o}C/ms. The formation of phenols was increased when TiO_2 (Rutile) based catalysts were applied. In particular, phenols increased from 25.6% in the non-catalytic runs to 37.2% after catalysed by the Pd/$CeTiO_2$ (Rutile). An important reduction was observed to phenols, acids and sugars after the treatment with ZrO_2&TiO_2 based catalysts. On the contrary, hydrocarbons, ketones and cyclopentanones were increased when the latter catalyst was applied. Specifically, the hydrocarbons increased from 0.1% (non catalytic runs) to 13.1% by ZrO_2&TiO_2 catalyst. Catalyst addition decreased the quantity of bio-oil yields but increased the quality of bio-oil in terms of calorific value, hydrocarbon distribution and removal of oxygenated groups.

The effect of MgO catalyst on pyrolysis yields was investigated by Putun et al. [76]. The experiments were divided in three sets in order to determine the effect of the pyrolysis temperature on pyrolysis yields, the effect of sweeping gas flow rate on product yields, and the effect of various amounts of MgO on pyrolysis yields (5, 10, 15, and 20 wt.% of raw material). The catalytic experiments were carried out in a fixed bed reactor with a length of 60 cm and an inner diameter of 2.5 cm. Pyrolysis vapours were condensed in a cold trap. The catalysts were mixed with 5grams of cotton seed and placed as a bed material inside the reactor. The optimum conditions used for the catalytic runs to maximise liquid yields were a pyrolysis temperature of 550^{o}C with a sweeping gas flow rate of 200 $mLmin^{-1}$. The pyrolysis products yields were influenced by the amount of catalyst. The amount of catalyst was directly proportional to gas and char yield and inversely proportional to the oil yields. Oxygen content was reduced from 9.56% to 4.90% when catalysts were applied. The conclusion regarding chemical distribution was that the bio-oil produced from the catalytic runs had lower weight hydrocarbons.

Torri investigated thoroughly the effects of a variety of metal oxide catalysts on pyrolysis vapours [77]. Catalyst screening was performed on 31 catalysts. The pyrolysis unit was a CDS Pyroprobe 1000 pyrolyser connected to a HP 5890 Series II gas chromatograph, and detection was carried out with an HP 5921A microwave induced plasma- atomic emission detector (MIP-AED). Tested catalysts included mesoporous silica supported metal oxides, bulk metal oxides, clays, zeolites and catalysts for methanol synthesis from syngas (MS). The catalysts were mixed with pine

sawdust at 1/1 (w/ w) ratio inside the quartz tube. A significant decrease in non-volatile fraction and slight decrease in bio-oil yield were obtained with ZnO, CuO, Fe_2O_3 and mixed oxide catalysts usually used for methanol synthesis from syngas.

3.3 Proprietary commercial catalysts (PCC)

Proprietary Commercial Catalysts (PCC) are designed with specific design properties for a specific company. The design properties such as pore size are not revealed in patents and are kept confidential [78].

Research was undertaken by Zabaniotou [79] using a commercial FCC catalyst to investigate the effect on pyrolysis vapours of five biomass residues. Corncobs and cornstalks, sunflower residues, olive kernels and olive tree prunings were used as raw materials. Pyrolysis experiments were performed using two different reactors, including a captive sample wire mess reactor and fixed bed reactor. Catalytic experiments were done only on the fixed bed reactor. The latter reactor had a height of 12.1 cm and a diameter of 1.25 cm. The liquid products were collected in a liquid bath. The amount of catalysts used in the bed was 0.7 g (or glass beads for the non-catalytic runs) and the biomass was 1.5 g. The pyrolysis reaction temperature was 500^{o}C. The pyrolysis products yields were influenced by the FCC catalyst. The greater liquid percentages for the non-catalytic runs were produced for olive kernels and corn residues, followed by olive tree prunings and sunflower residues. The addition of catalysts resulted in the reduction of the liquid yields, except for olive kernels and corncobs which had the opposite effect. The organic yields, though, were reduced for all biomass types. The most interesting results regarding the chemical distribution on bio-oil were the influence of FCC catalysts on phenol and hydrocarbon yields. A significant increase can be observed for the amount of phenols for all feedstocks, and specifically in the case of the corn cob and olive prunings. Sunflower residue showed the greater influence on hydrocarbons by FCC, followed by olive prunings and corn cob.

Euphorbia rigida and sesame stalk biomass were used to study the effect of DHC-32 (Ni-W/Al2O3) and HC-K 1.3Q (Ni-Mo/Al2O3) catalysts on their pyrolysis vapours [80]. The experimental apparatus used consisted of a bench fixed bed reactor and a liquid condenser system. Batch experiments were conducted at pyrolysis temperature of 500^{o}C and 750^{o}C, placing a mixture of 10 grams of biomass and different catalysts ratio (5, 10 and 20% w/w) inside the reactor. The pyrolysis products were influenced by

the various parameters. Optimum catalysts ratio for maximising pyrolysis oil yields were at 10% w/w for both feedstocks and both catalysts. Regarding the gas yields, a reduction was noticed with rising catalysts ratio at 500^{o}C, while at 750^{o}C was visa versa. Another outcome was that biomass type influenced the results. To specify for E. rigida, C and H values were reduced in the catalytic runs while oxygen content was increased. This was opposite with sesame stalk. Similar trend was observed with the chemical distribution in bio-oil. The catalytic pyrolysis of E. rigida reduced the aliphatic and aromatic chemical fractions and increased the polars. Concerning the catalytic pyrolysis of sesame stalk, a reverse tendency was noticed.

Further research on various zeolites and commercial zeolites was undertaken by French using a tubular quartz micro-reactor coupled with a molecular-beam mass spectrometry (MBMS) to analyse the pyrolysis vapours [81]. Forty catalysts were studied: 10 commercial zeolites (including ZSM-5, Y, and SAPO types), 22 ZSM-5 catalysts modified by substituting Al or hydrogen with different metals, four X and Y zeolites, and four different silica and alumina materials. Operation conditions involving a temperature range from 400℃ to 600℃ and catalys t-to-biomass ratios of 5– 10 by weight (10 mg of wood as biomass). The configuration used in the quartz tube was a layer of catalyst followed by the biomass sample and then the tube was inserted into flowing preheated gas. Findings of this study are with agreement with previous research. The highest yields of hydrocarbons (approximate 16wt%) were produced when nickel ZSM-5 was used, followed by cobalt, iron, and gallium-substituted ZSM-5. In addition, a commercial Zeolyst 8014 performed almost as well as the zeolite group. Zeolites with larger pores showed less de-oxygenation activity.

3.4 Natural catalyst

Naturally occurring catalysts, such as chars and clays, are found in the environment. These catalysts do not need to be synthesised. Some zeolites, such as Clinoptilolite, are found in the natural environment.

Research has been undertaken by Putun using a natural zeolite Clinoptilolite to study the effect of natural zeolite content on pyrolysis products of cotton-seed [82]. The effect of pyrolysis reaction temperature and the sweeping gas flow on Clinoptilolite was also investigated. The volume of the fixed bed reactor was 400 cm^3 and the pyrolysis

vapours were condensed in cold traps. The experimental work was divided into two sets.

The first one included the mixture of various amounts of natural zeolite (1%, 5%, 10% and 20%) with 10g of biomass. The pyrolysis reaction temperatures used were 400, 500, 550 or 700^{o}C at a constant heating rate of 7^{o}C min^{-}1 and held there for a minimum of 30 min at a static atmosphere. Maximum pyrolysis liquids yields were produced at 550^{o}C for 20% of zeolite. The addition of catalyst increased liquid yields.

The second set of experiments investigated the effect of sweeping gas flow (50, 100, 200 and 400 cm^{3} min-1) on pyrolysis products. This involved the mixture of 20% of Clinoptilolite with 10g of biomass at 550^{o}C (optimum operational conditions for maximum liquid production obtained from the first set of experiments). The greatest liquid yields were obtained at 100 cm^{3} min^{-1} instead at the highest flow of 400 cm^{3} min^{1}. An explanation can be that the cooling system used was insufficient. The use of sweeping gas increased the liquid yields from 30.87% to 35.77% for the same conditions.

The addition of catalyst in the process of pyrolysis improve the quality of the oil. It caused removal of oxygen and increased heating value and stability. The chemical distribution also showed that the oxygenated species decreased. Another observation was that catalytically treated oil showed an increase of the low C numbered hydrocarbons.

ATES [83] used the in-situ configuration to perform pyrolysis experiments in a fixed bed reactor with two selected commercial catalysts, namely Criterion-534, activated alumina, and natural zeolite (Clinoptilolite). The biomass feedstock used was Euphorbia rigida. The reactor system configuration had been described above. Various amounts of catalysts (5%, 10%, 20% and 25%) were mixed with 10g of biomass. The pyrolysis reaction temperature used was 550^{o}C at a constant heating rate of 7^{o}C min^{-}1 and held there for a minimum of 30 min at a static atmosphere.

The increase of catalysts mass resulted in the increase of liquid yields which is with agreement with the previous study [82], even if different biomass feedstocks were used. It was established that the pyrolysis oil yield rises in conjunction with increasing

catalyst percentage and reaches its maximum with using 20% by weight natural zeolite and Criterion-534 and 10% by weight activated alumina.

The oils produced were separated into two parts included n-pentane soluble (deasphalted oil) and insoluble (asphaltenes). Overall conclusions regarding the deasphalted and asphaltenes fraction of the oils showed that the catalysts have not any significant influence. The further separation of the deasphalted oil into hydrocarbons and polars shown that the all the catalysts increased the polar amount. The natural zeolite showed the greater increase, followed by Criterion-534 and activated alumina. In addition, the natural catalyst showed the highest increase on aliphatics, followed by activated alumina and Criterion-534.

The important finding of this study was that bio-oil yields were increased and the percentage from the use of each catalysts was 27.5% with the use of natural zeolite, 31% with Criterion-534 and 28.1% with activated alumina, while it was only 21.6% without any catalyst.

The summary of continuous catalytic pyrolysis experiments discussed throughout the literature review is listed in Table 3-1 below.

Table 3-1: Summary of continuous catalytic pyrolysis experiments

Ref.	Catalyst	Objective	Biomass type	Equipment	catalytic configuration	Operational conditions	Quality effect
55, 56	H-ZSM-5	effect of ZSM-5 on pyrolysis products yields and chemical distribution / influence of the regeneration of the former zeolite	mixture of wood types	fluidised bed reactor with a series of condensers to trap the pyrolysis vapours	The catalyst was placed in the reactor freeboard as a fixed bed (in-situ configuration)	0.216 and 0.228 kg h –l, 200g ZSM-5, WHSV 1.05 to 1.14 h-1, 550^{o}C pyrolysis reactor, 500^{o}C catalytic reactor	increased monocyclic and polycyclic aromatic hydrocarbons, reduced molecular weight and oxygenated compounds, regeneration of ZSM-5 reduced its effectiveness
57		influence of zeolite ZSM-5 catalyst deactivation on pyrolysis vapours				Same as above + The run was stopped at 10, 20, 30, 60, 120 and 180 minutes to enable the sampling of catalyst. This was used to observe the coke development during time.	Reduction of catalyst effectiveness with time
58		effect of catalyst dilution with steel balls on product yields and chemical distribution				100g of catalyst, WHSMV approximate 2 h^{-1} / 550^{o}C for pyrolysis reactor, 500^{o}C catalytic reactor catalyst to steel ratios of 1:0, l:l, 1:2, 1:3 and 0:3v/v	Steel increased monocyclic and polycyclic aromatic hydrocarbons, optimum conditions catalyst to steel ratio: 1:2v/v
59		influence of catalyst temperature on pyrolysis vapours	rice husks			400^{o}C – 600^{o}C	aromatic increased with temperature increase, but organic yields reduced
62	Na-ZSM-5, H-ZSM-5,Y, activated	effect of different zeolite structures and incorporation of a metal into	mixture of wood types	fluidised bed reactor with liquid	In situ fixed bed	0.216 and 0.228 kg h –l, 200g of catalyst, WHSV	Reduction of organic yields

	alumina	the ZSM-5 structure on pyrolysis vapours		condensation		between of 1.05 and 1.14 h-1 / 550^{o}C for pyrolysis reactor, 500^{o}C catalytic reactor	Production of aromatics Y highest coke Most effective was ZSM-5
63	proton forms of Beta, Y, ZSM-5 and Mordenite zeolites	effect of different zeolite structures on pyrolysis vapours	pine wood	a fluidised bed reactor, condensers, a char removal system and a screw feeder	catalyst as bed material inside the reactor	12 g catalyst and 30 g of pine biomass. Feeding rate of 20 g/h. Pyrolysis temperature of 450^{o}C	ZSM-5 high level of ketones and phenols, highest yields of PAHs formation Y highest coke
64	different acidities of the H-Beta zeolite	investigate the effect of different zeolite acidities on bio-oil and pyrolysis products					higher acidity: • less organics, more water + char • higher PAHs
65	beta, Y, ferrierite zeolites and their iron modifications	compare the proton forms of beta, Y, and ferrierite zeolites with their iron modification			In situ fluidised bed		De-oxygenation Most active Beta>Y>ferrierite Increase of levoglucosan
60	H-ZSM-5	Effect of reaction temperature and WHSV on H-ZSM-5	sawdust	Fluidised bed reactor	Secondary fixed bed reactor	Run duration of 80min, temperatures of 390, 410, 450, 470, 500, or 550^{o}C, and WHSV of 1 to 5 h^{-1}, respectively.	acid and ketones decreased, aromatics increased
74	Commercial zinc oxide	Effect of zinc oxide on pyrolysis products	Bark-free sawdust pine sawdust	Fluidised bed reactor (1kg/h)	Secondary catalytic fixed bed reactor	Pyrolysis reaction temperature 525^{o}C, catalytic reaction temperature 400^{o}C.	mild catalyst, decomposed the diethyl ether-insoluble fraction (water-soluble anhydrosugars and polysaccharides), lower viscosity

3.5 Key factors on catalytic fast pyrolysis

3.5.1 Temperature

The effect of temperature on pyrolysis yields for catalytic pyrolysis follows the same trend as for the non-catalytic experiments. The organic yields reach a maximum at approximately 500^{o}C and further temperature increase results in a reduction of liquid yields. In contrast, reaction water yields rise with an increase in temperature. In the case of gas yields, an increase is observed with rising temperature. The opposite trend is observed with char yields [59, 60, 84].

In addition, temperature has an effect on the chemical distribution for catalytic pyrolysis. Specifically, for both studies with temperature increase the amount of monocyclic and dicyclic aromatic hydrocarbons were greater when ZSM-5 was applied [59, 60].This is an interesting finding, since hydrocarbons are a desirable product in terms of bio-oil quality. Even though the chemicals increased the organic yields were decreased significantly.

3.5.2 Residence time

The residence time plays an important role to the catalytic pyrolysis products yields and distribution. The increase of residence time results to an increase of the thermal cracking of pyrolysis vapours. Horne at al. studied the effect of residence time using a ZSM-5 catalyst [58]. Concerning the products yields, an increase of residence time, decreased the pyrolysis liquid yields, coke and char yields. The gas yields showed an opposite trend. In terms of chemical distribution, the monocyclic and dicyclic aromatic hydrocarbons were greater.

3.5.3 Weight hour space velocity (WHSV)

The weight hour space velocity is defined by the weight of reactant per hourly divided by the weight of catalyst. Li et al. investigated the influence of various WHSV on ZSM-5 [60]. The liquid yields reached a maximum at 3h^{-1} and further increase resulted in a reduction. In the case of char yields, an increase was observed with rising temperature and the opposite tendency occurred for gas.

3.6 Chapter conclusions

The following catalysts were selected for screening tests using the Py-GC/MS. The catalysts choice was also depended from their availability on the market.

H-ZSM-5: is selected because it can enhanced de-oxygenation and cracking reactions, as well as the synthesis of aromatic hydrocarbons. Research was undertaken in terms of the effect of ZSM-5 on pyrolysis products yields and chemical distribution; influence of the regeneration of the former zeolite; influence of de-activation of ZSM-5 on pyrolysis vapours; catalyst dilution; operating conditions [55-59]. The existing studies would be interesting to use in comparison with the present study of H-ZSM-5.

CoMo: is known as a catalyst that enhance de-oxygenation reactions in the hydro-treating process. CoMo was also used in the pyrolysis process by Ates and Pattiya [83, 97]. This catalyst improved cracking reactions, increased light hydrocarbons and de-oxygenate the bio-oil.

NiMo: also used in the hydro-treating process. Since research showed that CoMo has a potential in pyrolysis process, NiMo could also prove to be an interesting catalyst for bio-oil upgrading.

FCC: it is a commercial proprietary catalyst and previous research showed that it is a promising catalysts for phenol and hydrocarbon production [79].

ZnO: this is a metal oxide catalyst that seemed promising to improve viscosity and stability of bio-oil [74].

ZrO, Fe_3O_2 and TiO: since ZnO seemed to be a potential catalyst for improvement of viscosity and stability of bio-oil, it is worth it to investigate more metal oxides. The selection of ZrO was due its market availability, as well as its potential for cracking the lignin derivative compounds in bio-oil. This was indicated from the oxidation of tar and ammonia in gasification gas cleaning process by ZrO [85]. A red mud based catalyst was used to upgrade bio-oil and it was showed that the upgraded bio-oil contained less carbonyl-containing and polar oxygenated compounds and more saturated hydrocarbons [86]. This result caused interesting to test red mud based catalyst, such as Fe3O2 and TiO. Additionally, the low cost and high availability of the red mud based catalysts made the catalysts attractive.

CuCr: is selected because it has potential for improving bio-oil stability and de-oxygenate the bio-oil [84]. Additionally, it was used for hydrogenation of carbonyl groups, under hydrogen atmosphere and high pressure [87].

Used CoMo: It was the catalyst that was recovered after the laboratory catalytic experiments. Further details about the laboratory experiments can be found in section 8.6.

Regenerated CoMo: This catalyst was recovered after the laboratory experiments (used CoMo) and was heated in air at 700^{o}C for one hour.

4 PYROLYSIS REACTOR SYSTEMS EMPLOYED AND PYROLYSIS PRODUCTS ANALYSIS

This chapter describe the pyrolysis reactor systems employed, ranging from analytical equipment, bench scale reactors to laboratory reactors. It includes an overview of thermogravimetric analysis (TGA), pyroprobe gas chromatographic/ mass spectrometry (Py-GC/MS), 100g/h and 300g/h bench scale fluidised reactor units, 1kg/h fluidised reactor unit and the 1kg/h circulate fluidised reactor unit of ECN. The mass balance methodology is also discussed. Additionally, the methodology used for the analysis of the pyrolysis products is presented in this chapter.

4.1 Thermogravimetric analysis – TGA

Analytical pyrolysis experiments were conducted using a micro-scale Perkin Elmer Pyris 1 TG analyser following the E 1131-03 ASTM standard Test Method for Compositional Analysis by Thermogravimetry. The equipment is able to measure the weight change in a sample as temperature varies. The data produced from thermogravimetric analysis (TGA)enables the calculation of volatilisation rate and peak temperature. Also, it produces kinetic data including activation energy and rate constants, but this is not further considered in this research.

TGA was used in this study for two reasons; to compare the thermal characteristics of various biomass types; to investigate the effect of pre-treatment on the thermal characteristics of untreated biomass. TGA is suitable to accomplish these two objectives since different biomass types have different physical and chemical characteristics and consequently different thermal degradation mechanisms. TGA can record those thermal degradation mechanisms. TGA has been used widely, since it is an easy technique to evaluate various feedstocks [88, 89, 90]. Figure 4-1 shows a micro-scale Perkin Elmer Pyris 1 TG, micro furnace, and a sample with a TGA crucible [91].

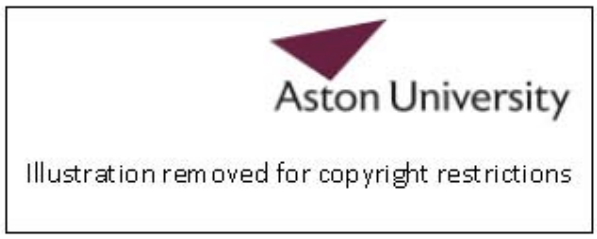

Figure 4-1: Micro-scale Perkin Elmer Pyris 1 TG,micro furnace, sample with TGA crucible [91]

Each sample was ground and sieved. The particle size of the feedstocks used for thermogravimetric analysis was 0.355-0.500mm. Each experiment was carried out in duplicates. Approximately 6 mg of each sample was placed on the TGA ceramic crucible and then placed in the autosampler. Then, the crucible with the biomass sample was placed inside the micro furnace in a nitrogen atmosphere for analytical pyrolysis. The sample was heated at 25^{o}C/min in a purge of nitrogen at a flow rate of 30 ml/min with the maximum temperature of 900^{o}C and each sample was held at the maximum temperature for 15 min. The procedure used for the TGA experiments is shown in Table 4-1.

Table 4-1: Procedure applied for the TGA experiments

Steps	**Methodology**
Drying Step	Sample heated from 40^{o}C to 105^{o}C using a heating rate of 10^{o}C/min Hold up 10 min at 105^{o}C
Devolatization Step	Sample heated from 105^{o}C to 905^{o}C using a heating rate of 25^{o}C/min Hold up 15 min at 905^{o}C

Weight loss (TG) and differential weight loss (DTG) graphs were produced for each sample.TG graph illustrates the percentage of weight loss as a temperature function, while DTG graph shows the rate of weight loss as a temperature function.

4.2 Pyroprobe- Gas Chromatograph / Mass Spectrometer (Py-GC/MS)

Micro-scale pyrolysis experiments were carried out with a Pyroprobe coupled with a Gas Chromatograph and a Mass Spectrometer. Due to equipment break-down, it was necessary to use two different equipment.

The majority of the characterisation experiments with raw and pre-treated feedstocks were carried out by a Pyroprobe- CDS AS-2500 Pyrolysis Auto Sampler coupled with a Perkin Elmer Autosystem XL Gas Chromatograph and a TurboMass Gold Mass Spectrometer. Each experiment was conducted in triplicates. The column used was an Elite-1701 (crossbond 14%, cyanopropylphenyl-85% dimethyl polysiloxane / 60m, 0.25 mm i.d., 0.25 µm df). Pyroprobe-GC/MS was used to perform pyrolysis experiments at the miligram scale. The gas chromatograph used for compound separation had a split ratio of 1:125 (Helium flow rate of 125ml/min). The compound mass range (m/z) was set between 28-600 and the data processing and the electron impact mass spectra (M/Z) were obtained using the Perkin Elmer TurboMass Gold spectrometer software package (version 6.0).

The catalytic experiments, as well as the characterisation of aquathermolised wheat straw and steamed poplar used another Py-GC/MS equipment. Each experiment was conducted in duplicates. The characterization of feedstocks with catalysts was done using a Pyroprobe 5000 Series coupled with a Varian 450 - Gas Chromatograph and a Varian 220 - Mass Spectometer. The column used was a factor four capillary column(30m, 25 mm i.d., 0.25 µm df). The gas chromatograph used for compound separation had a split ratio of 1:75 (Helium flow rate of 1ml/min). The molar mass (m/z) was set between 45-300 and the data processing and the electron impact mass spectra (M/Z) were obtained using the MS data review (version 6.9.2) and the varian MS workstation NIST/EPA/NIH (version 2.0).

The Py-GC/MS equipment is able to characterise the volatiles that are formed from the pyrolysis process. The gas chromatograph separates compounds in the volatile mixture by their boiling points and the mass spectrometer identifies and “semi-quantifies” them. The biomass sample is placed in a quartz silica tube, between two layers of hygroscopic wool and then is placed into the pyroprobe chamber, where the pyrolysis process is conducted. Figure 4-2 below illustrates the configuration of the biomass sample in the quartz tube used for the Pyroprobe.

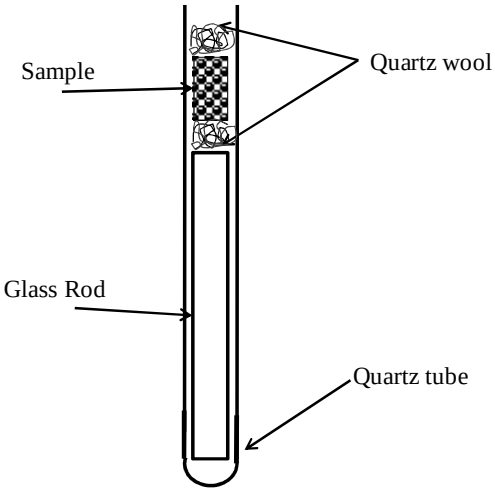

Figure 4-2:Configuration of biomass sample in quartz tube for Pyroprobe analysis

The pyrolysis vapours pass into the GC and travels through the GC column. The compounds in the volatile mixture are separated by their boiling points as they interact with the column. Then, the separate molecules pass to the mass spectrometry, which creates charged particles (radical cautions) from the molecules. The detector of the mass spectrometry analyses the ions and provides information concerning the molecular weight of the compound and its chemical structure. Further details regarding the mass spectrometry are provided in literature [92].

4.3 100 gh^{-1}fluidised bed reactor

4.3.1 Description of equipment

The 100 gh-1fluidised bed reactor has capacity of 100g/h and is constructed of a stainless steel tube with 40 mm diameter and 260 mm high. The range of biomass particle size was 355-500μm. This allows the 100 gh1 fluidised bed to perform without any blockages. The fluidizing gas is nitrogen whereas sand is used as a fluidising and heat transfer medium. The flow rate of nitrogen used is sufficient to provide three times the minimum fluidising velocity to the bed. The residence time of the pyrolysis vapours in the reactor is approximately 1 s. Further details regarding the operating conditions can be found in Chapter 7. Figure 4-3 and Figure 4-4 below show the main apparatus of the fast pyrolysis unit, which consists of the feeder, the reactor and the liquid product collection system [93]. The temperatures at different positions in the unit can be recorded using five thermocouples, which are located on the fluidised bed, reactor freeboard, cyclone, transition pipe.

The feeder consists of a tubular storage hopper, a stirrer and an entrainment tube. The feed rate of the biomass is controlled by the speed of the stirrer, the entrainment

nitrogen flow rate and the feeder top nitrogen flow rate. The rpm and the flow rate depend on the biomass type.

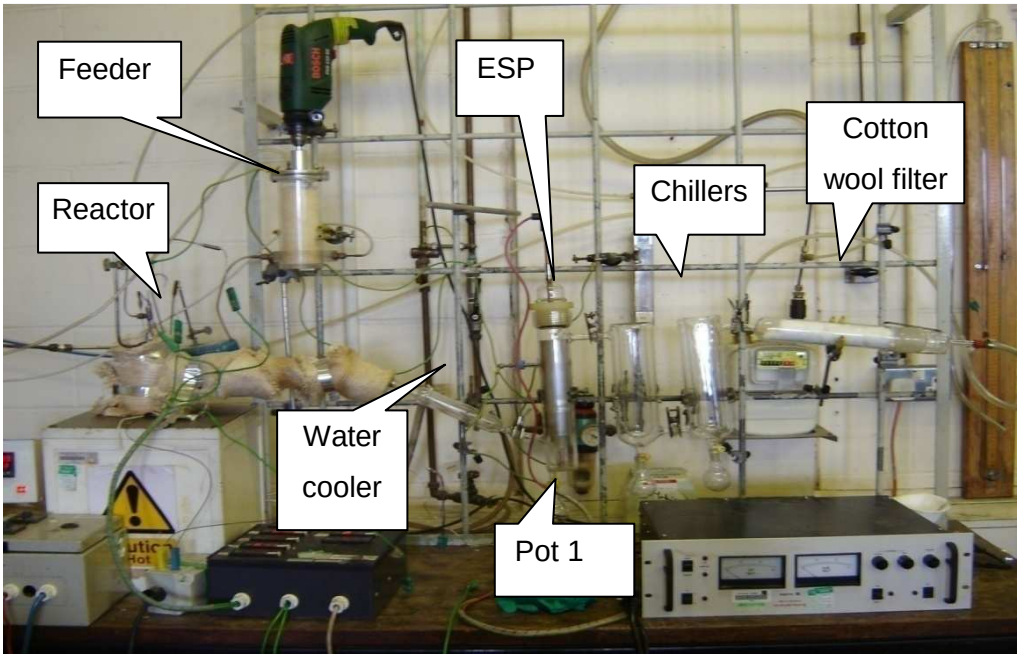

Figure 4-3: Photo of 100 g/h fluidised bed fast pyrolysis reactor

Figure 4-4: Experimental apparatus. Adapted from Coulson [93]

The reactor system is composed mainly of the reactor, cyclone and char pot. The cyclone part is responsible for the separation of the char from the gas stream. The fast pyrolysis process takes place in the fluidised bed and then the pyrolysis vapours and char enters the cyclone. The char is removed from the vapour stream using the cyclone

and collected in the char pot. The pyrolysis vapours exiting the cyclone pass into the liquid collection system.

The liquid collection system consists of a water condenser, an electrostatic precipitator (ESP), two dry ice/acetone condensers (chillers) and a cotton wool filter. The pyrolysis vapours passes through the first condenser (room temperature) followed by the ESP (room temperature) which traps the liquid products in aerosol form. The next two condensers are both at -20^{o}C using dry ice in acetone. Finally, the non-condensable gases passes through the cotton wool filter, which is used to protect the gas meter, and then to the GC.

4.3.2 Methodology

Fast pyrolysis of biomass produce a main liquid product and by-products of gas and char. The calculation of the mass balance uses the weight of the biomass feedstock used, while the output is the weight of the pyrolysis products. The mass balance closure is expressed in percentage (on dry biomass basis) for the amount of organic, char and gas produce.

The mass balance closure was calculated by weighing all the unit components of the 100g/h system before and after the run. Table 4-2 shows the mass balance closure calculations. The mass difference of the feeder before and after the experimental run is the input for the mass balance calculations. The char can be collected in the main reactor, sand, cyclone, char pot, transition pipes and a small amount in the water condenser and ESP (approximate 0.2wt%). The liquids can be collected in the water condenser, the ESP, the two dry ice/acetone condensers (chillers) and the cotton wool filter. Finally, the total volume of gases is the difference between initial and final gas meter readings.

Table 4-2: Mass balance closure calculations for the 300g/h fluidised bed reactor system

Pyrolysis Products	**Mass balance**	**Unit components**	**Measured techniques**
Char	Output	Reactor+sand+cyclone/ char pot/transition pipe/glass transition pipe/water condenser/ESP/cotton wool	Mass difference
Liquid	Output	Water condenser/ESP/dry ice condensers/cotton wool	Mass difference
Gas	Output	Gas meter	Gas meter and gas chromatography
Biomass fed	Input	Feeder	Mass difference

4.4 300 gh^{-1} fluidised bed reactor

4.4.1 Description of equipment

There are two important differences between the two bench scale reactor systems, the feeding system and product collection system. The 100g/h fluidized bed unit has a pneumatic feeder and water cooler, ESP and twin low temperature chillers while the 300g/h fluidized bed reactor has a screw feeder and is usually fitted with a quench column coupled to an ESP. Both reactor systems used in this study employed the liquid product collection system from the 100 g/h unit. The product collection system from the 100 g/h unit was used on the 300 g/h unit for more effective comparison and also because there is much more experience on this layout and it provides very good mass balance closures of better than 95%.

Several biomass particle size ranges were used with this reactor system. This includes the following: 0.355-0.500 mm, 0.500-0.600 mm, and 0.355-2mm. The N_2 flow rate was different for each range, as well as the sand particle size. The N_2 velocity was three times higher than the minimum fluidisation velocity. Details of the operating conditions for each experiment can be found in Chapter 6.

Significant problems in feeding were encountered during pyrolysis runs, so the experimental work was divided in two sections; experiments with the old feeding system which only had a single metering screw and a new feeding system with a metering screw and fast feed screw. The temperatures at different positions in the unit can be recorded using three thermocouples located on the fluidised bed, reactor freeboard and transition pipe.

4.4.2 Measurements

The calculation of the mass balance uses the weight of the biomass feedstock used, while the output is the weight of the pyrolysis products. The description of the calculations for the mass balance are the same with the 100g/h system and it was described in Section 4.3.2 above.

Table 4-3: Mass balance closure calculations for the 300g/h fluidised bed reactor system

Pyrolysis Products	Mass balance	Unit components	Measured techniques
Char	Output	Sand/ char pot/transition pipe/glass transition pipe/water condenser/ESP/cotton wool	Mass difference
Liquid	Output	Water condenser/ESP/dry ice condensers/cotton wool	Mass difference
Gas	Output	Gas meter	Gas meter and gas chromatography
Biomass fed	Input	Feeder	Mass difference

4.5 300 gh^{-1} fluidised bed reactor with secondary catalytic reactor

4.5.1 Description of equipment

This unit consists of the existing 300g/h fluidised bed reactor system (Section4.4.1) with the addition of a secondary catalytic fixed bed reactor. An illustration of the pyrolysis unit, as well as a photo, can be found in Figure 4-5 and Figure 4-6, respectively.

The secondary catalytic fixed bed reactor was constructed of stainless steel with 10 mm diameter and 400 mm length. It is placed in a horizontal tube furnace, which is located after the cyclone and before the liquid collection product system. This configuration provides the advantage of the removal of char from the pyrolysis vapour stream before it enters the catalytic bed. Also, the placement of the catalyst in a separate reactor enables the selection of different temperatures on the catalytic bed from the fluidised bed. The place of the catalyst bed in downstream horizontal tube furnace avoids the fluidisation of the catalytic bed.

The length of the catalytic bed was 200mm. SolidWorks software was used to draw the catalytic fixed bed reactor. A photo of the reactor design using SolidWorks, as well as the mechanical drawing of the reactor can be seen in APPENDIX C.

Catalytic runs were performed using ground wheat straw pellets as the biomass feedstock and CoMo as the catalyst. The range of wheat straw particle sizes was 0.355-2 mm. The catalyst was in pellets with diameter of 1mm. The nitrogen velocity was three times higher than the minimum fluidisation velocity. Details of the operating conditions can be found in Chapter 8. The catalyst was supported in the fixed bed by a ring of metal mesh and glass wool. Approximate 1g of glass wool was placed before and after the catalysts to capture fine char particles that the cyclone was unable to separate.

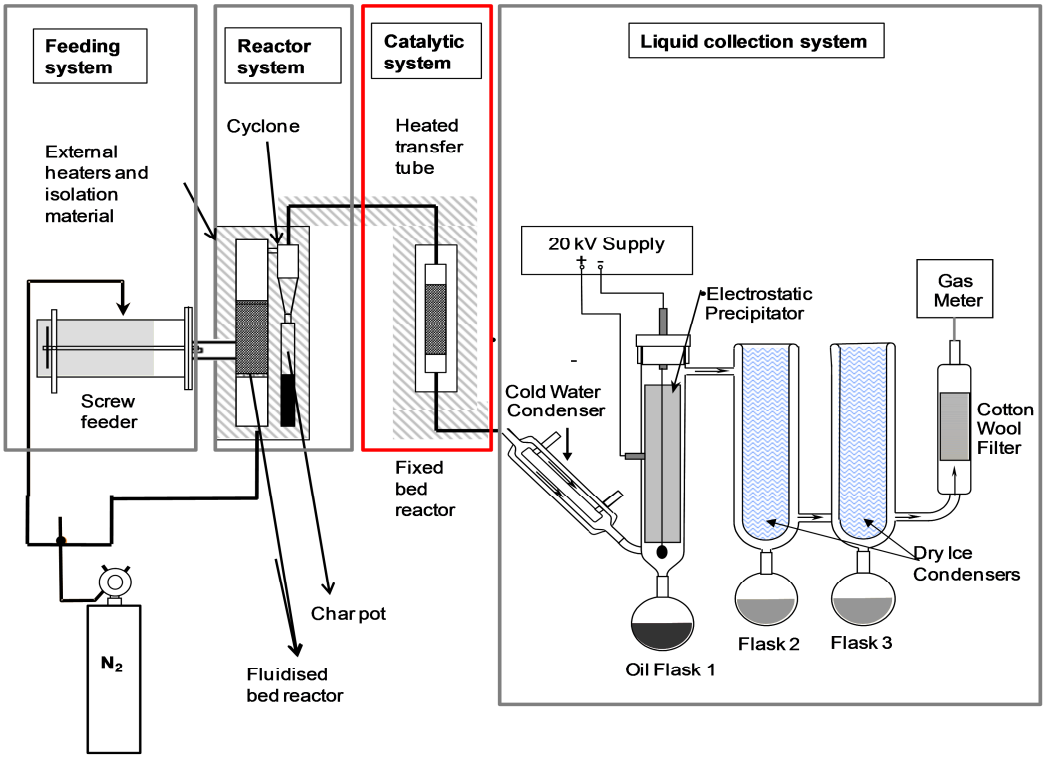

Figure 4-5: 300gh^{-1} fluidised bed reactor with a secondary catalytic fixed bed reactor

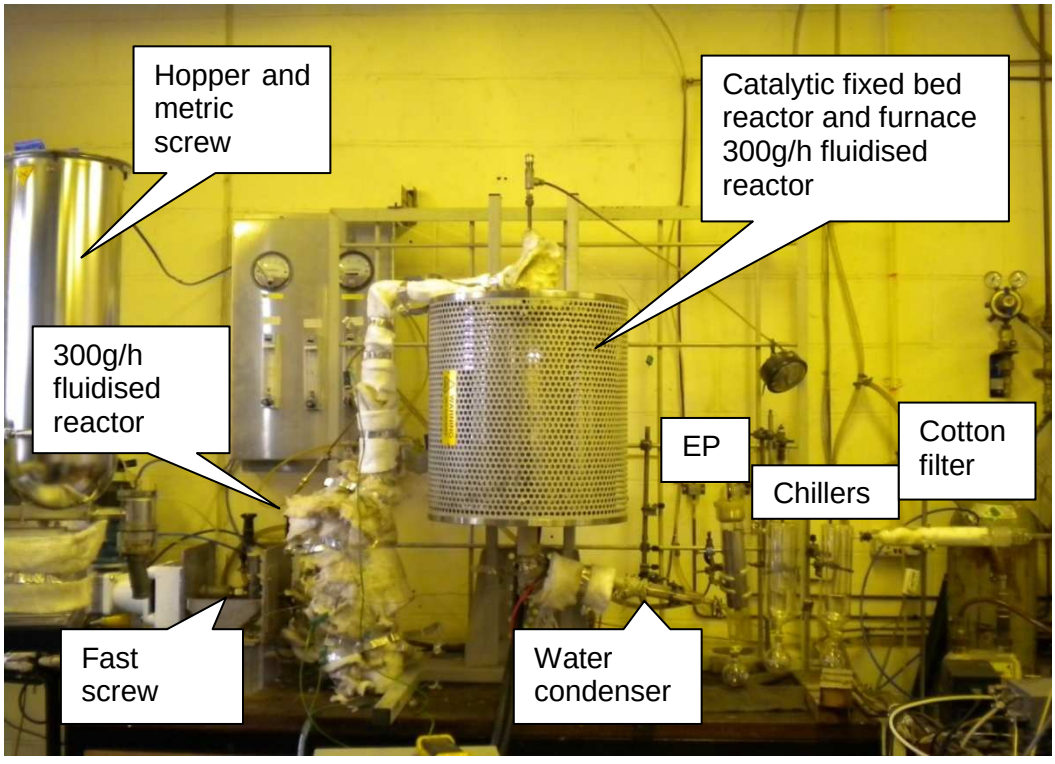

Figure 4-6: Photo of the 300gh^{-1} fluidised bed reactor with a secondary catalytic fixed bed reactor

Summarising, the main apparatus of the fast pyrolysis unit consists of the feeder, the primary fluidised bed reactor, secondary catalytic fixed bed reactor and the liquid

product collection system. The temperature in the catalytic fixed bed reactor is recorded by a K type thermocouple located on the freeboard of the catalytic bed.

4.5.2 Mass balance calculations

Fast pyrolysis of biomass produce a main liquid product and by-products of gas and char. The calculation of the mass balance uses the weight of the biomass feedstock used, while the output is the weight of the pyrolysis products. The mass balance closure is expressed in percentage (on dry biomass basis) for the amount of organic, char and gas produce.

The mass balance closure was calculated by weighing all the unit components of the catalytic system, before and after the run. The mass difference of the feed before and after the experimental run is the input for the mass balance calculations. The primary char can be collected in the main reactor, sand, cyclone, char pot, transition pipes and a small amount in the water condenser and ESP (approximate 0.2wt% from the ESP). The secondary char or coke can be collected in catalytic bed and the glass wool. The feeder, primary reactor, and cyclone are impossible to weight, in comparison with the 100g/h system. The liquids can be collected in the water condenser, the ESP, the two dry ice/acetone condensers and the cotton wool filter. Finally, the total volume of gases is the difference between initial and final gas meter readings.

Table 4-4: Mass balance closure calculations for the 300g/h fluidised bed reactor system coupled with a secondary catalytic fixed bed reactor

Pyrolysis Products	**Mass balance**	**Unit components**	**Measured techniques**
Char	Output	Sand/char pot/transition pipe/fixed bed reactor/glass transition pipe/water condenser/ESP/cotton wool	Mass difference
Coke	Output	Glass wool/catalytic bed	Mass difference
Liquid	Output	Water condenser/ESP/dry ice condensers/cotton wool	Mass difference
Gas	Output	Gas meter	Gas meter and gas chromatography
Biomass fed	Input	Feed	Mass difference

4.6 1 kg/h fluid bed reaction system at Aston

4.6.1 Description of equipment

The 1kg/h fluidised bed reactor is a screw fed reactor with a quench column coupled to an ESP, water cooler and 2 dry ice – acetone coolers. The reactor has capacity of 1000g/h and is constructed of a stainless steel tube of 7.29cm diameter and 42.24cm high. The fluidizing gas is nitrogen whereas sand is used as a fluidising and heat

transfer medium. The flow rate of nitrogen use is sufficient to provide three times the minimum fluidising velocity (MFV) to the bed.

The feeder consists of a tubular storage hopper, a metering screw and fast feed screw. The feed rate of the biomass is controlled by the speed of the metering screw.

The reactor system is composed mainly of the fluidised bed reactor, two cyclone and two char pot for the separation of the char from the pyrolysis gas stream. The fast pyrolysis process takes place in the fluidised bed and then the pyrolysis vapours and char enters the first cyclone. The majority of the char is removed from the vapour stream using the cyclone and collected in the char pot. The pyrolysis vapours with small quantities of char enters the second cyclone and a small amount of char is collected in the second char pot. The pyrolysis vapours exiting the second cyclone pass into the liquid collection system.

The liquid collection system consists of a quench column coupled to an ESP, water cooler 2 dry ice – acetone coolers (chillers), and a cotton wool filter. The pyrolysis vapours passes through the quench column (room temperature) coupled to an ESP which traps the liquid products by condensation and in aerosol form, respectively. The water cooler is at room temperature and the next two condensers are both at -20^{o}C using dry ice in acetone. Finally, the non-condensable gases passes through the cotton wool filter, which is used to protect the gas meter, before venting.

4.6.2 Mass balance calculations

The description of the calculations for the mass balance are similar with the bench scale systems and was described in Section 4.3.2. Table 4-5 shows the mass balance closure calculations for the 1kg/h fluidised bed reactor system.

Table 4-5: Mass balance closure calculations for the 1kg/h fluidised bed reactor system

Pyrolysis Products	**Mass balance**	**Unit components**	**Measured techniques**
Char	Output	Sand/ 1st and 2ndchar pot	Mass difference
Liquid	Output	Bio-oil weight from quench column coupled with ESP/water condenser/dry ice condensers/cotton wool	Mass difference
Gas	Output	Gas meter	Gas meter and gas chromatography
Biomass fed	Input	Feed	Mass difference

4.7 1 kg/h fluidised bed reactor system at ECN

4.7.1 Description of equipment

Pyrolysis experiments were performed in the fluidised bed reactor system (Figure 4-7) with capacity of 1kg/h. The main apparatus of the bubbling fluid bed (BFB) unit consists of the main reactor, soxhlet filter and the knock out pot for the collection of the heavier pyrolysis products. The fluidizing gas is argon whereas sand is the medium. The biomass is fed by a screw feeder in a stream of nitrogen and is delivered to the bed in the lower region of the fluidization zone. A part of the gaseous product is sampled and the char is removed from the gas stream using the soxhlet filter. The gases exiting the soxhlet filter pass to the knock out pot for the collection of the heavier pyrolysis products.

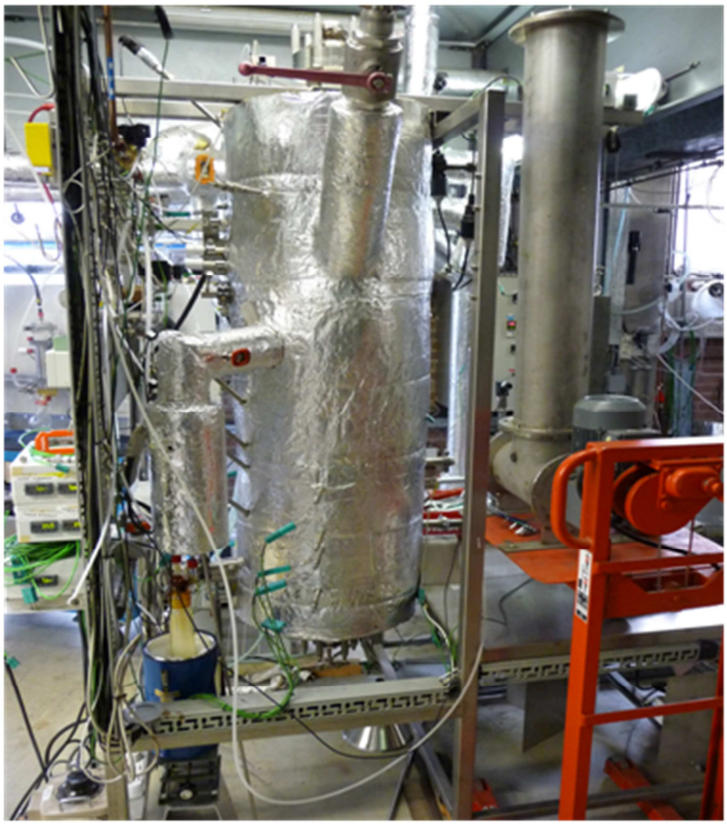

Figure 4-7: Fluidised bed reactor (BFB)

The bubbling fluid bed unit is connected to the PYPO system, and the latter is shown in Figure 4-8. This system consists of an electrostatic precipitator (ESP) and one condenser. The ESP is at room temperature and the condenser is at -20^{o}C using water salt mixture. Finally, the gas passes through the soxhlet filter, which is used to protect the gas meter.

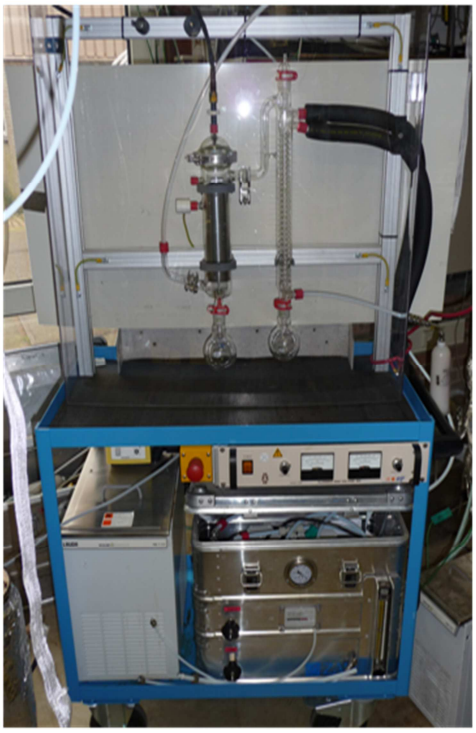

Figure 4-8: PYPO (PYrolysis Products Observation)

4.7.2 Measurements

Detail description of the mass balance calculations can be found in literature by de Wild [94].

4.8 Pyrolysis products analysis

4.8.1 Bio-oil

4.8.1.1 Water

The water content of bio-oil is determined by using a Metrohm 758 KFD Titrino applying a technique known as Karl Fisher (KF) titrometry. Three liquid samples from each pyrolysis experiment were subjected to water content analysis. These included the liquid of pot 1 (main bio-oil) and a liquid mixture of pot 2 and pot 3 (light ends). Each sample was tested in triplicate. In the case of the liquid products of the 1kg/h system, the analysis included the liquid of pot 1 (main bio-oil), the liquid of pot 2 and a liquid mixture of pot 3 and Pot 4 (light ends).

4.8.1.2 Elemental

The elemental analysis was done by MEDAC Ltd., Surrey, UK. The liquid obtained from pot 1 were subjected to carbon, hydrogen and nitrogen (CHN) analysis using CE-440 and Carlo Erba elemental analysers with ±0.3% absolute accuracy. To calculate the elemental analysis of the bio-oil on dry basis it was necessary to deduct the

hydrogen and oxygen weight of water. The oxygen content of bio-oil was calculated by difference of the dry basis carbon, hydrogen and nitrogen.

4.8.1.3 Heating values

The higher heating value (HHV) of the bio-oil is calculated based on Equation 4-1 developed by Channiwala et al. [95].

Equation 4-1:
HHV_{dry} (MJ/kg)= 0.3491*C+1.1783*H+0.1005*S-0.1034*O-0.015N-0.0211A
Where C, H, S, O, N and A represent mass percentages on dry basis of carbon, hydrogen, sulphur, oxygen, nitrogen and ash contents of bio-oil, respectively.

The ash content was not taken into consideration because it is close to zero. The char fines in bio-oil for wood derived oil is in the range of 0.2 to 1wt% [38], whereas for rice straw is 0.1-3wt% [96]. An estimation of the ash content in bio-oil can be done by assuming that the solids present in bio-oil contains 5 wt% of ash [97]. This results, in a really low value for the ash content, which is not going to significantly affect the result of the Equation 4-1.

The higher heating value wet (HHV_{wet}) of the bio-oil is calculated based on Equation 4-1 [98].
Equation 4-2: $HHV_{wet} = HHV_{dry} * (1-H_2O/100)$

The low heating value on dry basis is calculated from Equation 4-3 [98].
Equation 4-3: LHV_{dry}(MJ/kg)= HHV_{dry} – 2.442*8.936*H/100

The low heating value on wet basis is calculated from Equation 4-4 [98].
Equation 4-4: LHV_{wet} (MJ/kg)= LHV_{dry}*(1-H_2O/100)-2.442*H_2O/100

4.8.1.4 pH

The instrument for pH analysis is a Metrohm 713 pH meter, which is used at room temperature. The equipment is calibrated with liquid calibration standards of pH 4, 7 and 9. The pyrolysis liquid products collected from pot 1 and a liquid mixture of Pot 2 and Pot 3 oils were conducted to pH determination.

4.8.1.5 Molecular weight

Molecular weight distribution of pyrolysis liquids was determined using gel permeation chromatography (GPC) technique. The instrument used was an integrated GPC

system, PL-GPC50 from Polymer Laboratories, UK, equipped with a PLgel 3 µm MIXED-E column, 300×7.5 mm, and a refractive index (RI) detector. The Cirrus 3.0 software was used to calculate the molecular weight of the sample using an area based calculation.

The solvent used to dissolve the bio-oil samples was a HPLC-grade THF (tetrahydrofuran) at a concentration of approximate 0.01 g/ml.

4.8.1.6 Chemical analysis

The identification of the compounds present in bio-oils was done by a gas chromatography/mass spectrometry (GC/MS). Due to equipment break-down, it was necessary to use two different equipment. The majority of the characterisation experiments with raw and pre-treated feedstocks were carried out by a Perkin Elmer Autosystem XL Gas Chromatograph and a TurboMass Gold Mass Spectrometer. The catalytic experiments, as well as the characterisation of aquathermolised wheat straw and steamed poplar used another GC/MS equipment. The characterization of feedstocks with catalysts was done using a Varian 450 - Gas Chromatograph and a Varian 220 - Mass Spectometer. Further details can be found in Section 4.2. The samples were dissolved in a solvent (ethanol) at a concentration of approximately 25wt% organics.

4.8.2 Non-condensable gases

The non-condensable gases are connected during the fast pyrolysis experiments on-line, with a CP-4900 micro gas chromatograph with a thermal conductivity detector (TCD) from Varian Chromatography System Inc. This on-line configuration enables the sampling of the gases every three minutes. The software used for the analysis was a Star Chromatography Workstation 6.0. The equipment has two different columns for the separation of gases by their boiling points. A molecular-sieve coated capillary column (CP-Molsieve 5A) is used for the separation of hydrogen (H_2), oxygen (O_2), nitrogen (N_2), methane (CH_4) and carbon monoxide (CO) from the gas stream. The second column is a CP-PoraPLOT column and is used to separate nitrogen (N_2), methane (CH_4), carbon dioxide (CO_2), ethylene (C_2H_4), ethane (C_2H_6), propylene (C_3H_6) and propane (C_3H_8) from the non-condensable gas stream. The equipment is calibrated using standard gas mixtures.

5 CHARACTERIZATION OF BIOMASS FEEDSTOCKS

Analytical characterisation of a variety of raw and pre-treated biomass was conducted in this chapter using a thermogravimetric analyser (TGA) and pyrolysis-gas chromatography/mass spectrometry (Py-GC/MS). Proximate, ultimate and heating value analyses were also carried out on the samples.

5.1 Biomass feedstocks

The types of biomass selected by the Consortium included agricultural wastes as wheat straw, softwood as spruce, hardwood as poplar, pre-treated wood as torrefied spruce, torrefied poplar, steamed poplar, pre-treated agricultural wastes as aquathermolised wheat straw and bio-ethanol refinery residues as DDGS.

Each sample was ground and sieved. The particle size of the feedstocks used for analytical characterisation (TGA and Py-GC/MS experiments) was 0.355-0.500mm. The latter particle biomass size range was chosen because it was used for the laboratory pyrolysis experiments.

5.2 Pre-treatment methods

The pretreatment processes that have been applied to the feedstocks were torrefaction, steam treatment and aquathermolysis. This study examines the influence of these various pre-treatment methods on pyrolysis vapour quality. Torrefaction, steam pre-treatment and aquathermolysis were applied by de Wild at ECN [6, 43, 94] to poplar, spruce wood and wheat straw to investigate the effect of the pre-treatment process on pyrolysis liquids. Table 5-1 shows the pre-treatment process that was applied to each untreated biomass.

Table 5-1: Pre-treatment process applied to each untreated biomass

Untreated biomass	**Pre-treatment process**	
Poplar	Torrefaction	Steam
Spruce	Torrefaction	
Wheat straw	Aquathermolysis	

5.3 Experimental methodology

All of the feedstocks were characterised by a range of standard methods as described below.

5.3.1 Ultimate Analysis

The ultimate analysis was carried out by an external company (MEDAC Ltd., Surrey, UK) using a Carlo-Erba 1108 elemental analyser EA1108 in order to determine the basic elemental composition of the biomass samples. The analysis were on duplicates of each dry sample. The oxygen content was calculated by difference.

5.3.2 Calorific value calculations

The higher heating values (HHV) of the feedstocks were calculated based on Equation 4-1 developed by Channiwala et al.[95].

Equation 4-1:

HHVdry (MJ/kg)= 0.3491*C+1.1783*H+0.1005*S-0.1034*O-0.015N-0.0211A

Where C, H, S, O, N and A represent mass percentages on dry basis of carbon, hydrogen, sulphur, oxygen, nitrogen and ash contents of biomass, respectively.

The low heating value on dry basis is calculated from Equation 4-3 [98].

LHV_{dry}(MJ/kg)= HHV_{dry} – 2.442*8.936*H/100

Where H represent mass percentages on dry basis of hydrogen content of biomass.

5.3.3 Thermogravimetric Analysis (TGA)

The description of the TGA equipment, as well as the methodology used, was discussed in Chapter4. Micro-scale pyrolysis experiments were conducted in duplicates using the TGA to investigate the decomposition behaviour of the samples. The number of repeats was sufficient to obtain a representative result.

Weight loss (TG) and differential weight loss (DTG) graphs were produced for each sample. TG graph illustrates the percentage of weight loss as a temperature function, while DTG graph shows the rate of weight loss as a temperature function.

5.3.4 Pyroprobe-GC/MS

The characterisation of raw and pre-treated feedstocks was conducted by a Pyroprobe coupled with a Gas Chromatograph and a Mass Spectrometer. Each experiment was conducted in triplicates to achieve a representative result. Due to equipment break-down, it was necessary to use two different equipment.

Analytical pyrolysis of the feedstocks was done using a Perkin Elmer Pyris 1 TG analyser and a Pyroprobe CDS AS-2500 Pyrolysis Auto Sampler coupled with a Perkin

Elmer Autosystem XL Gas Chromatograph and a TurboMass Gold Mass Spectometer. The characterisation of aquathermolised wheat straw and steamed poplar was carried out by a Pyroprobe 5000 Series coupled with a Varian 450 - Gas Chromatograph and a Varian 220 - Mass Spectometer. Further details concerning the equipment can be found in Section 4.2.

The comparison of the results from the different equipment should be used only as an indicator. The different GC column could cause a diverse separation of the chemicals in the column. The molar mass (m/z) was set differently for each equipment, resulting in a limitation of chemicals.

5.3.5 Proximate Analysis (moisture, combustible matter and ash)

The proximate analysis was performed according to the ASTM standard test methods for measuring moisture, combustible matter and ash contents, which are ASTM E1756-01, E872-82 and E1755-01, respectively. The tests were carried out in triplicate as follows: weight of crucible; approximate 2 g of feedstock was placed in the crucible; placement of crucible in a muffle oven at 105^{o}C at air; weight the dry sample and crucible after six hours; the difference in weight is due the evaporation of the biomass moisture.

The ash content was determined by placing the crucible with the dry sample into the muffle oven for 5 hours at 575^{o}C at air. The weight of the sample after 5 hours was the ash weight. The combustible matter content was calculated by difference.

5.4 Results and discussion

5.4.1 Analysis of untreated and pre-treated feedstocks

The mean values of ultimate, proximate and heating value of the feedstocks are presented in Table 5-2 below. The ash content of DDGS and wheat straw, which can be seen in the proximate analysis, is significantly higher than the woods. This could imply higher level of inorganic compounds, resulting that the process of fast pyrolysis for those feedstocks could be subjected to stronger catalytic effect. Furthermore, the ash content of torrefied wood is nearly twice the ash content of untreated wood. This was not expected, since it is known that after the process of pre-treatment the residue left (torrefied poplar and spruce) was around 60 -70wt% of the untreated biomass. This is an error due the biomass particle distribution and it is possible that a smaller particle size could provide a more homogeneous sample [99]. Pre-treatment of poplar and spruce by steam and hot pressurised water (aquathermolysis) reduced the char content, in comparison with the untreated feedstocks.

Table 5-2: Analysis of untreated and pre-treated biomass

Feedstocks	Poplar	Tor' poplar	Steamed poplar	Spruce	Tor' spruce	Wheat straw	Aqua' wheat straw	DDGS
Ultimate analysis (wt%, dry basis)								
C	47.35	56.08	51.36	47.24	55.34	43.80	47.47	46.20
H	6.06	6.41	5.93	6.19	6.42	5.40	5.66	6.00
N	N.D.	0.10	0.10	<0.05	0.1	0.20	0.1	3.80
O (by difference)	46.59	37.41	42.62	46.52	38.14	50.60	46.77	44.00
Proximate analysis (wt%, dry basis)								
Ash	1.16	2.00	0.30	0.22	0.46	8.80	5.4	6.65
Combustible matter	98.94	98.00	99.70	99.78	99.54	91.20	94.6	92.35
Moisture (as received)	8.61	3.45	3.60	6.96	2.94	8.74	4.2	10.01
Heating value (MJ kg-1, dry basis)								
HHVdry	18.83	23.43	20.50	18.97	22.98	16.23	18.29	18.45
LHVdry	17.51	22.03	19.21	17.62	21.58	15.05	17.05	17.09

In the case of pre-treated feedstocks, the high and low heating values were increased. This was apparent for all pre-treated feedstocks, in comparison with the untreated. This was expected, since pre-treatment removed hemicellulose, resulting in an increase on char proportion.

5.4.2 Study of pre-treated biomass

An objective of this study was the comparison of different feedstocks and pre-treated feedstocks. The selection of the thermogravimetric method is suitable to accomplish the objective since different biomass types have different physical and chemical characteristics and consequently different thermal degradation mechanisms. TGA can record those thermal degradation mechanisms.

5.4.2.1 Torrefaction

Figure 5-2 illustrates the TGA and DTG profiles of fresh and torrefied wood. It can be observed that maximum rate of weight loss was higher on torrefied samples than fresh samples, particularly for spruce. This is probably due to the higher proportion of cellulose and the absence of hemicellulose that normally has a structure-stabilising role. The temperature of maximum rate of weight loss (peak temperature) was lower on torrefied spruce (399^{o}C) and torrefied poplar (382^{o}C) than fresh spruce (402^{o}C) and fresh poplar (384^{o}C). A low peak temperature is desirable due to less energy required for optimum weight loss, though the temperature difference between fresh and pre-treated samples was small. Also, according to the DTG profiles, torrefaction yields a reduction in hemicellulose. Torrefaction has broken down hemicellulose, hence the

hemicellulose peak cannot be seen on the DTG profile in the case of pre-treated woods. Moreover, this had resulted in a higher proportion of cellulose in the sample. Both fresh spruce and poplar had a peak between 300-350^{o}C, which was absent in their torrefied version, indicating the hemicellulose loss and possibly limited devolatilisation and carbonisation of lignin. Additionally, the volatile content of both fresh samples was higher than the torrefied samples. This result was expected, since it is known that during pre-treatment process (torrefaction) volatile matter was reduced.

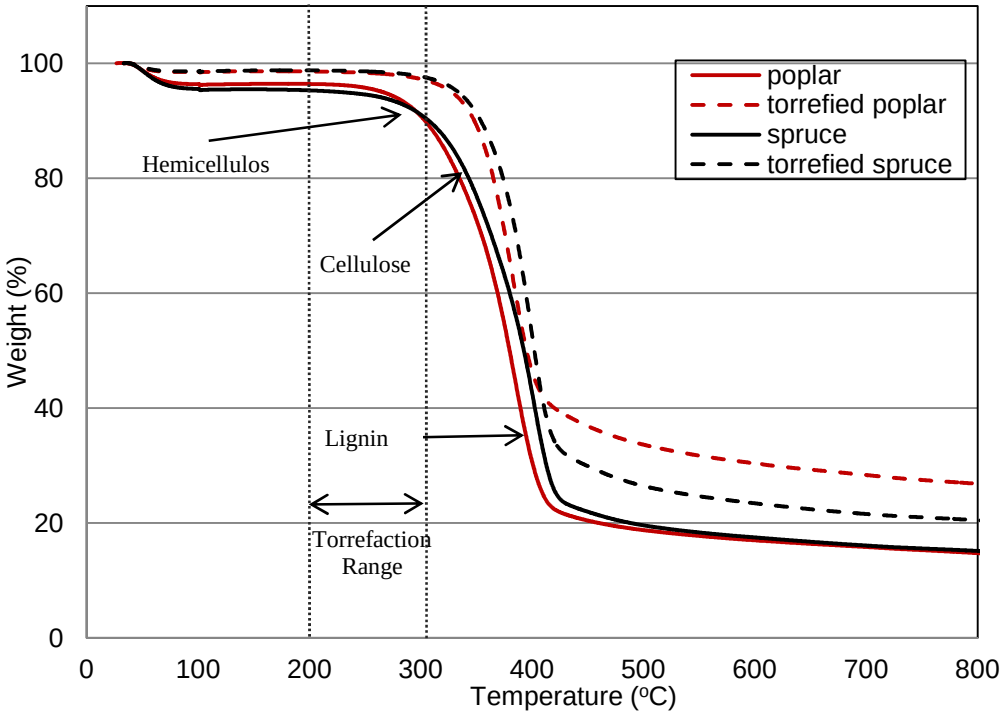

Figure 5-1: TG profile for spruce, poplar and their torrefied version

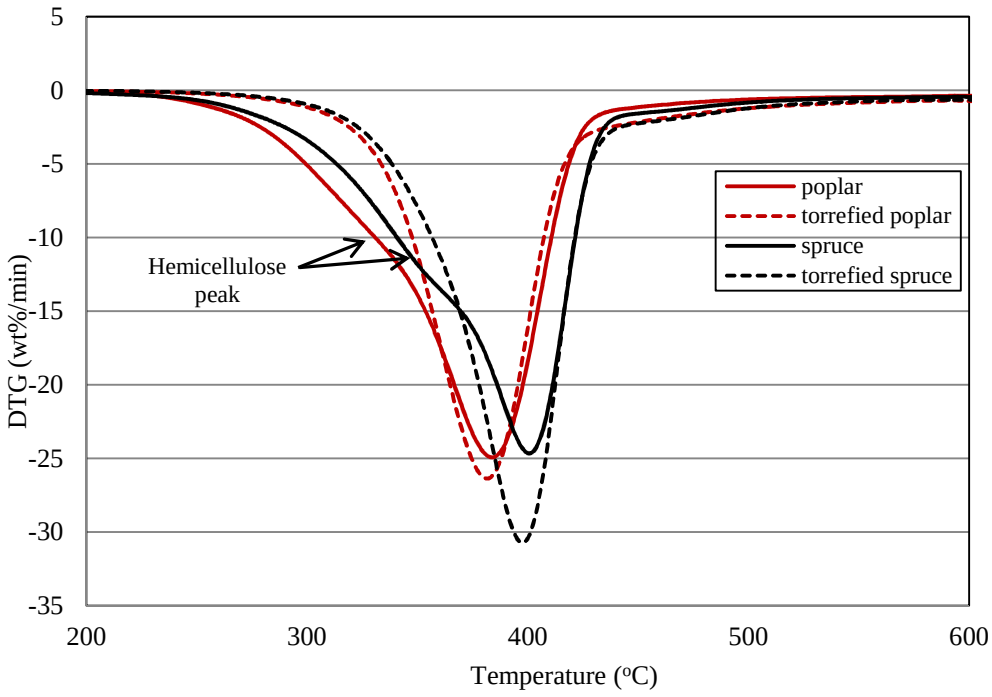

Figure 5-2: DTG profiles for spruce, poplar and their torrefied version

Regarding the screening of the fresh and torrefied woods by Py-GC/MS, only the larger chromatographic peak areas were identified and are shown below in Figure 5-3 to Figure 5-6 and Table 5-3 to Table 5-6. A comparison between fresh samples and torrefied samples revealed some interesting outcomes. Firstly, torrefied samples showed an increase in cellulose derived compounds. Secondly, torrefaction has resulted in a reduction in hemicellulose and from Py-GC-MS an increased in phenolic compounds can be seen, particularly in the case of compounds 7, 8, 9, 10, and 12 shown in Table 5-7. An explanation might be that pre-treatment had caused pre-decomposition of the material prior to Py-GC-MS analysis. As it was mentioned above the decomposition of hemicellulose and limited decomposition of lignin have been occurred during torrefaction. Thirdly, light volatile reduction (acetic acid, compound 9 and 10 for torrefied spruce and poplar, respectively) is seen in the chromatograms for torrefied wood (see Figure 5-4 for key) and this was possible due the torrefaction process temperature (270-300^{o}C).

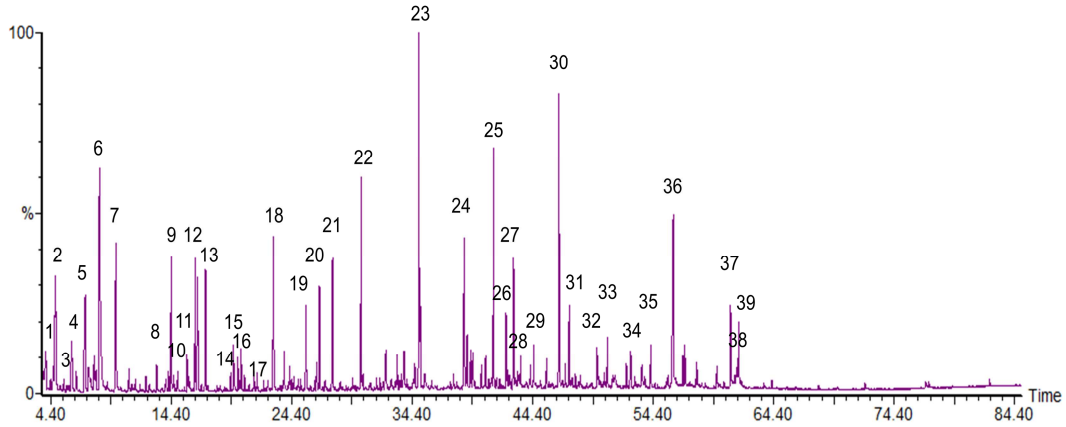

Figure 5-3. Chromatogram obtained by Py-GC-MS and chemical identification, spruce. See Table 5-3 for key.

Table 5-3. Identification of chemicals from spruce by Py-GC/MS

1: Acetaldehyde/Acetic aldehyde/Ethanal;
2: Methylglyoxal/2-oxopropanal/pyruvaldehyde;
3: 2-methyl-furan/alpha-Methylfuran; 5-Methylfuran;
4: 2.3 Butanedione/Butanedione/Diacetyl;
5: Hydroxyacetaldehyde/Glycolaldehyde;
6: Acetic acid/Ethanoic acid;
7: Hydroxypropanone/1-Hydroxy-2-propanone/Acetone alcohol;
8: Propenoic acid/Propionic acid/Ethanecarboxylic acid;
9: 3-Hydroxypropanal;
10: 2(3H)-Furanone;
11: 3(2H)-Furanone;
12: Butanedial/Succinaldehyde;
13: Furfural/furan-2-carboxaldehyde/fural/furfuraldehyde/2-furaldehyde/pyromucic aldehyde;
14: 5-Methyl-2(3H)-furanone/a-Angelica lactone/2.3-Dihydro-5-methyl-2-furanone
15: 2-Furanmethanol/2-Furfuryl alcohol;
16: 2-Ethyl-butanal;
17: Methoxy-dihydrofuran ;
18:2.3-Dihydro-5-methylfuran-2-one;
19: (5H)-furan-2-one;
20: 4-Hydroxy-5.6-dihydro-(2H)-pyran-2-one
21: 2-Hydroxy-1-methyl-1-cyclopentene-3-one/Maple lactone & 2.5-Dimethylcyclopentanone
22: 2-Methoxyphenol/Guaiacol/Guaicol;
23: 2-Methoxy-4-methyl phenol/Creosol/p-Methylguaiacol/4-Methylguaiacol;
24: 4-Ethyl-2-methoxyphenol/4-Ethyl guaiacol/4-Hydroxy-3-methoxy ethylbenzene/p-Ethylguaiacol;
25: 2-Methoxy-4-vinylphenol/4-Vinylguaiacol/p-Vinylguaiacol/4-Hydroxy-3-methoxystyrene;
26: Eugenol/2-Methoxy-4-allylphenol/2-Methoxy-1-hydroxy-4-allybenzene/Allylguaiacol;
27: 5-(Hydroxymethyl)-2-Furancarboxaldehyde/5-(Hydroxymethyl)-2-furfural/HMF/5-(Hydroxymethyl)-2-furaldehyde;
28: 2,6-Dimethoxy phenol/Syringol/1,3-Dimethoxy-2-hydroxybenzene/Pyrogallol dimethylether;
29,30: 2-Methoxy-4-(1-propenyl)phenol/Isoeugenol,c&t/4-Propenylguaiacol/4-Hydroxy-3-methoxypropenylbenzene;
31: Vanillin/2-Methoxy-4-formylphenol/4-Hydroxy-3-methoxybenzaldehyde;
32: Homovanillin;
33:1-(4-Hydroxy-3-methoxyphenyl)ethanone/Acetoguaiacone;
34: 1-(4-hydroxy-3-methoxyphenyl)-2-Propanone/Guaiacylacetone/Vanillyl methyl ketone/4-Hydroxy-3-methoxyphenyl acetone;
35: Coniferyl alcohol (cis)
36: 1,6-Anhydro-b-D-glucopyranose/Levoglucosan;
37: 4-((1E)-3-Hydroxy-1-propenyl)-2-methoxyphenol/Coniferol/Coniferyl alcohol;
38: 1.6-Anhydro-b-D-glucofuranose;
39: Coniferaldehyde

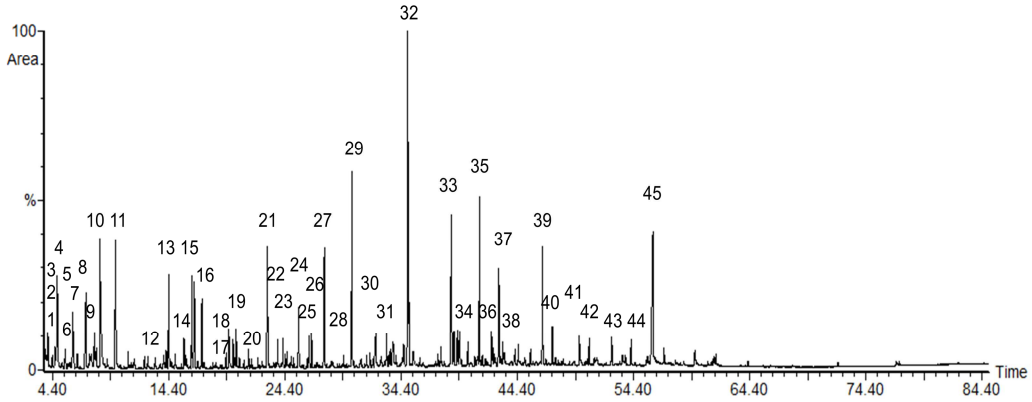

Figure 5-4.Chromatogram obtained by Py-GC-MS and chemical identification, torrefied spruce. See Table 5-4 for key.

Table 5-4. Identification of chemicals from torrefied spruce by Py-GC/MS

1: Acetaldehyde/Acetic aldehyde/Ethanal;
2:Furan/Furfuran/Furane/Oxacyclopentadiene;
3:2-Propenal/Acrylic aldehyde/Aqualin/2-Propen-1-one;
4: Methylglyoxal/2-oxopropanal/pyruvaldehyde;
5: 2-methyl-furan/alpha-Methylfuran; 5-Methylfuran;
6: 2.3 Butanedione/Butanedione/Diacetyl;
7: Hydroxyacetaldehyde/Glycolaldehyde;
8:2-Butenal/Crotonaldehyde/Crotonal;
9: Acetic acid/Ethanoic acid;
10: Hydroxypropanone/1-Hydroxy-2-propanone/Acetone alcohol;
11: Propenoic acid/Propionic acid/Ethanecarboxylic acid;
12: 3-Hydroxypropanal;
13: 2(3H)-Furanone;
14: 3(2H)-Furanone;
15: Butanedial/Succinaldehyde;
16: Furfural/furan-2-carboxaldehyde/fural/furfuraldehyde/2-furaldehyde/pyromucic aldehyde;
17: 5-Methyl-2(3H)-furanone/a-Angelica lactone/2.3-Dihydro-5-methyl-2-furanone
18: 2-Furanmethanol/2-Furfuryl alcohol;
19: 2-Ethyl-butanal;
20: Methoxy-dihydrofuran ;
21:2.3-Dihydro-5-methylfuran-2-one;
22: Dihydro-methyl-furanone;
23:5-Methyl-2-furancarboxaldehyde/5-Methylfurfural/2-Formyl-5-methylfuran/2-Methyl-5-formylfuran;
24: (5H)-furan-2-one;

25: 4-Hydroxy-5.6-dihydro-(2H)-pyran-2-one;
26:5-Methyl-2(5H)-furanone/b-angelica lactone;
27:2-Hydroxy-1-methyl-1-cyclopentene-3-one/Maple lactone & 2.5-Dimethylcyclopentanone;
28: Phenol;
29: 2-Methoxyphenol/Guaiacol/Guaicol;
30:methyl-butyraldehyde derivate;
31:4-Methyl-5H-furan-2-one/4-Methyl-2(5H)-furanone;
32: 2-Methoxy-4-methyl phenol/Creosol/p-Methylguaiacol/4-Methylguaiacol;
33: 4-Ethyl-2-methoxyphenol/4-Ethyl guaiacol/4-Hydroxy-3-methoxy ethylbenzene/p-Ethylguaiacol;
34:1.4:3.6-Dianhydro-a-d-glucopyranose;
35: 2-Methoxy-4-vinylphenol/4-Vinylguaiacol/p-Vinylguaiacol/4-Hydroxy-3-methoxystyrene;
36: Eugenol/2-Methoxy-4-allylphenol/2-Methoxy-1-hydroxy-4-allybenzene/Allylguaiacol;
37: 5-(Hydroxymethyl)-2-Furancarboxaldehyde/5-(Hydroxymethyl)-2-furfural/HMF/5-(Hydroxymethyl)-2-furaldehyde;
38: Catechol;
39: 2-Methoxy-4-(1-propenyl)phenol/Isoeugenol,c&t/4-Propenylguaiacol/4-Hydroxy-3-methoxypropenylbenzene;
40: Vanillin/2-Methoxy-4-formylphenol/4-Hydroxy-3-methoxybenzaldehyde;
41: Homovanillin;
42:1-(4-Hydroxy-3-methoxyphenyl)ethanone/Acetoguaiacone;
43: 1-(4-hydroxy-3-methoxyphenyl)-2-Propanone/Guaiacylacetone/Vanillyl methyl ketone/4-Hydroxy-3-methoxyphenyl acetone;
44: Coniferyl alcohol (cis)
45: 1,6-Anhydro-b-D glucopyranose/Levoglucosan;

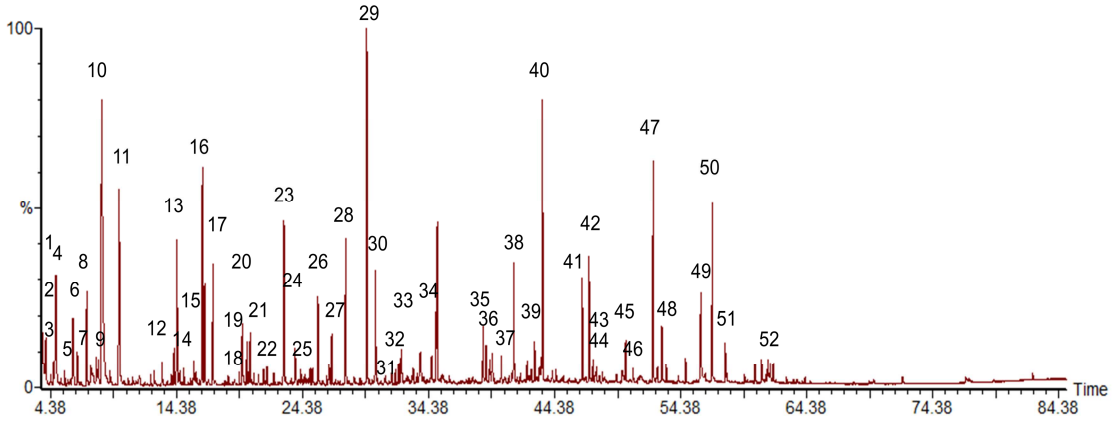

Figure 5-5. Chromatogram obtained by Py-GC-MS and chemical identification, poplar. See Table 5-5 for key.

Table 5-5. Identification of chemicals from poplar by Py-GC/MS

1: Acetaldehyde/Acetic aldehyde/Ethanal;
2:Furan/Furfuran/Furane/Oxacyclopentadiene;
3:2-Propenal/Acrylic aldehyde/Aqualin/2-Propen-1-one;
4: Methylglyoxal/2-oxopropanal/pyruvaldehyde;
5: 2-methyl-furan/alpha-Methylfuran; 5-Methylfuran;
6: 2.3 Butanedione/Butanedione/Diacetyl;
7:3-Pentanone/Pentan-3-one/Diethyl ketone (DEK);
8:Hydroxyacetaldehyde/Glycolaldehyde;
9:2-Butenal/Crotonaldehyde/Crotonal
10: Acetic acid/Ethanoic acid;
11: Hydroxypropanone/1-Hydroxy-2-propanone/Acetone alcohol;
12: Propenoic acid/Propionic acid/Ethanecarboxylic acid;
13: 3-Hydroxypropanal;
14: 2(3H)-Furanone;
15: 3(2H)-Furanone;
16: Butanedial/Succinaldehyde;
17: Furfural/furan-2-carboxaldehyde/fural/furfuraldehyde/2-furaldehyde/pyromucic aldehyde;
18: 5-Methyl-2(3H)-furanone/a-Angelica lactone/2.3-Dihydro-5-methyl-2-furanone
19: 2-Furanmethanol/2-Furfuryl alcohol;
20:1-Acetyloxy-2-propanone/1-Acetoxypropane-2-one/2-Oxopropyl acetate;
21: 2-Ethyl-butanal;
22:4-Cyclopentene-1.4-dione;
23:2.3-Dihydro-5-methylfuran-2-one;
24: Dihydro-methyl-furanone;
25:5-Methyl-2-furancarboxaldehyde/5-Methylfurfural/2-Formyl-5-methylfuran/2-Methyl-5-formylfuran;
26: (5H)-furan-2-one;
27: 4-Hydroxy-5.6-dihydro-(2H)-pyran-2-one;
28:2-Hydroxy-1-methyl-1-cyclopentene-3-one/Maple lactone & 2.5-Dimethylcyclopentanone;
29: Phenol;
30: 2-Methoxyphenol/Guaiacol/Guaicol;
31: Methyl 2-furoate/2-Furancarboxylic acid, methyl ester;
32:o-cresol/2-Methyl phenol;
33:methyl-butyraldehyde derivate;
34: 2-Methoxy-4-methyl phenol/Creosol/p-Methylguaiacol/4-Methylguaiacol;
35: 4-Ethyl-2-methoxyphenol/4-Ethyl guaiacol/4-Hydroxy-3-methoxy ethylbenzene/p-Ethylguaiacol;
36:4-Hydroxy-3-methyl-(5H)-furanone;
37:1.4:3.6-Dianhydro-a-d-glucopyranose;
38: 2-Methoxy-4-vinylphenol/4-Vinylguaiacol/p-Vinylguaiacol/4-Hydroxy-3-methoxystyrene;
39: 5-(Hydroxymethyl)-2-Furancarboxaldehyde/5-(Hydroxymethyl)-2-furfural/HMF/5-(Hydroxymethyl)-2-furaldehyde;
40:2,6-Dimethoxy phenol/Syringol/1,3-Dimethoxy-2-hydroxybenzene/Pyrogallol dimethylether;
41: 2-Methoxy-4-(1-propenyl)phenol/Isoeugenol,c&t/4-Propenylguaiacol/4-Hydroxy-3-methoxypropenylbenzene;
42: 4-Methyl syringol/2,6-Dimethoxy-4-methylphenol;
43: Vanillin/2-Methoxy-4-formylphenol/4-Hydroxy-3-methoxybenzaldehyde;
44: Hydroquinone/1.4-Benzenediol/4-Hydroxyphenol/Dihydroxybenzene;
45:4-ethyl-Syringol;
46:1-(4-Hydroxy-3-methoxyphenyl)ethanone/Acetoguaiacone;

47:4-Vinyl-2.6-dimethoxyphenol/Syringol-4-vinyl;
48:2.6-Dimethoxy-4-(2-propenyl)-Phenol;
49: 1,6-Anhydro-b-D-glucopyranose/Levoglucosan;
50:trans-4-Propenyl-2.6-dimethoxyphenol/Methoxyeugenol;
51:4-Hydroxy-3.5-dimethoxybenzaldehyde/Syringaldehyde/Syringe aldehyde/Cedar aldehyde;
52:1-(4-Hydroxy-3-dimethoxyphenyl)ethanone/Acetosyringone/3.5-dimethoxy-1-hydroxyacetophenone/Acetosyringon;

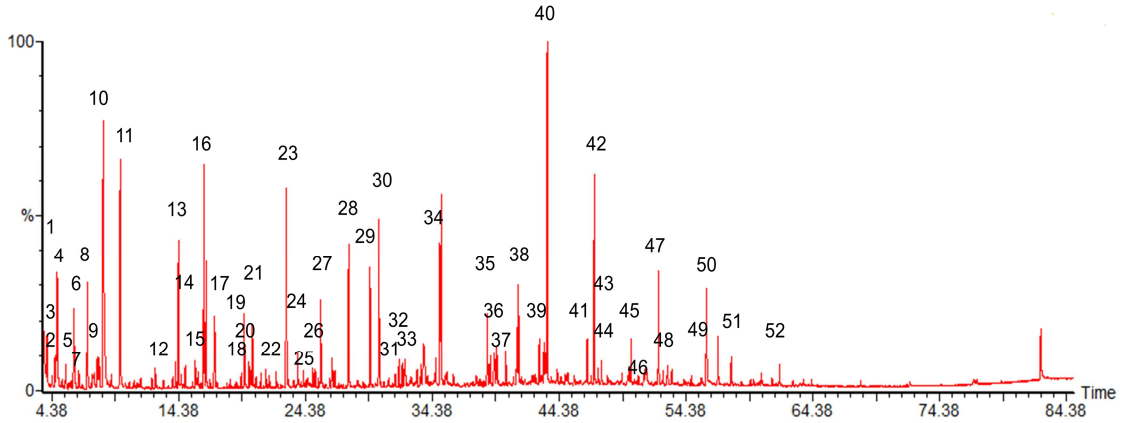

Figure 5-6.Chromatogram obtained by Py-GC-MS and chemical identification, torrefied poplar. See Table 5-6 for key.

Table 5-6. Identification of chemicals from torrefied poplar by Py-GC/MS

1: Acetaldehyde/Acetic aldehyde/Ethanal;
2:Furan/Furfuran/Furane/Oxacyclopentadiene;
3:2-Propenal/Acrylic aldehyde/Aqualin/2-Propen-1-one;
4: Methylglyoxal/2-oxopropanal/pyruvaldehyde;
5: 2-methyl-furan/alpha-Methylfuran; 5-Methylfuran;
6: 2.3 Butanedione/Butanedione/Diacetyl;
7:3-Pentanone/Pentan-3-one/Diethyl ketone (DEK);
8:Hydroxyacetaldehyde/Glycolaldehyde;
9:2-Butenal/Crotonaldehyde/Crotonal
10: Acetic acid/Ethanoic acid;
11: Hydroxypropanone/1-Hydroxy-2-propanone/Acetone alcohol;
12: Propenoic acid/Propionic acid/Ethanecarboxylic acid;
13: 3-Hydroxypropanal;
14: 2(3H)-Furanone;
15: 3(2H)-Furanone;
16: Butanedial/Succinaldehyde;
17: Furfural/furan-2-carboxaldehyde/fural/furfuraldehyde/2-furaldehyde/pyromucic aldehyde;
18: 5-Methyl-2(3H)-furanone/a-Angelica lactone/2.3-Dihydro-5-methyl-2-furanone
19: 2-Furanmethanol/2-Furfuryl alcohol;
20:1-Acetyloxy-2-propanone/1-Acetoxypropane-2-one/2-Oxopropyl acetate;
21: 2-Ethyl-butanal;
22:4-Cyclopentene-1.4-dione;
23:2.3-Dihydro-5-methylfuran-2-one;
24: Dihydro-methyl-furanone;
25:3-Methyl-2-cyclo-penten-1-one**;**
26:5-Methyl-2-furancarboxaldehyde/5-Methylfurfural/2-Formyl-5-methylfuran/2-Methyl-5-formylfuran;
27: (5H)-furan-2-one;
28:2-Hydroxy-1-methyl-1-cyclopentene-3-one/Maple lactone & 2.5-Dimethylcyclopentanone;
29: Phenol;
30: 2-Methoxyphenol/Guaiacol/Guaicol;
31: Methyl 2-furoate/2-Furancarboxylic acid, methyl ester;
32:o-cresol/2-Methyl phenol;
33:methyl-butyraldehyde derivate;
34: 2-Methoxy-4-methyl phenol/Creosol/p-Methylguaiacol/4-Methylguaiacol;
35: 4-Ethyl-2-methoxyphenol/ 4-Ethyl guaiacol/4-Hydroxy-3-methoxy ethylbenzene/p-Ethylguaiacol;
36:4-Hydroxy-3-methyl-(5H)-furanone;
37:1.4:3.6-Dianhydro-a-d-glucopyranose;
38: 2-Methoxy-4-vinylphenol/4-Vinylguaiacol/p-Vinylguaiacol/ 4-Hydroxy-3-methoxystyrene;
39: 5-(Hydroxymethyl)-2-Furancarboxaldehyde/5-(Hydroxymethyl)-2-furfural/HMF/ 5-(Hydroxymethyl)-2-furaldehyde;
40:2.6-Dimethoxy phenol/Syringol/1,3-Dimethoxy-2-hydroxybenzene/Pyrogallol dimethylether;

41: 2-Methoxy-4-(1-propenyl)phenol/Isoeugenol,c&t/4-Propenylguaiacol/4-Hydroxy-3-methoxypropenylbenzene;
42: 4-Methyl syringol/2,6-Dimethoxy-4-methylphenol;
43: Vanillin/2-Methoxy-4-formylphenol/4-Hydroxy-3-methoxybenzaldehyde;
44: Hydroquinone/1.4-Benzenediol/4-Hydroxyphenol/Dihydroxybenzene;
45:4-ethyl-Syringol;
46:1-(4-Hydroxy-3-methoxyphenyl)ethanone/Acetoguaiacone;
47:4-Vinyl-2.6-dimethoxyphenol/Syringol-4-vinyl;
48:2.6-Dimethoxy-4-(2-propenyl)-Phenol;
49: 1.6-Anhydro-b-D-glucopyranose/ Levoglucosan;
50:trans-4-Propenyl-2.6-dimethoxyphenol/Methoxyeugenol;
51:4-Hydroxy-3.5-dimethoxybenzaldehyde/ Syringaldehyde/Syringe aldehyde/ Cedar aldehyde;
52:1-(4-Hydroxy-3-dimethoxyphenyl)ethanone/Acetosyringone/ 3.5-dimethoxy-1-hydroxyacetophenone/Acetosyringon;

A number of compounds were selected to signify the difference in peak area between poplar, spruce and torrefied poplar, spruce, which are shown in Table 5-7. These are common to all the chromatograms and have peak areas greater than 1% of the total peak area. The relatively percentage of each identified compound is the peak area divided by the total peak area of all compounds on the chromatogram.

Table 5-7: Peak area percentages of chemical compounds for poplar, torrefied poplar, spruce and torrefied spruce where there are significant differences

ID	Compound name synonyms	Torrefied. poplar	Poplar	Torrefied. spruce	Spruce
1	2.3 Butanedione/Butanedione/ Diacetyl	1.65	1.03	0.15	1.32
2	Acetic acid/Ethanoic acid	4.84	5.69	4.70	5.53
3	Hydroxypropanone 1-Hydroxy-2-propanone Acetone alcohol	3.84	2.57	3.53	3.17
4	Butanedial/Succinaldehyde	3.51	2.05	1.69	1.95
5	2.3-Dihydro-5-methylfuran-2-one	3.36	1.75	2.48	2.41
6	Phenol	1.41	3.80	0.15	ND
7	2-Methoxyphenol/Guaiacol	2.36	1.10	3.79	2.88
8	2-Methoxy-4-methyl phenol Creosol/p-Methylguaiacol/ 4-Methylguaiacol	1.98	0.75	6.34	4.24
9	4-Ethyl-2-methoxyphenol 4-Ethyl guaiacol 4-Hydroxy-3-methoxy ethylbenzene p-Ethylguaiacol	1.20	0.59	4.18	2.68
10	2,6-Dimethoxy phenol Syringol 1,3-Dimethoxy-2-hydroxybenzene Pyrogallol dimethylether	4.44	0.45	ND	0.30
11	2-Methoxy-4-(1-propenyl)phenol Isoeugenol, c&t 4-Propenylguaiacol 4-Hydroxy-3-methoxypropenylbenzene	0.67	1.11	1.97	3.99
12	4-Methyl syringol 2,6-Dimethoxy-4-methylphenol	2.93	1.05	ND	ND
13	1,6-Anhydro-b-D-glucopyranose/Levoglucosan	3.14	1.24	4.04	3.89

Table 5-7 shows that there is a difference in peak area due to the pre-treatment process and feedstock type. The torrefaction process had an effect for poplar compounds (1, 4, 5, 6, 10, 12 and 13) but in the case of spruce for the same compounds, this effect is not found. Moreover, the torrefaction process appeared to affect compound 11 for spruce but not for poplar.

5.4.2.2 Steam pre-treatment

Figure 5-7 illustrates the DTG profiles of fresh and pre-treated poplar. It can be observed that maximum rate of weight loss was higher on pre-treated samples than fresh samples. This was more pronounced for the process of steam pre-treatment. An explanation of the greater maximum rate of weight loss for the case of pre-treatment samples is probably due to the higher proportion of cellulose and the absence of hemicellulose that normally has a structure-stabilising role. Torrefaction had broken down hemicellulose (hence hemicellulose peak not seen). Moreover, this has resulted in a high level of cellulose in the sample. Regarding the process of steam treatment the hemicellulose peak disappeared, when compared with the DTG of the untreated poplar. A peak appeared at 216^{o}C, which indicates that the lignin may be softened and decomposed by the process.

The temperature of maximum rate of weight loss (peak temperature) is lower on torrefied poplar (382^{o}C) than fresh poplar (384^{o}C). A low peak temperature is desirable due to less energy required for optimum weight loss. Fresh poplar had a shoulder between 300-350^{o}C indicating the hemicellulose loss and possibly limited devolatilisation and carbonisation of lignin. For steamed poplar the effect was reversed. The temperature of maximum rate of weight loss (peak temperature) is lower on fresh poplar (384^{o}C) than steamed poplar (391^{o}C). The difference on peak temperature is very low between fresh and pre-treated samples.

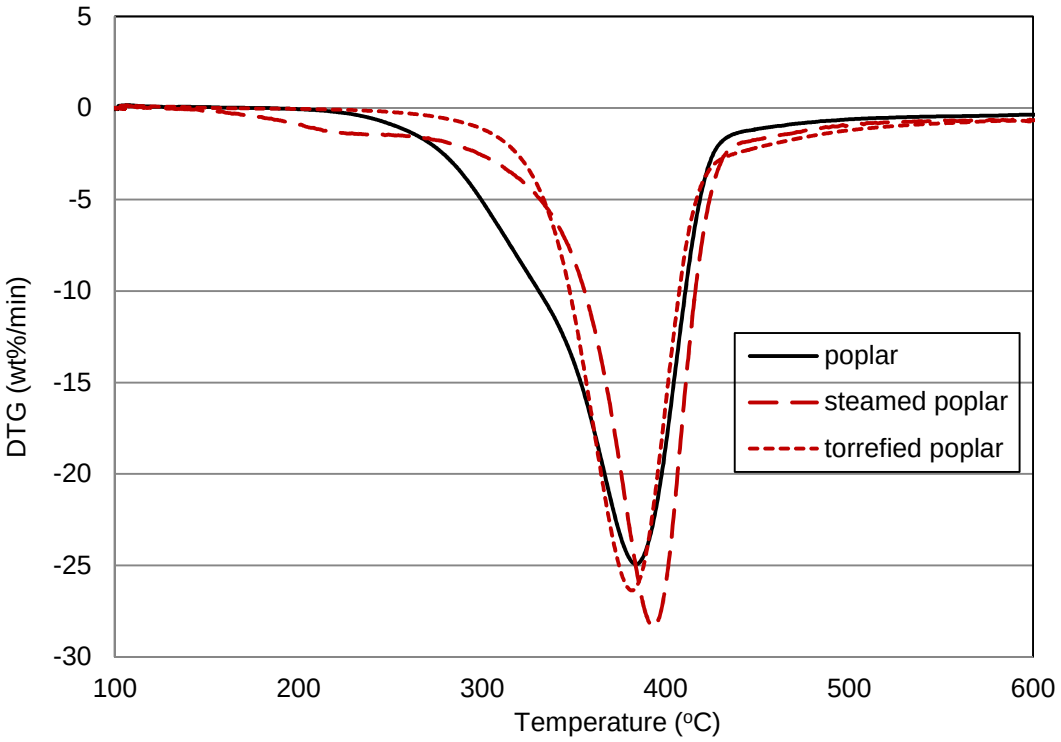

Figure 5-7: DTG profiles for untreated poplar, torrefied poplar and steamed poplar

Regarding the screening of the fresh, torrefied and steamed poplar by the Py-GC/MS, only the larger chromatographic peak areas were identified and are shown above in Figure 5-5, Figure 5-6, Table 5-5, Table 5-6 and below in Figure 5-8 and Table 5-8 respectively. A comparison between fresh poplar and pre-treated samples revealed some interesting outcomes. Fresh poplar is the reference sample. Firstly, torrefied poplar showed an increase in cellulose derived compounds, whereas for steam poplar was vice versa. Secondly, torrefaction had resulted in a reduction in hemicellulose and from Py-GC-MS an increase in phenolic compounds can be seen, particularly in the case of compounds 7, 8, 9, 10, and 12 and is shown in Table 5-7. A more pronounced increase in phenolics compounds can be observed for the case of steam poplar in Table 5-9. An explanation might be that pre-treatment had caused pre-decomposition of the material prior to Py-GC-MS analysis. As it mentioned above the decomposition of hemicellulose and limited decomposition of lignin have been occurred during torrefaction and steam treatment. Thirdly, light volatile reduction (acetic acid, compound 10 and 1 for torrefied and steamed poplar, respectively) is seen in the chromatograms for both torrefied and steamed poplar and this is possible due to both process temperatures. The reduction of acetic acid is more apparent in the case of steamed poplar. Lastly, an elimination of sugars can be observed for the case of steam poplar and specific for levoglucosan.

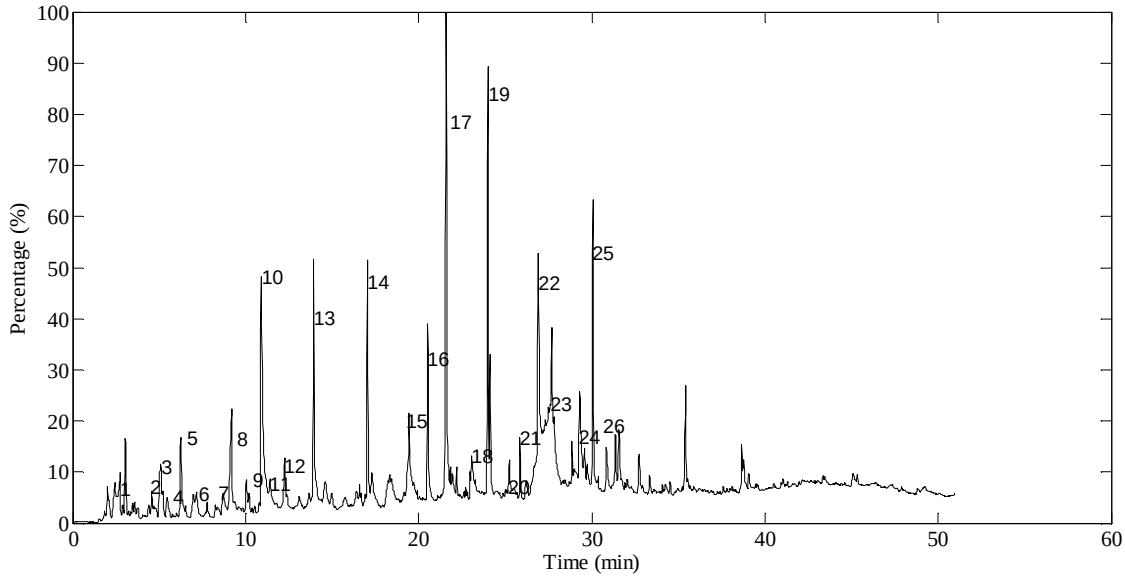

Figure 5-8: Chromatogram obtained by Py-GC/MS and chemical identification, steamed poplar. See Table 5-8 for key.

Table 5-8: Identification of chemicals from steamed poplar by Py-GC/MS

1	Acetic acid/Ethanoic acid
2	Toluene/methyl benzene
3	Propylene Carbonate/1.3-Dioxolan-2-one, 4-methyl-/Carbonic acid, cyclic propylene ester
4	(5H)-furan-2-one/2(5H)-Furanone
5	2.5-dimethyl-furan
6	2-Furanmethanol/2-Furfuryl alcohol
7	3.4-dihydro-2H-pyran
8	5-methyl-2(3H)-furanone/a-Angelica lactone
9	5-Methyl-2-furancarboxaldehyde/5-Methylfurfural/2-Formyl-5-methylfuran/2-Methyl-5-formylfuran
10	Phenol
11	3.4-dihydro-2H-pyran
12	2-Hydroxy-1-methyl-1-cyclopentene-3-one/Maple lactone/2-Hydroxy-3-methyl-2-cyclopenten-1-one
13	Mequinol/4-methoxy phenol/p-Methoxyphenol/p-Guaiacol or 2-methoxy
14	2-Methoxy-4-methyl phenol/Creosol/p-Methylguaiacol/4-Methylguaiacol
15	4-Ethyl-2-methoxy-phenol/4-Ethyl-guaiacol
16	2-Methoxy-4-vinylphenol/4-Vinylguaiacol/p-Vinylguaiacol/4-Hydroxy-3-methoxystyrene
17	2,6-Dimethoxy phenol/Syringol/1,3-Dimethoxy-2-hydroxybenzene/Pyrogallol dimethylether
18	Vanillin/2-Methoxy-4-formylphenol/4-Hydroxy-3-methoxybenzaldehyde
19	1, 2, 4- Trimethoxybenzene/1, 2, 4-Trimethoxy-1 benzene
20	2-Methoxy-4-(1-propenyl)phenol/Isoeugenol,c&t/4-Propenylguaiacol/4-Hydroxy-3-methoxypropenylbenzene
21	5-tert-Butylpyrogallol/ 1.5-tert-Butyl-1,2,3-Benzenetriol
22	1-(4-hydroxy-3-methoxyphenyl)-2-Propanone/Guaiacylacetone/Vanillyl methyl ketone/4-Hydroxy-3-methoxyphenyl acetone
23	2.6-Dimethoxy-4-(2-propenyl)-phenol
24	4-Hydroxy-3.5-dimethoxybenzaldehyde/Syringaldehyde/Syringe aldehyde/Cedar aldehyde
25	2.6-Dimethoxy-4-(2-propenyl)-phenol
26	1-(4-Hydroxy-3-dimethoxyphenyl)ethanone/Acetosyringone/3.5-dimethoxy-1-hydroxyacetophenone/Acetosyringon

Table 5-9 shows the difference in peak area between poplar, torrefied poplar and steamed poplar. These are common to all the spectra and have peak areas greater than 2% of the total peak area. The percentage of each identified compound is the peak area divided by the total peak area of all compounds on the chromatogram.

Table 5-9: Peak area percentages of chemical compounds for poplar, torrefied poplar and steamed poplar where there are significant differences

ID	Compound name/synonyms	Poplar	Torrefied. Poplar	Steamed poplar
1	Acetic acid/Ethanoic acid	5.69	4.84	**1.24**
2	2.6-Dimethoxy-4-(2-propenyl)-Phenol	0.63	0.46	**10.54**
3	1, 2, 4- Trimethoxybenzene/1, 2, 4- Trimethoxy-1 benzene	N.D.	N.D.	6.44
4	1-(4-hydroxy-3-methoxyphenyl)-2-Propanone/ Guaiacylacetone/Vanillyl methyl ketone/4-Hydroxy-3-methoxyphenyl acetone	N.D.	N.D.	5.58
5	4-Hydroxy-3.5-dimethoxybenzaldehyde/Syringaldehyde/ Syringe aldehyde/Cedar aldehyde	0.23	0.37	4.29
6	Phenol	3.80	1.41	4.79
7	2,6-Dimethoxy phenol/Syringol/1,3-Dimethoxy-2-hydroxybenzene/Pyrogallol dimethylether	0.45	4.44	7.75
8	5-Methyl-2(3H)-furanone/a-Angelica lactone/2.3-Dihydro-5-methyl-2-furanone	0.12	0.20	3.09
9	Vanillin/2-Methoxy-4-formylphenol/4-Hydroxy-3-methoxybenzaldehyde	0.31	0.25	2.37
10	2-Methoxy-4-methyl phenol/Creosol/p-Methylguaiacol/4-Methylguaiacol	0.75	1.98	3.10

There is a considerable difference in peak area due to the pre-treatment process. To specify, the process of torrefaction had a mild effect on biomass decomposition behaviour, in comparison with the process of steam pre-treatment. The steam process had a significanteffect for poplar compounds (1, 2, 3, 4, 5, 7, 8, 9 and 10) but in the case of torrefied poplar for the same compounds, this effect is not found. Moreover, the torrefied process appears to affect compound 6 (phenol) for poplar. To conclude, the process of steam pre-treatment reduced the acetic levels, as well increased significantly the phenolics compounds (phenols, guaiacols, syringols).

5.4.2.3 Aquathermolysis

Figure 5-9 illustrates the TG and DTG profiles of fresh and pre-treated wheat straw. It can be observed that maximum rate of weight loss is higher on pre-treated sample than fresh sample. As it was discussed above for the other pre-treated processes, an explanation of the greater maximum rate of weight loss for the case of pre-treated samples is probably due to the higher proportion of cellulose. Aquathermolysis had broken down hemicellulose (hence hemicellulose peak not seen), in comparison with fresh wheat straw. Moreover, this has resulted in a high proportion of cellulose in the sample. Fresh wheat straw has a shoulder between 300^{o}C indicating the hemicellulose loss and possibly limited devolatilisation and carbonisation of lignin. Another observation is that the main part of the thermal analysis curve has shifted towards higher temperature. This shift indicates that the pre-treated sample is thermally more stable than the fresh one. The temperature of maximum rate of weight loss (peak temperature) is lower on fresh wheat straw (357^{o}C) than aquathermolised wheat straw (408^{o}C).

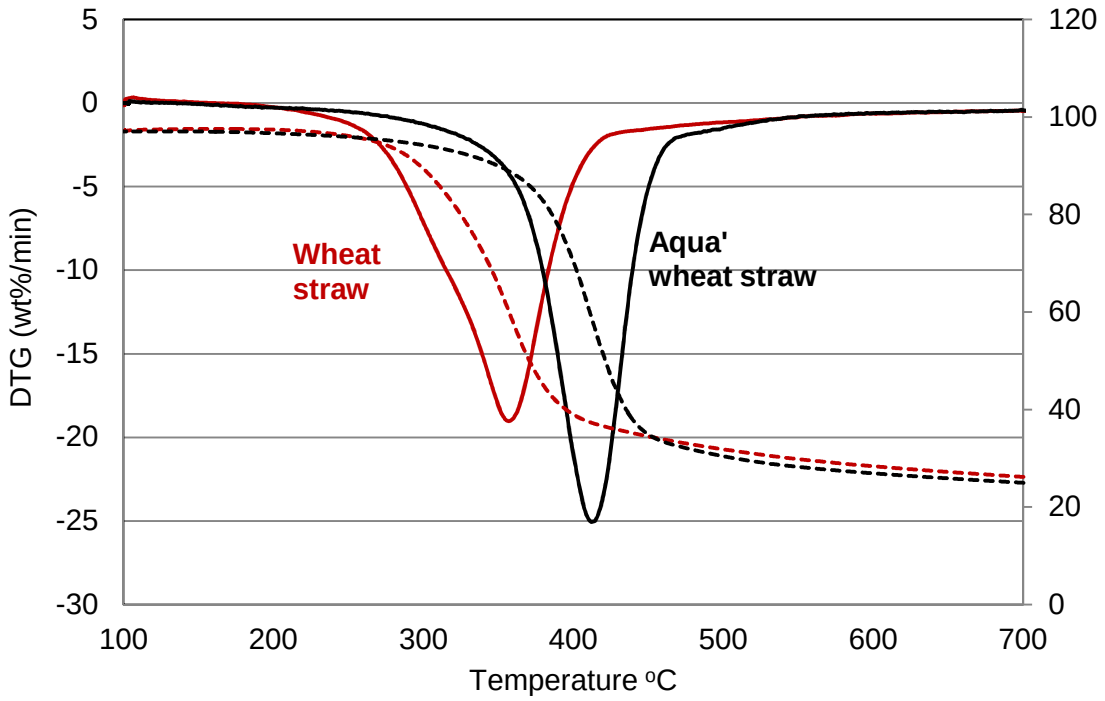

Figure 5-9: TG and DTG profiles for untreated wheat straw and aquathermolised wheat straw

With reference to the screening of the fresh and aquathermolised wheat straw by Py-GC/MS , only the larger chromatographic peak areas were identified and are shown below in Figure 5-10 and Figure 5-13 respectively and Table 5-10 and Table 5-13 respectively. A comparison between fresh and pre-treated straw reveals some interesting outcomes. Fresh wheat straw is the reference sample. Firstly, aquathermolised wheat straw showed a significant increase in levoglucosan yields (Figure 5-10, compound 21). Secondly, light volatile reduction (acetic acid, compound 1) is seen in the chromatograms for aquathermolised wheat straw and this is possible due to process temperature (270-300^{o}C). Thirdly, an important increase on syringols levels and a small reduction on guaiacols levels can be observed for pre-treated straw.

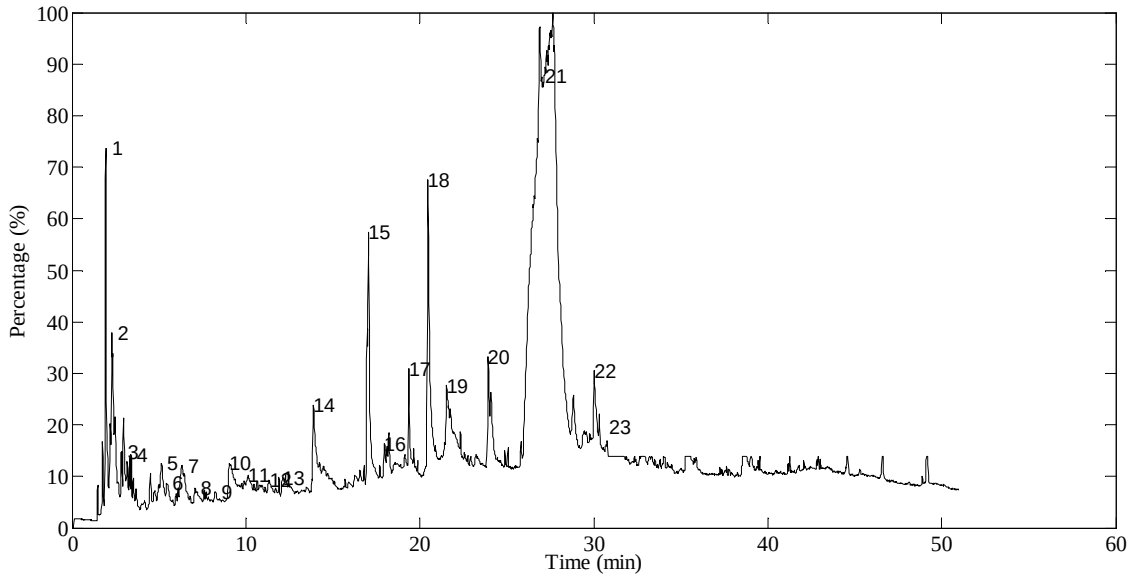

Figure 5-10: Chromatogram obtained by Py-GC/MS and chemical identification, aquathermolised wheat straw. See Table 5-10 for key.

Table 5-10: Identification of chemicals from aquathermolised wheat straw by Py-GC/MS

1	2.5-Furandione, dihydro-3-methyllene-	15	2-methoxy-4-methyl-phenol/p-Cresol, 2-methoxy-/p-Creosol/p-Methylguaiacol
2	2-ethyl-butanal		
3	3-hydroxy-butanal		
4	2.5-dimethyl-furan	16	1.4:3.6-Dianhydro-a-glucopyranose
5	Propylene Carbonate/1.3-Dioxolan-2-one, 4-methyl-/Carbonic acid, cyclic propylene ester	17	4-Ethyl-2-methoxyphenol/4-Ethyl guaiacol/4-Hydroxy-3-methoxy ethylbenzene/p-Ethylguaiacol
6	(5H)-furan-2-one/2(5H)-Furanone	18	2-Methoxy-4-vinylphenol/4-Vinylguaiacol/p-Vinylguaiacol/4-Hydroxy-3-methoxystyrene
7	Furfural/furan-2-carboxaldehyde/fural/furfuraldehyde/2-furaldehyde/pyromucic aldehyde	19	2,6-Dimethoxy phenol/Syringol/1,3-Dimethoxy-2-hydroxybenzene/Pyrogallol dimethylether
8	Ethylbenzene		
9	2-Methyl-2-Cyclopenten-1-one/2-Methyl-2-Cyclopentenone		
10	2-Furanmethanol/2-Furfuryl alcohol	20	1, 2, 4- Trimethoxybenzene/1, 2, 4-Trimethoxy-1 benzene
11	5-Methyl-2-furancarboxaldehyde/5-Methylfurfural/2-Formyl-5-methylfuran/2-Methyl-5-formylfuran	21	1,6-Anhydro-b-D-glucopyranose/Levoglucosan
12	3.4-dihydro-2-methoxy-2H-pyran	22	2.6-Dimethoxy-4-(2-propenyl)-phenol
13	2-Hydroxy-1-methyl-1-cyclopentene-3-one/Maple lactone & 2.5-Dimethylcyclopentanone	23	1-(4-Hydroxy-3.5-dimethoxyphenyl)ethanone/Acetosyringone
14	2-Methoxyphenol/Guaiacol/Guaicol		

Table 5-11 shows the difference in peak area between fresh wheat straw and pre-treated wheat straw. These are common to all the spectra and have peak areas greater than 2% of the total peak area. Table 5-11 is with agreement regarding the above outcomes. Compound 14 shows the outstanding increase of levoglucosan, while compound 1 presents the elimination of acetic acid.

Table 5-11: Peak area percentages of chemical compounds for wheat straw and aquathermolised wheat straw where there are significant differences

ID	Compound name/synomyms	Wheat straw	Aqua' wheat straw
1	**Acetic acid/Ethanoic acid**	**10.13**	**N.D.**
2	Hydroxypropanone/1-Hydroxy-2-propanone/Acetone alcohol	4.55	N.D.
3	Methylglyoxal/2-oxopropanal/pyruvaldehyde	3.16	N.D.
4	Butanedial/Succinaldehyde	2.90	N.D.
5	2.3-Dihydro-5-methylfuran-2-one	2.72	N.D.
6	2-Methoxy-4-vinylphenol/4-Vinylguaiacol/p-Vinylguaiacol/4-Hydroxy-3-methoxystyrene	6.27	3.70
7	3-Hydroxypropanal	2.07	N.D.
8	2.3 Butanedione/Butanedione/Diacetyl	1.97	N.D.
9	Furfural/furan-2-carboxaldehyde/fural/furfuraldehyde/2-furaldehyde/pyromucic aldehyde	3.05	1.12
10	2-methoxy-4-methyl-phenol/p-Cresol, 2-methoxy-/p-Creosol/p-Methylguaiacol	0.82	2.93
11	2.6-Dimethoxy-4-(2-propenyl)-phenol	N.D.	2.56
12	1, 2, 4- Trimethoxybenzene/1, 2, 4- Trimethoxy-1 benzene	N.D.	2.77
13	2,6-Dimethoxy phenol/Syringol/1,3-Dimethoxy-2-hydroxybenzene/Pyrogallol dimethylether	1.56	4.71
14	**1,6-Anhydro-b-D-glucopyranose/Levoglucosan**	**1.20**	**32.75**

5.4.3 Comparison of various biomass feedstocks

Comparison of poplar, spruce, wheat straw and DDGS using DTG profiles shown in Figure 5-11 below, shows some interesting results:

Firstly, the lowest temperature that at which maximum rate of decomposition occurred (peak temperature) is seen in wheat straw (357ºC). Secondly, the comparison of various biomass types through the DTG profile showed that maximum rate of weight loss occurred at 384ºC on poplar sample. Thirdly, the decomposition region of the samples is dissimilar; spruce has a narrow decomposition region while DDGS has a wide region. DDGS is a bio-ethanol refinery by-product containing starch, protein, crude fibre and crude fat [100]. Furthermore, the DDGS composition is reflecting in the DTG showing a number of prominent peaks when compared with the other biomass. A low temperature peak is strongly present in DDGS, possible due high hemicellulose content in the sample. Moreover, a shoulder feature can be noticed at 440ºC. This may be due to higher levels of lignin remaining in the sample from the DDGS process.

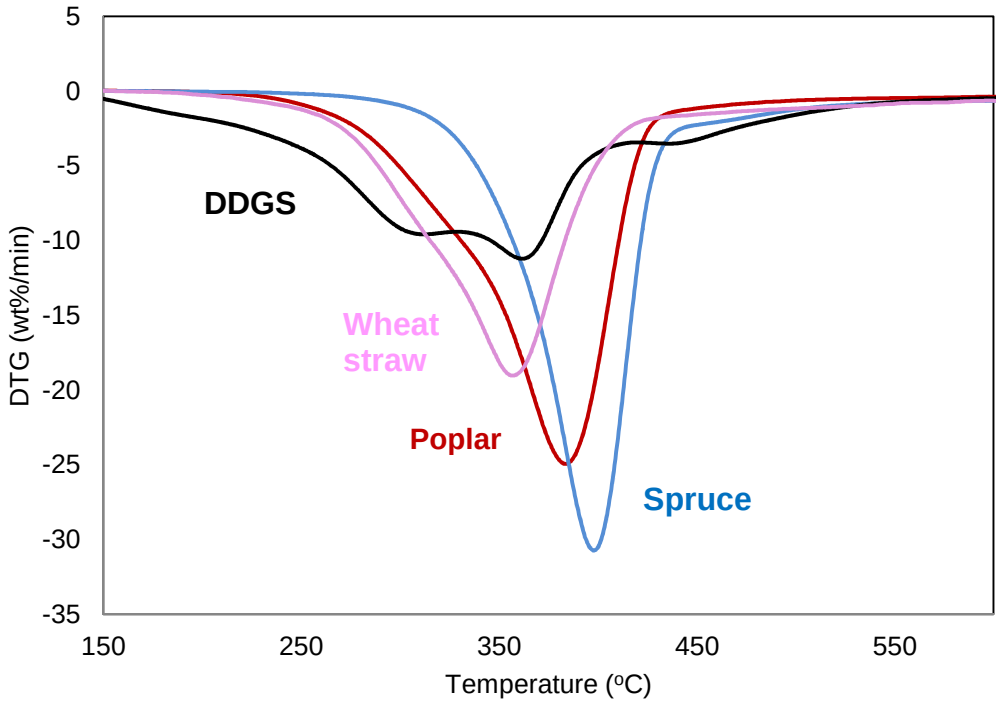

Figure 5-11. Comparison of poplar, spruce, DDGS and wheat straw using DTG profiles

The chemical compounds of DDGS and wheat straw were identified based on the chromatogram obtained from the Py-GC/MS and are illustrated below in Figure 5-12 and Table 5-12, respectively.

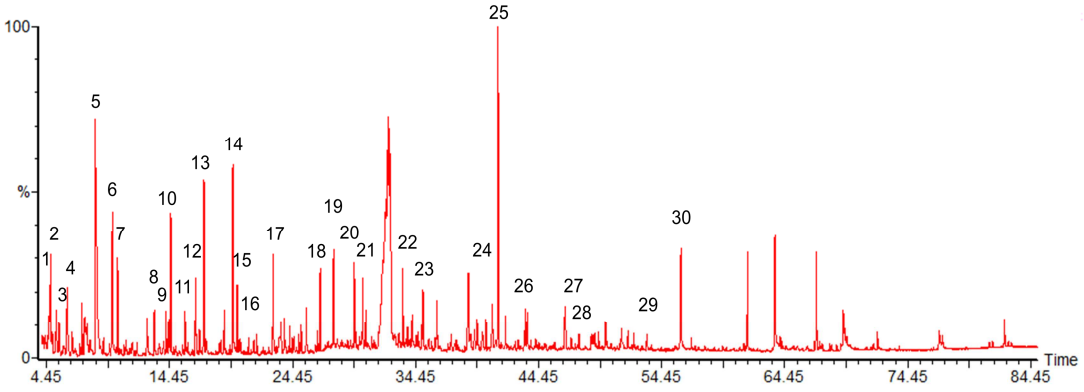

*Figure 5-12.*Chromatogram obtained by Py-GC/MS and chemical identification, DDGS. *See Table 5-12 for key.*

Table 5-12. Identification of chemicals from DDGS by Py-GC/MS

1:Furan/Furfuran/Furane/Oxacyclopentadiene;
2: methylglyoxal/ 2-oxopropanal/pyruvaldehyde;
3: 2-methyl-furan/alpha-Methylfuran;
4: 5-Methylfuran; 3-Pentanone/Pentan-3-one/Diethyl ketone (DEK);
5: Acetic acid/Ethanoic acid;
6: Hydroxypropanone/1-Hydroxy-2-propanone/Acetone alcohol;
7: Toluene/Methylbenzene;
8: 2-Propenoic acid methyl ester;
9: 1-Hydroxy-2-butanone;
10: 3-Hydroxypropanal;
11: 3(2H)-Furanone;
12: 2-Hydroxy-3-oxobutanal;
13: Furfural/furan-2-carboxaldehyde/fural/furfuraldehyde/2-furaldehyde/pyromucic aldehyde;
14: 2-Furanmethanol/2-Furfuryl alcohol;
15: 1-Acetyloxy-2-propanone/1-Acetoxypropane-2-one/2-Oxopropyl acetate;

16: 4-Cyclopentene-1.3-dione;
17:2.3-Dihydro-5-methylfuran-2-one;
18: 4-Hydroxy-5.6-dihydro-(2H)-pyran-2-one;
19: 2-Hydroxy-1-methyl-1-cyclopentene-3-one;
20: Phenol;
21: 2-Methoxyphenol/Guaiacol/Guaicol;
22: o-Cresol/2-Methyl phenol;
23: 2-Methoxy-4-methyl phenol/Creosol/p-Methylguaiacol/4-Methylguaiacol;
24: 1.5-Anhydro-arabinofuranose;
25: 2-Methoxy-4-vinylphenol/4-Vinylguaiacol/p-Vinylguaiacol/ 4-Hydroxy-3-methoxystyrene;
26: 2.6-Dimethoxy phenol/Syringol/1,3-Dimethoxy-2-hydroxybenzene/ Pyrogallol dimethylether;
27: 4-Methyl syringol/2.6-Dimethoxy-4-methylphenol;
28: Vanillin/2-Methoxy-4-formylphenol/ 4-Hydroxy-3-methoxybenzaldehyde;
29: 1-(4-hydroxy-3-methoxyphenyl)-2-Propanone/Guaiacylacetone/Vanillyl methyl ketone/4-Hydroxy-3-methoxyphenyl acetone;
30: 1.6-Anhydro-b-D-glucopyranose/ Levoglucosan

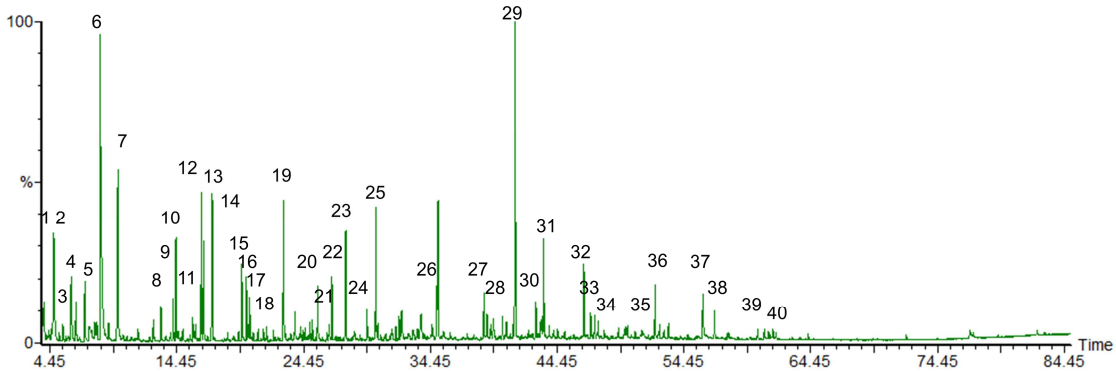

Figure 5-13.Chromatogram obtained by Py-GC/MS and chemical identification, wheat straw. See Table 5-13 for key

Table 5-13. Identification of chemicals from wheat straw by Py-GC/MS

1: Acetaldehyde/Acetic aldehyde/Ethanal;
2: Methylglyoxal/2-oxopropanal/pyruvaldehyde;
3: 2-methyl-furan/alpha-Methylfuran; 5-Methylfuran;
4: 2.3 Butanedione/Butanedione/Diacetyl;
5: Hydroxyacetaldehyde/Glycolaldehyde;
6: Acetic acid/Ethanoic acid;
7: Hydroxypropanone/1-Hydroxy-2-propanone/Acetone alcohol;
8: Propenoic acid/Propionic acid/Ethanecarboxylic acid;
9: 1-Hydroxy-2-butanone;
10: 3-Hydroxypropanal;
11: 3(2H)-Furanone;
12: Butanedial/Succinaldehyde;
13: 2-Hydroxy-3-oxobutanal;
14: Furfural/furan-2-carboxaldehyde/fural/furfuraldehyde/2-furaldehyde/pyromucic aldehyde;
15: 2-Furanmethanol/2-Furfuryl alcohol;
16: 1-Acetyloxy-2-propanone/1-Acetoxypropane-2-one/2-Oxopropyl acetate;
17: 2-Ethyl-butanal;
18: 1-(2-Furanyl)ethanone/Acetylfuran/2-Acetylfuran/Furyl methyl ketone;
19: Dihydro2.3-Dihydro-5-methylfuran-2-one;
20: (5H)-furan-2-one;
21: beta lactose derivate;
22: 4-Hydroxy-5.6-dihydro-(2H)-pyran-2-one;
23: 2-Hydroxy-1-methyl-1-cyclopentene-3-one;
24: Phenol;
25: 2-Methoxyphenol/Guaiacol/Guaicol;
26: 2-Methoxy-4-methyl phenol/Creosol/p-Methylguaiacol/4-Methylguaiacol;
27: 4-Ethyl-2-methoxyphenol/4-Ethyl guaiacol/4-Hydroxy-3-methoxy ethylbenzene/p-Ethylguaiacol;
28: 4-Hydroxy-3-methyl-(5H)-furanone;
29: 2-Methoxy-4-vinylphenol/4-Vinylguaiacol/p-Vinylguaiacol/4-Hydroxy-3-methoxystyrene;
30: 5-(Hydroxymethyl)-2-Furancarboxaldehyde/5-(Hydroxymethyl)-2-furfural/HMF/5-(Hydroxymethyl)-2-furaldehyde;
31: 2,6-Dimethoxy phenol/Syringol/1,3-Dimethoxy-2-hydroxybenzene/Pyrogallol dimethylether;
32: 2-Methoxy-4-(1-propenyl) phenol/Isoeugenol,c&t/4-Propenylguaiacol/4-Hydroxy-3-methoxypropenylbenzene;

33: 4-Methyl syringol/2.6-Dimethoxy-4-methylphenol;
34: Vanillin/2-Methoxy-4-formylphenol/4-Hydroxy-3-methoxybenzaldehyde;
35: 1-(4-Hydroxy-3-methoxyphenyl)ethanone/Acetoguaiacone;
36: 1-(4-hydroxy-3-methoxyphenyl)-2-Propanone/Guaiacylacetone/Vanillyl methyl ketone/4-Hydroxy-3-methoxyphenyl acetone;
37: 1.6-Anhydro-b-D-glucopyranose/Levoglucosan;
38: trans-4-Propenyl-2.6-dimethoxyphenol/Methoxyeugenol;
39: 4-((1E)-3-Hydroxy-1-propenyl)-2-methoxyphenol/Coniferol/Coniferyl alcohol;
40: Coniferaldehyde

The comparison of untreated feedstocks was done using the chromatograms obtained by Py-GC-MS shown in Figure 5-3, Figure 5-5, Figure 5-12 and Figure 5-13. An important result was the peak area percentage of lignin and cellulose derivates compounds for the samples and it is presented in Figure 5-14 below. The distinction between lignin and cellulose derived chemicals was done using literature by matching the chemicals produced in the chromatogram to the biomass components [101]. The results show that spruce contained the higher amount of lignin derivates while DDGS had the lowest. Figure 5-14 only includes the peak area percentages of the identified compounds and the results are not conclusive. For example DDGS seems to contain the lowest proportion of lignin derivates, but also only accounts for the lowest proportion of total products identified. For example according to Figure 5-12 it is noticeable that there are a number of unidentified compounds with high peak areas which may be high molecular weight lignin derivates.

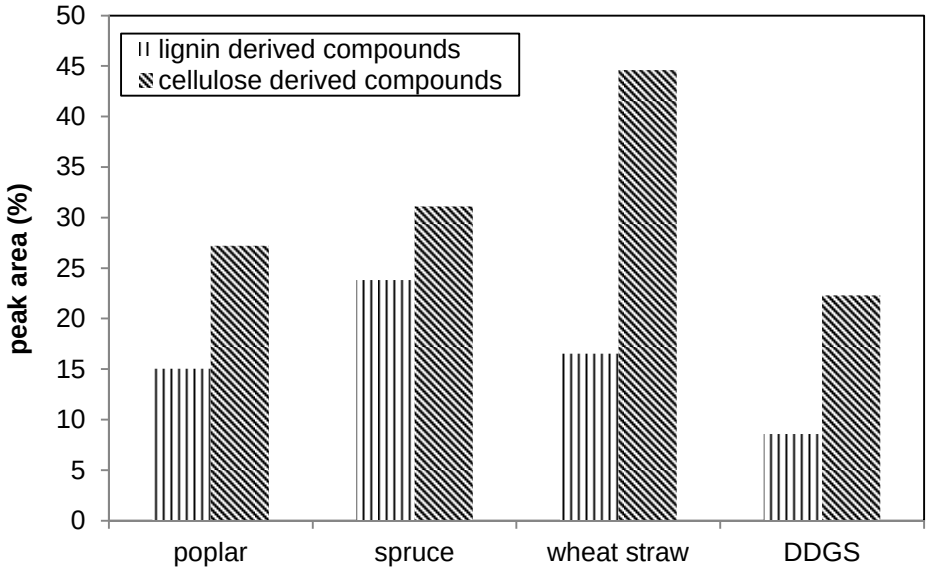

Figure 5-14. Peak area percentages of lignin and cellulose derivates compounds for poplar, spruce, wheat straw and DDGS

A number of compounds were selected to signify the difference in peak area between poplar, spruce, wheat straw and DDGS and can be found in Figure 5-15 below. It is noticeable that spruce has the higher peak area for levoglucosan, when compared with the rest feedstocks. This could be due to the low ash content and implies a low level of

inorganic compounds. This result is in agreement with the literature, showing that the removal of metals from biomass favours production of levoglucosan [8, 9]. Furthermore, a high amount of acetic acid can be seen for wheat straw although this cannot yet be explained. Another important result obtained from the comparison of the feedstocks is the identification of an aromatic hydrocarbon (toluene) for DDGS.

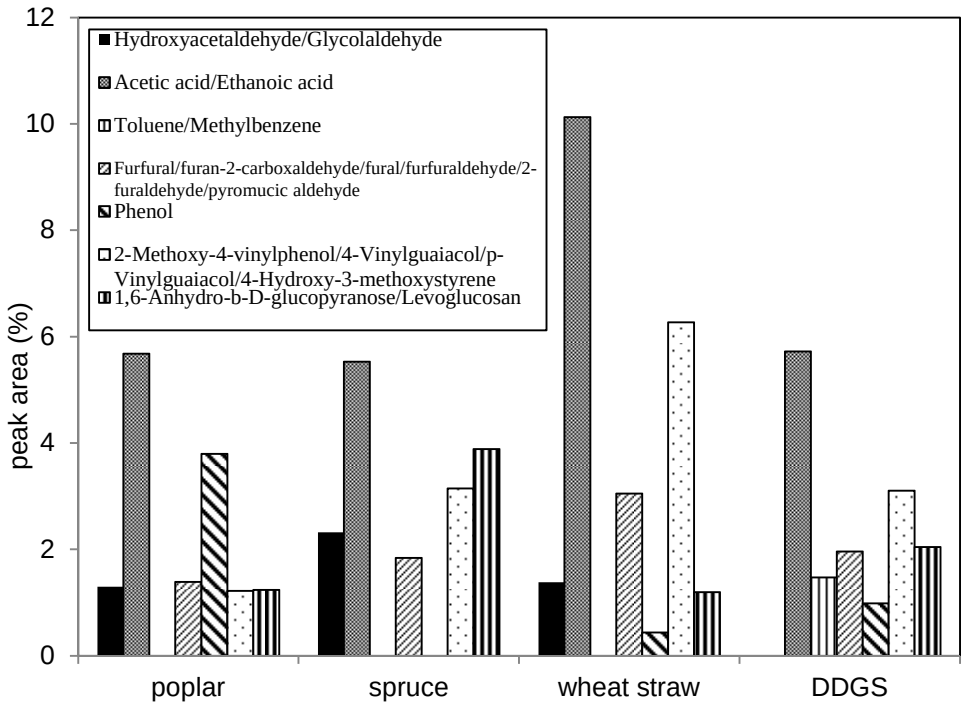

Figure 5-15.Peak area percentages of major common chemical compounds for poplar, spruce, wheat straw and DDGS

5.5 Chapter conclusion

The objective of this study was to investigate the influence of various untreated and treated biomass types on the thermochemical characteristics. The results can be divided in two main categories including:

Comparison of pre-treated (torrefied poplar and spruce, steamed poplar, aquathermolised wheat straw) and fresh samples (poplar, spruce and wheat straw)

- Pre-treatment of biomass by torrefaction caused a reduction of the temperature that at which maximum rate of decomposition occurs. Moreover, maximum rate of weight loss is higher on torrefied samples than fresh samples, particularly for spruce. Furthermore, this pre-treatment decreased hemicellulose content as shown by TGA.
- Torrefied samples showed an increase in cellulose derived compounds. This pre-treatment by torrefaction decreased hemicellulose content. Py-GC-MS analysis results showed an increase in phenolic compounds. Also, light volatile reduction

(acetic acid content) is observed in the chromatograms for torrefied wood and this is possible due to the torrefaction process temperature (270-300ºC).

- Pre-treatment of biomass causes the maximum rate of weight loss to be higher on pre-treated samples than fresh samples, particularly for spruce and wheat straw.
- Pre-treatment of wheat straw by aquathermolysis increased significantly the levoglucosan yields, while eliminated acetic acid yields.
- Elimination of sugars can be observed for the case of steam poplar. Also, a noteworthy increased of phenolics compounds can been seen.
- To specify, the process of torrefaction had a mild effect on biomass decomposition behaviour, in comparison with the process of steam pre-treatment.

Comparison of untreated biomass (poplar, spruce, wheat straw and DDGS)

- Firstly, the lowest temperature of maximum rate of weight loss (peak temperature) is seen in wheat straw (357ºC). Secondly, further analysis through the DTG profile showed that maximum rate of weight loss occurred at 384ºC on poplar sample. Thirdly, the decomposition region of the samples showed dissimilar characteristics; spruce had a narrow region while DDGS had a wide decomposition region. DDGS is a bio-ethanol refinery by-product containing starch, protein, crude fibre and crude fat [100]. Furthermore, the DDGS composition reflected in the DTG profile, showed a number of prominent peaks in comparison with the other biomass. A low temperature peak was more apparent in DDGS, possible due to high hemicellulose content in the sample. A shoulder feature can be noticed at 440ºC.
- Results from Py-GC-MS showed that spruce contained the greater amount of lignin derivates while DDGS had the lowest. It is noticeable that spruce had the higher peak area for levoglucosan in comparison with the other feedstocks. Furthermore, a high amount of acetic acid can be seen for wheat straw. Another interesting result is the identification of toluene from DDGS.

6 FAST PYROLYSIS OF WHEAT STRAW

This chapter describes the fast pyrolysis experiments with wheat straw in terms of pyrolysis products yields and chemical distribution on bio-oil. Optimum temperature is investigated to maximise the liquid yields for further catalytic experiments. In addition, limitations of the equipment and recommendations for improvement are discussed.

6.1 Introduction

Fast pyrolysis experiments were performed on the 300 g/h and 1kg/h fluidised bed reactor systems. The aim of this work was to study the effect of pyrolysis reaction temperature on the liquid yield and bio-oil quality.

Significant problems in feeding were encountered, so the experiments have been divided in two sections; experiments with the original feeding system which only had a single metering screw and a modified feeding system with a metering screw and fast feed screw.

6.2 Original feeding system

6.2.1 Results

Of the 42 fast pyrolysis runs carried out in total, 6 were used to investigate the effect of pyrolysis reaction temperature on the yield and quality of fast pyrolysis products. The results from these runs are summarised in Table 6-1.

Table 6-1: Mass balances of fast pyrolysis runs using wheat straw on 300g/h & 1kg/h continuous fast pyrolysis units

Test reference	301109	151209	270110	100110	130509	91209
Capacity of bed reactor	300g/h	300g/h	300g/h	1kg/h	300g/h	300g/h
Feed rate	117g/h	84g/h	93g/h	700g/h	154g/h	102g/h
Run time (min)	87	78	51	60	30	92
Vapour residence time (sec)	1.09	1	0.66	1	0.96	0.96
Product collection system	Cooler + ESP	Cooler + ESP	Cooler + ESP	Quench + ESP	Cooler + ESP	Cooler + ESP
Fluidised N_2 velocity (l/min)	8	8	12	40	8	8
Fluidising medium	sand	sand	sand	sand	sand	sand
Sand particle size	355-500	355-500	500-600	610-710	355-500	355-500
Feedstock	**Wheat straw**	**Wheat straw**	**Wheat straw**	**Wheat straw**	**Wheat straw**	**Wheat straw**
Particle size (μm)	< 1mm	< 1mm	< 1mm	< 1mm	< 1mm	< 1mm
Moisture content (wt%, wet basis)	9.5	9.02	8.78	8.89	6.61	9.48
Ash content (wt%, dry basis)	8.8	8.8	8.8	8.8	8.8	8.8
Minimum Pyrolysis T (^oC)	386	468	480	468	506	509
Average Pyrolysis T (^oC)	421	484	492	500	518	518
Maximum Pyrolysis T (^oC)	469	514	522	512	527	550
Product yields (wt%, dry feed)						
Char in char pot	16.11	12.33	28.29	15.56	2.51	12.33
Char in agglomerates in bed	23.57	19.28	N.D.	7.64	21.4	19.28
Char total	42.52	33.73	31.74	26.05	27.83	33.73
Liquids total	34.8	24.25	43.32	43.29	36.8	24.25
Organics	18.92	14.07	21.75	29.57	13.86	14.07
Reaction water	15.88	10.17	21.57	13.72	23	10.17
Gas	16.7	30.13	13.13	21.99	24.6	30.13
H2	0.04	0.27	0.03	0.02	0.12	0.27
CH4	0.67	1.98	0.38	0.71	1.47	1.98
CO	5.05	N.D.	3.89	6.55	8.26	N.D.
C2H4	0.13	0.56	0.12	0.12	0.35	0.56
C2H6	0.16	0.36	0.38	0.18	0.24	0.36
C3H8	0.06	0.11	0.03	0.08	0.35	0.11
C3H6	0.15	0.43	0.1	0.17	0.09	0.43
C4H10	0.02	0.08	0.02	0.01	0.1	0.08
CO2	10.42	16.33	8.17	14.14	13.62	16.33
Closure (wt%, dry basis)	94.02	88.11	88.19	91.33	89.24	88.11
	Feed problems, bed T drop, phase separated bio-oil, agglomeration		Feed problems, bed T drop, phase separate bio-oil,	bed T drop, **homogeneous bio-oil,** agglomeration	Feed problems, bed T drop, phase separate bio-oil, agglomeration	

6.2.2 Operating problems encountered

6.2.2.1 Feeding and blockages

The calculation of the mass balance uses the weight of the biomass feedstock used, while the output is the weight of the pyrolysis products. The difficulty of the existing screw feeder consists in an accurate weight of the biomass feedstock used, resulting in a low mass balance. A meteric feeder will avoid this difficulty, since it could calculate accurate the weight of the feedstock used.

Bridging of wheat straw in the feeder and pre-pyrolysis of wheat straw at the end of the screw are both responsible for the reproducibility and the low mass balance of the experiments. Both problems are attributable to the feeder construction, requiring the design of a new feeder. Theoretically, a feeder with a meteric screw (slow screw) connected to a fast screw (more than 100rpm) should be able to overcome the above problems. Figure 6-1 below illustrates the bridging phenomenon in the original feeder.

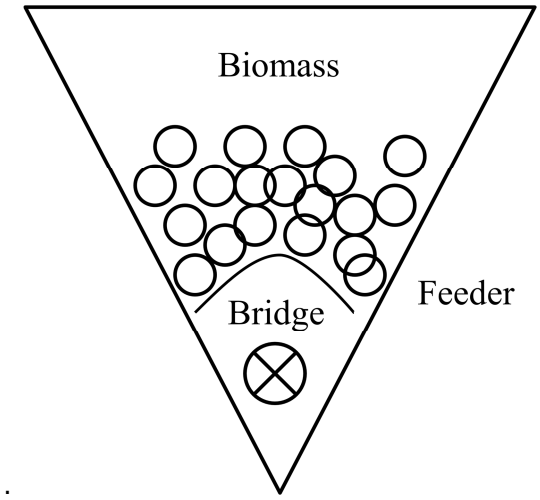

Figure 6-1: Bridging in the old feeding system

6.2.2.2 Char pot

The duration of the runs influences the mass balance in a small scale system. Longer duration runs will allow the production of a more representative bio-oil. Specifically, in the case of wheat straw a larger char pot will increase the duration of the runs, due to the high ash content of the feedstock. Runs using the 300g/h system with the original char pot was described in Table 6-1 above, showed a full char pot.

6.2.2.3 Agglomeration phenomenon

The nature of wheat straw (ash content of 8.8wt% on dry biomass basis, K content of 1.4wt% on dry biomass basis) seemed to be the main reason that caused the agglomeration phenomenon. This phenomenon took place during the runs with

reference 301109, 130509, 091209, 151209 (300g/h rig-Coolers) and 100110 (1Kg/h-Quench). See Table 6-1 as key.

Agglomeration is a phenomenon that seems to occur for high ash feedstocks with particular inorganic elements present. This phenomenon was the main problem of fast pyrolysis of wheat straw. The agglomeration of sand particles with char particles produced big chunks in the fluidised bed, resulting in a temperature drop. During the experiments, the bed temperature dropped more than 50^{o}C, resulting in the end of the run. An attempt to continue the experiments was to stop feeding during the runs and continue the fluidization of the bed to remove the char outside of the bed and increase the bed temperature. Unfortunately, it was not possible to increase the bed temperature and continue the run.

This could be due to the feedstock nature (ash content of 8.8wt% on dry biomass basis, K content of 1.4wt% on dry biomass basis). When the reactor was cooled down and it was feasible to open the bed, chunks of sand and char were visible. An additional explanation for agglomeration could be the N_2 fluidization velocity. The run with reference 270110 showed no agglomeration. It is the only run with the 300g/h rig with higher N_2 fluidization velocity (12 l/min compare to 8 l/min).

Also, pre-treatment of wheat straw could reduce the ash content and consequently the inorganic compounds. It is possible that this could eliminate the agglomeration phenomenon during the fast pyrolysis of wheat straw. The processing of aquathermolised wheat straw by fast pyrolysis will be studied in Chapter 7.

6.2.3 Discussion of results

Table 6-1 illustrates the mass balance closures of the runs and the yields of pyrolysis liquids, char and gas. It can be seen that the mass balance varies on the range of 88-94 wt% dry basis. The presence of extra peaks was noticed in the gas chromatograms. Those peaks could not be identified, due to the GC column limitations. This could imply that the unidentified and undetectable permanent gases may be one of the reasons for the loss in the mass balance.

6.2.3.1 Liquid yields

It can be seen from Table 6-1 that higher liquid yields was obtained at average pyrolysis temperature of 500^{o}C and 492 ^{o}C, which are the runs with reference 100110 (1Kg/h-Quench) and 270110 (300g/h rig-Chillers) respectively. The higher liquid yield

of fast pyrolysis of wheat straw is 43.2wt%, dry basis which is considered low when compared to wood biomass (approximate 70wt%, d.b.).

Both runs that produced the higher liquid yield had an approximate average pyrolysis temperature of 500^{o}C. The run with reference 91209 with average pyrolysis temperature of 518^{o}C and maximum temperature of 550^{o}C showed an reduction on liquid yields. This could be due the higher reaction temperature used, causing the secondary volatiles decomposition [17].

It should be mentioned that both reaction water and organic part of bio-oil are listed in Table 6-1. The organic part of bio-oil is the non-water part and contains the desirable products. Table 6-1 and Figure 6-2 show that the run with reference 100110 gave higher organics (29.57%), whereas run 091209 produced the lower (8.93%).

Low liquid yield may be caused due to the higher ash content of wheat straw compared to woods. This could imply higher level of inorganic compounds, resulting that the process of fast pyrolysis of wheat straw could be subjected to stronger catalytic effect [8, 9]. The catalytic effect in fast pyrolysis process results in the reduction of liquid yields and the formation of char and non-condensable gases.

6.2.3.2 Gas and char yields

Furthermore, the highest gas yield was produced at the average pyrolysis temperature of 518 ^{o}C (run 91209) and the highest char yield at average pyrolysis temperature of 420^{o}C (run 301109). Runs with references 091209 and 301109 have both mass balances over 90%, hence they are more reliable for comparison. It can be noticed that increasing temperature led to lower char yields and higher gas yields. This is in agreement with previous studies [25, 26, 28]. The reduction of char yields with increasing temperature could be due to greater primary decomposition of the biomass at higher temperature and/or secondary thermal decomposition of the char formed before being entrained out of the reaction zone. The increase of gas yields with increasing temperature is possibly due to a combination of secondary thermal cracking of the evolved pyrolysis vapours and the char secondary decomposition.

An illustration of the liquid, char and gas yields, expressed on wt.% on dry biomass basis for fast pyrolysis of wheat straw can be found in Figure 6-2 below.

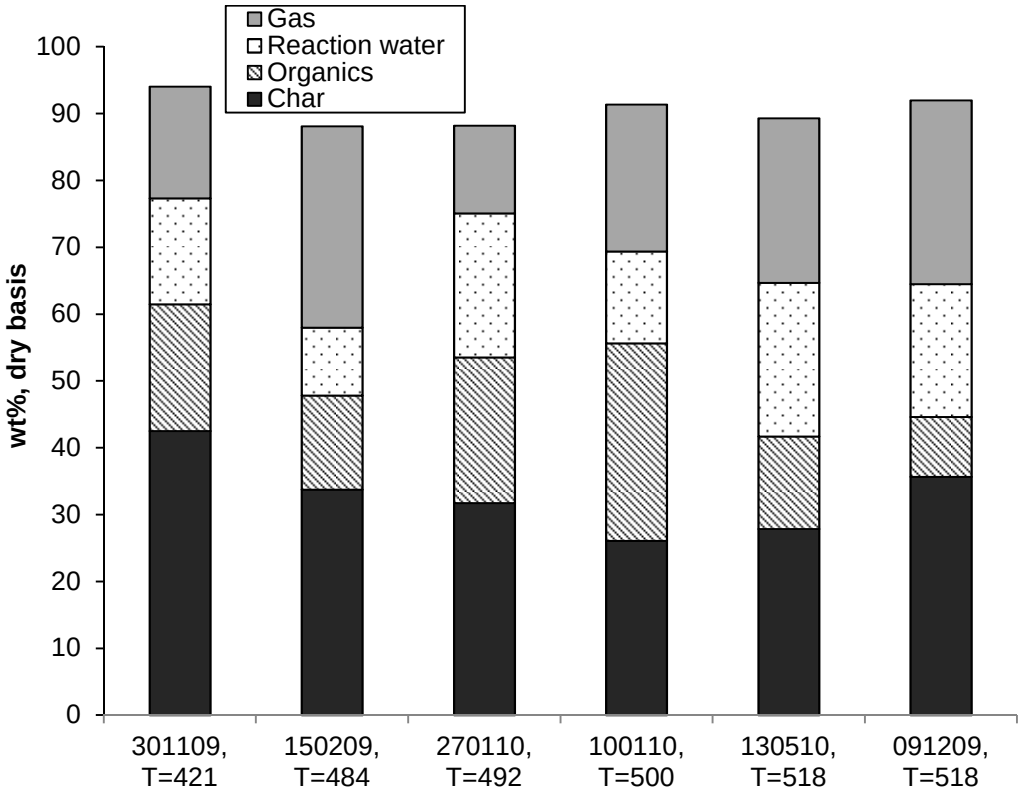

Figure 6-2: Yields of liquid, gas and char from fast pyrolysis of wheat straw, wt% on dry feed basis.

Figure 6-3 shows the gas composition from pyrolysis experiments of wheat straw feedstock at different reaction temperatures. The data represents on dry basis the composition on weight percent (wt.%, dry basis) of each gas evolved with the total gas yield in Table 6-1.

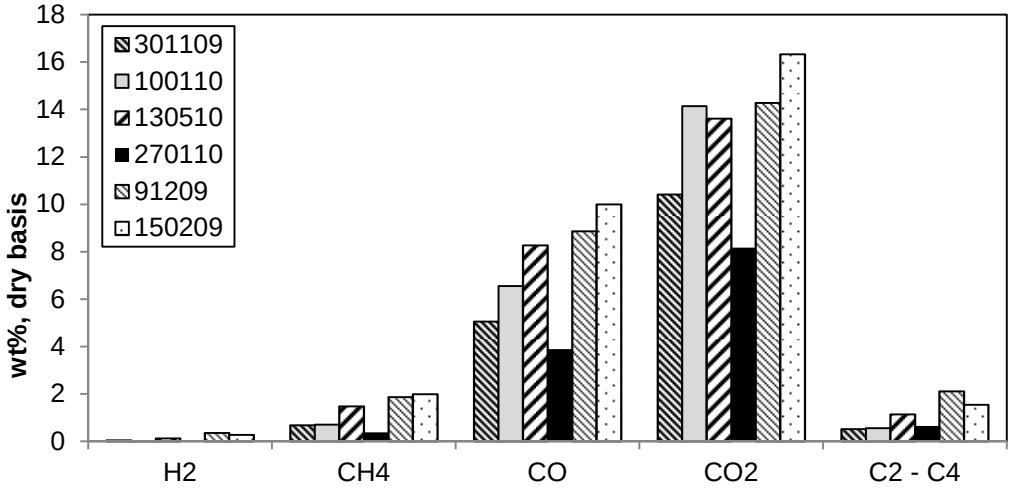

Figure 6-3: Gas composition on dry basis of weight percent (wt %, dry basis) from the fast pyrolysis runs using wheat straw

According to Figure 6-3 the gaseous products contain mainly of carbon dioxide and carbon monoxide with small portions of C_1 - C_4 hydrocarbon and hydrogen gases. It can

be observed from Figure 6-3 that for all the experiment the formation of CO_2 was greater in comparison with CO. Run with reference 91209 (518^{o}C average pyrolysis temperature) shows an increase for C_2 - C_4, production, when comparing with runs 270110, 301109, 100110.

6.3 Modified feeding system

Fast pyrolysis experiments with wheat straw have been conducted using the 300g/h fluidised bed reactor system with the new feeding system. The new feeding system comprises of a meteric screw and a fast screw, which are controlling the feeding rate and the speed of biomass entering in the fluidised bed respectively.

6.3.1 Operating problems encountered

The aim of the new feeding system was to overcome the problems mentioned in subsection 6.2.2.1. Unfortunately, problems also occurred with fast pyrolysis of wheat straw using the new system. Table 6-2 below summarised the operating conditions of the runs and the problems obtained.

Table 6-2: Operating conditions-Problems and observations

Test reference	21110	91110	131210	070111A	070111B	80211	140211
Reactor configuration	300 g reactor + 100 g glass ware	300 g reactor + 100 g glass ware	300 g reactor + 100 g glass ware	300 g reactor + 100 g glass ware	300 g reactor + 100 g glass ware	300 g reactor + 100 g glass ware	300 g reactor + 100 g glass ware
Nominal capacity of reactor	300g/h	300g/h	300g/h	300g/h	300g/h	300g/h	300g/h
Feed moisture (%)							5.02
Average feed rate	100g/h	100g/h	100g/h	120g/h	360g/h	100g/h	117g/h
Run time (min)	1	1	30	30	30	15	103
Product collection system	Cooler + ESP	Cooler + ESP	Cooler + ESP	-	-	Cooler + ESP	Cooler + ESP
Fluidised N_2 velocity (l/min)	16	14	16	-	-	8	2
Feeder N_2 velocity (l/min)	2	2	2	2	2	15	15
Fluidising medium	Sand	Sand	Sand	Sand	Sand	Sand	Sand
Sand particle size microns	355-500	355-500	610-710	-	-	500-600	355-500
Fast screw (rpm)	150	100	100	105	105	105	105
Feedstock	**Wheat straw**	**Wheat straw**	**Wheat straw from ground pellets**	**Wheat straw**	**Wheat straw from ground pellets**	**Wheat straw**	**Wheat straw from ground pellets**
Feed particle size (mm)	0.225-1	0.225-1	0.225-1	0.225-1	0.225-1	0.225-1	0.225-1
Pyrolysis T (^oC) average	550	515	520	Cold	Cold	477	471.81
Pressure in reactor at start of run (ins water)							5
Pressure in reactor at end of run (ins water)							6
Pressure in feeder at start of run (ins water)							16
Pressure in feeder at end of run (ins water)							20
Feeding wheat straw	Feeding was	Feeding was	Feeding worked,	Feeding worked well			Feeding

to pyrolyser	not possible	not possible	but stopped after 15 min		worked well
Problem	Feed blockage at entrance to fast screw	Sand was fluidised at entrance to fast screw	Feed blockage at entrance to fast screw	2 leaks 1 Gas and vapour leak from glass and metal ball into water cooler 2 Gas leak from glass ball from cooler to ESP	Char did not leave the bed-Char pot was empty, Agglomeration in the bed
Cause	1. Probably due to low bulk density of material 2. Probably higher pressure in bed than feeder	Probably higher pressure in bed than feeder	1. Probably due to low bulk density of material 2. Higher pressure in bed than feeder	Probably due to high pressure on the glassware system	Not proper fluidization in the bed, Nature of wheat straw
Solution	1. Increase bulk density by pelletising wheat straw 2. Increase pressure in the feeder by increasing N_2 flow rate	Increase pressure in the feeder by increasing N_2 flow rate	1. Increase bulk density by pelletising wheat straw 2. Increase pressure in the feeder by increasing N_2 flow rate		Probably an increase on N_2 flow rate in feeder
Observations				Pyrolysis vapours stopped entering water cooler for 10 minutes No observed hold up in feeder Inlet to fast screw blocked Operation of fast screw did not move straw from inlet pipe	

Regarding the runs with reference 021110, 091110 and 131210 feeding of wheat straw was not possible. After few minutes the wheat straw was blocked in the pipe that connects the meteric screw with the fast one (picture below). This indicated that it was difficult to feed this feedstock, due to its low bulk density. In run 091110, sand was also fluidised in the pipe that connects the meteric screw with the fast one. This could be caused from higher pressure in the bed than the feeder.

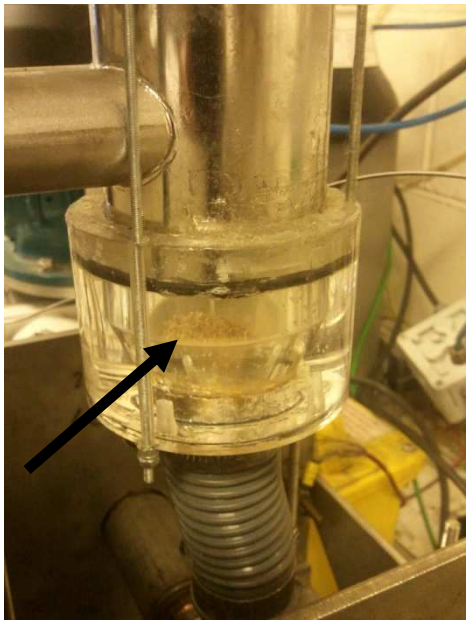

Figure 6-4: Shows blockage in feeder upstream of fast feeding screw in run 131210

The next step was to exclude the feeding problem. Two cold runs have been performed (070111A, 070111B) in cold conditions to investigate the feeding problem. The same feeder with the same settings was used for both runs. Measurements of both runs are listed in Table 6-3 below. Feeding was regular and without any problems.

Table 6-3: Measurements of runs with reference 070111A and 070111B using the new feeding system

Test reference	0701101	0701102
Feed material	Wheat straw	Ground pelletized wheat straw
Time (min)	Weight (g) delivered	Weight (g) delivered
5	10.06	29.63
10	11.29	33.81
15	10.76	32.55
20	10.72	32.29
25	11.04	32.76
30	11.00	31.18
Feed rate	120g/h	360g/h

The bulk density of wheat straw and ground pellets can be found below in Figure 6-5. The bulk density of ground pellets was approximate three times higher the bulk density

of ground wheat straw, confirming the results obtained from the cold runs mentioned above.

Ground wheat straw	Pellets	Ground pellets
Particle size: < 1mm Bulk density (min): 0.146 g/cm^3 Bulk density (min): 0.163 g/cm^3		Particle size: < 1mm Bulk density (min): 0.351 g/cm^3 Bulk density (min): 0.391 g/cm^3

Figure 6-5: Photos of ground wheat straw, pellets and ground pellets respectively.

Regarding the run 080211, feeding was possible with an increase in the N_2 velocity of the feeder. Leakages were occurred on the glassware though, possible because they are designed for lower pressure. After 15 min wheat straw was still blocked in the pipe that connects the meteric screw with the fast one. Feeding wheat straw was regular only on run 140211. The bed fluidisation occurred by fluidisation through the feeder.

6.3.2 Discussion of results

Table 6-4 shows the pyrolysis products yields obtained by fast pyrolysis of ground pellets wheat straw using the new feeding system. The organic yields produced was 10.32 wt% dry basis, which is considered low in comparison with the results from Table 6-1.

The main cause for the low liquid and organic yields is the agglomeration phenomenon. It can be seen that the char yield formed in the bed was 32.6 wt%, dry basis. Higher nitrogen fluidization velocity of 15l/min (instead of 8l/min and 12l/min on Table 6-1) was used for the run with reference 140211. The fluidization using the new feeding system for run 140211 was through the feeder instead of the fluidised bed. This may be the reason that agglomeration still occurred for run 140211, even the increase of the fluidisation velocity.

Table 6-4: Mass balance of fast pyrolysis experiment of ground pellets wheat straw using the 300g/h reactor with the new feeding system

Test reference	140211
Minimum Pyrolysis T (^{o}C)	463
Average Pyrolysis T (^{o}C)	472
Maximum Pyrolysis T (^{o}C)	489
Product yields (wt.%, dry feed)	
Char in char pot	0.37
Char in agglomerates in bed	32.60
Char	**37.41**
Liquids total	**33.72**
Organics	10.32
Reaction water	23.40
Gas	**19.32**
H_2	0.05
CH_4	1.13
CO	5.03
C_2H_4	0.25
C_2H_6	0.46
C_3H_8	0.44
C_3H_6	0.32
C_4H_{10}	0.25
CO_2	11.39
Closure (wt%, dry basis)	90.45

6.4 Bio-oil analysis

The properties of bio-oil obtained from fast pyrolysis of wheat straw have been studied. This includes water, pH value, basic elemental composition, molecular weight distribution, heating values and chemical composition.

It is imperative to highlight that the bio-oil produced from the 300g/h fluidised reactor were collected in three fractions (pot 1, pot 2 and pot 3) as mentioned in Section4.4. Pot 1 contained phase separated oil and it was divided in aqueous light fraction and heavy organic fraction. The oil produced from the 1kg/h reactor system was collected in four fractions and it is described in section 4.6. It should be noted that the run 100110 (1kg/h reactor system) formed a brown homogeneous colour oil in comparison with the oil produced from the 300g/h reactor system.

With regards to the water content and pH value, pot 1 (aqueous light fraction and heavy organic fraction) and a mixture of pot 2 and pot 3were analysed. In the case of the 1 kg/h reactor system, the main bio-oil (pot 1) and a mixture of pot 2, pot 3, and pot 4 were analysed. The determination of elements, molecular weight and chemical compounds were done only in the aqueous light fraction and heavy organic fraction (pot 1). This can be justified by the high water content (> 70%) of pot 2 and pot 3. Concerning the 1 kg/h reactor system only the main bio-oil (pot 1) was subjected to analysis.

6.4.1 Water content

The water in bio-oil derived from the original moisture in the feedstock and from pyrolysis as a product from dehydration reactions. Bio-oil water content ranges from typically 15 to 35 % and the variation of the water content depends on the feedstock water content and the process severity in terms of secondary reactions [38].

The reaction water content was discussed above in Section 6.2.3.1. The amount of water present in bio-oils is important because this effects its quality. As the water content of bio-oil increases, its heating value, flame temperature and ignition properties reduce. Conversely, the high water content can improve the flow characteristics of bio-oil resulting in a closer to uniform temperature profile in the cylinder of a diesel engine. This can be an advantage in diesel engines and in general in power generation as it lowers NO_x emissions and ignition delay [38-41].

Table 6-5 shows the percentage of water content produced from wheat straw using the 300g/h and 1kg/h fluidised bed reactors. Wheat straw derived bio-oil is a phase separate oil. The aqueous phase water content is in the range of 54-77 wt.% (aqueous phase of bio-oil basis), while the heavy phase is 9-13wt.% (heavy phase of bio-oil basis). An interesting finding is that the run with reference 100110 (1kg/h- Quench + ESP) produced a homogenous oil with water content of 23.28 wt.% (bio-oil basis).

Table 6-5: Water content of bio-oil produced from wheat straw

Test reference	301109	140211	151209	270110	100110	130509	91209
Minimum Pyrolysis T (^oC)	386	463	468	480	468	506	509
Average Pyrolysis T (^oC)	421	472	484	492	500	518	518
Maximum Pyrolysis T (^oC)	469	489	514	522	512	527	550
Homogeneity	Phase separated	Phase separated	Phase separated	Phase separated	**Homo-geneous**	Phase separated	Phase separated
Water content %							
Pot 1							
Aqueous phase	56.03	77.50	57.66	53.75	23.28	67.4	77.52
Heavy phase	10.50	11.90	9.5	9.3		11.2	13.2
Pot 2+3	68.34	64.82	64.95	75.24	81.32	73.7	78.52

6.4.2 Basic elemental composition, molecular weight distribution and pH value analysis

The molecular weight distribution, pH value, elemental composition, and heating value analysis are listed in Table 6-6 below. It was found that the pot 2+3 oils were more acidic than the pot 1 oils for all the samples. The low pH values of bio-oils are caused

by the presence of carboxylic compounds such as formic and acetic acids in large proportion.

The percentages of carbon, hydrogen, nitrogen and oxygen expressed on dry basis of the organic heavy fraction of wheat straw oils were within the range of 66-72%, 6.5-8% and 18-26% respectively. The percentages of carbon, hydrogen, and oxygen expressed on dry basis of the light aqueous fraction of wheat straw oils were within the range of 34-58%, 6.5-12.5% and 35-51% respectively. The HHV_{wet} in the case of run 100110 was 16.72 MJ/kg and it was an homogenous oil. This is in agreement in literature, in which the HHV_{wet} was 17.3 MJ/kg [102]. The wet heating values for all the runs are lower than the dry values, due the consideration of water into the results. The wet heating value is interesting, since the bio-oil is going to be used as produced in any application.

Table 6-6: pH and molecular weight bio-oil produced from wheat straw

Test ref.	301109		100110	130509		270110		91209		151209		140211	
Feed	**Wheat straw**											**Wheat straw from ground pellets**	
Phase	Aqueous Light fraction	Organic Heavy fraction	**Homo-genous oil**	Aqueous Light fraction	Organic Heavy fraction	Aqueous Light fraction	Organic Heavy fraction	Aqueous Light fraction	Organic Heavy fraction	Aqueous Light fraction	Organic Heavy fraction	Aqueous Light fraction	Organic Heavy fraction
Molecular weight(g/mol)													
Mw	430	472	321	265	581	495	621	272	415	255	598	231	600
Mn	240	174	127	182	238	238	255	154	169	175	246	139	245
PD	1.79	2.71	2.53	1.46	2.44	2.08	2.43	1.76	2.45	1.46	2.43	1.66	2.45
pH													
Pot 1	2.96	2.89	Pot 1: 3.97	3.08	2.80	3.36	3.11	4.07	4.01	3.2	2.7	4.1	3.6
Pot 2 + 3	1.95		Pot 2: 2.91 Pot 3+4: 3.46	2.29		2.10		2.94		2.35		2.4	
Elemental analysis (wt%, dry basis)													
C	41.16	65.63	46.43	49.29	68.05	57.69	68.19	34.30	73.00	48.18	66.57	39.64	71.77
H	7.83	7.32	7.72	9.24	7.27	6.48	6.45	11.24	7.47	7.31	6.68	12.48	7.89
N	0.20	1.21	0.52	0.00	0.00	0.43	1.01	0.49	1.64	0.24	0.88	0.44	0.92
O	50.77	25.82	45.32	41.47	24.68	35.36	24.34	53.93	17.89	44.28	25.86	47.43	19.42
Heating value (MJ/Kg)													
HHV_{dry}	18.35	28.85	20.61	23.80	29.77	24.11	28.87	19.63	32.41	20.85	28.42	23.64	32.33
HHV_{wet}	8.07	25.82	15.81	7.76	26.44	11.15	26.18	4.41	28.13	8.83	25.72	5.32	28.48
LHV_{dry}	16.75	27.25	19.01	22.21	28.17	22.52	27.27	18.04	30.81	19.25	26.83	22.04	30.73
LHV_{wet}	6.00	24.14	14.02	5.59	24.74	9.10	24.51	2.16	26.42	6.74	24.05	3.07	26.78

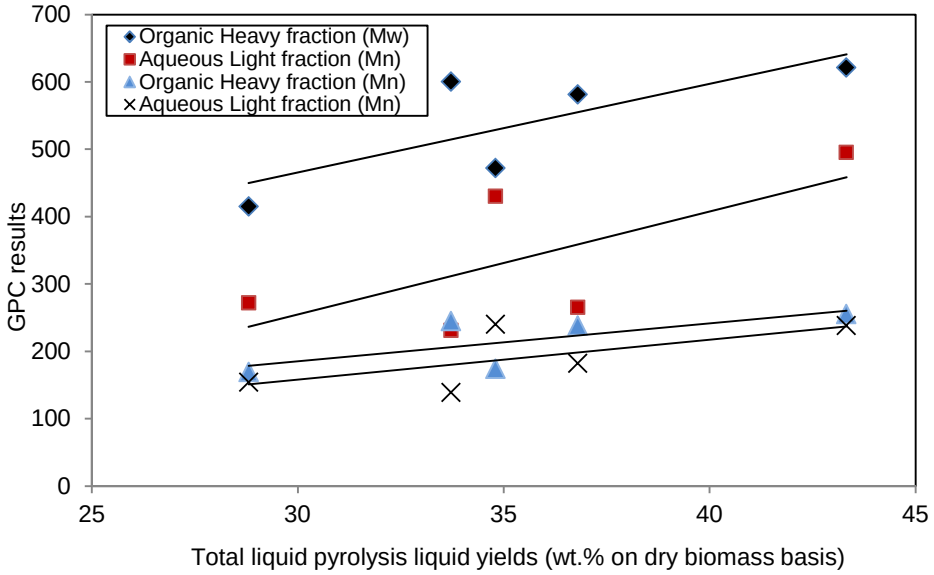

Figure 6-6: Total liquid pyrolysis liquid yields (wt.% on dry biomass basis) versus GPC results

Figure 6-6 above shows the linear relationship between the total liquid pyrolysis liquid yields (wt.% on dry biomass basis) versus the molecular weight and number of the pyrolysis runs discussed in Table 6-6. It seems that a higher liquid yield contained higher molecular weight derived compounds [16]. The run 100110 (homogeneous oil – 1kg/h) was not included in Figure 6-6, due to the use of a different reactor and the homogeneity of the oil. Additionally, run 151209 was not included, due to its low mass balance and very low liquid yield.

6.4.3 GC-MS analysis

The analysis of bio-oil obtained from fast pyrolysis of wheat straw was performed by gas chromatography/mass spectrometry (GC/MS) technique. The aim of this analysis is to identify and 'semi-quantify' the chemical compounds present in wheat straw derived oil. The term 'semi-quantify' is used because the GC/MS cannot quantify the chemicals without calibration; the peak areas obtained from the chromatograms do not directly relate to the concentration. Peak area should be used with caution, since it shows the amount of one chemical as a percentage of the total chemicals measures by the chromatogram.

Chromatograms obtained by GC/MS analysis of the organic heavy fraction and aqueous light fraction of pot 1 wheat straw derived oil are illustrated in Figure 6-7 - Figure 6-8 respectively. It is also important to mention that the organic heavy fraction of pot 1 was dissolved in a solvent (ethanol) at a concentration of approximately 25 wt% organics.

The similarities of the chromatograms from the runs with reference 180110 and 270110 are noticeable. Comparison of these chromatograms is interesting because it revealed that the chemical distribution is similar even different reactor and collection product systems have been applied. To add to this, the oil obtained from the run with reference 180110 (1kg/h, Quench) was on homogenous phase, whereas the oil from run 270110 (300g/h, Coolers) was on phase separation.

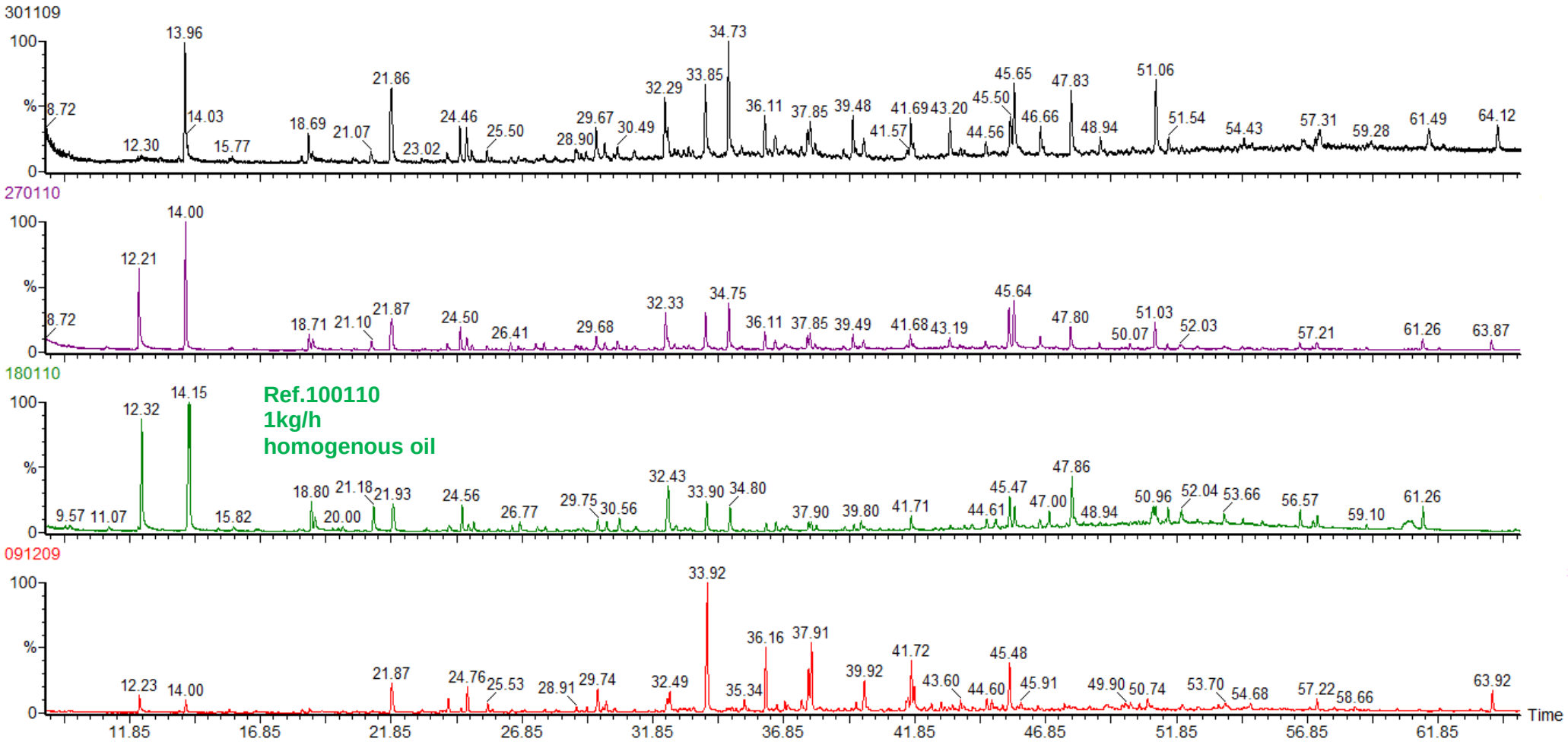

Figure 6-7: Chromatograms obtained by the GC/MS analysis of organic heavy fraction (pot 1) of wheat straw derived oil

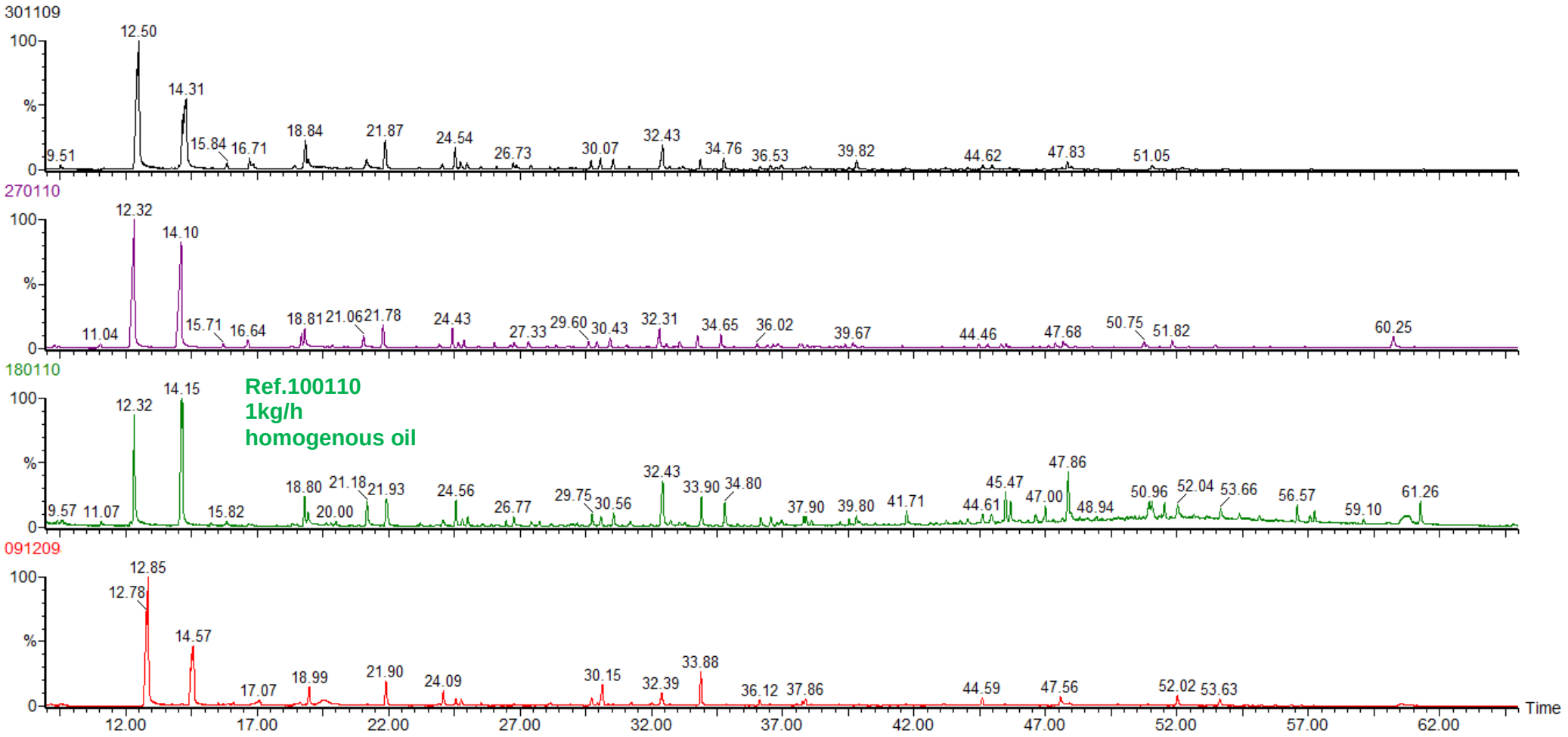

Figure 6-8:Chromatograms obtained by the GC/MS analysis of aqueous light fraction(pot 1) of wheat straw derived oil

The chemical compounds that were identified in the organic heavy fraction of pot 1 of wheat straw derived oil including their compound name, retention time (R/T), molecular formula, molecular weight (MW) and group are listed in Table 6-7 below.

According Table 6-7 the heaviest molecule that GC/MS was able to identify is trans-methoxyeugenol (ID-81) with molecular weight of 194.23 g/mol. Comparing the results obtained from Table 6-6 and Table 6-7 it could be concluded that the GC/MS technique is not able to identify all molecules in the bio-oils. According to Table 6-6, the average molecular weight (Mw) of wheat straw bio-oils were in the range of 321-621 g/mol and 231-495 g/mol for the organic heavy fraction and aqueous light fraction respectively.

The chemical distribution of different runs and different bio-oil fractions (organic heavy fraction and aqueous light fraction of pot 1) was studied by applying seven bio-oil samples in GC-MS analysis. The percentage of each identified compound is the peak area divided by the total peak area of all compounds on the chromatogram is presented in Table 6-8.

Table 6-7: Identification of chemical compounds present in the organic heavy fraction and aqueous light fraction of Pot 1 of wheat straw derived oil

ID	Compound name/synomyms	R/T	Formula	MW	Group
1	2.3 Butanedione/Butanedione/Diacetyl	9.57	$C_4H_6O_2$	86.09	Ketones
2	Hydroxyacetaldehyde/Glycolaldehyde	11	$C_2H_4O_2$	60.05	Misc. Oxygenates
3	Acetic acid/Ethanoic acid	12.8	$C_2H_4O_2$	60.05	Acids
4	Hydroxypropanone/1-Hydroxy-2-propanone/Acetone alcohol	14.57	$C_3H_6O_2$	74.08	Misc. Oxygenates
5	3-Penten-2-one	15.7	C_5H_8O	84	Ketones
6	3-Hydroxy-2-butanone/2-Hydroxy-3-butanone	15.8	$C_4H_8O_2$	88.11	Misc. Oxygenates
7	3-Hydroxypropanal	17.1	$C_3H_6O_2$	74.08	Misc. Oxygenates
8	(5H)-furan-2-one/2(5H)-Furanone	18.5	$C_4H_4O_2$	84.07	Furans
9	1-Hydroxy-2-butanone	19	$C_4H_8O_2$	88.11	Misc. Oxygenates
10	Butanedial/Succinaldehyde	21.2	$C_4H_6O_2$	86.09	Aldehydes
11	Furfural/furan-2-carboxaldehyde/fural/furfuraldehyde/2-furaldehyde/pyromucic aldehyde	21.9	$C_5H_4O_2$	96.08	Aldehyde
12	2-Methyl-furan	21.9	C_5H_6O	82	Furans
13	2-Furanmethanol/2-Furfuryl alcohol	24.1	$C_5H_4O_2$	98	Furans
14	1-Acetyloxy-2-propanone/1-Acetoxypropane-2-one/2-Oxopropyl acetate	24.6	$C_5H_8O_3$	116.12	Misc. Oxygenates
15	2-Methyl-2-Cyclopenten-1-one	24.8	C_6H_8O	96	Ketones
16	2-Ethyl-butanal/Tetrahydro-4-methyl-3-furanone	25	$C_6H_{12}O$	100.16	Aldehydes
17	1-(2-Furanyl)ethanone/Acetylfuran/2-Acetylfuran/Furyl methyl ketone	25.5	$C_6H_6O_2$	110.11	Furans
18	2-ethyl-5-methyl-furan	25.5	$C_7H_{10}O$	110	Furans
19	2.5-diethoxytetrahydro-furan	26.1	$C_8H_{16}O_3$	160	Furans
20	5-Methyl-2(3H)-Furanone/a-Angelica lactone2.3-Dihydro-5-methylfuran-2-one	27.4	$C_5H_6O_2$	98.1	Furans
21	5-Methyl-2-furancarboxaldehyde/5-Methylfurfural/2-Formyl-5-methylfuran/2-Methyl-5-formylfuran	28.9	$C_6H_6O_2$	110.11	Furans
22	3-Methyl-2-Cyclopenten-1-one/3-Methyl-2-Cyclopentenone	29.7	C_6H_8O	96	Ketones
23	Tetrahydro-2-furanol	29.9	$C_5H_{10}O_2$	102	
24	4- hydroxy-butanoic acid	30.1	$C_4H_8O_3$	104	
25	3.4-dimehtyl-2-Cyclopenten-1-one	30.4	$C_7H_{10}O$	110	Ketones
26	5-Methyl-2(5H)-Furanone/β-Angelica lactone	31.16	$C_5H_6O_2$	98.1	Furans
27	2-Hydroxy-1-methyl-1-cyclopentene-3-one/Maple lactone & 2.5-Dimethylcyclopentanone	32.3	$C_6H_8O_2$ & $C_7H_{12}O$	112	Ketones
28	2.3-dimethyl-2-Cyclopenten-1-one	32.42	$C_7H_{10}O$	110	Ketones
29	4-Methyl -5H-furan-2-one/4-Methyl-2(5H)-furanone	32.69	$C_5H_6O_2$	98	Furans
30	Phenol	33.9	C_6H_6O	94.11	Phenols

31	1-Methylindene/1-Methyl-1H-indene	34.7	$C_{10}H_{10}$	130	Aromatic Hydrocarbons
32	3-Methylindene/3-Methyl-1H-indene	34.8	$C_{10}H_{10}$	130	Aromatic Hydrocarbons
33	2-Methoxyphenol/Guaiacol/Guaicol	34.9	$C_7H_8O_2$	124.14	Guaiacols
34	3-ethyl-2-cyclopenten-1-one	35.3			Ketones
35	o-cresol/2-Methyl phenol	36.1	C_7H_8O	108.14	Phenols
36	3-Ethyl-2-Hydroxy-2-Cyclopenten-1-one/1.3-Ethyl-2-Hydroxy-2-Cyclopenten-1-one	36.5	$C_7H_{10}O_2$	126	Ketones
37	1H-indene, 1-Methylene-	37.5	$C_{10}H_8$	128	Aromatic Hydrocarbons
38	p,m-Cresol/3,4-Methyl phenol	37.9	C_7H_8O	108.14	Phenols
39	Anhydrosugar: unknown	39.06			
40	2-Methoxy-4-methyl phenol/Creosol/p-Methylguaiacol/4-Methylguaiacol	39.5	$C_8H_{10}O_2$	138.17	Guaiacols
41	Xylenols/Dimethyl phenol (2.3-; 2.4-; 2.5-)	39.9	$C_8H_{10}O$	122.17	Phenols
42	3,4,5-Trimethyl phenol	40.8	$C_9H_{12}O$	136	Phenols
43	Ethyl phenol (2-; 3-; 4-;)	41.7	$C_8H_{10}O$	122.17	Phenols
44	2-Ethyl-4-methyl-phenol	42.2	$C_9H_{12}O$	136	Phenols
45	2-Methyl-naphthalene	42.5	$C_{11}H_{10}$	142	Aromatic Hydrocarbons
46	3.4-Dimethyl phenol	42.9	$C_8H_{10}O$	122.17	Phenols
47	4-Ethyl-2-methoxyphenol/4-Ethyl guaiacol/4-Hydroxy-3-methoxy ethylbenzene/p-Ethylguaiacol	43.2	$C_9H_{12}O_2$	152.19	Guaiacols
48	1 H-Indene, 1-ethyidene	43.3	$C_{11}H_{10}$	142	Aromatic Hydrocarbons
49	2-Ethyl-6-methylphenol	43.6	$C_9H_{12}O_2$	136	Guaiacols
50	1,4:3,6-Dianhydro-.alpha.-D-glucopyranose	44.6	$C_6H_8O_4$	144.13	Sugars
51	1H-inden-1-one, 2,3-Dihydro-	44.6	C_9H_8	132	Aromatic Hydrocarbons
52	3-Ethyl-5-methylphenol	45.2	$C_9H_{12}O_2$	136	Guaiacols
53	4-Vinylphenol	45.3			Phenols
54	2.3-Dihydro-benzofuran	45.4	C_8H_8O	120	Phenols
55	2-Methoxy-4-vinylphenol/4-Vinylguaiacol/p-Vinylguaiacol/4-Hydroxy-3-methoxystyrene	45.6	$C_9H_{10}O_2$	150.18	Guaiacols
56	Eugenol/2-Methoxy-4-allylphenol/2-Methoxy-1-hydroxy-4-allybenzene/Allylguaiacol	46.6	$C_{10}H_{12}O_2$	164.2	Guaiacols
57	1.2-Benzenediol	47.6	$C_6H_6O_2$	110	Phenols
58	2,6-Dimethoxy phenol/Syringol/1,3-Dimethoxy-2-hydroxybenzene/Pyrogallol dimethylether	47.8	$C_8H_{10}O_3$	154.17	Syringols
59	4-(2-propenyl)-phenol	50.1			Guaiacols
60	2-methyl-Benzofuran	50.7	C_9H_8O	132	Phenols
61	9-.BETA.-D-ARABINOFURANOSYLGUANINE	50.9			Sugars
62	2-Methoxy-4-(1-propenyl)phenol/Isoeugenol,c&t/4-Propenylguaiacol/4-Hydroxy-3-methoxypropenylbenzene	51	$C_{10}H_{12}O_2$	164.2	Guaiacols
63	4-Methyl syringol/2,6-Dimethoxy-4-methylphenol	51.5	$C_9H_{12}O_3$	168.19	Syringols

64	Hydroquinone/1.4-Benzenediol/4-Hydroxyphenol/Dihydroxybenzene	52	$C_6H_6O_2$	110.11	Phenols
65	4-hydroxybenzaldehyde/4-Formylphenol	52.4	$C_7H_6O_2$	122.12	Misc. Oxygenates
66	2-Methyl-1.4-benzenediol/2-methylcatechol/Homocatechol/Toluene-3.4-diol	53.6	$C_7H_8O_2$	124.24	Phenols
67	4-Methyl-1.2-benzenediol/4-methylcatechol/Homocatechol/Toluene-3.4-diol	53.9	$C_7H_8O_3$	124.24	Phenols
68	4-ethyl-Syringol	54.4	$C_{10}H_{14}O_3$	182.22	Syringols
69	1-(4-Hydroxy-3-methoxyphenyl)ethanone/Acetoguaiacone	54.9	$C_9H_{10}O_3$	166.18	Guaiacols
70	4-Vinyl-2.6-dimethoxyphenol/Syringol-4-vinyl	56.6			Syringols
71	1-(4-hydroxy-3-methoxyphenyl)-2-Propanone/Guaiacylacetone/Vanillyl methyl ketone/4-Hydroxy-3-methoxyphenyl acetone	57.1	$C_{10}H_{12}O_3$	180.20	Guaiacols
72	4-Propenyl-2.6-dimethoxyphenol/Methoxyeugenol (sis)	59.1	$C_{11}H_{14}O_3$	194.23	Guaiacols
73	1,6-Anhydro-b-D-glucopyranose/Levoglucosan	60.6	$C_6H_{12}O_5$	162.14	Sugars
74	trans-4-Propenyl-2.6-dimethoxyphenol/Methoxyeugenol (trans)	61.4	$C_{11}H_{14}O_3$	194.23	Guaiacols

Table 6-8: Peak area percentages of chemical compounds present in the organic heavy fraction and aqueous light fraction of Pot 1 of wheat straw derived oil

ID	180110	270110	301109	91209	270110	301109	91209
	Homogeneous	Organic heavy fraction			Aqueous light fraction		
1	0.35	N.D.	N.D.	N.D.	N.D.	N.D.	N.D.
2	N.D.	N.D.	N.D.	N.D.	0.99	N.D.	N.D.
3	9.41	6.87	0.55	1.27	28.07	30.04	31.78
4	16.29	11.01	5.51	0.79	24.10	19.18	17.84
5	N.D.	N.D.	N.D.	0.18	N.D.	N.D.	N.D.
6	N.D.	0.16	0.22	N.D.	0.45	N.D.	N.D.
7	1.49	0.22	0.48	0.23	1.49	1.39	2.35
8	1.11	0.96	0.68	0.26	1.21	1.20	0.36
9	2.39	1.20	1.12	0.30	1.46	3.28	2.83
10	2.51	0.98	0.46	N.D.	1.89	2.09	N.D.
11	3.21	4.78	5.07	N.D.	3.31	3.80	N.D.
12	N.D.	N.D.	N.D.	2.79	N.D.	N.D.	4.00
13	0.53	0.62	0.50	0.96	N.D.	0.60	1.99
14	1.73	1.93	1.34	0.26	1.95	1.98	0.84
15	0.49	1.06	1.33	0.20	0.56	0.75	0.87
16	0.63	0.42	0.38	N.D.	0.82	0.63	N.D.
17	N.D.	0.38	0.46	0.60	N.D.	N.D.	N.D.
18	N.D.	N.D.	N.D.	N.D.	N.D.	N.D.	N.D.
19	N.D.	N.D.	N.D.	N.D.	0.60	0.40	N.D.
20	0.29	0.60	N.D.	N.D.	0.92	0.44	N.D.
21	0.10	0.34	0.56	0.42	0.15	N.D.	0.15
22	1.02	1.58	1.64	2.13	0.83	N.D.	1.27
23	N.D.	N.D.	N.D.	N.D.	N.D.	N.D.	3.76
24	0.76	N.D.	0.86	0.82	N.D.	1.14	4.23
25	N.D.	N.D.	N.D.	0.36	N.D.	N.D.	0.60
26	0.54	0.67	0.57	N.D.	0.42	0.39	N.D.
27	4.79	4.13	2.73	1.79	2.73	3.66	2.38
28	N.D.	N.D.	0.36	N.D.	N.D.	N.D.	N.D.
29	0.39	0.42	0.30	N.D.	0.34	0.32	N.D.
30	2.48	3.64	4.07	10.14	1.23	1.00	5.04
31	N.D.	N.D.	N.D.	0.21	N.D.	N.D.	N.D.
32	N.D.	N.D.	N.D.	0.20	N.D.	N.D.	N.D.
33	1.92	4.35	5.07	0.29	1.61	1.48	N.D.
34	0.15	N.D.	N.D.	1.10	0.11	0.10	N.D.
35	0.65	1.65	1.77	4.33	0.57	0.36	0.82
36	N.D.	0.99	1.09	N.D.	N.D.	0.54	N.D.
37	N.D.	N.D.	N.D.	1.03	N.D.	N.D.	N.D.
38	0.53	0.92	0.97	3.00	0.27	0.19	0.52
39	0.07	N.D.	N.D.	N.D.	0.54	1.55	N.D.
40	0.37	1.19	1.60	N.D.	0.26	0.23	N.D.
41	0.29	0.86	0.95	0.64	0.18	0.18	0.16
42	N.D.	N.D.	N.D.	0.28	N.D.	N.D.	N.D.
43	1.04	1.21	2.15	3.33	0.19	N.D.	0.25
44	N.D.	N.D.	N.D.	0.24	N.D.	N.D.	N.D.
45	N.D.	N.D.	N.D.	0.66	N.D.	N.D.	N.D.
46	N.D.	N.D.	N.D.	0.63	N.D.	N.D.	N.D.
47	0.24	1.18	1.67	0.17	N.D.	0.25	N.D.
48	N.D.	N.D.	N.D.	0.36	N.D.	N.D.	N.D.
49	N.D.	N.D.	N.D.	0.71	N.D.	N.D.	N.D.
50	0.70	N.D.	N.D.	N.D.	0.43	0.62	1.22
51	N.D.	N.D.	N.D.	0.88	N.D.	N.D.	N.D.
52	N.D.	N.D.	N.D.	0.40	N.D.	N.D.	N.D.
53	N.D.	N.D.	N.D.	N.D.	N.D.	N.D.	N.D.
54	2.13	N.D.	1.84	0.22	N.D.	0.15	0.22
55	1.50	3.91	3.16	N.D.	0.32	0.16	N.D.

56	N.D.	1.25	1.14	N.D.	0.13	N.D.	N.D.
57	N.D.	N.D.	N.D.	N.D.	N.D.	N.D.	1.93
58	4.26	2.40	3.31	N.D.	0.89	0.96	N.D.
59	N.D.	N.D.	0.57	0.67	N.D.	N.D.	N.D.
60	N.D.	N.D.	N.D.	0.46	N.D.	N.D.	N.D.
61	0.91	N.D.	N.D.	N.D.	0.42	0.60	0.27
62	1.52	0.58	0.82	N.D.	0.18	N.D.	N.D.
63	1.08	0.49	0.78	N.D.	0.10	0.13	N.D.
64	1.67	0.96	N.D.	N.D.	0.79	0.47	1.74
65	0.24	0.42	N.D.	N.D.	0.17	N.D.	N.D.
66	N.D.	N.D.	N.D.	N.D.	N.D.	N.D.	1.17
67	0.90	0.70	N.D.	N.D.	0.42	0.33	N.D.
68	0.62	0.35	0.81	N.D.	N.D.	N.D.	N.D.
69	0.42	0.38	N.D.	N.D.	0.18	N.D.	N.D.
70	1.16	0.59	0.84	N.D.	N.D.	N.D.	N.D.
71	0.41	0.21	0.50	N.D.	0.11	N.D.	N.D.
72	0.29	0.27	N.D.	N.D.	N.D.	N.D.	N.D.
73	2.57	N.D.	N.D.	N.D.	2.00	N.D.	1.00
74	1.45	0.54	1.71	N.D.	0.13	N.D.	N.D.

Table 6-9 shows the relatively peak area percentages of chemical groups and the reaction temperature effect for wheat straw.

Table 6-9: The effect of temperature and different reactor systems on pyrolysis products. Cells highlighted in green show a significant variation from wheat straw at 500°C for the 300g and 1 kg system (270110 and 180110 respectively)

Relatively peak area (%)-chemical groups	**180110 Homo-geneous**	**270110**	**301109**	**91209**	**270110**	**301109**	**91209**
		Organic heavy fraction			**Aqueous light fraction**		
Minimum Pyrolysis T (°C)	468	480	386	509	480	386	509
Average Pyrolysis T (°C)	500	492	421	518	492	421	518
Maximum Pyrolysis T (°C)	512	522	469	550	522	469	550
Acids	9.41	6.87	0.55	1.27	28.07	30.04	31.78
Aldehydes	6.35	6.18	5.92	N.D.	6.01	6.52	N.D.
Aromatic Hydrocarbons	N.D.	N.D.	N.D.	3.34	N.D.	N.D.	N.D.
Furans	2.95	4.01	3.07	5.49	3.63	3.36	6.50
Sugars	4.18	N.D.	N.D.	N.D.	2.85	1.22	2.49
Ketones	6.79	7.75	7.16	5.76	4.24	5.05	5.12
Misc. Oxygenates	22.14	14.94	8.67	1.58	30.61	25.84	23.86
Phenols	9.69	9.94	11.76	22.57	3.66	2.67	12.03
Guaiacols	8.11	13.86	16.26	2.49	2.93	2.12	N.D.
Syringols	7.12	3.83	5.73	N.D.	0.99	1.08	N.D.

Conclusions can be drawn only for significant variation from the runs 180110 and 270110. Noteworthy variations were:

- Aldehydes were eliminated with the increase of reaction temperature.
- The formation of aromatic hydrocarbons occurred for run with reference 91209 (greater reaction temperature).

- Sugars were produced only on the aqueous light fraction of the runs 270110, 301109, 91209 (300g reactor system) and in 180110 (1kg reactor system – homogeneous oil).
- The reduction of misc. oxygenates followed the temperature decrease.
- Phenols increased significant for run 91209, while guaiacols and syringols decreased.

6.5 Chapter conclusions

Wheat straw is an interesting feedstock because it is abundance and it is an agricultural residue. The thermochemical processing of straw by fast pyrolysis revealed that several problems occurred. Feeding and blockages to the existing equipment were due to the feedstock type. The low bulk density of the straw, as well as the nature of the feedstock, were the main reasons for the feeding problems. The high ash content caused pre-pyrolysis and agglomeration on both the 300g/h and 1 kg/h fluidised bed reactor systems. The main conclusion concerning the existing 300g/h system is that the modified feeding system is beneficial for processing of wheat straw, in comparison with the original feeding system. Further work needs to be conducted to establish optimum fluidisation velocity for avoiding the agglomeration phenomenon.

The wheat straw derived bio-oil that was produced from the 300g/h reactor system (chillers) was phase separated. This could be a significant problem for the use of the oil as a fuel. The 1kg/h reactor system (quench column) formed a homogenous oil. This could be due the different cooling system of the 1kg reactor system. The cooling of the pyrolysis vapours was probably more effective with the latter cooling system and it seems to be beneficial for the homogenous nature of the oil. Further research could be conducted on the effect of various cooling systems on the bio-oil production.

The pyrolysis reaction temperature had a significant effect on pyrolysis product yields. It seems that with a temperature increase, the organic yields reached a maximum around 500^{o}C and then a reduction was obtained. Char yields were reduced with a temperature increase. Concerning the gas yields the reverse tendency was noticed.

Regarding the chemical distribution absolute conclusions cannot be draw due the phase separate nature of the bio-oil and the high temperature drop. General conclusions are that in wheat straw derived oil, the chemicals produced in a significant level were the carboxylic acids and the phenolics compounds (phenols, guaiacols, syringols).

7 RESULTS FROM PYROLYSIS OF RAW AND PRE-TREATED FEEDSTOCKS

This chapter compares the fast pyrolysis results obtained from untreated and pre-treated biomass, in terms of pyrolysis products yields and chemical distribution on bio-oil. The influence of pre-treatment methods on bio-oil quality is also examined. Further, limitations of the equipment and recommendations are discussed.

7.1 Introduction

This chapter investigates the influence of the pre-treatment processes of torrefaction, aquathermolysis and steamed pre-treatment on pyrolysis products. Further details with reference to the pre-treatment processes can be found in Section 2.4.1.

Fast pyrolysis experiments have been performed with untreated and pre-treated poplar, spruce and wheat straw. The equipment used was the 100g/h fluidized bed reactor with a pneumatic feeder and the 300g/h fluidized bed reactor with a screw feeder. The pathways used in the current work are depicted in Figure 7-1 for wheat straw, poplar and spruce.

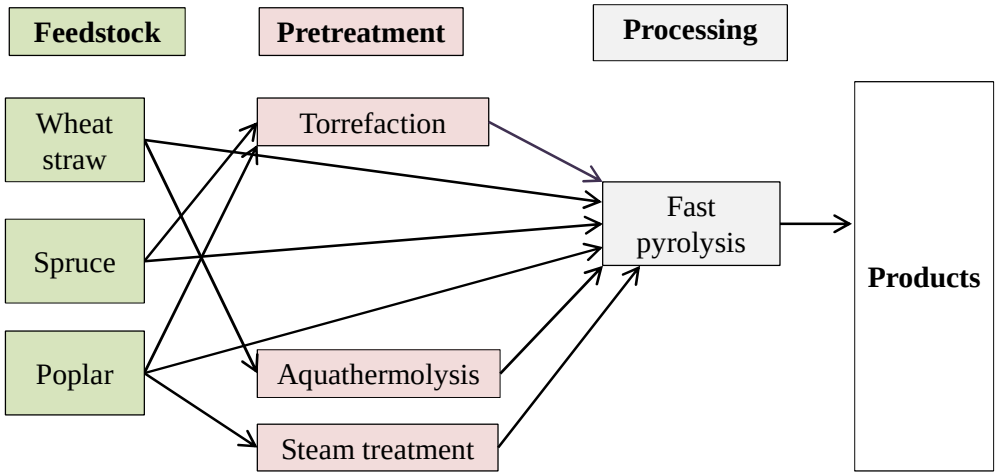

Figure 7-1: Combinations for product production by pre-treatment and fast pyrolysis

A larger scale experiment was performed with torrefied poplar using the 1000g/h bubbling fluidized bed reactor system of ECN, which was described in Chapter 4. This was used for comparison with Aston's bench scale system.

7.2 100 g/h and 300g/h units at Aston

7.2.1 Results

Of the 42 fast pyrolysis runs carried out in total, 10 were used to investigate the effect of pre-treatment on the yield and quality of fast pyrolysis products. The results from

these runs are summarised in Table 7-1, which includes the operating conditions, the yields of pyrolysis liquids, char and gases and the mass balance closures of the runs.

Table 7-1: Mass balances of fast pyrolysis runs using untreated and Pre-treated poplar, spruce and wheat straw on 100g/h and 300g/h

Test reference	31108	281008*	200309	81008	111208*	131008*~	120309*~	160211#	270110#	140709#
Nominal capacity of reactor	100g/h	100g/h	100g/h	100g/h	100g/h	100g/h	100g/h	300g/h	300g/h	300g/h
Vapour residence time (sec)	1.26	1.23	1.25	1.28	1.28	1.33	1.34	0.56	0.66	1.00
Average feed rate	73.9g/h	65.3g/h	64.4g/h	63.1g/h	65.7g/h	63.8g/h	42.6g/h	35g/h	93g/h	99.7g/h
Run time (min)	22	60	70	70	66	55	60	51	51	41
Product collection system	Cooler + ESP	Cooler + ESP	Cooler + ESP	Cooler + ESP	Cooler + ESP	Cooler + ESP	Cooler + ESP	Cooler + ESP	Cooler + ESP	Cooler + ESP
Fluidised N_2 flow rate (l/min)	6	6	6	6	6	6	6	2	12	8
Feeder N_2 flow rate (l/min)	1	1	1	1	1	1	1	14	2	2
Fluidising medium	Sand	Sand	Sand	Sand	Sand	Sand	Sand	Sand	Sand	Sand
Sand particle size	355-500	355-500	355-500	355-500	355-500	355-500	355-500	355-500	500-600	355-500
Feedstock	**Torrefied spruce**	**Spruce**	**Spruce**	**Poplar**	**Poplar**	**Torrefied poplar**	**Torrefied poplar**	**Steamed poplar**	**Wheat straw**	**Aqua' wheat straw**
Particle size (mm)	355-500	355-500	355-500	355-500	355-500	355-500	355-500	355-500	< 1mm	355-500
Moisture content (wt%, wet basis)	2.29	6.96	3.85	8.61	6.38	3.45	3.31	3.84	8.78	4.09
Ash content (wt%, dry basis)	0.46	0.22	0.22	1.16	1.2	2	2.1	0.35	8.8	5.4
Average pyrolysis T (^oC)	527	551	538	516	516	485	482	499	492	489
Product yields (wt%, dry feed)										
Char	**36.88**	**31.95**	**12.72**	**14.1**	**9.89**	**25.13**	**19**	**8.32**	**31.74**	**24.85**
Liquids	**49.25**	**62.29**	**68.65**	**74.65**	**73.6**	**57.7**	**58.6**	**68.62**	**43.32**	**47.91**
Organics	32.86	56.21	56.22	64.78	65.11	50.2	44.01	49.45	21.75	41.73
Gases	**7.75**	**13.48**	**15.58**	**7.89**	**10.28**	**7**	**13.6**	**15.9**	**13.13**	**21.94**
H_2	N.D.	0.02	0.08	0.03	0.05	0.17	0.06	0.05	0.03	0.1
CH_4	0.6	0.43	0.80	0.37	0.56	0.67	0.68	0.86	0.38	1.61
CO	3.53	5.23	6.98	3.60	4.53	2.44	5.29	4.96	3.89	12.96
C_2H_4	3.38	0.08	0.16	0.04	0.12	0.10	0.09	0.55	0.12	0.76
C_2H_6	0.07	0.08	0.08	0.07	0.09	0.10	0.10	0.51	0.38	0.23
C_3H_8	0.07	0.07	0.11	0.06	0.10	0.10	0.09	1.62	0.03	0.46
C_3H_6	0.06	0.04	0.03	0.01	0.02	0.06	0.04	0.85	0.10	0.05
C_4H_{10}	0.02	0.01	0.02	0.01	0.04	0.01	0.01	0.95	0.02	0.11
CO_2	N.D.9	7.53	7.32	3.71	4.74	3.31	7.25	5.54	8.17	5.65
Closure (wt%, dry basis)	93.89	107.72	96.95	96.58	93.76	89.83	91.2	92.84	88.19	94.7
# using 300 g/h unit with screw feed due to feeding problems										
*run had to stop several times to unblock the entrainment tube; probably oxygen went through the system										
~blockages were caused in the feeding tube inside the reactor and in the water cooled condenser, probably due to fractionation of the heavy components										

7.2.2 Operating problems encountered

7.2.2.1 Feeding and blockages

The main limitation of the 100g/h fluidised reactor system is the pneumatic feeding system. The feeder consists of a tubular storage hopper, a stirrer and an entrainment tube. The feed rate of the biomass is controlled by the speed of the stirrer, the entrainment nitrogen flow rate and the feeder top nitrogen flow rate. The cooling of the entrainment tube is by air and it is not sufficient, resulting in pre-pyrolysis of biomass and limits the variety of feedstocks that could be used with the existing system. The feeding system is illustrated in detail in Figure 7-2 below [103].

Figure 7-2: 100g/h fluidised bed reactor and entrainment tube [103]

Several problems occurred during the fast pyrolysis runs with untreated poplar and spruce. Blockages inside the entrainment tube occurred during the run with reference 281008 and 111208. The runs had to be stopped to unblock the tube which typically took 5 to 10 minutes. The nitrogen tube that was connected to the entrainment tube had to be removed to unblock the tube, and this probably caused air to go through the system. This could be

an explanation of the higher gas content for run 111208 (poplar). Especially for the run 281008 (spruce) the tube blocked several times during the run. This could explain the bad mass balance (107 %) and the higher char content (31.95%).

In the case of torrefied wood (poplar and spruce) several problems also occurred. Feeding was possible, but irregular. In both cases blockages were caused in the feeding tube inside the reactor and in the water cooled condenser, probably due to fractionation of the heavy components. Another explanation could be the nature of the feedstock, which had become brittle and very easy to become powder. The separation efficiency of the cyclone becomes very low when it comes to fine particle size. To add to this, the pre-treatment of woods by torrefaction increased the proportion of char content, due the removal of hemicellulose. It was observed that it was an increase in pressure on the cyclone, while the feeder pressure was stable. This indicated a blockage after the cyclone.

Feeding only for few seconds was possible for wheat straw using the 100g/h fluidised bed reactor system. Pre-pyrolysis of wheat straw occurred inside the entrainment tube possibly due the high ash content and subsequently high alkali metals level of the feedstock. Feeding of wheat straw was not possible even after pre-treatment by aquathermolysis, which reduced the amount of inorganic compounds. The pre-treatment made the material brittle and the pneumatic feeder did not have the capacity to feed it. A screw feeding system was necessary, resulting into the use of the 300g/h reactor system.

7.2.2.2 Temperature control

The operating conditions in particular pyrolysis reaction temperatures vary to some extent due to uncontrollable situations. The 100g reactor used an external furnace as a heat source, while the 300g reactor used two external heaters. Fluctuations on temperature control, due to limitations of the furnace heaters, occurred for both reactor systems, causing difficulties to obtain the desirable pyrolysis temperature. This could also cause differences on the pyrolysis products yield.

7.2.3 Discussion of results

It can be seen from Table 7-1that the mass balance closures varies in the range of 88.2 to 107.0 wt% dry biomass basis. An explanation of the low mass balance could be due the undetectable permanent gases. The presence of extra peaks was noticed in the gas chromatograms. Those peaks could not be identified, due to the GC column limitations.

This could imply that the unidentified and undetectable permanent gases may be one of the reasons for the loss in the mass balance.

7.2.3.1 Effect of pre-treatment processes on liquid yields of woods

Figure 7-3 below shows that higher liquid yields were obtained from the processing of untreated poplar in comparison with torrefied poplar. Similar findings are found for untreated and torrefied spruce. This observation was expected, since the ash content and consequently the inorganic compounds on the feedstocks were increased during the pre-treatment process of torrefaction. The production of liquid yield could be reduced owing to the catalytic effect of alkali metals. The comparison of pre-treatment methods shows that higher liquid yields was produced for the steamed treated poplar (68.62%) than the torrefied poplar (57.7%). During steam treatment ash levels was reduced, indicating removal of alkali metals. In conclusion, the processing of pre-treated feedstocks by torrefaction caused a reduction on liquid yields for both woods.

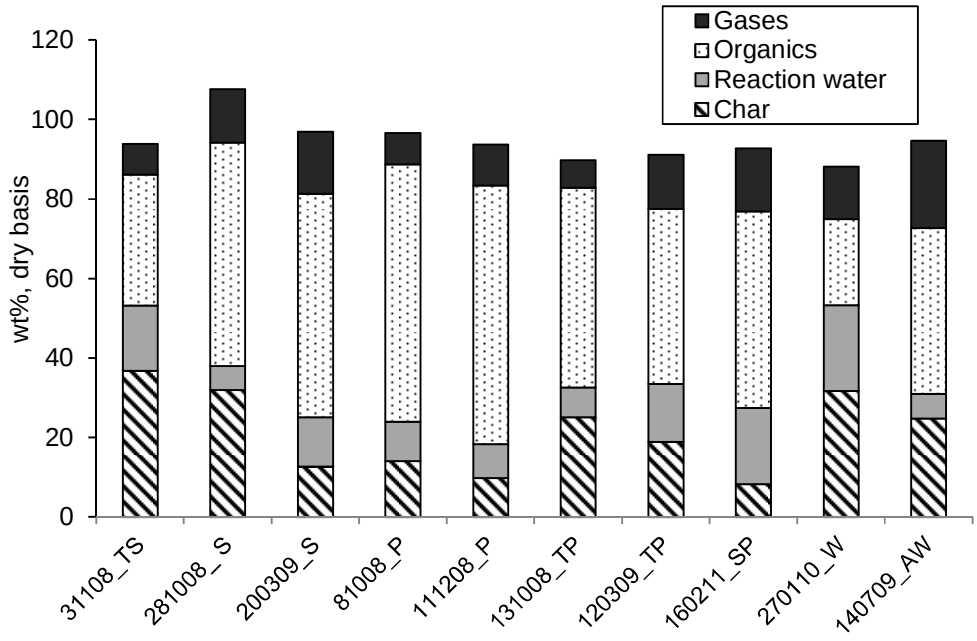

Figure 7-3: Pyrolysis products yields expressed on dry biomass basis

The water in bio-oil is derived from the original moisture in the feedstock and from pyrolysis as a product from dehydration reactions. The organic part of bio-oil is the non-water part that contains the desirable products. It should be mentioned that only the organic part of bio-oil is listed in Table 7-1. The pyrolysis of steamed treated poplar gave higher liquid yields, even though the organic parts of both torrefied and steamed poplar are

similar. In the case of spruce, lower organic yields were observed from run 31108 for pyrolysis of torrefied spruce.

7.2.3.2 Effect of pre-treatment on poplar char yields

It was reported in Section 2.4.1 that both torrefaction and hot pressurised steam treatment significantly reduced hemicellulose in poplar. Results are in agreement with thermogravimetry analysis (TGA) and were discussed in Chapter 5 above. This is also in agreement with other studies [104, 105]. Torrefaction caused hemicellulose to degrade; cellulose proportion and char content increased. The runs with reference 131008 and 120309 also proved it, since the char content was 25 wt% and 19 wt% respectively whereas the char content for fresh poplar was 10 – 14wt%. This is illustrated in Figure 7-4 below. Another finding is that steamed pre-treatment reduced the char content. According the run with reference 160211 char content was reduced when is compared with untreated poplar.

7.2.3.3 Effect of Aquathermolysis on liquid and char yields of wheat straw

Hot pressurised water treatment (aquathermolysis) caused the water soluble minerals (particularly potassium) to be reduced by a considerable amount. The biomass decomposition behavior would be affected, since the metal compounds are known to have catalytic effect and increased the yields of gases and H_2O. This could be an explanation for the lower amount of reaction water and higher level of gas when comparing with untreated wheat straw.

Figure 7-4-Figure 7-6 show the gas composition from pyrolysis experiments of untreated and pre-treated feedstocks. The data represents on a nitrogen free and dry biomass basis, the composition on weight percent (wt %, dry basis) of each gas evolved with the total gas yield in Table 7-1. According to Figure 7-4 - Figure 7-6 the gaseous products contain mainly of carbon dioxide and carbon monoxide with small portions of C_1-C_4 hydrocarbon and hydrogen gases.

7.2.3.4 Influence of Torrefaction on gases for both woods

It can be noticed from Figure 7-4 that the processing of torrefied poplar led to an increase in CO_2 proportion and a decrease in CO proportion. The same observation could be made for pre-treated spruce according to Figure 7-5. This could be possible caused by the increase of char levels and consequently the inorganic level in ash.

7.2.3.5 Influence of Steam treatment on gases for poplar

Regarding the hot pressurised steam treatment (steamed poplar) Figure 7-4 shows a reduction in CO_2 and CO levels and a significant increase in C_2-C_4 yields. An explanation could be that the steam pre-treatment lowered the ash content and removed inorganic compounds of the original feedstock.

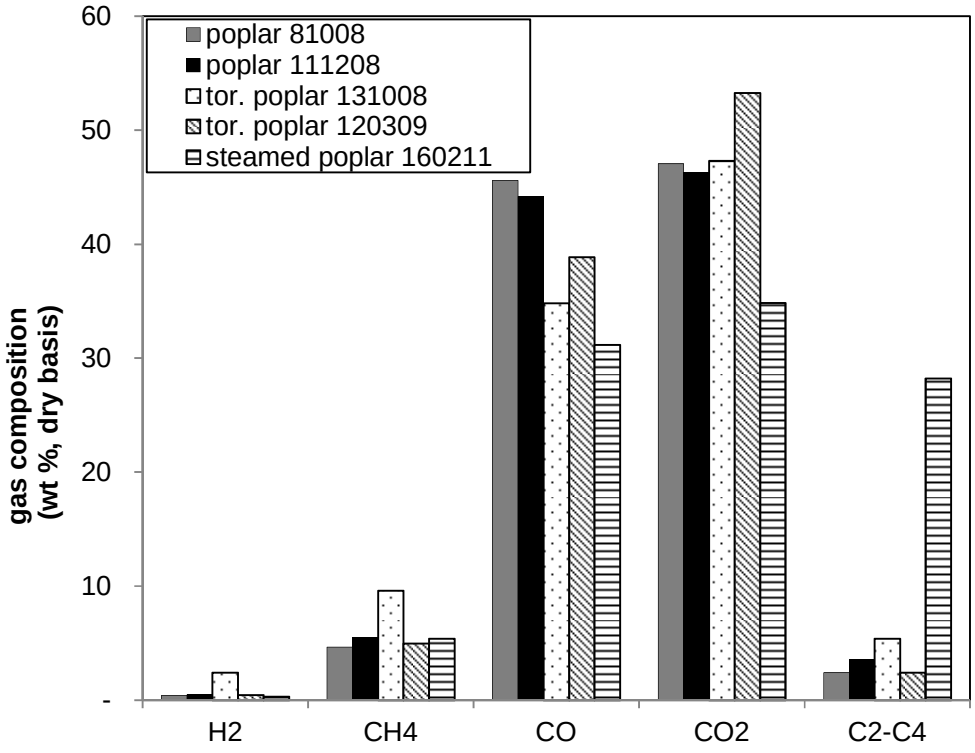

Figure 7-4: Gas composition on a nitrogen free and dry biomass basis of weight percent (wt %, dry basis) from the fast pyrolysis runs using untreated and pre-treated poplar

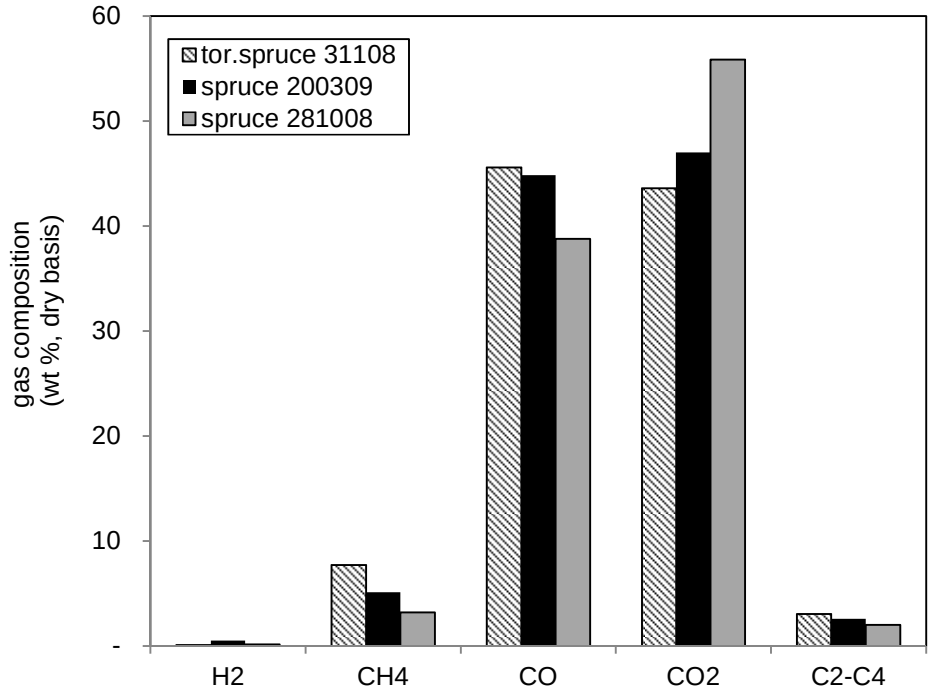

Figure 7-5: Gas composition on a nitrogen free and dry biomass basis of weight percent (wt %, dry basis) from the fast pyrolysis runs using untreated and pre-treated spruce

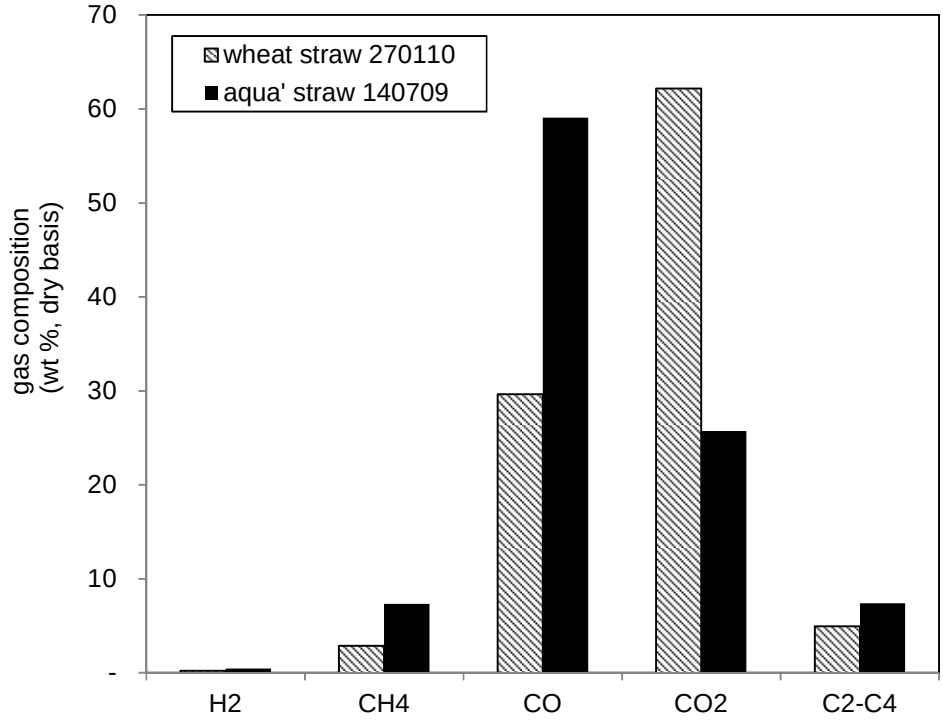

Figure 7-6: Gas composition on a nitrogen free and dry biomass basis of weight percent (wt %, dry basis) from the fast pyrolysis runs using untreated and pre-treated wheat straw`

7.2.3.6 Influence of Aquathermolysis on gases from wheat straw

For the case of aquathermolised wheat straw Figure 7-6 illustrates the effect of pre-treatment on wheat straw pyrolysis gases. CO_2 levels has significant decreased, while CH_4, C_2-C_4, CO and H_2 yields increased. This observation could be justified by the removal of the water soluble minerals (potassium) to a considerable level by aquathermolysis. The removal of minerals in the case of aquathermolysis is more apparent when comparing with the process of steam treatment and this could be due to the initial higher ash content of straw.

7.2.4 Bio-oil analysis

The properties of bio-oil obtained from fast pyrolysis of untreated and pre-treated poplar, spruce, and wheat straw, were studied. This includes water, pH value, basic elemental composition, heating value, molecular weight distribution, and chemical composition by GC/MS analysis.

It is important to highlight that the bio-oil produced from the 100 g/h and 300g/h fluidised reactor were collected in three locations (pot 1, pot 2 and pot 3) as mentioned in Section4.8.1. In the case of wheat straw (run 270110) pot 1 contained phase separated oil and it is divided in aqueous light fraction and heavy organic fraction.

Concerning the water content and pH value, pot 1 and a mixture of pot 2 and pot 3were analysed. The determination of elements, molecular weight and chemical compounds were done only in the fraction of pot 1. This could be justified by the high water content (> 70%) of pot 2 and pot 3.

7.2.4.1 Water content

As it has been discussed before in section 6.4.1 the water in bio-oil derived from the original moisture in the feedstock and from pyrolysis as a product from dehydration reactions. The variation of bio-oil water content depends on the feedstock water content and the process severity in terms of secondary reactions [38].

The reaction water content was discussed above in Section 7.2.3.1. The amount of water present in bio-oils is important because this effects its quality.

Table 7-2 shows the percentage of water content produced from untreated and pre-treated poplar, spruce and wheat straw using the 100g/h and 300g/h reactor systems. Wheat straw derived bio-oil is a phase separate oil. The aqueous phase water content is 67 %, while the heavy phase is 13%. An interesting finding is that the run with reference 140709 (aquathermolised wheat straw) produced a homogenous oil with water content of 7.14 %, whereas fresh wheat straw derived bio-oil was a phase separate oil. For the case of wheat straw, pre-treatment of biomass influence the homogeneity of the bio-oil.

For steamed poplar the water content was increased, while treatment by torrefaction reduced it. In the case of torrefied spruce the water content increase when the run 200309 is taken as reference, since it was the run with no problems.

7.2.4.2 Basic elemental composition, molecular weight distribution and pH value analysis

The elemental composition, heating value, molecular weight distribution and pH value analysis are listed in Table 7-3 below.

It was found that the Pot 2+3 oils were more acidic than the Pot 1 oils. The low pH values of bio-oils are caused by the presence of carboxylic compounds such as formic and acetic acids in large proportion. The comparison of pre-treated and untreated derived oils shows no significant differences in terms of pH content.

Pre-treatment had an influence on the molecular weight of bio-oils. For all feedstocks a reduction on molecular weight was observed, after pre-treatment.

Table 7-2: Water content of bio-oil produced from fast pyrolysis of untreated and pre-treated poplar, spruce and wheat straw

Test ref.	31108	281008	200309	81008	111208	131008	120309	160211	140709	270110	
Feed	**Tor' spruce**	**Spruce**	**Spruce**	**Poplar**	**Poplar**	**Tor' poplar**	**Tor' poplar**	**Steam' poplar**	**Aqua' wheat straw**	**Wheat straw**	
T (°C)	527	551	538	516	516	485	482	499	489	492	
Water content %										**Aqueous light fraction**	**Heavy organic fraction**
Pot 1	28.81	34.74	16.59	18.09	19.49	8.34	16.59	25.6	7.14	67	13
Pot 2+3	90.53	73.38	68	63.84	62	62.62	70.41	64.6	79.29	75.24	-

Table 7-3: pH and molecular weight of bio-oil produced by fast pyrolysis of untreated and pre-treated poplar, spruce and wheat straw

Test ref.	281008	200309	81008	111208	131008	120309	160211	270110		140709
Feed	Spruce	Spruce	Poplar	Poplar	Torrefied poplar	Torrefied poplar	Steamed poplar	Wheat straw		Aqua' wheat straw
								Aqueous Light fraction	Organic Heavy fraction	
Molecular weight (g/mol)										
Mw	467	463	547	573	397	381	252	495	621	295
Mn	259	307	303	332	230	269	140	238	255	191
PD	1.80	1.51	1.80	1.73	1.73	1.42	1.80	2.08	2.43	1.54
pH										
Pot 1	2.15	2.6	2.74	2.56	2.67	2.29	3.47	3.36	3.11	2.82
Pot 2 +3	2.26	1.99	2.12	2.08	1.99	2.11		2.1		2.14
Elemental analysis (wt%, dry basis)										
C	55.90	53.31	54.88	55.66	51.61	55.39	62.67	80.88	71.09	55.74
H	6.50	7.01	6.65	6.46	6.68	6.63	6.02	4.65	6.26	6.76
N	0.21	0.12	0.21	0.20	0.11	0.12	0.20	0.64	1.07	0.28
O	37.39	39.57	38.27	37.70	41.60	37.87	31.14	13.89	21.59	37.23
Heating values (MJ/kg)										
HHV_{dry}	23.30	22.78	23.04	23.15	21.59	23.23	25.75	32.27	29.94	23.57
HHV_{wet}	15.21	19.00	18.87	18.63	19.79	19.37	19.15	10.65	26.05	21.89
LHV_{dry}	21.88	21.36	21.62	21.73	20.17	21.81	24.33	30.85	28.53	22.15
LHV_{wet}	13.43	17.41	17.27	17.02	18.28	17.79	17.47	8.55	24.50	20.40

7.2.5 Chemical analysis by GC/MS

The compounds in each sample are based on the chromatograms obtained from the GC/MS and were identified using both literature [106, 107, 108, 109, 110, 111] and from the mass spectra of the Perkin Elmer NIST computer library. The aim of this analysis was to identify and 'semi-quantify' the chemical compounds present in untreated and pre-treated poplar, spruce, and wheat straw derived oil. The term 'semi-quantify' is used because the GC/MS cannot quantify the chemicals; the peak areas obtained from the chromatograms are not a direct relation with concentration. Peak area should be used with caution, since it shows the relative amount of one chemical in relation with the total chemicals obtained by the chromatogram.

It should be mentioned that for run 270110 phase separated oils were produced and the fraction of pot 1 of organic heavy and aqueous light fraction were subjected to analysis. It is also important to add that the fraction of pot 1 was dissolved in a solvent (ethanol) at a concentration of approximately 25 wt% organics.

7.2.5.1 Analysis of torrefied spruce, torrefied poplar, and steamed poplar derived oil

Regarding the screening of the untreated and pre-treated poplar oil, the chromatographic peak areas that were over 0.5 % were identified and are shown below in Figure 7-7-Figure 7-9 and Table 7-4-Table 7-6. A detailed identification of the chemicals presented in pot 1 of fresh and pre-treated poplar derived oils are listed in APPENDIX - A in Table 12-1.

Overall observations from the analysis showed that bio-oil contained oxygenated compounds which are in the group of aldehydes, ketones, furans, carboxylic acids, sugars, and phenolics (phenols, guaiacols and syringols) chemical groups.

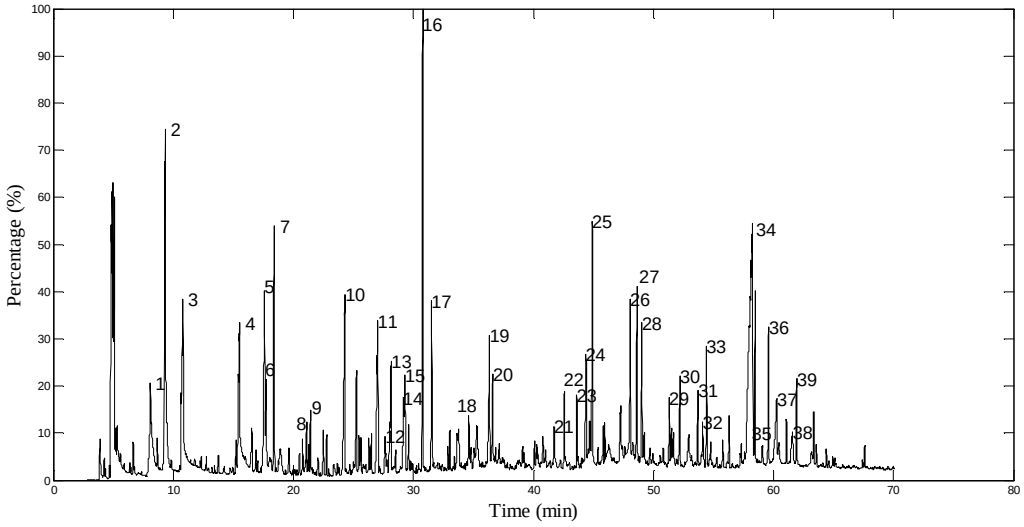

Figure 7-7: Chromatogram obtained by GC/MS and chemical identification, poplar derived oil. See Table 7-4 for key

Table 7-4: Identification of chemicals from poplar derived oil by GC/MS

1: Hydroxyacetaldehyde/Glycolaldehyde
2: Acetic acid/Ethanoic acid
3: Hydroxypropanone/1-Hydroxy-2-propanone/Acetone alcohol
4: 3-Hydroxypropanal
5: Butanedial/Succinaldehyde
6: 2-Hydroxy-3-oxobutanal
7: Furfural/furan-2-carboxaldehyde/fural/furfuraldehyde/2-furaldehyde/pyromucic aldehyde
8: 1-Acetyloxy-2-propanone/1-Acetoxypropane-2-one/2-Oxopropyl acetate
9: 2-Ethyl-butanal/Tetrahydro-4-methyl-3-furanone
10: 2.3-Dihydro-5-methylfuran-2-one
11: (5H)-furan-2-one/2(5H)-Furanone
12: 2(5H)-FURANONE, 5-METHYL-
13: 4-Hydroxy-5.6-dihydro-(2H)-pyran-2-one
14: 2-Hydroxy-1-methyl-1-cyclopentene-3-one/Maple lactone/2-Hydroxy-3-methyl-2-cyclopenten-1-one
15: 2-Hydroxy-1-methyl-1-cyclopentene-3-one/Maple lactone & 2.5-Dimethylcyclopentanone
16: Phenol
17: 2-Methoxyphenol
18: methyl-butyraldehyde derivate
19: 2-Methoxy-4-methyl phenol/Creosol/p-Methylguaiacol/4-Methylguaiacol
20: anhydrosugar:unknown
21: 1.4:3.6-Dianhydro-a-d-glucopyranose
22: 2-Methoxy-4-vinylphenol/4-Vinylguaiacol/p-Vinylguaiacol/4-Hydroxy-3-methoxystyrene
23: Eugenol/2-Methoxy-4-allylphenol/2-Methoxy-1-hydroxy-4-allylbenzene/Allylguaiacol
24: 5-(Hydroxymethyl)-2-Furancarboxaldehyde/5-(Hydroxymethyl)-2-furfural/HMF/5-(Hydroxymethyl)-2-furaldehyde
25: 2,6-Dimethoxy phenol/Syringol/1,3-Dimethoxy-2-hydroxybenzene/Pyrogallol dimethylether
26: 2-Methoxy-4-(1-propenyl)phenol/Isoeugenol,c&t/4-Propenylguaiacol/4-Hydroxy-3-methoxypropenylbenzene
27: 4-Methyl syringol/2,6-Dimethoxy-4-methylphenol
28: Vanillin/2-Methoxy-4-formylphenol/4-Hydroxy-3-methoxybenzaldehyde
29: Homovanillin
30: 1-(4-Hydroxy-3-methoxyphenyl)ethanone/Acetoguaiacone
31: 4-Vinyl-2.6-dimethoxyphenol/Syringol-4-vinyl
32: 1-(4-hydroxy-3-methoxyphenyl)-2-Propanone/Guaiacylacetone/Vanillyl methyl ketone/4-Hydroxy-3-methoxyphenyl acetone
33: trans-4-Propenyl-2.6-dimethoxyphenol/Methoxyeugenol
34: 1,6-Anhydro-b-D-glucopyranose/Levoglucosan
35: trans-4-Propenyl-2.6-dimethoxyphenol/Methoxyeugenol (trans)
36: 4-Hydroxy-3.5-dimethoxybenzaldehyde/Syringaldehyde/Syringe aldehyde/Cedar aldehyde
37: 4-Hydroxy benzoic acid
38: Anhydrosugar: unknown

39: 1-(4-Hydroxy-3-dimethoxyphenyl)ethanone/Acetosyringone/3.5-dimethoxy-1-hydroxyacetophenone/Acetosyringon

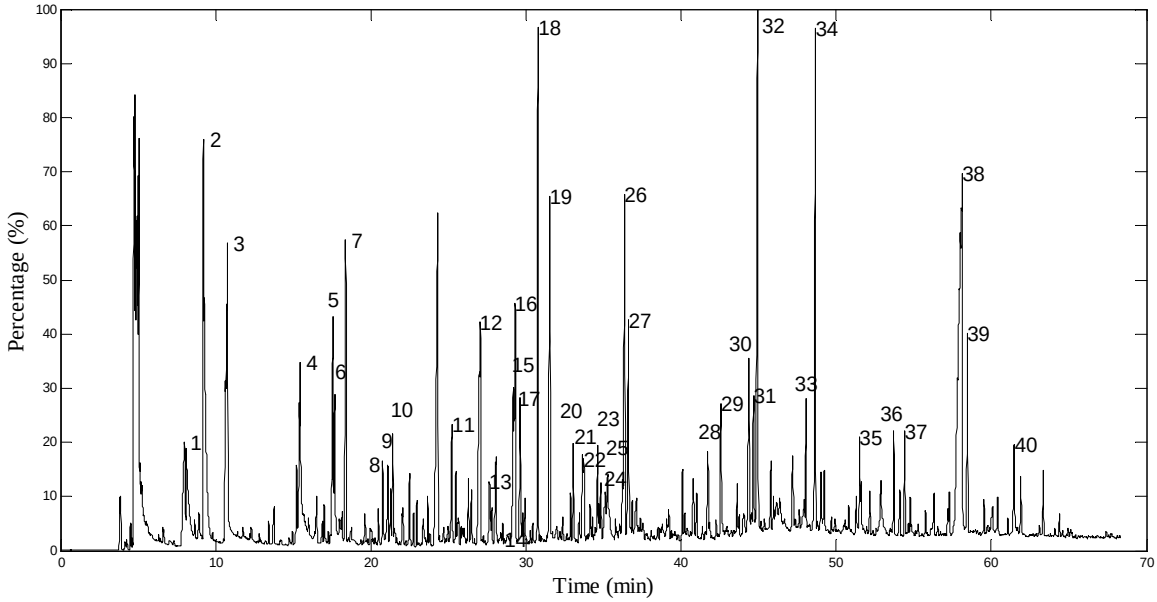

Figure 7-8: Chromatogram obtained by GC/MS and chemical identification, torrefied poplar derived oil. See Table 7-5 for key

Table 7-5: Identification of chemicals from torrefied poplar derived oil by GC/MS

1: Hydroxyacetaldehyde/Glycolaldehyde
2: Acetic acid/Ethanoic acid
3: Hydroxypropanone/1-Hydroxy-2-propanone/Acetone alcohol
4: 3-Hydroxypropanal
5: Butanedial/Succinaldehyde
6: 2-Hydroxy-3-oxobutanal
7: Furfural/furan-2-carboxaldehyde/fural/furfuraldehyde/2-furaldehyde/pyromucic aldehyde
8: Unknown
9: 1-Acetyloxy-2-propanone/1-Acetoxypropane-2-one/2-Oxopropyl acetate
10: 2-Ethyl-butanal
11: Dihydro-methyl-furanone
12: (5H)-furan-2-one/2(5H)-Furanone
13: 5-Methyl-2(5H)-Furanone/β-Angelica lactone
14: 4-Hydroxy-5.6-dihydro-(2H)-pyran-2-one
15: Unknown
16: 2-Hydroxy-3-methyl-2-cyclopentene-one
17: Anhydro-hexo-furanose
18: Phenol
19: 2-Methoxyphenol/Guaiacol/Guaicol
20: o-cresol/2-Methyl phenol
21: Unknown
22: Unknown
23: 4-METHYL-5H-FURAN-2-ONE/4-Methyl-2(5H)-furanone
24: Unknown
25: 2-FURANMETHANOL, TETRAHYDRO-5-METHYL-, TRANS-
26: 2-Methoxy-4-methyl phenol/Creosol/p-Methylguaiacol/4-Methylguaiacol
27: Anhydrosugar: unknown
28: Unknown
29: 2-Methoxy-4-vinylphenol/4-Vinylguaiacol/p-Vinylguaiacol/4-Hydroxy-3-methoxystyrene
30: 5-(Hydroxymethyl)-2-Furancarboxaldehyde/5-(Hydroxymethyl)-2-furfural/HMF/5-(Hydroxymethyl)-2-furaldehyde
31: 1,2-BENZENEDIOL
32: 2,6-Dimethoxy phenol/Syringol/1,3-Dimethoxy-2-hydroxybenzene/Pyrogallol dimethylether
33: 2-Methoxy-4-(1-propenyl)phenol/Isoeugenol,c&t/4-Propenylguaiacol/4-Hydroxy-3-methoxypropenylbenzene
34: 4-Methyl syringol/2,6-Dimethoxy-4-methylphenol
35: 4-ethyl-Syringol
36: 4-Vinyl-2.6-dimethoxyphenol/Syringol-4-vinyl
37: 2.6-Dimethoxy-4-(2-propenyl)-Phenol
38: 1,6-Anhydro-b-D-glucopyranose/Levoglucosan
39: trans-4-Propenyl-2.6-dimethoxyphenol/Methoxyeugenol

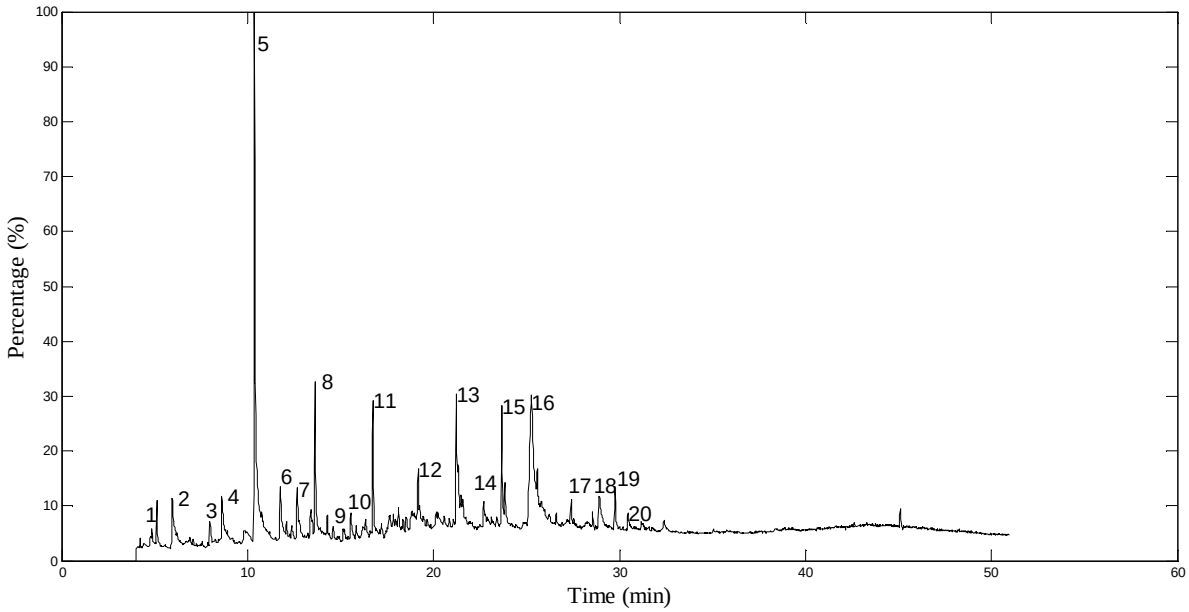

Figure 7-9: Chromatogram obtained by GC/MS and chemical identification, steamed poplar derived oil. See Table 7-6 for key

Table 7-6: Identification of chemicals from steamed poplar derived oil by GC/MS

1: 2-propenyidene-cyclobutene
2: 2.5-dimethyl-furan
3: 2-Methyl-Cyclopenten-1-one/2-Methyl-2-cyclopentenone
4: 5-methyl-2(3H)-Furanone
5: Phenol
6: 2-Hydroxy-1-methyl-1-cyclopentene-3-one/Maple lactone/2-Hydroxy-3-methyl-2-cyclopenten-1-one
7: 3-methyl-phenol/m-Cresol/1-Hydroxy-3-methylbenzene
8: 2-methoxy-phenol/o-methoxy-phenol/o-Guaiacol
9: Dimethyl phenol (2.3-; 2.4-; 2.5-)/Xylenols
10: Dimethyl phenol (3.5, 3,4)/Xylenols
11: 2-Methoxy-4-methyl phenol/Creosol/p-Methylguaiacol/4-Methylguaiacol
12: 4-Ethyl-2-methoxy-phenol/4-Ethyl-guaiacol
13: 2,6-Dimethoxy phenol/Syringol/1,3-Dimethoxy-2-hydroxybenzene/Pyrogallol dimethylether
14: 2-Methoxy-4-(1-propenyl)phenol/Isoeugenol,c&t/4-Propenylguaiacol/4-Hydroxy-3-methoxypropenylbenzene
15: 1, 2, 4- Trimethoxybenzene/1, 2, 4-Trimethoxy-1 benzene
16:1,6-Anhydro-b-D-glucopyranose/Levoglucosan
17: 4-Propenyl-2.6-dimethoxyphenol(sis)/Methoxyeugenol (trans)
18: 4-Hydroxy-3.5-dimethoxybenzaldehyde/Syringaldehyde/Syringe aldehyde/Cedar aldehyde
19: 4-Propenyl-2.6-dimethoxyphenol(trans)/Methoxyeugenol (trans)
20: 1-(4-Hydroxy-3-dimethoxyphenyl)ethanone/Acetosyringone/3.5-dimethoxy-1-hydroxyacetophenone/Acetosyringon

A comparison between fresh and torrefied poplar derived oil revealed some interesting outcomes. Firstly, peak area percentages of the hemicellulose-derived furans from torrefied wood derived oil (mainly furfural and furfuryl alcohol)were significantly decreased in comparison with untreated wood derived oil (mostly in poplar case). Secondly, light volatile reduction (acetic acid, compound 2) is seen in the chromatogram for torrefied poplar derived oil (Figure 7-8) and this is possible due the torrefaction process temperature (270-300^{o}C).

To present the effect ofpre-treatment methods on poplar derived oil the peak area percentages of the major known condensable organics are illustrated in Figure 7-10. It is noticeable that pre-treatment influenced pyrolysis products yields and composition.

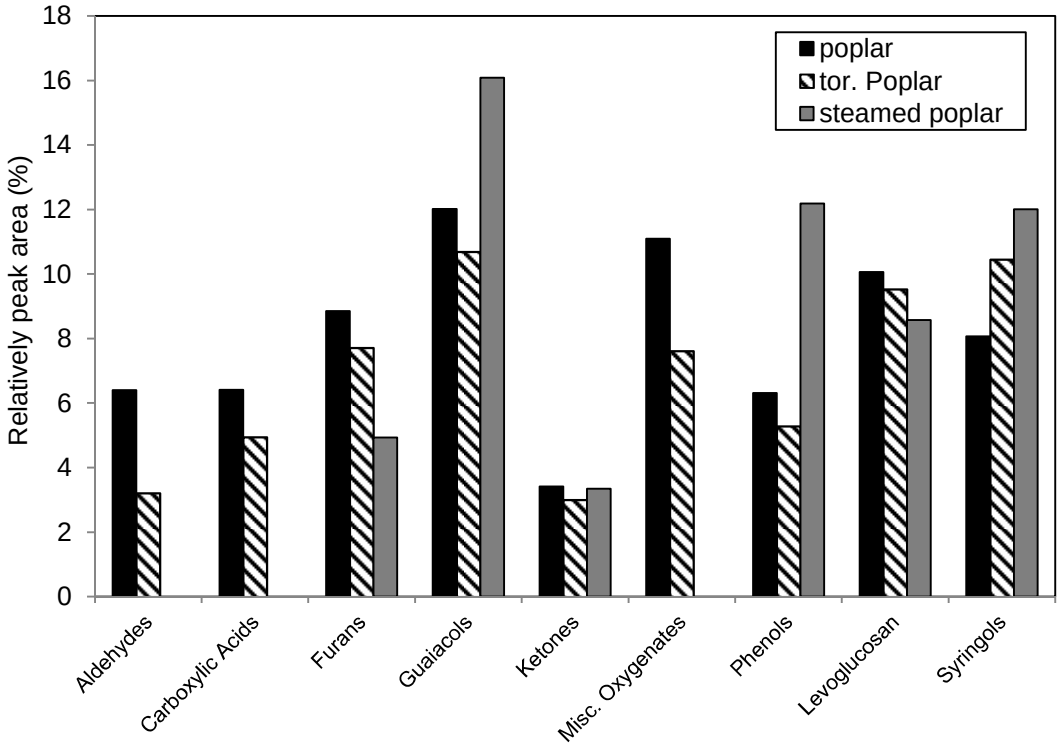

Figure 7-10: Peak area percentages of the major known condensable organics from fast pyrolysis of untreated and pre-treated poplar. Detailed data is listed in APPENDIX - A.

It can been noticed from Figure 7-10 that light volatile reduction occurred for both pre-treated poplar derived oils. Specifically, in the case of steamed poplar derived oil aldehydes and carboxylic acids could not be detected. The influence of steam treatment on poplar derived oil is distinguished; phenolics compounds (guaiacols, phenols and syringols) showed a major increase. For the case of torrefied oil, an increase in syringols levels is shown. In conclusion, the process of torrefaction did not have an important influence on poplar derived oil composition (cellulose derived products lowered from 47.6% to 38 % peak area), the steam treatment had a significant influence (cellulose derived products lowered from 47.6% to 17 % peak area/ lignin derived compounds increased from 26 to 40.85%).

A number of compounds were selected to signify the difference in peak area between the bio-oil derived frompoplar, torrefied poplar and steamed poplar, which are shown in Table 7-7. These have peak areas differences greater than 1.5 % and 2% of the total peak area for torrefied and steamed poplar oil respectively. The percentage of each

identified compound is the peak area divided by the total peak area of all compounds on the chromatogram.

Table 7-7: Peak area percentages of chemical compounds for poplar, torrefied poplar and steamed poplar derived oils where there are significant differences

Compound name/synonymous	**poplar**	**torrefied. poplar**	**steamed poplar**
2,6-Dimethoxy phenol	2.79	5.14	4.72
4-Methyl syringol	1.61	3.39	N.D.
2-Methoxy-4-methyl phenol	1.48	3.08	2.91
2-Hydroxy-3-methyl-2-cyclopentene-one	N.D.	1.95	N.D.
Phenol	5.03	3.27	6.92
Furfural/furan-2-carboxaldehyde/fural/furfuraldehyde/2-furaldehyde/pyromucic aldehyde	2.67	0.13	N.D.
3-Hydroxypropanal	3.30	0.37	N.D.
2.3-Dihydro-5-methylfuran-2-one	3.09	0.08	N.D.
2.5-dimethyl-furan	N.D.	N.D.	2.07
5-methyl-2(3H)-Furanone	N.D.	N.D.	2.87
3-methyl-phenol/m-Cresol/1-Hydroxy-3-methylbenzene	N.D.	N.D.	2.40
2-methoxy-phenol/o-methoxy-phenol/o-Guaiacol	N.D.	N.D.	3.31
4-Ethyl-2-methoxy-phenol/4-Ethyl-guaiacol	N.D.	N.D.	4.36
1, 2, 4- Trimethoxybenzene/1, 2, 4- Trimethoxy-1 benzene	N.D.	N.D.	3.61
4-Propenyl-2.6-dimethoxyphenol(sis)/Methoxyeugenol (trans)	N.D.	N.D.	2.48
Butanedial/Succinaldehyde	2.31	2.01	N.D.
Hydroxyacetaldehyde/Glycolaldehyde	2.47	1.59	N.D.
(5H)-furan-2-one/2(5H)-Furanone	2.58	2.77	N.D.
Hydroxypropanone/1-Hydroxy-2-propanone/Acetone alcohol	4.06	4.62	N.D.
Acetic acid/Ethanoic acid	6.15	4.94	N.D.

Regarding the screening of fresh and torrefied spruce derived oils, the chromatographic peak areas that were over 0.5 % were identified and are shown below in Figure 7-11 - Figure 7-12 and Table 7-8 - Table 7-9. A detailed identification of the chemicals presented in pot 1 of fresh and treated spruce are listed in APPENDIX - A.

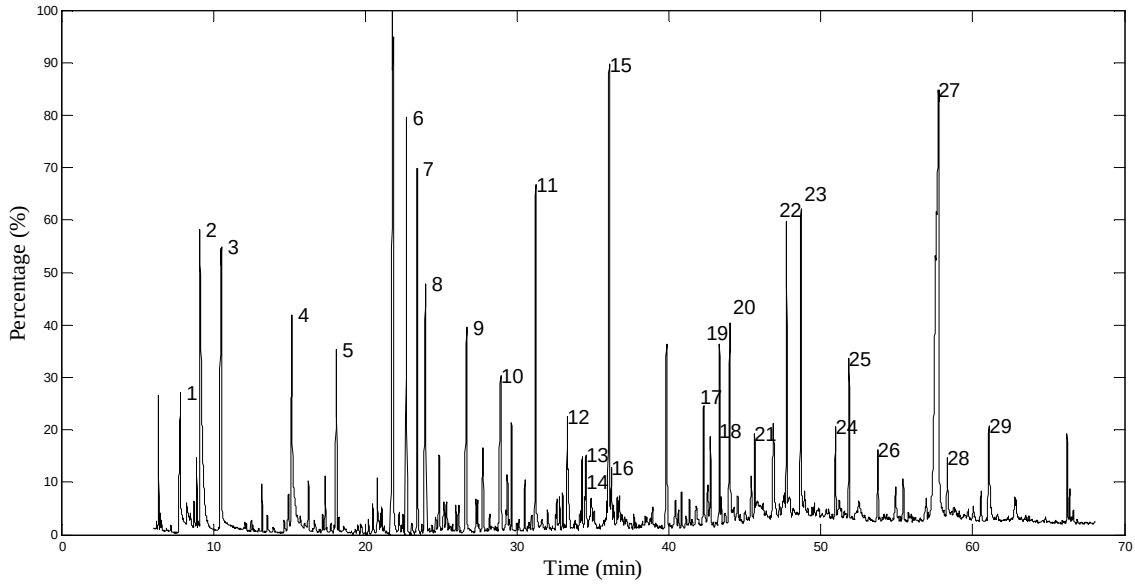

Figure 7-11:Chromatogram obtained by GC/MS and chemical identification, spruce derived oil. See Table 7-8 for key

Table 7-8: Identification of chemicals from spruce derived oil by GC/MS

1: Hydroxyacetaldehyde/Glycolaldehyde
2: Acetic acid/Ethanoic acid
3: Hydroxypropanone/1-Hydroxy-2-propanone/Acetone alcohol
4: 3-Hydroxypropanal
5: Furfural/furan-2-carboxaldehyde/fural/furfuraldehyde/2-furaldehyde/pyromucic aldehyde
6: 2.5-diethoxytetrahydro-furan
7: 2.5-diethoxytetrahydro-furan
8: 2.3-Dihydro-5-methylfuran-2-one
9: (5H)-furan-2-one/2(5H)-Furanone
10: 2-Hydroxy-1-methyl-1-cyclopentene-3-one/Maple lactone & 2.5-Dimethylcyclopentanone
11: 2-Methoxyphenol/Guaiacol/Guaicol
12: methyl-butyraldehyde derivate
13: p,m-Cresol/3,4-Methyl phenol
14: 2-FURANMETHANOL, TETRAHYDRO-5-METHYL-, TRANS-
15: 2-Methoxy-4-methyl phenol/Creosol/p-Methylguaiacol/4-Methylguaiacol
16: Anhydrosugar: unknown
17: 2-Methoxy-4-vinylphenol/4-Vinylguaiacol/p-Vinylguaiacol/4-Hydroxy-3-methoxystyrene
18: 4-METHYL-5H-FURAN-2-ONE/4-Methyl-2(5H)-furanone
19: Eugenol/2-Methoxy-4-allylphenol/2-Methoxy-1-hydroxy-4-allybenzene/Allylguaiacol
20: 5-(Hydroxymethyl)-2-Furancarboxaldehyde/5-(Hydroxymethyl)-2-furfural/HMF/5-(Hydroxymethyl)-2-furaldehyde
21: 2-Methoxy-4-(1 propenyl)phenol/Isoeugenol,c&t/4-Propenylguaiacol/4-Hydroxy-3-methoxypropenylbenzene
22: 2-Methoxy-4-(1-propenyl)phenol/Isoeugenol,c&t/4-Propenylguaiacol/4-Hydroxy-3-methoxypropenylbenzene
23: Vanillin/2-Methoxy-4-formylphenol/4-Hydroxy-3-methoxybenzaldehyde
24: Homovanillin
25: 1-(4-Hydroxy-3-methoxyphenyl)ethanone/Acetoguaiacone
26: 1-(4-hydroxy-3-methoxyphenyl)-2-Propanone/Guaiacylacetone/Vanillyl methyl ketone/4-Hydroxy-3-methoxyphenyl acetone
27: 1,6-Anhydro-b-D-glucopyranose/Levoglucosan
28: Dihydroconiferyl alcohol
29: Anhydrosugar

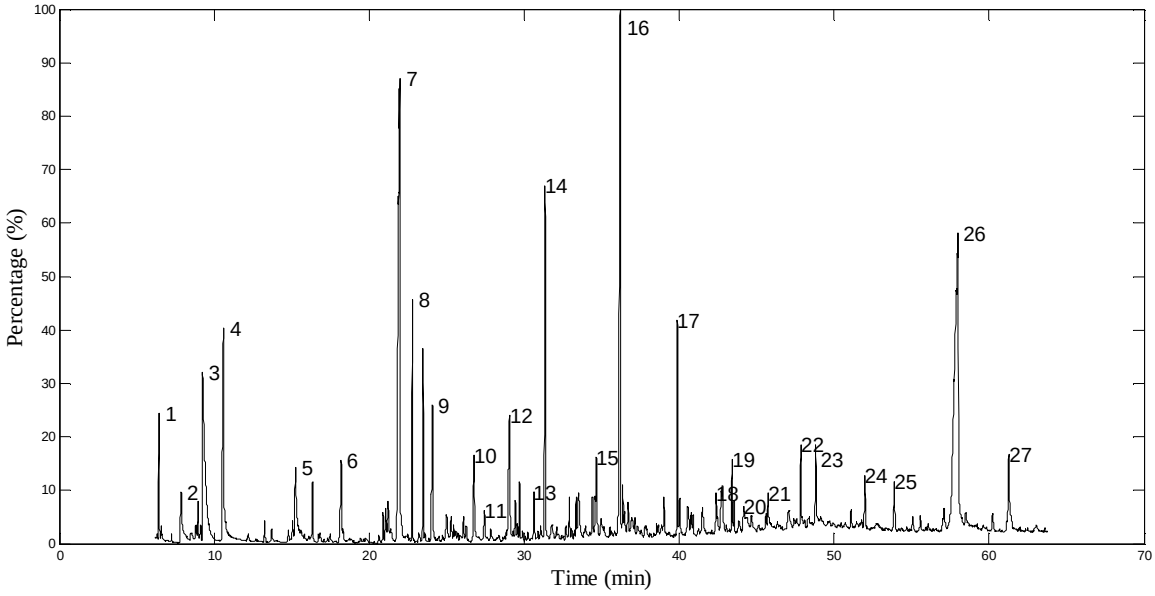

Figure 7-12: Chromatogram obtained by GC/MS and chemical identification, torrefied spruce derived oil. See Table 7-9 for key

Table 7-9: Identification of chemicals from torrefied spruce derived oil by GC/MS

1	3-Hydroxy-2-butanone
2	Hydroxyacetaldehyde/Glycolaldehyde
3	Acetic acid/Ethanoic acid
4	Hydroxypropanone/1-Hydroxy-2-propanone/Acetone alcohol
5	3-Hydroxypropanal
6	Furfural/furan-2-carboxaldehyde/fural/furfuraldehyde/2-furaldehyde/pyromucic aldehyde
7	2,2-Diethoxyethanol/Hydroxyacetaldehyde diethyl acetal/2,2-diethoxy ethanol/glycolaldehyde diethyl acetal
8	2.5-diethoxytetrahydro-furan
9	2-Hydroxy-2-cyclopenten-1-one
10	(5H)-furan-2-one/2(5H)-Furanone
11	5-Methyl-2(5H)-Furanone/β-Angelica lactone
12	2-Hydroxy-1-methyl-1-cyclopentene-3-one/Maple lactone & 2.5-Dimethylcyclopentanone
13	Phenol
14	2-Methoxyphenol/Guaiacol/Guaicol
15	p,m-Cresol/3,4-Methyl phenol
16	2-Methoxy-4-methyl phenol/Creosol/p-Methylguaiacol/4-Methylguaiacol
17	Unknown
18	2-Methoxy-4-vinylphenol/4-Vinylguaiacol/p-Vinylguaiacol/4-Hydroxy-3-methoxystyrene
19	Eugenol/2-Methoxy-4-allylphenol/2-Methoxy-1-hydroxy-4-allybenzene/Allylguaiacol
20	5-(Hydroxymethyl)-2-Furancarboxaldehyde/5-(Hydroxymethyl)-2-furfural/HMF/5-(Hydroxymethyl)-2-furaldehyde
21	2-Methoxy-4-(1-propenyl)phenol/Isoeugenol,c&t/4-Propenylguaiacol/4-Hydroxy-3-methoxypropenylbenzene
22	2-Methoxy-4-(1-propenyl)phenol/Isoeugenol,c&t/4-Propenylguaiacol/4-Hydroxy-3-methoxypropenylbenzene
23	Vanillin/2-Methoxy-4-formylphenol/4-Hydroxy-3-methoxybenzaldehyde
24	1-(4-Hydroxy-3-methoxyphenyl)ethanone/Acetoguaiacone
25	1-(4-hydroxy-3-methoxyphenyl)-2-Propanone/Guaiacylacetone/Vanillyl methyl ketone/4-Hydroxy-3-methoxyphenyl acetone
26	1,6-Anhydro-b-D-glucopyranose/Levoglucosan
27	Anhydrosugar: unknown

The results show that the torrefaction process change the peak area percentages of cellulose and hemicellulose spruce derived products (cellulose derived products increased from 52% to 55 % peak area/ lignin derived compounds from 25.4% to 34 % peak area).

Treatment of spruce by torrefaction lowered the light volatiles and increased the phenolics (phenols and guaiacols/syringols not detected) levels in bio-oil. The concentration of phenolics in bio-oil could be useful for the resins industry.

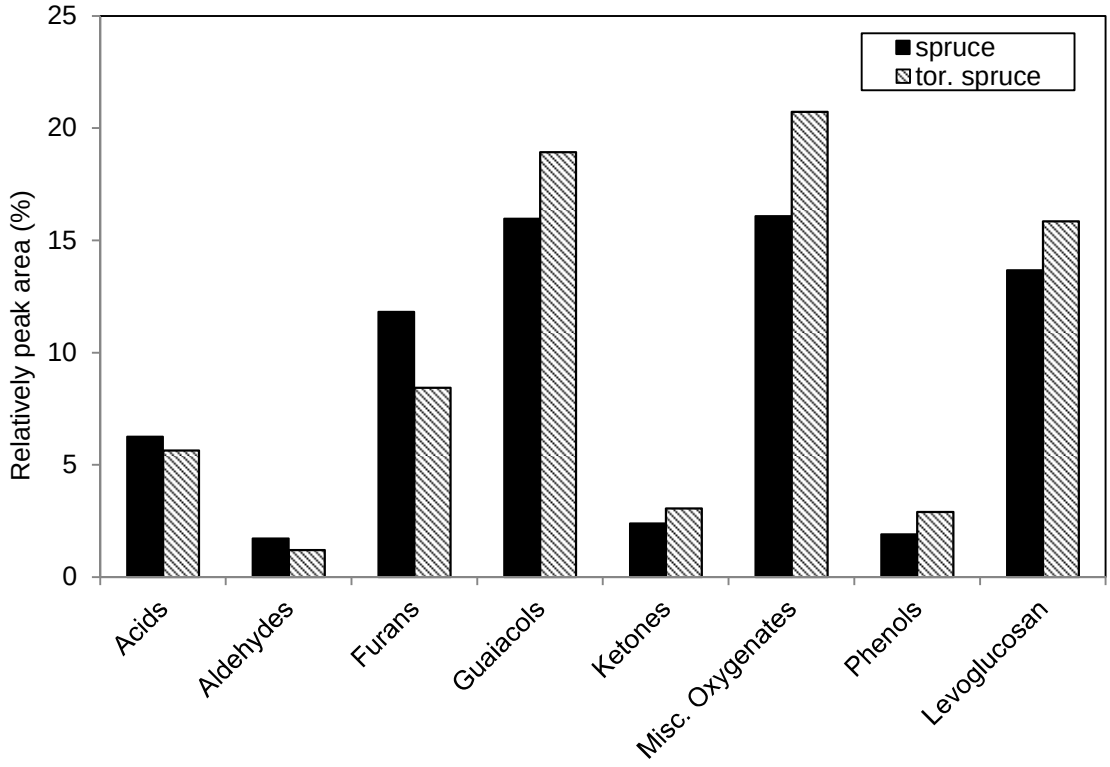

Figure 7-13: Peak area percentages of the major known condensable organics from fast pyrolysis of untreated and pre-treated spruce.

Table 7-10: Peak area percentages of chemical compounds for spruce and torrefied spruce derived oils where there are significant differences

Compound name/synonyms	**spruce**	**torrefied. spruce**
2,2-Diethoxyethanol/Hydroxyacetaldehyde diethyl acetal/2,2-diethoxy ethanol/glycolaldehyde diethyl acetal	6.14	11.87
2-Methoxy-4-methyl phenol/Creosol/p-Methylguaiacol/4-Methylguaiacol	3.82	8.38
1,6-Anhydro-b-D-glucopyranose/Levoglucosan	13.67	15.85
2-Methoxyphenol/Guaiacol/Guaicol	2.79	4.69
5-(Hydroxymethyl)-2-Furancarboxaldehyde/5-(Hydroxymethyl)-2-furfural/HMF/5-(Hydroxymethyl)-2-furaldehyde	2.13	1.10
3-Hydroxypropanal	2.85	1.39
Vanillin/2-Methoxy-4-formylphenol/4-Hydroxy-3-methoxybenzaldehyde	2.74	1.03

7.2.5.2 Analysis of aquathermolised wheat straw derived oil

With reference to the screening of the untreated and pre-treated wheat straw derived oils, the chromatographic peak areas that were over 0.5 % were identified and are shown below in Figure 7-14 and Table 7-11. A detailed identification of the chemicals presented in pot 1 of fresh and treated wheat straw are listen in APPENDIX - A.

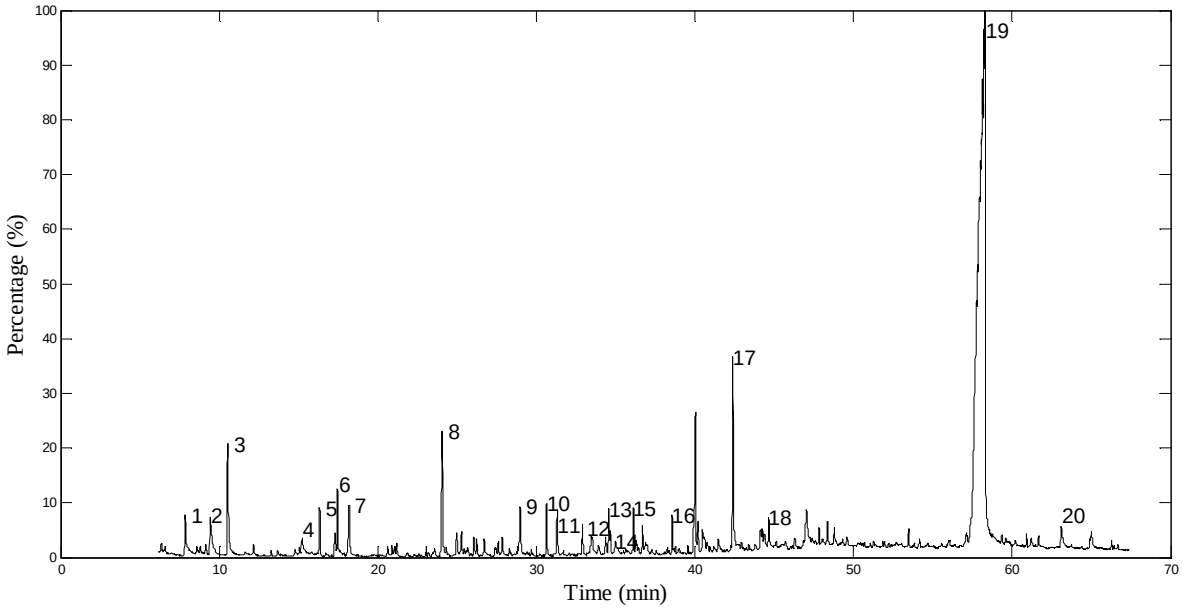

Figure 7-14: Chromatograms obtained by GC/MS and chemical identification, aquathermolised wheat straw derived oil. See Table 7-11 for details

Table 7-11: Identification of chemicals from aquathermolised wheat straw derived oil by GC/MS

1	Hydroxyacetaldehyde/Glycolaldehyde
2	Acetic acid/Ethanoic acid
3	Hydroxypropanone/1-Hydroxy-2-propanone/Acetone alcohol
4	3-Hydroxypropanal
5	Unknown
6	Acetic anhydride
7	Furfural/furan-2-carboxaldehyde/fural/furfuraldehyde/2-furaldehyde/pyromucic aldehyde
8	2-Hydroxy-2-cyclopentene-1-one
9	2-Hydroxy-1-methyl-1-cyclopentene-3-one/Maple lactone & 2.5-Dimethylcyclopentanone
10	Phenol
11	2-Methoxyphenol/Guaiacol/Guaicol
12	Unknown
13	p,m-Cresol/3,4-Methyl phenol
14	2-Furanmethanol,tetrahydro-5-methyl-/Furfurylalcohol/Tetrahydro-5-methyl-2-furanmethanol
15	2-Methoxy-4-methyl phenol/Creosol/p-Methylguaiacol/4-Methylguaiacol
16	Ethyl phenol (2-; 3-; 4-;)
17	4-Vinylphenol/4- ethenyl phenol/4-ethenylphenol/4- hydroxystyrene
18	2,6-Dimethoxy phenol/Syringol/1,3-Dimethoxy-2-hydroxybenzene/Pyrogallol dimethylether
19	1,6-Anhydro-b-D-glucopyranose/Levoglucosan
20	1,6-ANHYDRO-.BETA.-D-GLUCOFURANOSE

The comparison between untreated and treated wheat straw derived oil is complicated, since the aquathermolised derived oil is on homogenous phase while the untreated one is phase separated. For that reason only the apparent differences between chemical levels could be discussed.

Outstanding differences between fresh and treated wheat straw oils were the significant decrease on acid levels and hydroxypropanone. In contrast, levoglucosan

yields were increased. This is presented in Figure 7-15 below. An explanation of the considerable increase of levoglucosan levels could be due the leach out of the alkali metals from wheat straw during the pre-treatment process. Another important results was the reduction of furfural, indicating that furfural is water soluble and it could be absorbed by the hot water treatment.

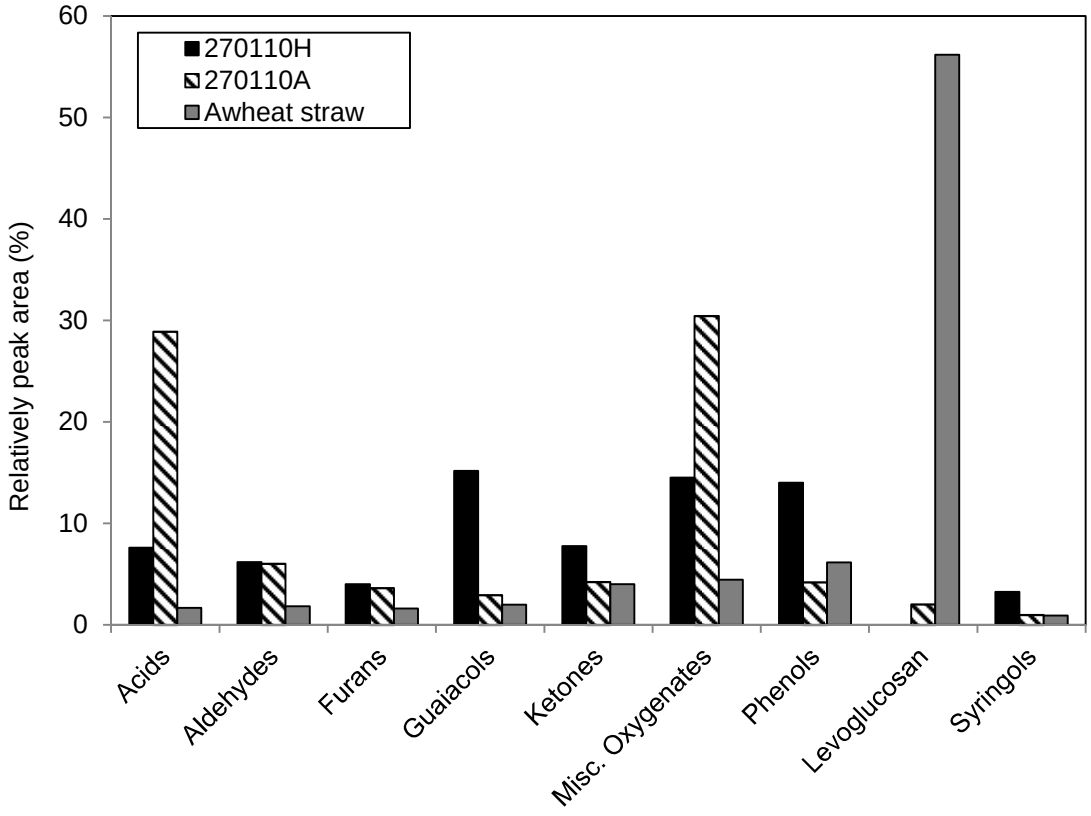

Figure 7-15: Peak area percentages of the major known condensable organics from fast pyrolysis of untreated (270110H-heavy fraction and 270110A-aqueous fraction) and pre-treated (Awheat straw-aquathermolised) wheat straw.

A number of compounds were selected to signify the difference in peak area between wheat straw and aquathermolised wheat straw derived oils, which are shown in Table 7-12. These have peak areas greater than 2% of the total peak area for untreated and pre-treated straw derived oils, respectively. The percentage of each identified compound is the peak area divided by the total peak area of all compounds on the chromatogram.

Table 7-12: Peak area percentages of chemical compounds for wheat straw and aquathermolised wheat straw derived oils where there are significant differences

Compound name/synonyms	270110 Heavy fraction	270110 Aqueous fraction	Aqua-thermolised wheat straw
1,6-Anhydro-b-D-glucopyranose/Levoglucosan	**N.D.**	**2.00**	**56.18**
4-Vinylphenol/4- ethenyl phenol/4- ethenylphenol/4-hydroxystyrene	3.21	0.37	3.29
2-Hydroxy-2-cyclopentene-1-one	N.D.	N.D.	2.60
1-Hydroxy-2-butanone	1.20	1.46	0.13
Butanedial/Succinaldehyde	0.98	1.89	0.45
2-Hydroxy-1-methyl-1-cyclopentene-3-one/Maple lactone & 2.5-Dimethylcyclopentanone	4.13	2.73	1.02
1-Acetyloxy-2-propanone/1-Acetoxypropane-2-one/2-Oxopropyl acetate	1.93	1.95	0.12
Hydroxypropanone/1-Hydroxy-2-propanone/Acetone alcohol	**11.01**	**24.10**	**2.13**
Acetic acid/Ethanoic acid	**6.87**	**28.07**	**1.33**
Phenol	3.64	1.23	0.82
Furfural/furan-2-carboxaldehyde/fural/furfuraldehyde/2-furaldehyde/pyromucic aldehyde	4.78	3.31	1.21
2-Methoxyphenol/Guaiacol/Guaicol	4.35	1.61	0.69
2-Methoxy-4-vinylphenol/4-Vinylguaiacol/p-Vinylguaiacol/4-Hydroxy-3-methoxystyrene	3.91	0.32	N.D.

7.3 1 kg/h unit at ECN

7.3.1 Experimental method

Section 4.7 describes the experimental method used to obtain the pyrolysis products yield, as well as the mass balance. This also includes a description of the bubbling fluidised bed reactor system of ECN.

7.3.2 Results and discussion

7.3.2.1 Mass balance

A large scale experiment was conducted using the 1000g/h continuous bubbling fluidised bed reactor system of ECN with torrefied poplar. Operating conditions, as well as pyrolysis products yield and mass balance closures are listed in Table 7-13.

.

Table 7-13: Mass balance and operation conditions of fast pyrolysis of torrefied poplar using the 1000g/h continuous bubbling fluidised bed reactor system of ECN

Test reference	TP_ECN
Nominal capacity of reactor	1000g/h
Average feed rate	150g/h
Run time (min)	180
Product collection system	Cooler + ESP
Fluidised gases	Ar + N_2
Fluidised Ar flow rate (l/min)	20
Feeder N_2flow rate (l/min)	1
Fluidising medium	Sand
Sand particle size	0.1- 0.5 mm
Feedstock	**Torrefied poplar**
Particle size (mm)	0.7 – 2mm
Average pyrolysis T (^oC)	500
Product yields (wt%, wet feed)	
Char	**17.4**
Liquids	**52.00**
Gases	**24.88**
Closure (wt%)	94.28

Pyrolysis liquid and char yields of run with reference TP_ECN are comparable with the yields obtained from the runs 131008 and 120309. The latter runs were carried out at Aston's 100g/h fluidised bed reactor and were discussed previously in Section 7.2.3. According to Table 7-13 gas yield of TP_ECN is higher when compared with runs 131008 and 120309 of Table 7-1. A possibly explanation for this could be the vapour residence time. Experiments that were performed with the 100g/h fluidised bed reactor system of Aston had a maximum residence time of 1 second, while the run with reference TP_ECN had a time of 2 seconds. This could have caused the secondary cracking of vapours which resulted in an increase of gas yield [17]. In addition, the secondary cracking of pyrolysis vapours could be an explanation for the production of CO than CO_2 [112]. This is illustrated in Figure 7-16 below. WOB_TI represents the temperature measurements in the reactor unit, while WOB_CO and WOB_CO_2 the volume measurement of CO and CO_2 that were produced during the experiment.

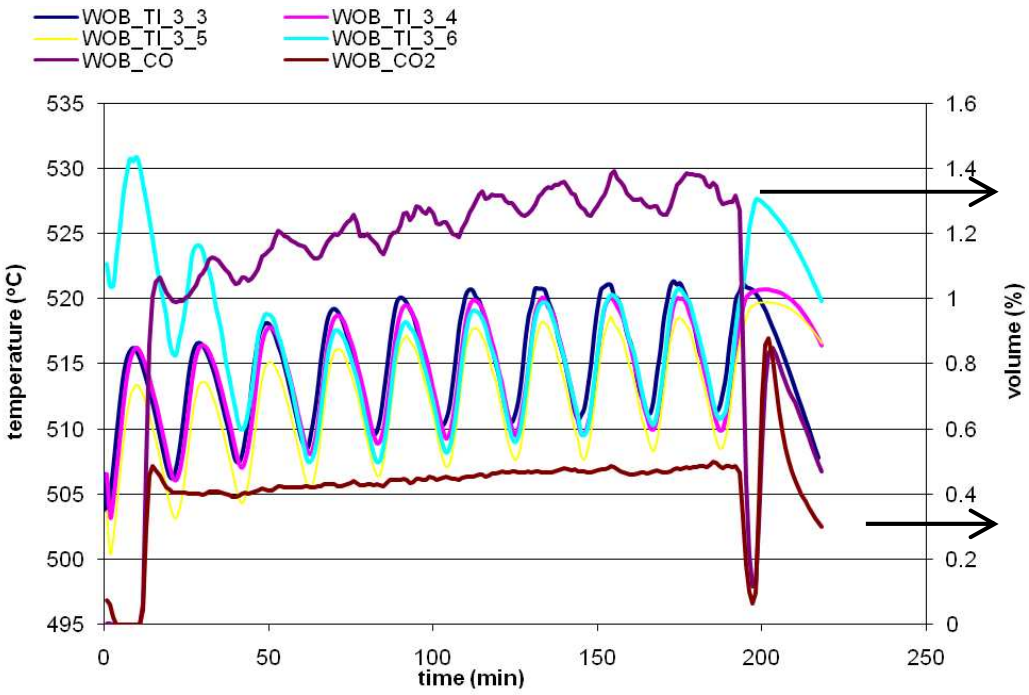

Figure 7-16: Temperature and gas volume versus time

7.3.2.2 Chemical analysis of bio-oil

A chemical analysis of the bio-oil obtained from fast pyrolysis of pre-treated poplar by torrefaction was conducted on ECN using a GC/MS/FID. It is imperative to highlight that the bio-oil produced from the 1 kg/h bubbling fluidised bed reactor of ECN was collected in three fractions (pot 1, pot 2 and pot 3). Details regarding the fractions could be found in Section 4.6.1.

Table 7-14 was provided by ECN and shows the chemical compounds that were identified. A chemical analysis by Aston was not possible due to confidentiality reasons. The compounds obtained on high levels are hydroxyacetaldehyde, hydroxyaceton, acetic acid, levoglucosan, pyrocatechol, methanol, phenol, 2(5H)-Furanone, 1-Hydroxy-2-butanon, 2-Furaldehyde, formic acid and methanol.

Table 7-14: Identification of chemical compounds from torrefied derived oil produced with the 1 kg/h bubbling fluidised bed reactor of ECN expressed on mg/Kg

	Pot 1	ESP	-20C cooler
Acetaldehyde	1274	907	2929
Methylformate	46	454	118
Propanal	283	454	1082
Furan	46	454	50
Isobutyraldehyde	46	454	50
Aceton	308	907	881
Methylacetate	46	454	111
Methanol	7457	2269	22611
Toluene	23	227	25
O-xylene	23	227	25
Hydroxyaceton	33717	21417	39824
Hydroxyacetaldehyde	106641	197226	39037
1-Hydroxy-2-butanon	3387	3367	3422
Angelicalactone	240	454	311
Acetic_acid	31102	15990	37210
2-Furaldehyde	2854	3086	3630
Formic_acid	2441	1815	2808
5-Methyl-2-furaldehyde	758	1382	483
2-Furanmethanol	1303	1998	188
Naphtalene	29	227	25
2(5H)-Furanone	3896	7104	748
2-Methoxyphenol	589	1219	129
4-Methylguaiacol	347	842	50
Phenol	6252	13671	1079
4-Ethylguaiacol	79	454	50
P-cresol	1060	2434	70
Acenaphthene	23	227	25
Eugenol	46	454	50
4-Ethylphenol	214	529	50
4-Propylphenol	540	1609	50
26-Dimethoxyphenol	46	454	50
Levulinic_acid	594	2269	250
Isoeugenol	46	454	50
4-Methylsyringol	219	761	50
Fluorene	101	340	25
5-(Hydroxymethyl)-2-furaldehyde	1781	3675	50
26-dimethoxy-4-(2-propenyl)-phenol	46	454	50
Vanilline	181	454	50
Aceto-vanillone	100	454	50
Pyrocatechol	7714	15482	50
Phenanthrene	23	227	25
Anthracene	23	227	25
Syringaldehyde	196	641	50
4-hydroxybenzaldehyde	61	454	50
2-Methoxyhydroquinone	92	907	100
4-Hydroxybenzylalcohol	92	907	100
Acetosyringone	96	907	100
4-Hydroxy_acetophenone	92	907	100
Hydroquinone	953	1937	50
Resorcinol	300	907	100
Fluoranthene	23	227	25
Coniferylalcohol	92	907	100
Pyrene	23	227	25

Levoglucosan	18454	73967	250
unknowns	195868	346983	103287

Comparison of the oil obtained by run TP_ECN and run 081008 revealed some interesting results. The chemicals obtained in the oil by run 081008 in significant amount are levoglucosan, acetic acid, phenol, 1-Hydroxy-2-propanone, 3-Hydroxypropanal, 2.3-Dihydro-5-methylfuran-2-one, syringol, 2-furaldehyde, 2(5H)-Furanone and hydroxyacetaldehyde. The analysis of the bio-oil obtained by Aston is comparable with the oil of ECN. It should be noted that the ECN results are given on mg/kg, while Aston's are on peak area percentages. Thus, the results should be used as an indication.

7.4 Chapter conclusions

Pre-treatment of biomass by torrefaction, aquathermolysis, and steam resulted in a significant effect on pyrolysis products in comparison with untreated biomass pyrolysis products. Effects included changes in the pyrolysis products yield, product composition and changes in the proportion of key components.

The comparison of the influence of pre-treatment processes on fast pyrolysis products revealed some interesting outcomes.

Torrefaction:

- Feedstock type had a influence on the effect of torrefaction on bio-oil.
- Torrefied wood caused irregularity of feeding with the pneumatic feeder.
- Peak area percentages of the hemicellulose-derived furans (mainly furfural and furfuryl alcohol) were significantly decreased after torrefaction treatment (mostly in poplar case).
- Light volatile reduction (reduction of acetic acid content) is seen in the chromatograms for torrefied wood derived oil and this is possible due the torrefaction process temperature (270-300^{o}C).
- Increase of phenolics levels for spruce; interesting candidate for the resins industry.

Hot pressurized steam pre-treatment:

- Steam pre-treatment increased significantly the phenolics in bio-oil, in comparison with untreated poplar derived oil.
- Light volatiles (acetic acid) were not detected.

Aquathermolysis:

- Performing pyrolysis on aquathermolised wheat straw altered the physical characteristics of the bio-oil produced, changing it from phase separate to homogeneous oil. Pyrolysis using wheat straw had some disadvantages such as pre-pyrolysis and agglomeration, which was discussed previously in more detail in Chapter 6. The use of aquathermolised wheat straw avoided these problems.
- The use of aquathermolised wheat straw as a raw material for fast pyrolysis changed the proportion of key components in bio-oil and increased significantly levoglucosan levels.

It was showed that the yields of pyrolysis products resulting from the large scale experiment with torrefied wood performed by ECN were similar to the yields produced using Aston's bench scale unit. The only important difference was in the gas yields. This could be a result of the longer vapour residence time, which caused the secondary cracking of pyrolysis vapours. The proportion of chemical key components was similar with the results obtained from Aston.

Value chemicals such as phenolics and levoglucosan, were produced from fast pyrolysis of pre-treated feedstocks studied in this work. Further research should be performed on the combine integration of both steps (staged degasification); evaluation of pre-treatment process combined with fast pyrolysis of the pre-treatment residue; increase on yields of target chemicals produced by pre-treatment using catalysts; separation technologies available for mixture of target chemical in bio-oil; potential markets for the target chemicals produced.

8 CATALYSTS

This chapter evaluates various catalysts for upgrading of pyrolysis vapours of untreated and pre-treated wheat straw. The evaluation of catalysts was conducted by analytical and laboratory equipment, including a Py-GC/MS, and a 300g/h fluidised bed reactor coupled with a secondary catalytic fixed bed reactor, respectively. The initial step was to apply analytical pyrolysis (Py-GC/MS) to determine whether catalysts have an effect on fast pyrolysis products. This was done in order to select certain catalysts for further laboratory fast pyrolysis processing. The effect of activation, temperature, and biomass pre-treatment on catalysts were also investigated.

8.1 Selection of catalysts

The selection of appropriate catalysts for pyrolysis runs was obtained from the literature review of Chapter 3. The catalysts choice was also depended from their availability on the market. The first step was to apply analytical pyrolysis (Py-GC/MS) to determine which catalysts had an effect on fast pyrolysis liquid, in order to select catalysts for further laboratory fast pyrolysis. Laboratory experiments were also conducted using the existing 300g/h fluidised bed reactor system with a secondary catalytic fixed bed reactor, as a later step.

8.2 Activation of catalysts

The catalysts that were activated prior the pyrolysis experiments were NiMo, H-ZSM-5, FCC, and CoMo. The methodology used was to place the catalyst in a muffle oven overnight at 105^{o}C. This was done to remove the moisture from the catalyst. The next step was to place the catalyst in a muffle oven for 2 hours at 400^{o}C at atmospheric conditions [97].

8.3 Feedstocks

Agricultural waste (wheat straw) was the feedstock used in Abengoa bio-refinery for the production of bio-ethanol. Wheat straw is abundance, easy to grow, an agricultural residue, resulting in a low-cost feedstock. The pre-treatment of wheat straw with hot pressurised water (aquathermolysis) seem interesting to use as a raw material in this

catalytic work. Aquathermolised wheat straw was used to study the effect of pre-treatment on catalysts.

8.4 Experimental methodology

8.4.1 Biomass material

The biomass material used in this study for the mg-scale experiments (Py-GC/MS) was wheat straw and pre-treated wheat straw (aquathermolised wheat straw). The analysis of the wheat straw and aquathermolised wheat straw are shown in Chapter 5. The particles of biomass sample with the size of 0.105-0.250 mm were selected for the analytical experiments.

Regarding the g-scale experiments (bench scale reactor) wheat straw was the chosen feedstock. Pellets made from wheat straw were ground to obtain a particle size of 0.255mm – 1 mm.

8.4.2 Py-GC/MS

The characterization of feedstocks with catalysts was done using a Pyroprobe 5000 Series coupled with a Varian 450 - Gas Chromatograph and a Varian 220 - Mass Spectometer. The column used was a factor four capillary column(30m, 25 mm i.d., 0.25 μm df).

Pyroprobe-GC/MS was used to perform pyrolysis experiments in a mg scale. Detailed discussion concerning the Pyroprobe-GC/MS equipment can be found in Section 4.2. The placement of the biomass sample and the catalyst in the quartz tube is illustrated in Figure 8-1. Approximate 0.5 mg of biomass sample and 1 mg of catalyst were weight in a Perkin Elmer Micro balance and then placed into a glass tube using quartz wool plugs.

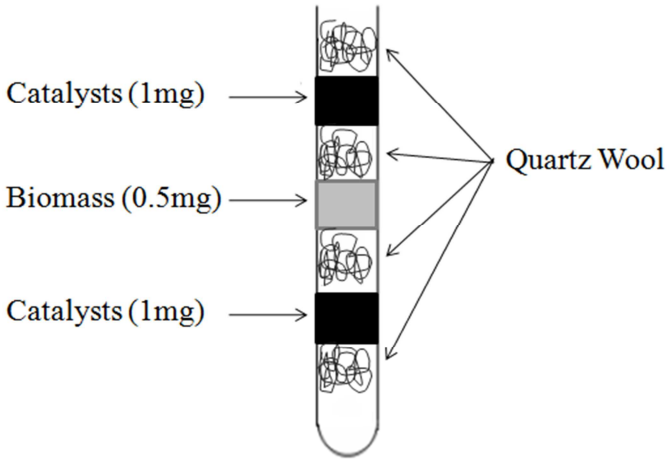

Figure 8-1: Configuration of catalyst and biomass in the quartz tube

The experimental work using the Py-GC/MS with catalysts and biomass is divided in four sets of experiments on duplicates. This is listed in Table 8-1.

Table 8-1: Procedure applied for the Py-GC/MS experiments with catalysts

Experiments	Methodology	Pyrolysis temperature
1st set of 10 experiments	Comparison of catalysts	500^{o}C
2nd set of 5 experiments	Influence of biomass pre-treatment	500^{o}C
3rd set of 3 experiments	Effect of catalyst activation	500^{o}C
4th set of 8 experiments	Influence of reaction temperature	500^{o}C 600^{o}C 700^{o}C

8.4.3 300g/h fluidised bed reactor unit coupled with a secondary catalytic fixed bed reactor

The methodology for experimentation is described and analysed in Section 4.4 and 4.4. This includes a description of the 300g/h fluidised bed reactor system and the 300g/h fluidised bed reactor unit coupled with a secondary catalytic fixed reactor, as well as the measurements taken to obtain the pyrolysis products yield and mass balance. The important difference between the two systems is the fixed bed catalytic reactor. Both reactor systems used in this project employed the liquid product collection system from the 100 g/h unit. This was done for more effective comparison and also because there is much more experience on this layout and it provides very good mass balance closures of better than 95%.

Table 8-2: Operational conditions of catalytic fast pyrolysis runs with ground wheat straw pellets and CoMo catalyst.

Test reference	280211C	80311C
Reactor configuration	**300 g reactor + catalytic fixed bed reactor+100 g glass ware**	**300 g reactor + catalytic fixed bed reactor+100 g glass ware**
Capacity of reactor	300g/h	300g/h
Feed rate	50g/h	39g/h
Run time (min)	40	24
Product collection system	Cooler + ESP	Cooler + ESP
Fluidised N_2 velocity (l/min)	1	1
Feeder N_2 velocity (l/min)	12	16
Fluidising medium	Sand	Sand
Particle size	355-500	355-500
Fast screw (rpm)	100	100
Feedstock	**Wheat straw from ground pellets**	**Wheat straw from ground pellets**
Particle size (mm)	0.225-1	0.225-1
Pyrolysis T (^oC) average	522	501
Pressure in reactor at start of run (ins water)	10	10
Pressure in reactor at end of run (ins water)	11	9
Pressure in feeder at start of run (ins water)	20	22
Pressure in feeder at end of run (ins water)	26	26
Pressure after cat. reactor at start of run (ins water)	-	8
Pressure after cat. reactor at end of run (ins water)	-	7
Catalyst	**Co-Mo**	**Co-Mo**
Weight catalyst	8.67g	9.9g

Catalytic runs were performed using ground wheat straw pellets as the biomass feedstock and CoMo as the catalyst. The operating conditions used for both experiments are listed in Table 8-2 above.

8.5 Evaluation by Py GCMS

8.5.1 Results and discussion

8.5.1.1 Comparison of catalysts

Analytical pyrolysis using the Py-GC/MS was applied to wheat straw with eleven catalysts at 500^{o}C. The catalysts used included NiMo, ZrO, Fe_3O_2, ZnO, CuCr, H-ZSM-5, TiO, FCC, CoMo, used CoMo and regenerated CoMo.

The percentage of each identified compound is the peak area divided by the total peak area of all compounds on the chromatogram. The chromatograms obtained from the Py-GC/MS for wheat straw and the combination of wheat straw with different types of catalysts are presented in Figure 8-2 and Figure 8-3 below. Further details can be also found in APPENDIX - B.

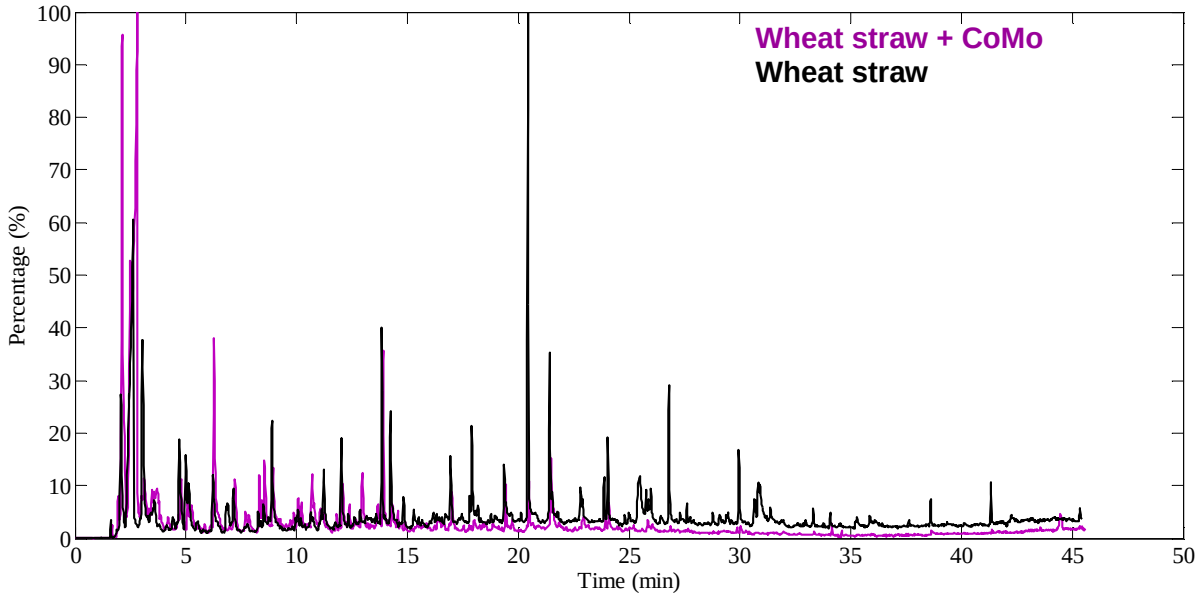

Figure 8-2: Chromatograms obtained from Py-GC/MS for wheat straw with Co-Mo catalyst at 500C

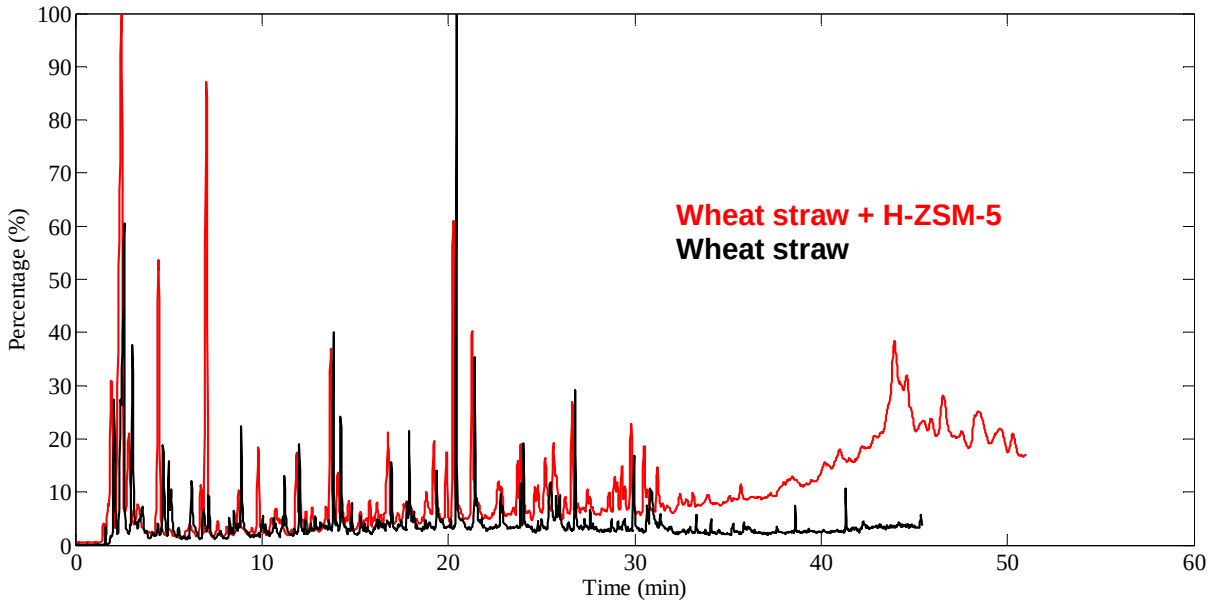

Figure 8-3: Chromatograms obtained from Py-GC/MS for wheat straw with H-ZSM-5 catalyst at 500C

Concerning the chromatograms above it can be observed that each catalyst had an effect on wheat straw pyrolysis vapours. However this effect cannot be evaluated from the results shown in the chromatograms and further investigation needs to be undertaken to categorise this effect.

Additionally, Figure 8-4 illustrates the chromatograms obtained from the Py-GC/MS for wheat straw and the combination of wheat straw with CoMo, used CoMo and regenerated CoMo.

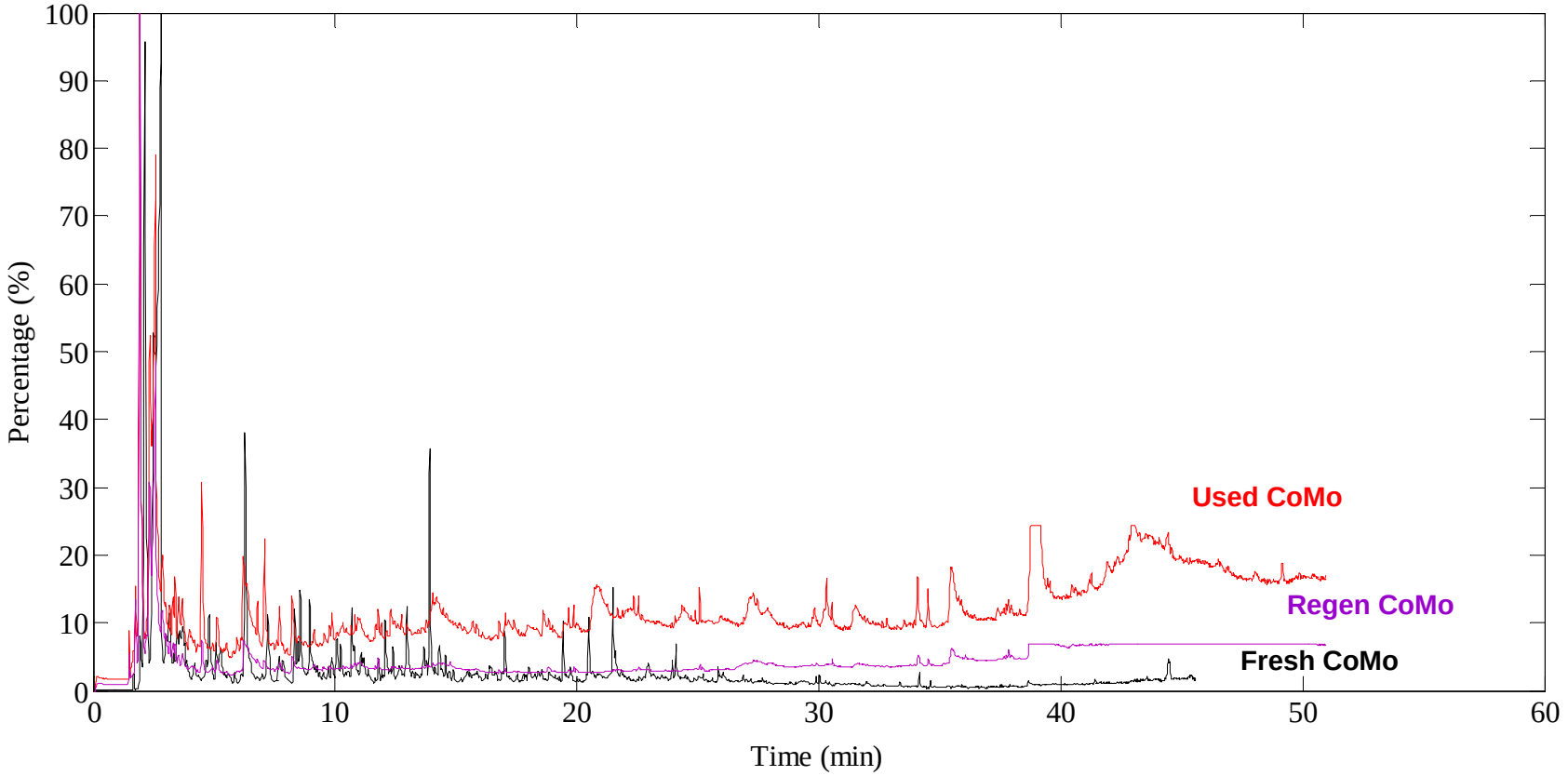

Figure 8-4: Chromatograms obtained from Py-GC/MS for wheat straw with fresh Co-Mo, regenerated Co-Mo and used Co-Mo (used as received from the laboratory experiments) catalyst at 500C

The chemical compounds that were identified based on the chromatograms Figure 8-2, Figure 8-3, Figure 8-4, and APPENDIX - B, were separated in chemical groups and are shown in Table 8-3.

Table 8-3: The effect of catalysts on pyrolysis products. Cells highlighted in green show a significant variation from wheat straw with no catalysts at 500^{o}C, cells in yellow show a reduction, and cell in grey show an increase.

Chemical groups- Relatively peak area (%)	Straw	NiMo	ZrO	Fe	ZnO	CuCr	ZSM	TiO	FCC	CoMo	CoMo used	CoMo regen
Aldehyde	6.40	19.73	4.85	5.88	11.52	18.96	0.40	1.91	8.60	16.95	15.59	34.76
Carboxylic acids	13.96	10.66	6.05	14.02	22.74	42.23	9.42	9.43	15.38	21.69	12.08	21.17
Ethers	1.99	0.68	1.56	1.86	N.D.	N.D.	0.21	2.12	1.50	1.62	N.D.	N.D.
Furans	5.99	11.38	5.02	1.53	4.05	1.06	1.06	6.36	8.26	12.02	10.22	12.62
Guaiacols	21.33	3.67	16.89	17.50	12.08	4.20	9.45	15.41	11.74	6.36	2.25	N.D.
Ketones	5.91	2.91	2.87	1.73	N.D.	N.D.	3.69	6.55	7.69	6.60	3.31	2.23
Misc. Oxygenates	8.65	N.D.	4.11	3.75	5.33	N.D.	N.D.	5.22	6.76	3.27	2.89	N.D.
Phenols	3.66	0.62	6.46	0.55	N.D.	N.D.	1.48	5.06	2.19	3.35	0.89	N.D.
Sugars	2.77	N.D.	N.D.	N.D.	N.D.	N.D.	1.13	2.17	N.D.	N.D.	N.D.	N.D.
Syringols	4.15	N.D.	9.89	9.08	1.36	1.17	0.41	3.70	6.58	1.65	0.17	N.D.
TOTAL	74.81	49.65	57.70	55.90	57.08	67.62	27.25	57.93	68.70	73.51	47.40	70.78
Aromatic Hydro-carbons	N.D.	8.89	1.47	2.15	N.D.	0.66	14.99	N.D.	N.D.	N.D.	8.77	4.37
Hydro-carbons	N.D.	N.D.	N.D.	N.D.	N.D.	N.D.	N.D.	N.D.	N.D.	N.D.	N.D.	N.D.
TOTAL	N.D.	8.89	1.47	2.15	N.D.	0.66	14.99	N.D.	N.D.	N.D.	8.77	4.37

The two main uses of bio-oil are to produce higher value fuels including biofuels and chemicals. Biofuels require well defined and carefully specified products that are either completely compatible with conventional fuels such as synthetic diesel or gasoline (i.e. hydrocarbons that will require complete de-oxygenation of bio-oil); or can be sufficiently carefully controlled in quality to be blendable in some proportions such as ethanol or a partially de-oxygenated product that is miscible with conventional fuels. The effect of catalysts on the level of aromatic hydrocarbons is shown in Table 8-3.

The formation of aromatic hydrocarbons was enhanced by seven catalysts. The ZSM-5was the most selective followed by NiMo, CoMo used, CoMo regenerated, Fe_3O_2, ZrO, CuCr. Additionally, hydrocarbons are also of interest due to their beneficial effect to bio-oil heating value.

Chemicals need to be able to meet product specification requirements for market acceptability. These may be oxygenated such as phenol where the requirement is

more on delivering a product that is of a sufficiently high concentration to justify separation and refining into a marketable chemical. The ZrO catalyst had the higher phenol yields followed by TiO.

Another important factor in determining the quality of bio-oil is the yields of carboxylic acid. The level of these acids present in bio-oil is responsible for its corrosive effect due to their low pH value. The influence of various catalysts on the production of acids is demonstrated in Table 8-3.

On the contrary, the high concentration of acetic acid could be beneficial for the market. For example, if the aim is a production of a less corrosive bio-oil, the ZrO should be selected for improving bio-oil quality. Therefore, if the objective is the production of acetic acid, the CuCr should be selected.

One of the main objectives is to crack the lignin-derived compounds in bio-oil by using catalysts. Both guaicyl and syringyl compounds are lignin derivatives and their yields are compared in Table 8-3.

Reduction of these compounds suggests that lignin and its derivatives are being successfully reacted and result in lower oxygen content in the final product. The summation of the percentages of all lignin compounds showed that less of lignin derivatives are contained in CoMo regenerated. The rest of the catalysts also decreased the lignin compounds, except ZrO and Fe_3O_2.

Another property of bio-oil is storage stability. Ketones present in bio-oil contribute to its instability and Table 8-3 shows that most of the ketones were decreased in the presence of catalysts apart from TiO, FCC and CoMo.

8.5.1.2 Influence of biomass pre-treatment

The effect of pre-treatment on catalysts is investigated in the current subsection. Four catalysts were used, which were CoMo, ZSM-5, Fe_3O_2, and NiMo. The chromatograms below depicted the influence of pre-treatment on catalysts.

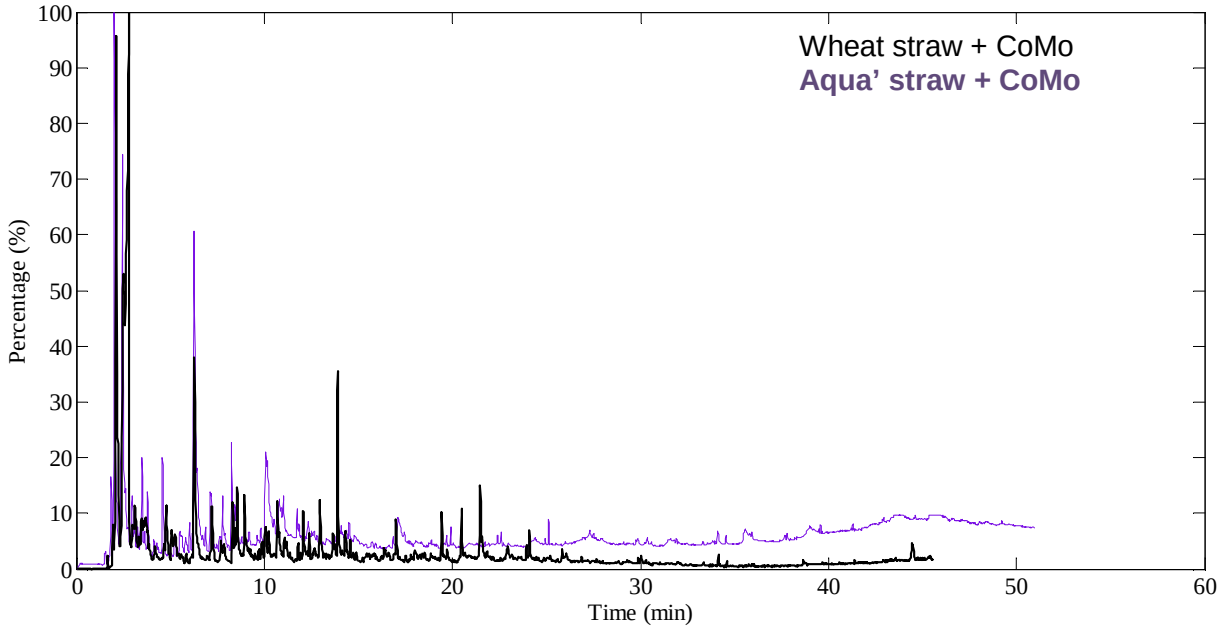

Figure 8-5: Chromatograms obtained from Py-GC/MS for wheat straw with Co-Mo catalyst and aquathermolised wheat straw with CoMo catalyst at 500C

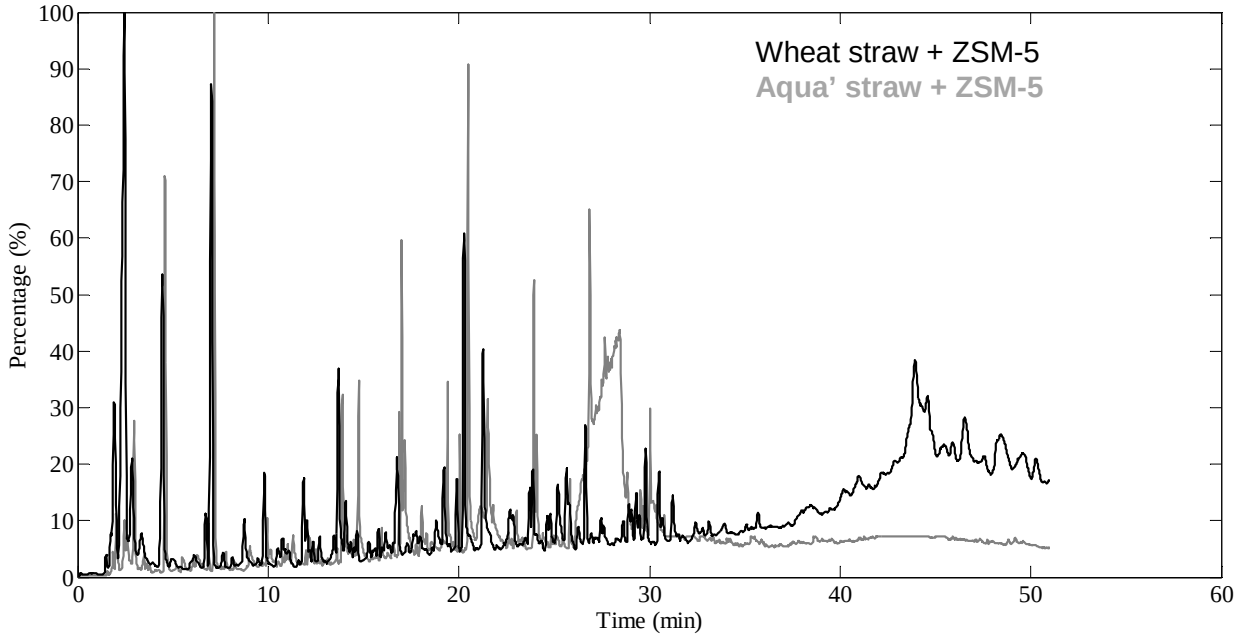

Figure 8-6: Chromatograms obtained from Py-GC/MS for wheat straw with H-ZSM-5 catalyst and aquathermolised wheat straw with H-ZSM-5 catalyst at 500C

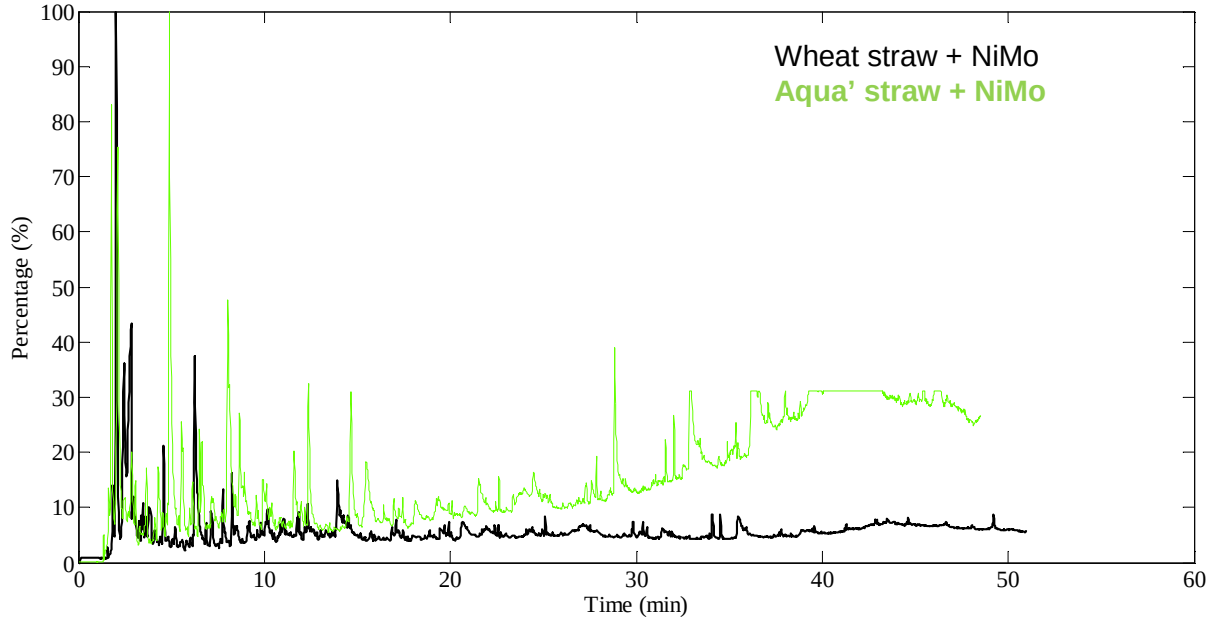

Figure 8-7: Chromatograms obtained from Py-GC/MS for wheat straw with Ni-Mo catalyst and aquathermolised wheat straw with NiMo catalyst at 500C

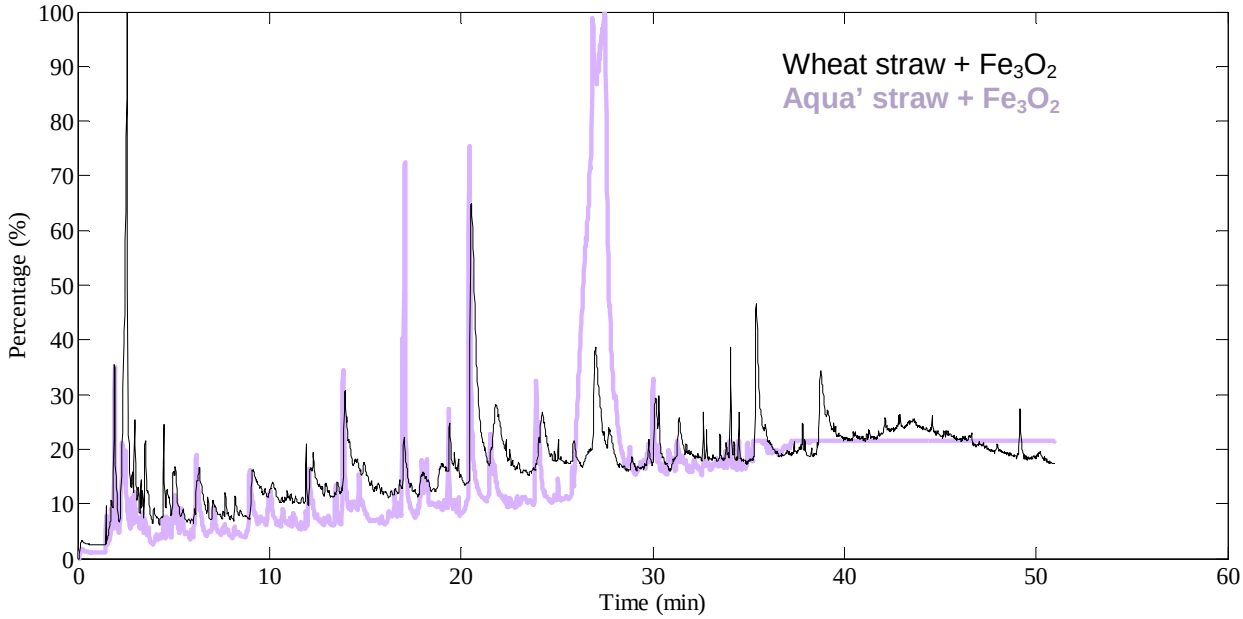

Figure 8-8: Chromatograms obtained from Py-GC/MS for wheat straw with Fe_3O_2 catalyst and aquathermolised wheat straw with Fe_3O_2 catalyst at 500C

The chemical compounds that were identified based on the chromatograms Figure 8-5- Figure 8-8 were separated in chemical groups and are shown in Table 8-4 below.

Table 8-4: The effect of catalysts and pre-treatment on pyrolysis products. Cells highlighted in green show a significant increase from wheat straw and aquathermolised wheat straw with no catalysts; cells in grey show a significant reduction.

Chemical groups- Relatively peak area (%)	**Aqua'**	**Aqua' + CoMo**	**Aqua' + ZSM-5**	**Aqua' + NiMo**	**Aqua' + Fe_3O_2**	Straw	Straw + CoMo	Straw + ZSM-5	Straw + NiMo	Straw + Fe_3O_2
Aldehyde	1.82	24.50	0.99	11.54	3.13	6.40	16.95	0.40	19.73	5.88
Aromatic Hydrocarbons	0.57	7.56	21.61	2.08	ND	ND	ND	14.99	8.89	2.15
Carboxylic acids	0.53	ND	0.46	ND	1.44	13.96	21.69	9.42	10.66	14.02
Furans	1.50	24.40	2.16	16.78	3.81	5.99	12.02	1.06	11.38	1.53
Guaiacols	12.74	1.49	14.45	5.21	10.83	21.33	6.36	9.45	3.67	17.50
Hydrocarbons	ND	0.80	0.27	ND	ND	ND	ND	ND	ND	ND
Ketones	0.51	2.48	0.40	4.01	0.77	5.91	6.60	3.69	2.91	1.73
Phenols	1.67	4.47	0.69	5.30	ND	3.66	3.35	1.48	0.62	0.55
Sugars	32.93	ND	28.68	1.96	29.87	2.77	ND	1.13	ND	ND
Syringols	9.24	ND	13.00	2.39	5.70	1.85	0.41	3.70	ND	4.30

The effect of catalysts on the level of aromatic hydrocarbons is shown in Table 8-4. The formation of aromatic hydrocarbons for aquathermolised wheat straw was enhanced by three catalysts. The ZSM-5 is the most selective followed by CoMo, NiMo. In the case of fresh wheat straw, the ZSM-5 is the most selective followed by NiMo, and Fe_3O_2.

With regards to the catalytic effect on phenol yields for aquathermolised wheat straw, the NiMo had the higher phenol yields followed by CoMo. For wheat straw, CoMo had no effect on phenol yields, while the rest catalysts decreased the yields of phenols.

An interesting result was that for aquathermolised wheat straw was not any noteworthy change concerning the carboxylic acidic yields. On the contrary, when CoMo was applied on fresh wheat straw a major change was observed. This indicated that biomass pre-treatment had an important influence on pyrolysis products as well as the catalyst type.

As it was mentioned in Subsection 8.5.1.1 the low concentration of both guaicyl and syringyl compounds could result in a lower oxygen content in the final product. The summation of the percentages of all lignin compounds showed that less of lignin derivatives was contained in CoMo, followed by NiMo and Fe_3O_2, whereas for ZSM-5 a significant increase was observed. In the case of wheat straw, NiMo showed the lower selectivity, followed by CoMo, ZSM-5 and Fe_3O_2.

The presence of NiMo increased the yield of ketones on aquathermolised pyrolysis vapours, followed by CoMo and Fe_3O_2. Opposing, a reduction was observed on wheat straw ketones yields for all the catalysts, apart from CoMo.

An important result was the significant reduction of sugars for aquathermolised wheat straw. The presence of CoMo and NiMo resulted on the elimination of a high percentage of sugars (32.93%).

8.5.1.3 Influence of pyrolysis reaction temperature

Three catalysts were subjected for analytical pyrolysis at different temperatures (500°C, 600°C, 700°C). The aim of this work was to investigate the effect of temperature on pyrolysis products composition and distribution. CoMo, ZSM-5 and Fe_3O_2 were the chosen catalysts, whereas wheat straw was the feedstock. The chromatograms obtained from Py-GC/MS for wheat straw at 500C, 600C and 700C, as well as the chromatograms obtained from Py-GC/MS for wheat straw with H-ZSM-5, CoMo and Fe_3O_2 catalyst at 500C, 600C and 700C can be found in APPENDIX B in Figure 13-8 to Figure 13-11. Table 8-5 shows the relatively peak area percentages of chemical groups and the reaction temperature effect for wheat straw and the three catalysts.

Table 8-5: The effect of pyrolysis reaction temperature on catalysts and pyrolysis products. Cells highlighted in green show a significant variation from wheat straw with no catalysts, cells in yellow show an decrease, cells in dark grey show an increase

Chemical groups- Relatively peak area (%)	**Straw 500**	**ST 600**	**ST 700**	**CoMo 500**	**CoMo 600**	**CoMo 700**	**ZSM 500**	**ZSM 600**	**ZSM 700**	**Fe 500**	**Fe 600**	**Fe 700**
Aldehyde	6.40	8.51	15.83	16.95	31.35	24.94	0.40	6.32	8.50	5.88	9.22	16.44
Carboxylic acids	13.96	13.50	19.92	21.69	16.89	15.88	9.42	1.85	6.88	14.02	11.91	21.23
Ethers	1.99	1.63	2.04	1.62	N.D.	N.D.	0.21	N.D.	N.D.	1.86	1.22	1.78
Furans	5.99	1.76	2.90	12.02	12.30	13.11	1.06	1.67	2.83	1.53	3.93	5.49
Guaiacols	21.33	10.65	13.86	6.36	N.D.	N.D.	9.45	4.82	5.24	17.50	15.08	8.63
Ketones	5.91	4.33	5.11	6.60	0.41	0.55	3.69	N.D.	N.D.	1.73	5.09	5.27
Misc. Oxygenates	8.65	6.53	9.22	3.27	4.75	N.D.	N.D.	N.D.	N.D.	3.75	4.30	7.63
Phenols	3.66	3.71	1.92	3.35	N.D.	1.96	1.48	N.D.	N.D.	0.55	0.81	0.27
Sugars	2.77	N.D.	N.D.	N.D.	N.D.	N.D.	1.13	N.D.	N.D.	N.D.	N.D.	N.D.
Syringols	4.15	4.01	7.23	1.65	4.17	N.D.	0.41	0.55	3.89	9.08	2.11	6.16
TOTAL	74.81	54.63	78.03	73.51	69.87	56.44	27.25	15.21	27.34	55.9	53.67	72.9
Aromatic Hydro-carbons	N.D.	3.04	3.88	N.D.	6.07	12.46	14.99	57.22	53.81	2.15	2.36	5.92
Hydro-carbons	N.D.	0.31	0.30	N.D.	N.D.	1.91		N.D.	N.D.		N.D.	N.D.
TOTAL	0	3.35	4.18	0	6.07	14.37	14.99	57.22	53.81	2.15	2.36	5.92

An illustration of the influence of temperature on hydrocarbons, as well as the summation of guaiacols, syringols, and carboxylic acids can be found in Figure 8-9, Figure 8-10, Figure 8-11 respectively.

The trend line for wheat straw and wheat straw combined with catalysts indicated that the increase of pyrolysis temperature was beneficial for the formation of hydrocarbons. Specifically, the hydrocarbons production showed a dramatic increase with temperature for ZSM-5 catalyst.

Figure 8-10, presents that greater temperature caused a reduction on guaiacols and syringols compounds. To focus, the correlation of temperature and lignin derived compounds seems linear for CoMo catalyst. Certain conclusions cannot be made for the ZSM-5.

The relatively peak area percentages of carboxylic acids seem to reduce on Figure 8-11, while for fresh wheat straw and Fe_3O_2 were vice versa. The similar behaviour of the Fe_3O_2 catalyst with fresh wheat straw (no catalyst) indicated that is not an effective catalyst, in comparison with CoMo and ZSM-5.

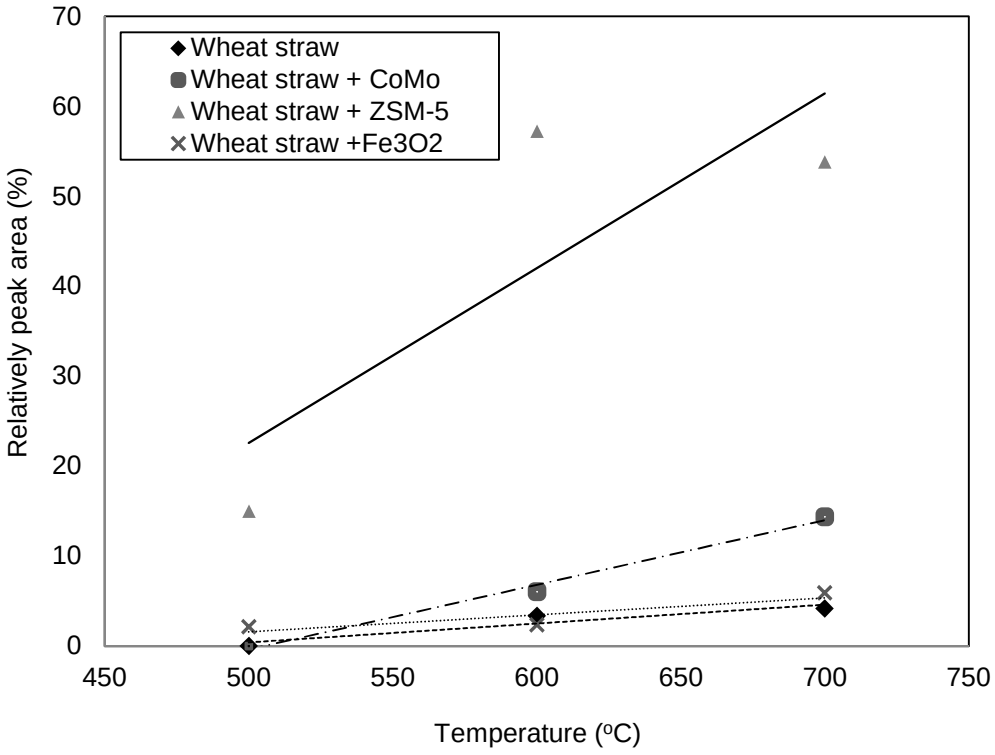

Figure 8-9: Influence of temperature on hydrocarbons

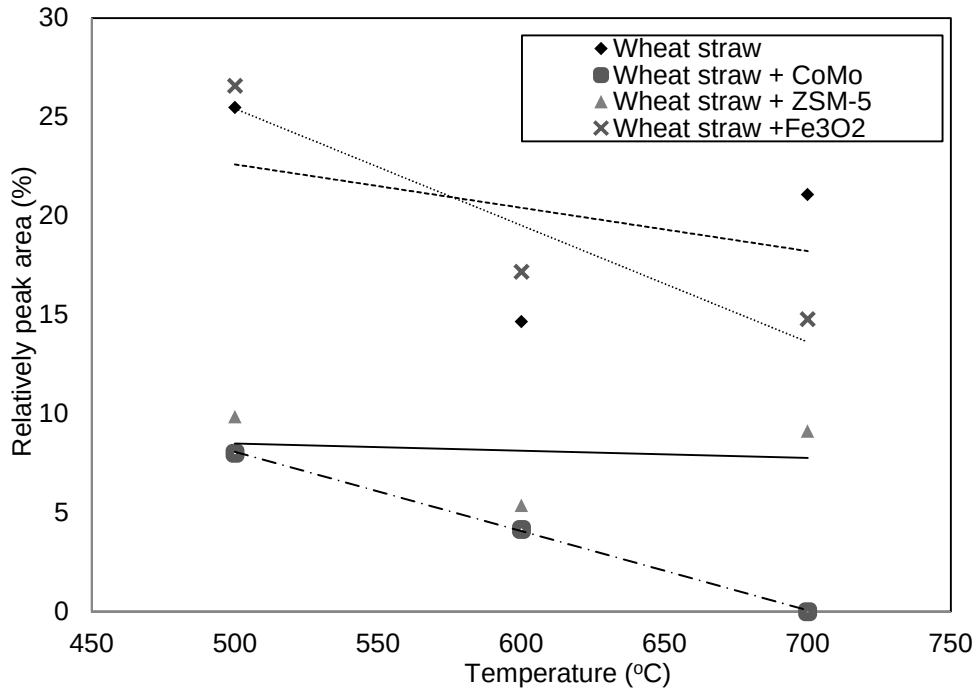

Figure 8-10: Influence of temperature on lignin derived - guaiacols and syringols

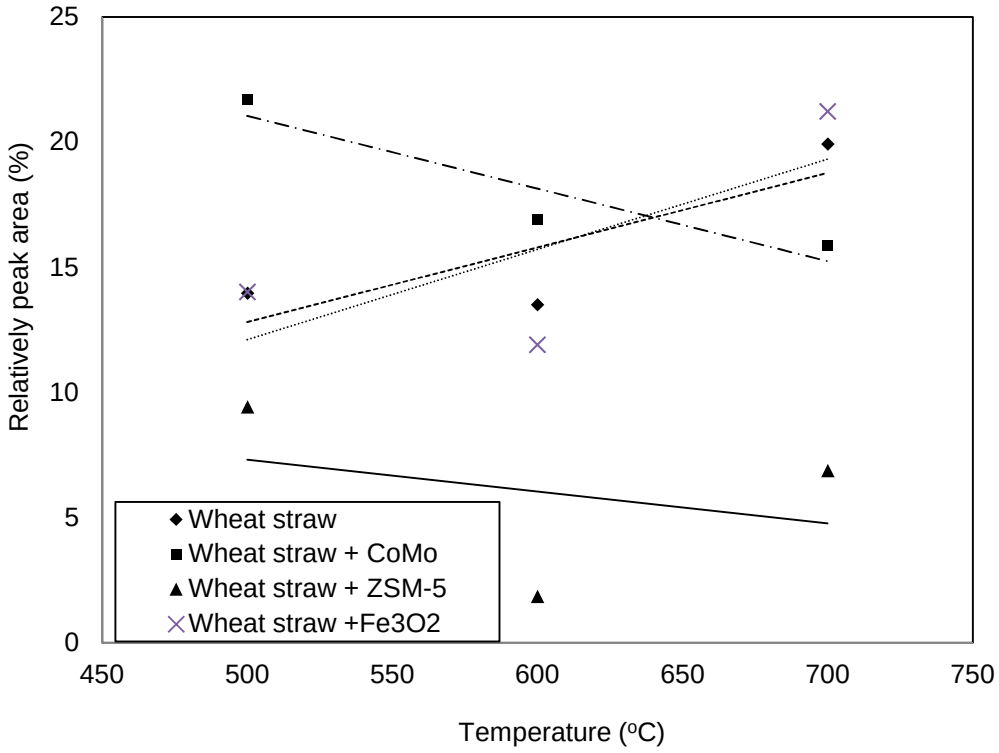

Figure 8-11: Influence of temperature on carboxylic acids

Table 12-7 in APPENDIX - B shows the relatively peak area percentages of chemical groups for wheat straw, all the catalysts, used and regenerated CoMo, catalysts at different temperatures.

8.5.1.4 Effect of catalyst activation

The last set of analytical experiments involved the study of the influence of catalysts activation on pyrolysis vapours. The CoMo, ZSM-5 and FCC catalysts were selected for analytical pyrolysis with wheat straw. The chromatograms obtained from the Py-GC/MS for activation and non- activation of the former catalysts can be found on Figure 8-12, Figure 8-13, Figure 8-14 respectively.

For all the catalysts it can be seen that the activation process had an influence on pyrolysis products. In the case of CoMo the non-activation caused the reduction of the higher molecular weight products of pyrolysis. Figure 8-12 illustrates the significant differences between the two chromatograms of activated and non-activated CoMo. It can been seen that for non-active CoMo a high peak is formed in a low retention time, which is identified as the dihydro-3-methyllene-2.5-furandione. A non-activated CoMo catalysts can be interesting, if the objective is to produce a bio-oil with high concentration of dihydro-3-methyllene-2.5-furandione.

The activation process had a significant influence on pyrolysis products for the H-ZSM-5 catalyst. It can be observed from Figure 8-13 that both chromatograms indicated stable catalysts. The non activate ZSM-5 had a different product distribution.

Figure 8-14 illustrates an unstable non-activated catalysts. The product distribution was similar, though the peaks obtained from the Py-GC/MS chromatogram seemed unstable in comparison with the activate FCC catalyst. The activation process for FCC catalyst indicated an influence on catalyst stability, on the contrary to the ZSM-5 catalyst that the effect focused on pyrolysis products distribution.

The effect of activation process on catalysts was different for each catalyst type. For CoMo the non-activation of the catalyst caused the reduction of the higher molecular weight products of pyrolysis. In the case of H-ZSM-5, non-activation changed the pyrolysis products distribution. The activation of FCC indicated an influence on catalyst stability, rather on pyrolysis products.

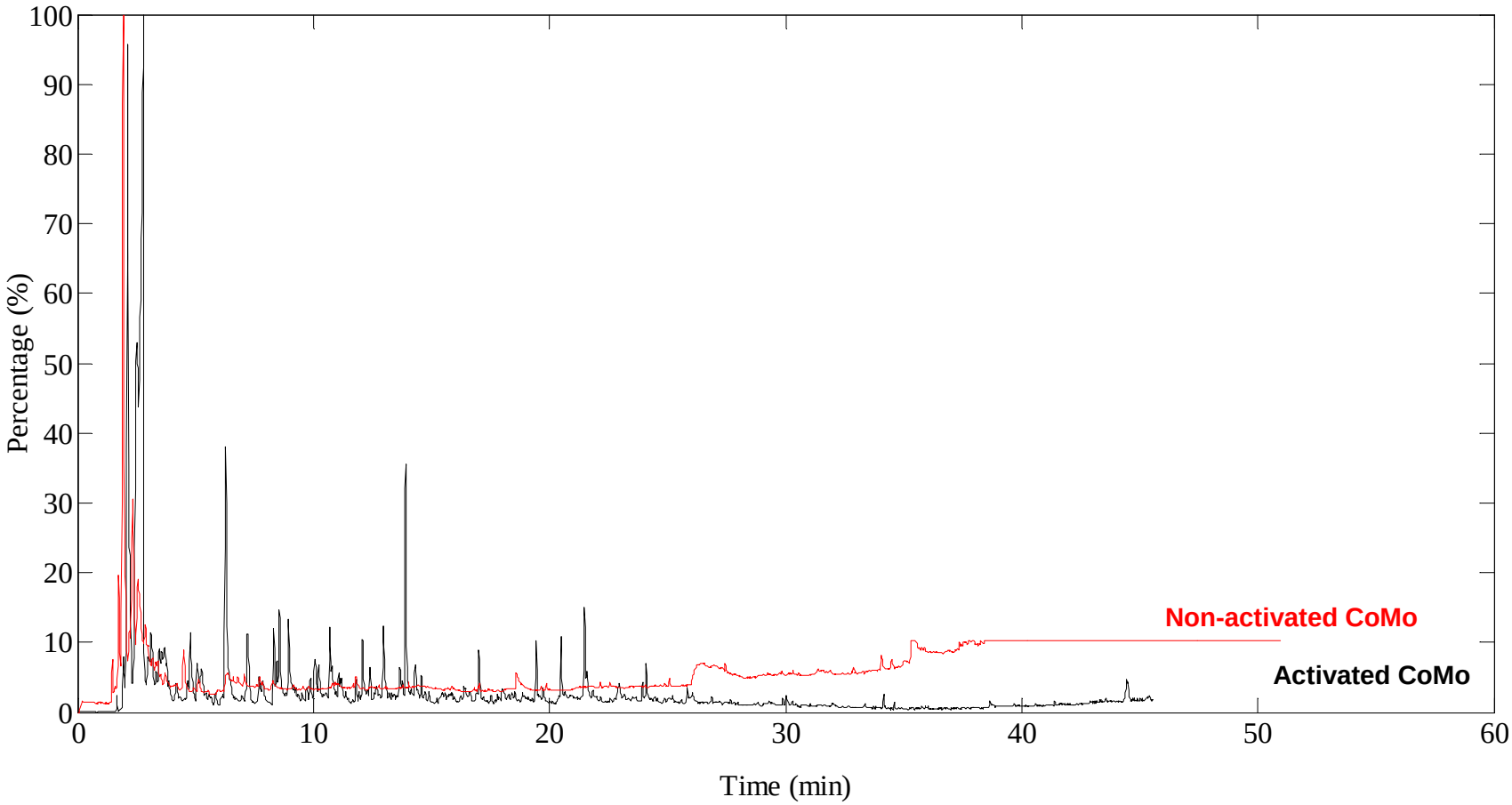

Figure 8-12: Chromatograms obtained by Py-GC/MS for activated and non activated CoMo with wheat straw

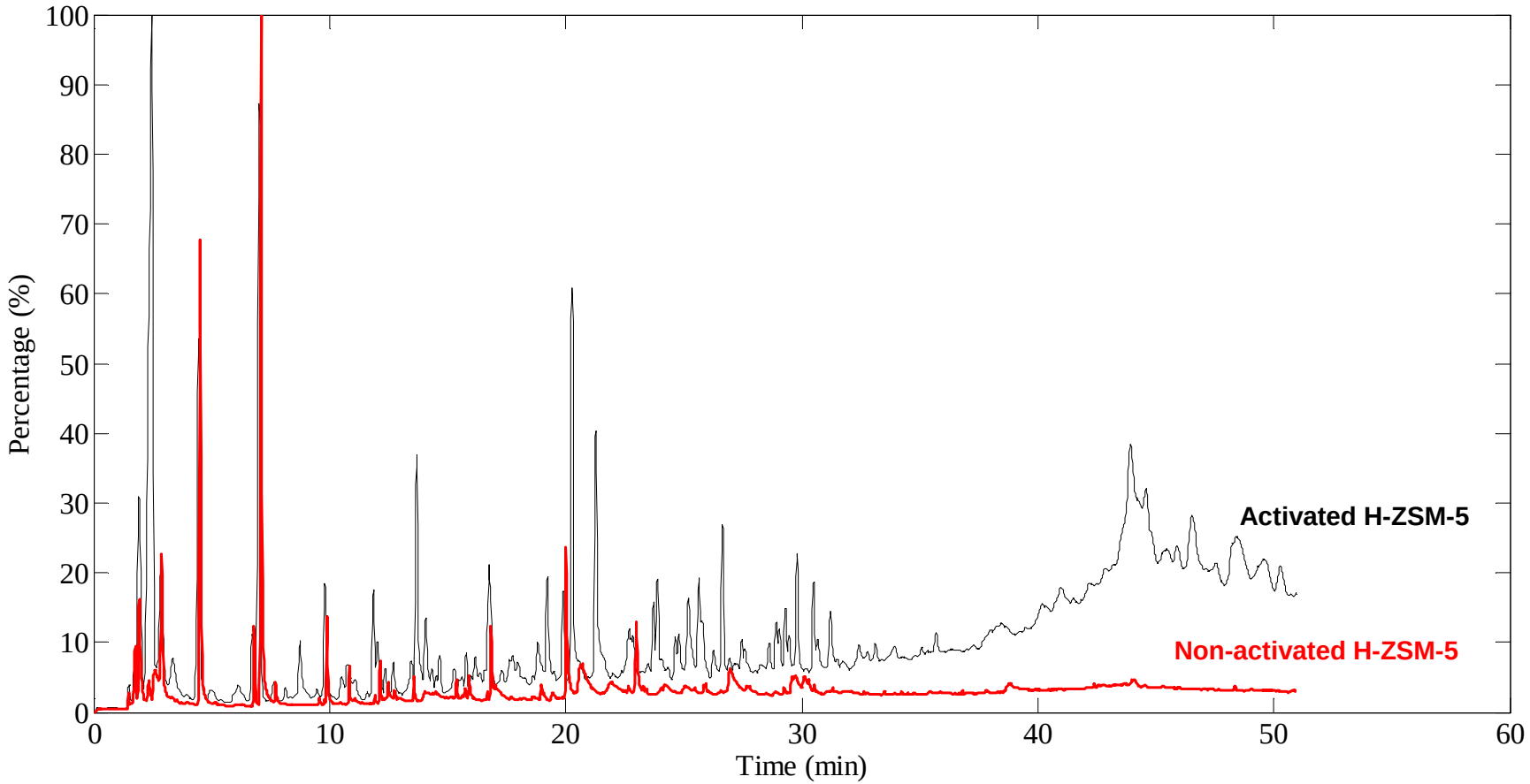

Figure 8-13: Chromatograms obtained by Py-GC/MS for activated and non activated H-ZSM-5 with wheat straw

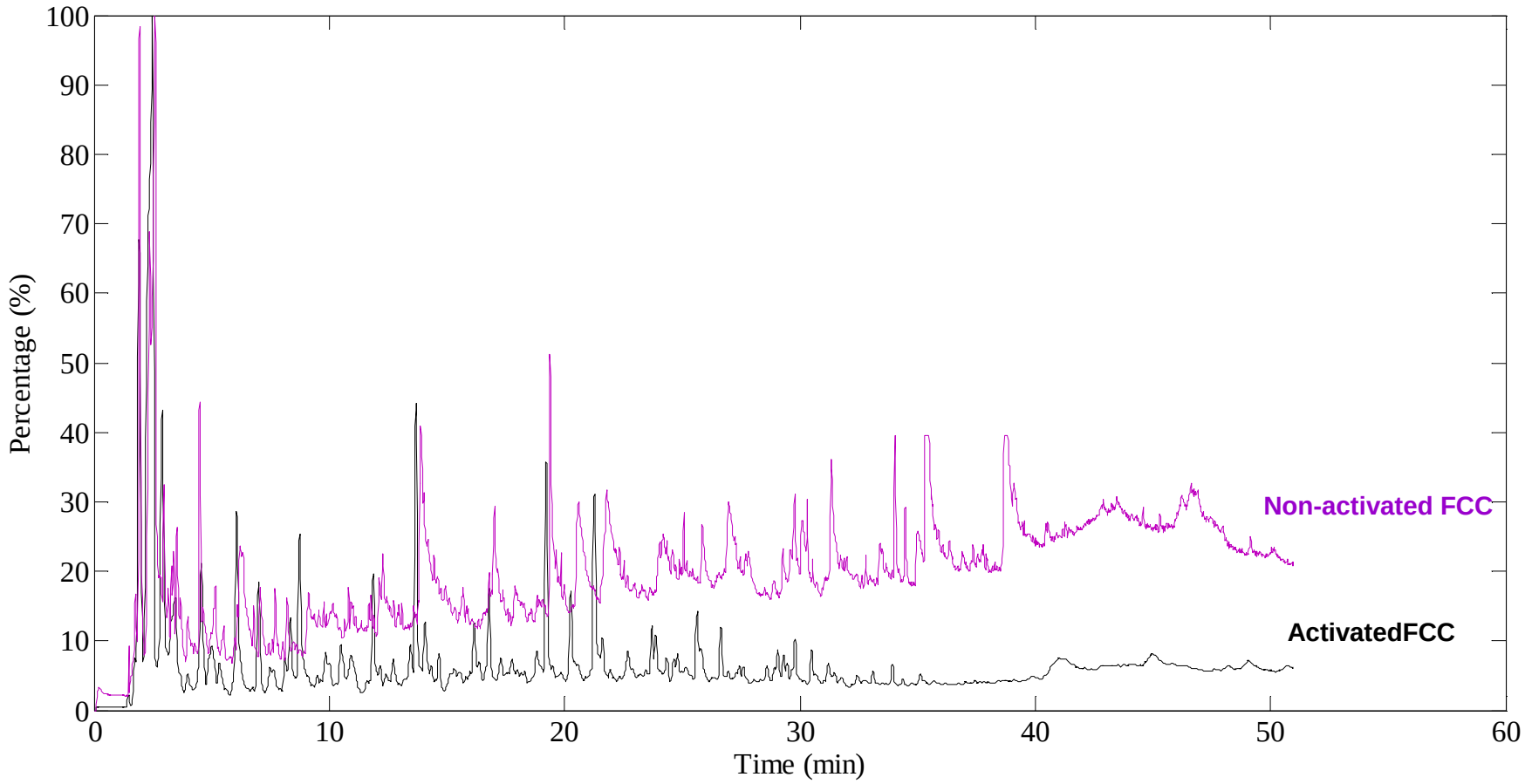

Figure 8-14: Chromatograms obtained by Py-GC/MS for activated and non activated FCC with wheat straw

8.6 Evaluation by laboratory testing

8.6.1 Results and discussion

8.6.1.1 Pyrolysis products yield

Two catalytic fast pyrolysis runs carried out in total and were used to investigate the effect of catalyst (CoMo) on the yield and quality of fast pyrolysis products. The experiments without catalyst with reference 270110 and 140211 were used for comparison. The results from these runs are summarised in Table 8-6. This summarises the operating conditions, the yields of pyrolysis liquids, char and gases and the mass balance closures of the runs.

Table 8-6: Mass balances of catalytic fast pyrolysis runs of wheat straw

Test reference	270110	140211	280211C	80311C
Reactor configuration	**300 g reactor +100 g glass ware**	**300 g reactor +100 g glass ware**	**300 g reactor + catalytic fixed bed reactor+100 g glass ware**	**300 g reactor + catalytic fixed bed reactor+100 g glass ware**
Nominal capacity of reactor	300g/h	300g/h	300g/h	300g/h
Average feed rate	93g/h	117g/h	50g/h	39g/h
Run time (min)	51	103	40	24
Product collection system	Cooler + ESP	Cooler + ESP	Cooler + ESP	Cooler + ESP
Fluidised N_2 flow rate (l/min)	12	2	1	1
Feeder N_2 flow rate (l/min)	2	12	12	16
Fluidising medium	Sand	Sand	Sand	Sand
Sand particle size	500-600	355-500	355-500	500-600
Feedstock	**Wheat straw**	**Wheat straw from ground pellets**	**Wheat straw from ground pellets**	**Wheat straw from ground pellets**
Particle size (mm)	< 1mm	0.255- 1	0.255- 1	0.255- 1
Moisture content (wt%, wet basis)	8.78	5.02	5.02	5.02
Ash content(wt%, dry basis)	8.8	8.8	8.8	8.8
Average pyrolysis T (^oC) in fluidised reactor	492	472	522	501
Catalyst	**Blank run**	**Blank run**	**Co-Mo**	**Co-Mo**
Weight catalyst	-	-	8.67g	9.9g
Catalyst coke	-	-	0.91 g	1g
Average pyrolysis T (^oC) in catalytic fixed reactor	-	-	500	505
Product yields (wt%, dry feed)				

Char in char pot	28.29	0.37	0.09	14.05
Char in agglomerates in bed	N.D.	32.60	67	6.29
Coke	-	-	2.73	6.41
Char	**31.74**	**37.41**	**67.3**	**32.14**
Liquids	**43.32**	**33.72**	**23.33**	**35.70**
Organics	21.75	10.32	5.66	10.29
Reaction water	21.57	23.40	17.67	25.41
Gases	**13.13**	**19.32**	**4.02**	**18.73**
H_2	0.03	0.05	0.04	0.13
CH_4	0.38	1.13	0.31	0.87
CO	3.89	5.03	0.94	4.71
C_2H_4	0.12	0.25	0.11	0.35
C_2H_6	0.38	0.46	0.13	0.35
C_3H_8	0.03	0.44	0.24	0.77
C_3H_6	0.10	0.32	0.16	0.56
C_4H_{10}	0.02	0.25	0.16	0.47
CO_2	8.17	11.39	1.93	7.57
Closure (wt%, dry basis)	**88.19**	**90.45**	**95**	**86.57**

Feeding	Feeding was possible	Feeding was possible	Feeding was possible	
Problem	bed T drop	Char did not leave the bed- Char pot was empty, Agglomeration in the bed	1. No vapours were visible in the EP for 12 min before the feed blockage 2. Feed blockage at entrance to fast screw	
Cause		Not proper fluidization in the bed, Nature of wheat straw	Blockage in the catalytic bed, due to catalysts coking Construct a larger catalytic fixed bed	
Solution		Probably an increase on N_2 flow rate in feeder		
Observations			1. Catalyst was black (due to coking) and difficult to remove from fixed bed 2.Agglomeration in fluidised bed 3. Aerosols were not visible in EP, indicating that they were trap in the catalytic bed	

Wheat straw as a biomass feedstock caused difficulties including feeding problems, agglomeration, reproducibility, phase separated pyrolysis oil. This problems were discussed in Chapter 6. It can been observed from Table 8-6 that agglomeration still occurred for the catalytic runs. The run with reference 80311C formed less char in the fluidised bed than the run 280211C. This was the cause for the liquid yields reduction.

It can be seen that the mass balance varies on the range of 95-55 wt% dry basis. Table 8-6 shows that higher liquid yield was obtained for the catalytic run with reference

80311C. The organic part of bio-oil is the non-water part that contains the desirable products. The catalytic run 80311C gave higher liquid yields, even though the organic parts of both catalytic run 80311C and the non- catalytic140211 are similar. The higher yield of reaction water in the catalytic run 80311C indicated that de-oxygenation of bio-oil took place through dehydration reactions.

The catalytic run 280211C produced lower liquid and organic yields than the catalytic run with reference 80311C. This can be explained by the agglomeration which occurred at run 280211C. The phenomenon of agglomeration at run 280211C, disturbed the fluidisation of the bed. This resulted to a high char content in the bed of 67% wt dry biomass basis and a lower liquid yield. For these reasons a higher nitrogen rate was used on run 80311C. The fluidisation nitrogen rate was increased from 12l/min to 16l/min to avoid the agglomeration phenomenon.

Figure 8-15: Agglomeration in fluidised bed

This is with totally agreement with the non-catalytic runs with reference 270110 and 140211. The experiment with reference 270110 produced higher liquid and organic yields in comparison with 140211. The biomass used were ground wheat straw and wheat straw from ground pellets respectively. The agglomeration phenomenon occurred only at run 140211, resulting in the production of a lower liquid yield.

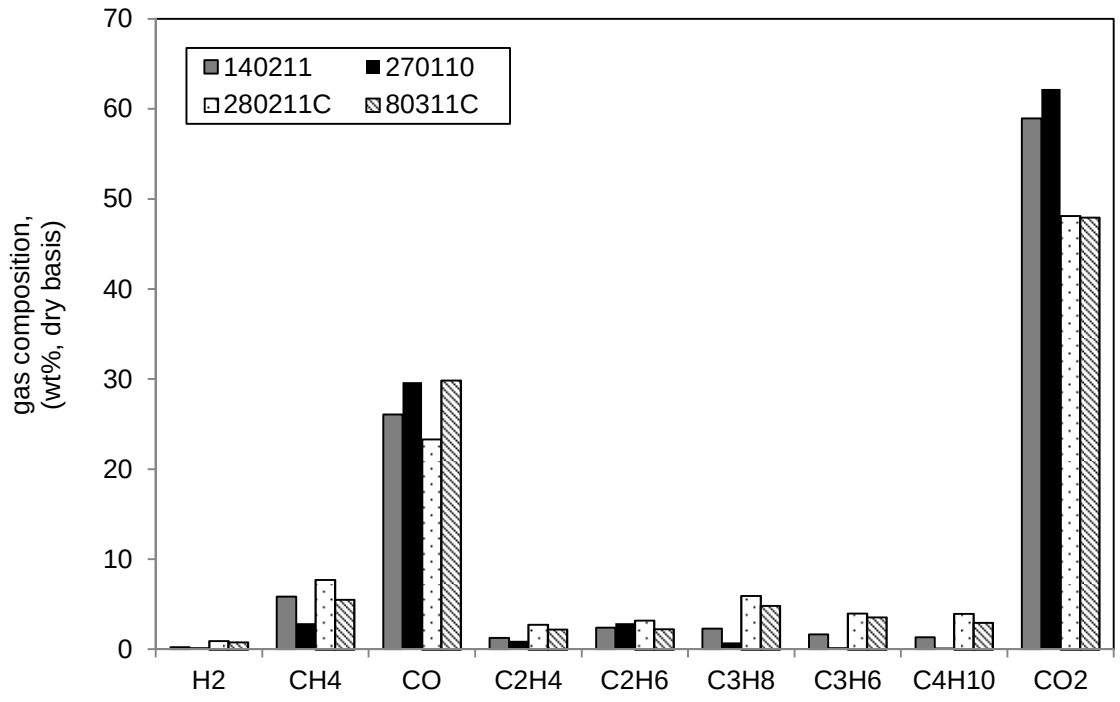

Figure 8-16: Gas composition on dry basis of weight percent (wt %, dry basis) from the fast pyrolysis runs using wheat straw and wheat straw + CoMo

It should be noticed that for both catalytic runs the yields of CO_2 were decreased, in comparison with the non-catalytic runs. It can be added that for both non catalytic runs, the yields of certain gases such as H_2, CH_4, C_2H_4, C_2H_6, C_3H_8, C_2H_6, and C_4H_{10} decreased, in comparison with both catalytic runs.

Figure 8-17 below shows the catalyst pellets before and after the catalytic runs. The black colour of the pellets indicated the coke formation on the catalyst. After the catalytic runs CoMo was crashed to become powder and it was observed that it was still black, indicated that coking took place inside the pores. Another finding was that the aerosols was not seen in the electrostatic precipitator (see Figure 8-18). This means that probably the aerosols was trapped in the catalyst pores.

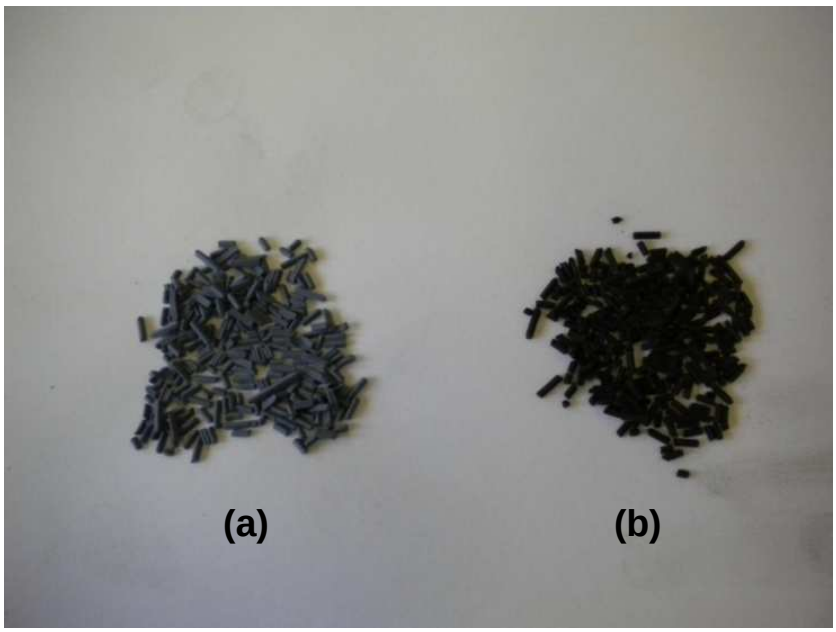

Figure 8-17: Co-Mo catalysts before (a) and after (b) run

Figure 8-18: EP after run 280211- Not aerosols in EP

The main bio-oil produced from the catalytic runs was phase separate. This can be observed from Figure 8-19 below.

Figure 8-19: Main bio-oil condensed in water condenser / Collection of main bio-oil in pot 1

8.6.1.2 Bio-oil analysis

The bio-oil obtained by the catalytic runs were subjected to analysis and Table 8-7 show the water content and pH values. Due to the high water content and the equipment limitations, a molecular weight analysis and elemental analysis were not possible.

It is important to highlight that the bio-oil produced from the 300g/h fluidised reactor with a secondary fixed bed reactor were collected in three locations (pot 1, pot 2 and pot 3) as mentioned in section 4.4. For both catalytic runs (run 280111C, 80311C) pot 1 contained phase separated oil, but it was not possible to divide it in aqueous light fraction and heavy organic fraction. A mixture of the aqueous and heavy fraction was used for the water content, pH and chemical analysis.

Table 8-7: Water content and pH analysis of bio-oil

Test ref.	140211		280211C	80311C
Water content %	Aqueous Light fraction	Organic Heavy fraction		
Pot 1	77.5	14.23	88.87	91.98
Pot 2+3	64.8		87.32	89.11
pH	Aqueous Light fraction	Organic Heavy fraction		
Pot 1	4.82	4.48	5.32	4.56
Pot 2+3	5.2		6.2	3.8

The pH value was higher for the catalytic runs, in comparison with the non-catalytic experiments. This is probably relevant to the higher water content of the catalytic experiments.

The determination of chemical compounds had only be performed on pot 1. The water content of pots 2 and 3 was too high (>87%) to perform any accurate analysis. Figure 8-20 illustrates the chromatograms obtained by the GC/MS and shows the difference of the bio-oil obtained from the catalytic runs with reference 280211C and 80311C. From Figure 8-20 and Table 8-8 it can be observed that both bio-oil samples shown similar chemical distribution, even the different pyrolysis products yields of Table 8-6.

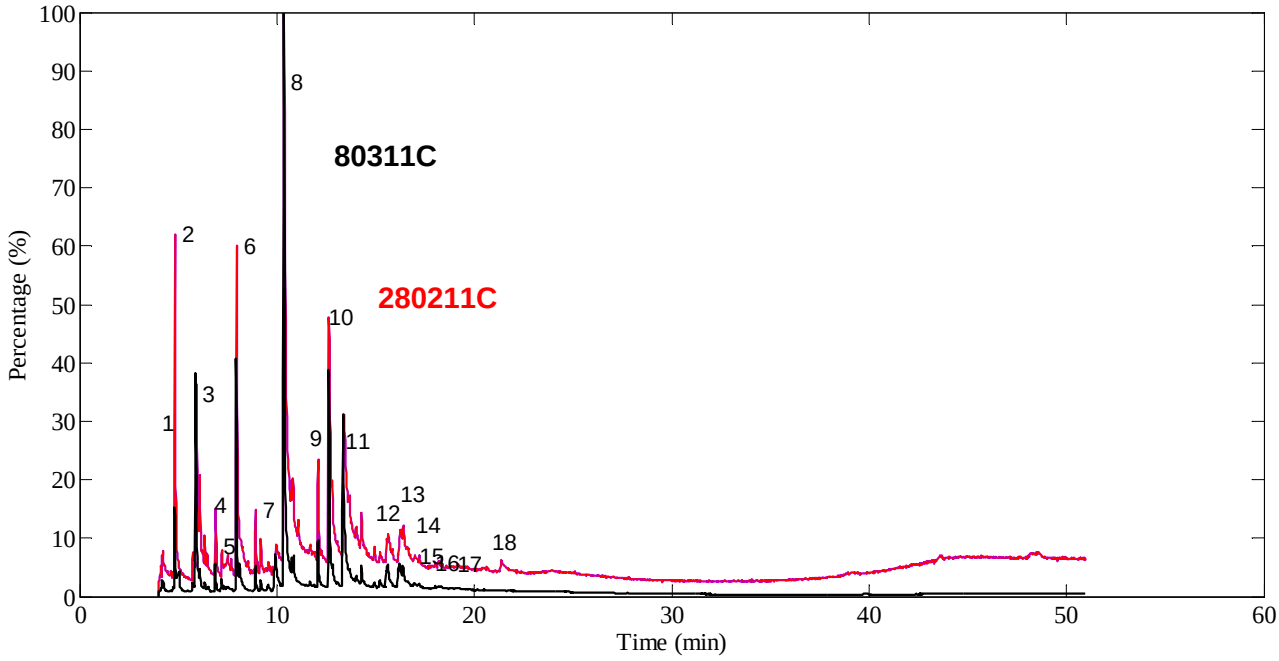

Figure 8-20: Chromatograms obtained by GC/MS and chemical identification, ground pellets from wheat straw + CoMo catalyst. See Table 8-8for details

Table 8-8: Identification of chemicals from ground pellets for wheat straw + CoMo catalyst by GC/MS

1	Toluene/methyl benzene	12	2.3-dimethyl-phenol
2	(5H)-furan-2-one/2(5H)-Furanone	13	2-ethyl-phenol
3	2-ethyl-2-butenal	14	3-ethyl-phenol
4	Ethylbenzene	15	2-methoxy-4-methyl-phenol/p-Cresol, 2-methoxy-/p-Creosol/p-Methylguaiacol
5	o-Xylene/1.2-Dimethyl-Benzene		
6	2-Methyl-2-Cyclopenten-1-one/2-Methyl-2-Cyclopentenone	16	4-ethyl-2-methyl-phenol
7	1.2.3-trimethyl-cyclopentene	17	4-Ethyl-2-methoxyphenol/4-Ethyl guaiacol/4-Hydroxy-3-methoxy ethylbenzene/p-Ethylguaiacol
8	Phenol		
9	2.3-dimehtyl-2-Cyclopenten-1-one	18	2-Methoxy-4-vinylphenol/4-Vinylguaiacol/p-Vinylguaiacol/4-Hydroxy-3-methoxystyrene
10	2-methyl-phenol/o-Cresol		
11	Mequinol/4-methoxy phenol/p-Methoxyphenol/p-Guaiacol		

In addition, Figure 8-21 is presented below to show the chromatogram of the aqueous and heavy phase of the non catalytic run 140211.

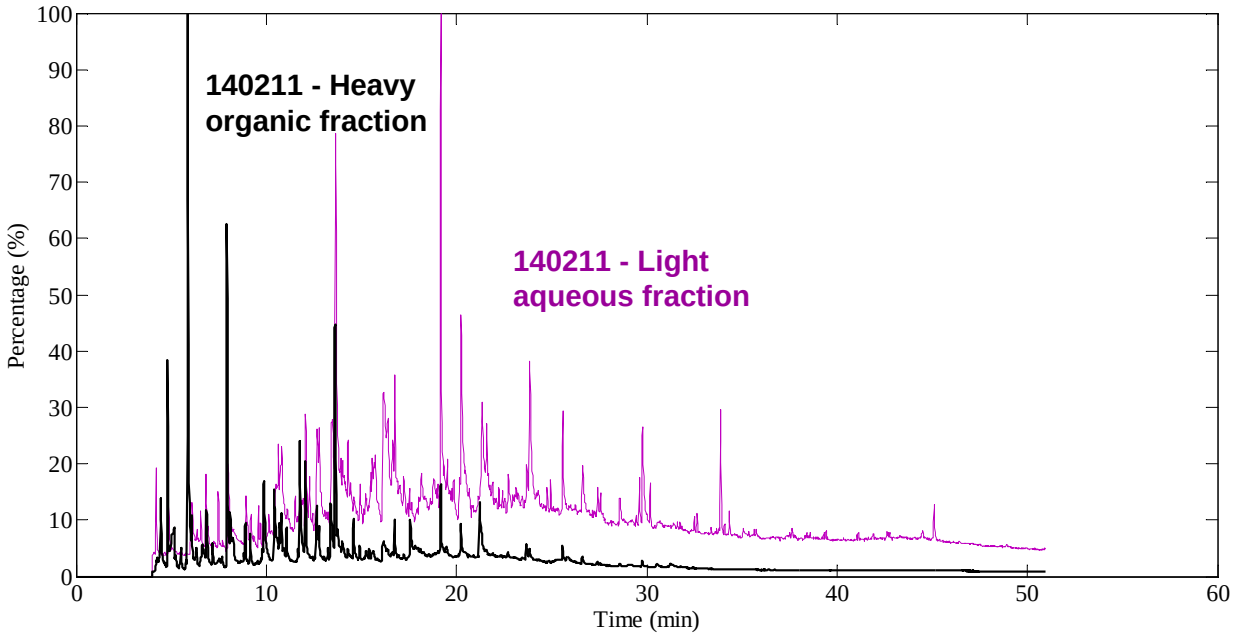

Figure 8-21: Chromatograms obtained by GC/MS, ground pellets from wheat straw

The chemical compounds that were identified based on the chromatograms on Figure 8-20 were separated in chemical groups and are shown in Table 8-9.

Table 8-9: The effect of CoMo catalysts on pyrolysis products. Cells highlighted in grey show a significant variation from wheat straw with no catalysts at 500^{o}C

Chemical groups- Relatively peak area (%)	140211 - light fraction	140211 - heavy fraction	80311C	280211C
Aldehyde	N.D.	0.47	1.10	3.20
Aromatic Hydrocarbons	N.D.	2.10	N.D.	0.50
Carboxylic acids	4.20	N.D.	N.D.	N.D.
Furans	14.63	0.02	11.97	10.34
Hydrocarbons	2.90	0.78	1.09	0.82
Ketones	19.92	4.17	11.80	11.93
Guaiacols	16.34	37.50	N.D.	1.34
Phenols	11.56	23.78	66.26	60.37
Syringols	4.10	5.42	N.D.	N.D.

The effect of CoMo catalyst on the level of phenolics compounds is shown in Table 8-9. The formation of phenols for wheat straw has been enhanced by the use of catalyst. Both bio-oil samples shown an increase for phenol yields. Figure 8-22 illustrates the phenols distribution on the catalytic bio-oil.

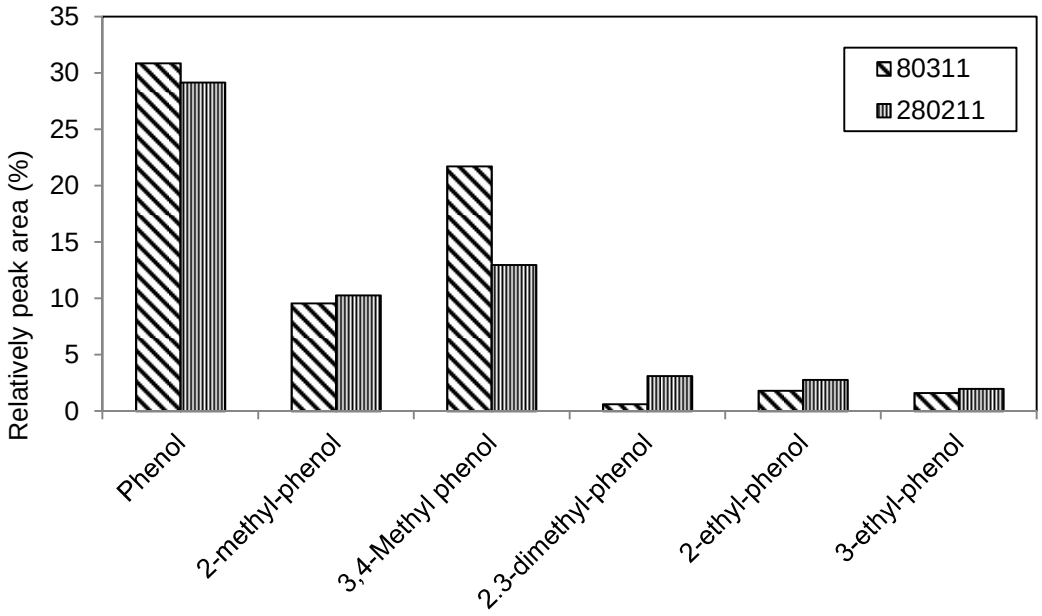

Figure 8-22: Relatively peak area percentages of phenols in wheat straw + CoMo derived bio-oil

As it was mentioned above the low concentration of both guaicyl and syringyl compounds could result in lower oxygen content in the final product. The summation of the percentages of all lignin compounds showed that less of lignin derivatives was contained in catalytic treated bio-oil by CoMo.

The presence of CoMo reduced the yield of ketones on wheat straw pyrolysis oil. Ketones present in bio-oil contribute to its instability and Table 8-9 shows that ketones yields were decreased in the presence of the CoMo catalyst.

8.7 Chapter conclusions

Eleven catalysts were tested for their effect on the pyrolysis products of wheat straw and aquathermolised wheat straw using a Py-GC/MS. Their influence on improving the quality of bio-oil were investigated in terms of reduction of lignin derived compounds, corrosiveness, and hydrocarbon production. The definition of bio-oil quality depends upon the different uses of bio-oil. The properties of bio-oil that could need improvement depend on each bio-oil application. Therefore, it is not possible to assume if the use of catalyst leads to overall stability improvement of bio-oil.

8.7.1 Comparison of catalysts

The conclusions from the screening of catalysts with straw are organised as follows:

- The ZSM-5 catalyst, showed the most significant increase in formation of aromatic hydrocarbons followed by NiMo, CoMo used, CoMo regenerated, compared to no catalyst. The other catalysts also showed a small increase in hydrocarbon formation.
- With regards to the phenol production, ZrO gives a higher yield by around 50% compared to no catalyst. ZnO, CuCr and CoMo regenerated eliminates phenols yields.
- The level of carboxylic acids present in bio-oil is responsible for its corrosive effect due to their low pH value. For this reason, the ZrO would be selected for improving bio-oil quality. Therefore, if the objective is the production of acetic acid, the CuCr would be selected.

In terms of overall catalysts performance and promise:

- TiO does not appear to be a promising catalyst for any application.
- FCC catalyst has some effect but the changes in product composition are not sufficiently significant to offer much promise.
- ZrO catalyst has an important effect on phenol production and reduction on carboxylic acids.
- CoMo and NiMo catalysts had a significantly different effect than the other catalysts and are therefore worthy of continued study, especially in multifunctional systems.
- As expected, ZSM-5 catalysts show significant improvement in hydrocarbon product and work on these materials should be developed.
- An interesting outcome was that CoMo used and CoMo regenerated shown an increase on hydrocarbon formation, whereas fresh CoMo had no effect.

8.7.2 Influence of biomass pre-treatment

In terms of the pre-treatment influence on catalyst:

- Fresh wheat straw and aquathermolised wheat straw shown a completely different product distribution. The noteworthy difference is the formation of a high peak of levoglucosan for pre-treated straw, compared with fresh straw.
- The ZSM-5 is the most selective catalysts for the formation of hydrocarbons followed by CoMo, NiMo.
- Regarding the catalytic effect on phenol yields for aquathermolised wheat straw, the NiMo has the higher phenol yields followed by CoMo. For wheat straw,

CoMo had no significant effect on phenol yields, while the rest catalysts decreased the yields of phenols.

- An interesting result was that for aquathermolised wheat straw was not any noteworthy change concerning the carboxylic acidic yields. On the contrary, when CoMo was applied on fresh wheat straw a major change was observed. This indicates that pre-treatment had an important influence on pyrolysis products as well as the catalyst type.
- The presence of NiMo increased the yield of ketones on aquathermolised pyrolysis vapours, followed by CoMo and Fe_3O_2. Opposing, a reduction was observed on wheat straw ketones yields for all the catalysts, apart from CoMo.
- An important result was the significant reduction of sugars for aquathermolised wheat straw. The presence of CoMo and NiMo resulted on the elimination of a high percentage of sugars (32.93%).

8.7.3 Influence of pyrolysis reaction temperature

- The trend line for wheat straw and wheat straw combined with catalysts indicated that the increase of pyrolysis temperature was beneficial for the formation of hydrocarbons. In specific, the hydrocarbons production showed a dramatic increase with temperature for ZSM-5 catalyst.
- Greater temperature caused a reduction on guaiacols and syringols compounds. To focus, the correlation of temperature and lignin derived compounds seems linear for CoMo catalyst. Certain conclusions cannot be made for the ZSM-5 catalyst.
- The relatively peak area percentages of carboxylic acids seemed to reduce with temperature increase, while for fresh wheat straw and Fe_3O_2wasvice versa.
- The increase of temperature for pyrolysis of wheat straw with the Fe_3O_2 catalyst showed a similar trend with the non-catalytic pyrolysis. This indicates that Fe_3O_2 catalyst is not such an effective catalyst, in comparison with CoMo and ZSM-5.

8.7.4 Effect of catalysts activation

- For all catalysts the activation process had an influence on pyrolysis products.
- For CoMo the non-activation of the catalyst caused the reduction of the higher molecular weight products of pyrolysis.
- In the case of H-ZSM-5, non-activation changed the pyrolysis products distribution.

- The activation process for FCC catalyst indicated an influence on catalyst stability, in contrast to the ZSM-5 catalyst whereby the effect focused on pyrolysis products distribution.

8.7.5 Laboratory experiments using CoMo with wheat straw

Applying the CoMo catalyst on fast pyrolysis process for wheat straw resulted to obtained a completely different bio-oil in comparison with non catalysts. The organic yields decreased significantly, whereas the reaction water increased. The increase of reaction water indicated that de-oxygenation occurred by dehydration reactions.

The most significant result was the massive increase on phenols levels in bio-oil. This is important for market acceptability. Phenols may be oxygenated but the requirement of the market could be less on de-oxygenation and more on delivering a product that is of a sufficiently high concentration to justify separation and refining into a marketable chemical. The introduction of CoMo catalyst in the fast pyrolysis process, resulted to a significant increase of phenol yields in bio-oil.

9 CONCLUSIONS

9.1 Response to the two main objectives

Objective 1: *Examine the influence of pre-treatment of biomass on the fast pyrolysis process and liquid quality*

It was found that pre-treatment had a significant effect on thermal decomposition of biomass. Differences included the maximum rate of weight loss, the temperature of maximum rate of heat loss, the pyrolysis products composition, and the proportion of key components in bio-oil.

1 The temperature of maximum rate of weight loss as showed by the DTG graph in the TGA was more pronounced for aquathermolised wheat straw and steamed poplar, and least for torrefied wood. An increase of temperature was observed for aquathermolised wheat straw and steamed poplar, and a small decrease for torrefied wood.

2 Hemicellulose was reduced significantly for all the pre-treated feedstocks. This was proved by the DTG graphs, in which the hemicellulose peak was not found in the case of the pre-treated feedstocks.

3 DTG and TG graphs obtained by TGA analysis showed that the pre-treatment of torrefaction was more effective for spruce, in comparison with poplar. Additionally, the Py-GC/MS showed that phenolics were increased after torrefaction and this was more apparent for spruce. This indicates that feedstock type had an influence on the effect of torrefaction on bio-oil composition.

4 The Py-GC/MS showed a small increase in phenolics for the torrefied samples compared to untreated wood. A noticeable increase in the amount of phenolics was recorded from steamed poplar.

5 The levoglucosan yields from fast pyrolysis of aquathermolised wheat straw increased significantly by a factor of over 27, while the acetic acid yields were eliminated. This was observed from the chromatograms obtained by the Py-GC/MS. An explanation could be that the alkali metals were washed out by this hot pressurised water process, resulting in an increase of levoglucosan yields. Additionally, light volatiles such as acetic

acids probably were removed due the aquathermolysis process temperature (180^{o}C).

6 Larger scale experiments using the 100g/h and 300g/h fluidised bed reactors with pre-treated feedstocks showed to be in agreement with the micro-scale Py-GC/MS experiments. Pyrolysis of pre-treated feedstocks changed the proportion of key components in bio-oil and pyrolysis vapours, in comparison with the untreated feedstocks; torrefaction increased phenolics; aquathermolysis increased significantly levoglucosan; steam pre-treatment increased considerable phenolics.

7 Both untreated and torrefied wood caused irregularity of feeding with the pneumatic feeder of the 100g/h fluidised bed reactor system.

8 Performing pyrolysis on aquathermolised wheat straw altered the physical characteristics of the bio-oil produced, changing it from phase separate to homogeneous oil. Pyrolysis using wheat straw had some disadvantages such as pre-pyrolysis and agglomeration. The use of aquathermolised wheat straw avoided these problems, possible due to the lower level of alkali metals and consequently a slower reaction rate.

9 Torrefaction proved to have a mild influence on pyrolysis products, when compared to aquathermolysis and steam pre-treatment.

Objective 2: *Study the influence of catalysts on fast pyrolysis liquids*

Screening by Py-GC/MS

1. TiO does not appear to be a promising catalyst for any application.
2. FCC catalyst has some effect but the changes in product composition are not sufficiently significant to offer much promise.
3. ZrO catalyst has an important effect on phenol production and reduction on carboxylic acids.
4. CoMo and NiMo catalysts had a significantly different effect than the other catalysts, such as the reduction of the higher molecular weight products of pyrolysis, and are therefore worthy of continued study, especially in multifunctional systems.
5. As expected, ZSM-5 catalysts show significant improvement in aromatic hydrocarbon product and work on these materials should be developed.
6. An interesting outcome was that CoMo used and CoMo regenerated shown an increase on hydrocarbon formation, whereas fresh CoMo had no effect.

Laboratory experiments

1. The screening of catalysts showed that CoMo was a highly active catalyst, which particularly reduced the higher molecular weight products of fast pyrolysis. From these screening tests, CoMo catalyst was selected for larger scale laboratory experiments.
2. Applying the CoMo catalyst on the fast pyrolysis of wheat straw resulted in an entirely different bio-oil in comparison to non catalytic runs. The organic yields decreased significantly, whereas the reaction water increased. The increase of reaction water indicated that de-oxygenation occurred by dehydration reactions.
3. The most significant result was the massive increase in phenol levels in bio-oil. This is important for market acceptability. Phenols may be oxygenated but the requirement of the market could be less on de-oxygenation and more on delivering a product that is of a sufficiently high concentration to justify separation and refining into a marketable chemical.

9.2 Response to sub-objectives

Sub-objective 1: *Compare biomass types in terms of fast pyrolysis liquid quality*

1. Concerning the thermal degradation behaviour of various biomass types it was found that biomass type has a significant effect on thermal decomposition. Differences included in the maximum rate of weight loss; the temperature of maximum rate of heat loss; the pyrolysis products composition, and the proportion of key components.
2. Specifically, wheat straw has the lowest temperature of maximum rate of weight loss, when compared with the poplar, spruce and DDGS. A low peak temperature is desirable due to less energy required for optimum weight loss. Further analysis through the DTG profiles showed that maximum rate of weight loss occurs on poplar sample. In addition, the decomposition region of the samples shows dissimilar characteristics; spruce has a narrow region while DDGS has a wide decomposition region. DDGS is a bio-ethanol refinery by-product containing starch, protein, crude fibre and crude fat. Furthermore, the DDGS composition reflected in the DTG profile, shows a number of prominent peaks in comparison with the other biomass. A low temperature

peak is more apparent in DDGS, possible due to high hemicellulose content in the sample. A peak feature can be noticed at 440ºC.

3. Results from Py-GC-MS show that spruce contains the greater amount of lignin derivates while DDGS has the lowest. It is noticeable that spruce has the higher peak area for levoglucosan in comparison with the other feedstocks. Furthermore, a high amount of acetic acid can be seen for wheat straw. Another interesting result is the identification of toluene for DDGS.

Sub-objective 2: *Understand and define the concept of bio-oil quality*

Before bio-oil can effectively be used in any application as a fuel and/or chemical source, there are several inherent properties that require consideration.

Biofuels require well defined and carefully specified products. These are either completely compatible with conventional fuels, such as synthetic diesel or gasoline (i.e. hydrocarbons that will require complete de-oxygenation of bio-oil), or can be sufficiently carefully controlled in quality to be blendable in some proportions, such as ethanol or a partially de-oxygenated product that is miscible with conventional fuels. Production of unique or dedicated biofuels such as ethanol, methanol or DME is also possible, but only through gasification to syngas and synthesis of the required product. This route is not considered further for the purpose of the present thesis.

The most important general quality requirements are:

4. All direct uses of bio-oil require a consistent and homogenous product, for which homogeneity is the most important for storage, handling and processing.
5. Low solids are important to avoid potential blockage of injectors, filters and catalyst beds.
6. Low alkali metals and other impurities such as traces of sulphur and chlorine are important in catalytic systems.

The most important quality requirements for production of transport fuels and chemicals by any method in addition to the points 1-3 above are:

- Water content.
- Acidity.

- Oxygen content.

Chemicals need to be able to meet product specification requirements for market acceptability. These may be oxygenated (such as acetic acid or phenol), whereby the requirement is less on de-oxygenation and more on delivering a product that is of a sufficiently high concentration, to justify separation and refining into a marketable chemical. Examples include precursors for phenol substitution in wood panel resin production; these may be whole bio-oil or extracts from bio-oil. Hydrocarbon chemicals are also of interest and may be produced along with biofuels from de-oxygenation.

Sub-objective 3: *Determine the optimum pyrolysis reaction temperature for wheat straw to obtain the highest organics yield*

Fast pyrolysis experiments were carried out using the 300g/h and 1kg/h fluidised bed reactor systems. Wheat straw is an economical interesting feedstock because it is in abundance and it is an agricultural residue. The thermochemical processing of wheat straw by fast pyrolysis revealed that several problems occurred.

1. Feeding and blockages to the existing equipment (300g/h system) were caused due to the nature of feedstock. The low bulk density of the straw was one of the reasons for the feeding problems. The high ash content caused pre-pyrolysis and agglomeration on both 300g/h and 1 kg/h fluidised bed reactor systems. The main conclusion concerning the existing 300g/h system is that the modified feeding system is beneficial for processing of wheat straw, in comparison with the original feeding system. Further work needs to be conducted to establish optimum fluidisation velocity for avoiding the agglomeration phenomenon.
2. The pyrolysis reaction temperature had a significant effect on pyrolysis product yields. It seems that with a temperature increase, the organic yields reached a maximum around 500^{o}C and then a reduction was obtained. Char yields were reduced with a temperature increase. Concerning the gas yields the reverse tendency was noticed.
3. The wheat straw derived bio-oil that was produced from the 300g reactor system was phase separated. This could be a significant problem for the use of the oil as a fuel. The 1kg/h reactor system (quench column) formed a

homogenous oil. A possible interpretation could be that the cooling system of the 1kg/h was beneficial for the homogenous nature of the oil.

4. Regarding the chemical distribution in wheat straw derived oil, the chemicals produced in a significant level were the carboxylic acids and the phenolics compounds (phenols, guaiacols, syringols). The results from the fast pyrolysis experiments using wheat straw indicated that the oil produced may be more suitable for producing chemicals than fuel.

10 RECOMMENDATIONS FOR FUTURE WORK

Pre-treatment

- Economic and technical evaluation of the synergies from integration of pre-treatment processes with fast pyrolysis of the pre-treated feedstocks.
- Economic and technical impact of combination of catalysts and pretreatment to increase yields of target chemicals.
- Review and investigate the separation technologies available to separate target chemicals in bio-oil.
- Potential markets for the target chemicals produced.
- Further investigation could be carried out on the effect of degradation on pre-treated feedstocks to understand mechanisms and pathways of selective processing and derived chemicals.
- Finally, the effect of pre-treatment on liquid yield and quality and the cost and energy effectiveness need to be further evaluated.

Catalytic work

- Different reactor configurations could be evaluated. The apparatus used in this work was a fluidised bed reactor combined with a secondary fixed bed reactor. Further catalytic work could investigate the combination of two or more secondary fixed bed reactor systems instead of one, to evaluate the progression of coking over time. Different liquid products collection systems for each catalytic fixed bed reactor are also required. This is necessary to observe the product distribution of bio-oil over time. Additionally, different lengths of fixed bed could be used.
- The secondary catalytic reactor used in this study was a fixed bed. It should be interesting to investigate the coking of catalysts in a secondary fluidised bed reactor. This configuration is interesting for future larger scale upgrading of the bench scale unit to an industrial unit. The industrial unit could be a primary fluidised bed reactor combined with a fluid catalytic unit cracking (FCC) and a catalyst regenerator. The FCC unit (fluidised bed) is an existing technology, which has been widely used in petroleum refineries to convert the high molecular weight hydrocarbons of crude oils to more valuable products, such as gasoline and olefinic gases [113, 114, 115].

- Further investigation could be conducted on the effect of various operating conditions to optimise pyrolysis products. With reference to the laboratory work, the effect of various weight hourly space velocities (WHSV) on pyrolysis products could be studied.
- Another parameter is the catalytic temperature. The placement of a catalyst in a secondary reactor provides the benefit of operating on different temperatures from the primary pyrolysis reactor. Further work could be conducted on investigating the influence of various catalytic temperatures to optimise pyrolysis products yields and distribution.
- Larger scale catalytic experiments should be performed to produce bio-oil in larger quantities. This will enable to apply further analysis methods such as viscosity, which was not possible in the present study due to the low quantities of bio-oil.
- It is recommended that the effect of various biomass to catalyst ratios could be explored using analytical equipment, such as the Py-GC/MS. The finding of a specific ratio that optimises a market product could be used for future laboratory work.
- Further work on the activation of catalysts is recommended. Parameters such as atmosphere and temperature, that affect the activation process should be studied.

Analysis of bio-oil

- The analysis of bio-oil was performed in this study by gas chromatography/mass spectrometry (GC/MS) technique. The disadvantage of this analysis was that it only 'semi-quantifies' the chemical compounds present in bio-oil. The term 'semi-quantify' is used because the GC/MS cannot quantify the chemicals; the peak areas obtained from the chromatograms do not directly relate to the concentration; peak area should be used with caution, since it shows the amount of one chemical as a percentage of the total chemicals measured by the chromatogram. For chemical quantification it is necessary to calibrate the liquid chromatographic system by preparing standard solutions with known amounts of compounds [116]. Quantification could be obtained accurately by using calibration graphs for the reference chemicals.

- It is suggested that a higher number of repeats (more than three) should be carried out using the pyroprobe-GC/MS to obtain an accurate result.

11 LIST OF REFERENCES

[1] Bridgwater A.V., Biomass, Bioenergy and Biofuels. Royal Society of Chemistry meeting, Nottingham, 12-14 September 2007.

[2] Bridgwater AV., *Review of fast pyrolysis of biomass and product upgrading.* Biomass and Bioenergy, 2011. p. 1-27.

[3] Börjesson, P. I. I., *Energy analysis of biomass production and transportation.* Biomass and Bioenergy, 1996. 11(4): p. 305-318.

[4] Goldstein, I.S., Organic chemicals from biomass. 1981. p. 320.

[5] Mohan, D., Pittman C.U., and Steele P.H., *Pyrolysis of wood/biomass for bio-oil: A critical review.* Energy & Fuels, 2006. 20, (3): p. 848-889.

[6] De Wild P., Den Uil H., Reith H., Lunshof A., Hendriks C., Van Eck E. R. H., , and Heeres E. J.,. *Bioenergy 2: Biomass valorisation by a hybrid thermochemical fractionation approach.* International Journal of Chemical Reactor Engineering 7, Article A51 (2009).

[7] Elliott, D.C., Issues in value-added products from biomass. In Progress in Thermochemical Biomass Conversion, Bridgwater, A.V., Ed., Blackwell Science: London, 2001. 2: p. 1186-1196.

[8] Fahmi, R., Bridgwater AV, Darvell LI, Jones JM, Yates N, Thain SC and Donnison IS, The effect of alkali metals on combustion and pyrolysis of Lolium and Festuca grasses, switchgrass and willow. Fuel.86(10-11): p. 1560-1569.

[9] Nowakowski, D.J., Woodbridge C.R., and Jones J.M., Phosphorus catalysis in the pyrolysis behaviour of biomass. Journal of Analytical and Applied Pyrolysis, 2008.83(2): p. 197-204.

[10] Main components of wood. [cited 2011 26th August]; Available from http://learn.forestbioenergy.net/learning-modules/module-6/unit-1/lesson-1

[11] Kontturi E. J., Surface chemistry of cellulose: from natural fibres to model surfaces. PhD Thesis.Eindhoven University of Technology, 2005

[12] Vamvuka, D., et al., Pyrolysis characteristics and kinetics of biomass residuals mixtures with lignite. Fuel.82(15-17): p. 1949-1960.

[13] Gronli, M.A, Theoretical and experimental study of the thermal degradation of Biomass. PhD Thesis, 1996. p. 15-145.

[14] Campbell IM, Biomass, catalysts and liquid fuels. London: Holt, Rinehart and Winston, 1983.

[15] Alén, R., E. Kuoppala, and P. Oesch, Formation of the main degradation compound groups from wood and its components during pyrolysis. Journal of Analytical and Applied Pyrolysis, 1996. 36 (2): p. 137-148.

[16] Fahmi, R., The characterisation and optimisation of modified herbaceous grasses for identifying pyrolysis-oil quality traits. PhD Thesis, May 2007, Aston University.

[17] Bridgwater, A.V., Principles and practice of biomass fast pyrolysis processes for liquids. Journal of Analytical and Applied Pyrolysis, 1999. 51(1-2): p. 3-22.

[18] Milne T.A., "Pyrolysis - The Thermal Behaviour of Biomass Below 600℃", A Survey of Biomass Gasification, Vol II, SERI TR-33-239, July 1979, p II:95-132.

[19] Tillman D.A., "Energy from Wastes: An Overview of Present Technologies and Programs", Fuels from Wastes, Anderson, L.L. and Tillman, D.A. (eds.), Academic Press, Inc. (London) Ltd, 1977, p 17-40.

[20] Bridgwater A.V., Biomass pyrolysis. In: Bridgwater A.V., Hofbauer H., van Loo S. (Eds.). Thermal biomass conversion. CPL Press, 2009, p.37-78, p.423-429.

[21] Onay, O., Kockar O.M., Slow, fast and flash pyrolysis of rapeseed. Renewable Energy, 2003.28(15): p. 2417-2433.

[22] Bridgwater, A.V. and G.V.C. Peacocke, Fast pyrolysis processes for biomass. Renewable and Sustainable Energy Reviews, 2000.4(1): p. 1-73.

[23] Scott, D.S., Majerski P., Piskorz J., Radlein D., A second look at fast pyrolysis of biomass - the RTI process. Journal of Analytical and Applied Pyrolysis, 1999.51(1-2): p. 23-37.

[24] Meier, D. and O. Faix, State of the art of applied fast pyrolysis of lignocellulosic materials - a review. Bioresource Technology, 1999. 68(1): p. 71-77.

[25] Scott, D.S., Piskorz J., Bergougnou M. A., Graham R., R. P. Overends. The role of temperature in the fast pyrolysis of cellulose and wood. Industrial & Engineering Chemistry Research, 1988.27(1): p. 8-15.

[26] Bridgwater, A.V., D. Meier, and D. Radlein, An overview of fast pyrolysis of biomass. Organic Geochemistry, 1999.30(12): p. 1479-1493.

[27] Piskorz, J, Majerski, P, Radlein, D et al. Fast pyrolysis of sweet sorghum and sweet sorghum bagasse, Journal of Analytical and Applied Pyrolysis, 1998. 46: p. 15-29.
[28] Horne, P.A. and P.T. Williams, Influence of temperature on the products from the flash pyrolysis of biomass. Fuel, 1996.75(9): p. 1051-1059.
[29] L.L. Baxter, Influence of ash deposit chemistry and structure on physical and transport properties, Fuel Processing Technology 56 (1998) 81–88.
[30] Agblevor, F.A. and S. Besler, Inorganic Compounds in Biomass Feedstocks. 1. Effect on the Quality of Fast Pyrolysis Oils. Energy & Fuels, 1996.10(2): p. 293-298.
[31] R. Fahmi, A.V. Bridgwater, I. Donnison, N. Yates, J.M. Jones, The effect of lignin and inorganic species in biomass on pyrolysis oil yields, quality and stability, Fuel 87 (2008) 1230–1240.
[32] A. Oasmaa, Y. Solantausta, V. Arpiainen, E. Kuoppala, K. Sipilä, Fast pyrolysis bio-oils from wood and agricultural residues, Energy and Fuels 24 (2010) 1380–1388.
[33] Nik-Azar, M., Hajaligol, M.R., Sohrabi, M. et al. (1997) Mineral matter effects in rapid pyrolysis of beech wood. Fuel Processing Technology, 51, p. 7-17.
[34] Liden, A.G., F. Berruti, and D.S. Scott, A kinetic model for the production of liquids from the flash pyrolysis of biomass. Chemical Engineering Communication, 1988.65: p. 207–221.
[35] Czernik, S., J. Scahill, and J.Diebold, The production of liquid fuel by fast pyrolysis of biomass. IECEC-93. Proceedings of the 28th Intersociety Energy Conversion
[36] Zhang, Q., Jie C., Tiejun W., Ying X.., Review of biomass pyrolysis oil properties and upgrading research. Energy Conversion and Management, 2007.48(1): p. 87-92.
[37] Diebold, J.P., A review of the chemical and physical mechanisms of the storage stability of fast pyrolysis bio-oils. In: A.V. Bridgwater, Editor, Fast pyrolysis of biomass: a handbook vol. 2, CPL Press, Newbury, UK, 2002: p. 424.
[38] Czernik, S. and A.V. Bridgwater, Applications of Biomass Fast Pyrolysis Oil. Energy Fuels, 2004.18(2): p. 590-598.
[39] Oasmaa, A. and K. Sipila, Pyrolysis Oil Properties: Use of Pyrolysis Oil As Fuel In Medium-Speed Diesel Engines. In: Bridgwater, A. V. & Hogan, E. N. (eds.). Bio-oil production & utilisation.Proc.2nd EU-Canada Workshop on Thermal Biomass Processing. Newbury: CPL Press, 1996: p. 175 - 185.
[40] Diebold, J., Overview of fast pyrolysis of biomass for the production of liquid fuels. The Fast Pyrolysis of Biomass: A Handbook, A. V. Bridgwater, S. Czernik, J. Diebold, D. Meier, A. Oasmaa, C. Peacocke, J. Piskorz and D. Radlein, eds., CPL Press, Newbury, UK: p. 14-32.
[41] Andrews, R.G. and P.C. Patnaik, A Biomass Derived Fuel For Industrial Gas Turbine Applications. In: Bridgwater AV, Hogan EN, editors. Bio-oil production and utilisation. Newbury, UK: CPL Press, 1996: p. 236-245.
[42] Chong, K. A methodology for the generation and evaluation of biorefinery process chain. PhD Thesis. 2011, Aston university.
[43] De Wild P., Den Uil H., Reith H. Kiel JHA, Heeres HJ. Biomass valorisation by staged degasification. A new pyrolysis-based conversion option to produce value-added chemicals from lignocellulosic biomass. J. Anal. Appl. Pyrol. 85, 124-133 (2008).
[44] Bergman, P.C.A. and J.H.A. Kiel, Torrefaction for Biomass Upgrading. ECN, Biomass, 2005.
[45] Mitchell, P., Kiel J., Livingston B., Dupont-Roc G., A Fore sighting Study into the Business Case for Pellets from Torrefied Biomass as a New Solid Fuel, in All Energy '07. May 2007.
[46] Peng, J. (2007) A Study of Torrefaction for the Production of High Quality Wood Pellets. Availably from http ://www.techtp.com/Torrefaction%20for%20High%20Quality %20Wood %20Pellets.pdf.
[47] Koukios EG. Progress in thermochemical, solid-state refining of biomass – from research to commercialization. Advances in thermochemical biomass conversion. Bridgwater AV. (Ed.), 2, 1678, (1993).
[48] Ayla U., Pre-treatment technologies and their effects on the international bioenergy supply chain logistics. PhD thesis, 2005.Utrecht University.
[49] Adjaye, J.D. and N.N. Bakhshi, Production of hydrocarbons by catalytic upgrading of a fast pyrolysis bio-oil. Part I: Conversion over various catalysts. Fuel Processing Technology, 1995.45(3): p. 161-183.
[50] Adjaye, J.D. and N.N. Bakhshi, Production of hydrocarbons by catalytic upgrading of a fast pyrolysis bio-oil. Part II: Comparative catalyst performance and reaction pathways. Fuel Processing Technology, 1995.45(3): p. 185-202.

[51] Bhatia, S., Zeolite Catalysis: Principles and Applications, CRC Press, Inc., Boca Raton,USA,1990,ISBN 0-8493-5628-8,pp.291.Applied Catalysis, 1991.70(1): p. N12-N14.
[52] S.M. Csicsery, Shape-selective catalysis in zeolites, Zeolites 4 (1984) 202–213
[53] H.V.C. van Bekkum, E.M. Flanigen, P.A. Jacobs, J.C. Jansen (Eds.), Introduction to zeolite science and practice. Studies in Surface Science and Catalysis 2001.
[54] McMurray, J. Organic Chemistry, 1992. Third edition, John Wiley and Sons Inc. London
[55] Williams, P.T. and P.A. Horne, The influence of catalyst regeneration on the composition of zeolite-upgraded biomass pyrolysis oils. Fuel, 1995.74(12): p. 1839-1851.
[56] Williams, P.T. and P.A. Horne, Analysis of aromatic hydrocarbons in pyrolytic oil derived from biomass. Journal of Analytical and Applied Pyrolysis, 1995.31: p. 15-37.
[57] Horne, P.A. and P.T. Williams, The effect of zeolite ZSM-5 catalyst deactivation during the upgrading of biomass-derived pyrolysis vapours. Ibid. 34(1): p. 65-85.
[58] Horne, P.A. and P.T. Williams, Upgrading of biomass-derived pyrolytic vapours over zeolite ZSM-5 catalyst: effect of catalyst dilution on product yields. Fuel, 1996.75(9): p. 1043-1050.
[59] Williams, P.T. and N. Nugranad, Comparison of products from the pyrolysis and catalytic pyrolysis of rice husks. Energy, 2000.25(6): p. 493-513.
[60] Li, H.-y., Y.-j.Yan, and Z.-w. Ren, Online upgrading of organic vapours from the fast pyrolysis of biomass. Journal of Fuel Chemistry and Technology, 2008.36(6): p. 666-671.
[61] Zhang, H., Xiao R., Huang H,, Xiao G., Comparison of non-catalytic and catalytic fast pyrolysis of corncob in a fluidized bed reactor. Bioresource Technology, 2009. 100(3): p. 1428-1434.
[62] Williams, P.T. and P.A. Horne, The influence of catalyst type on the composition of upgraded biomass pyrolysis oils. Journal of Analytical and Applied Pyrolysis, 1995.31: p. 39-61.
[63] Aho, A., N Kumar, K Eränen, T Salmi, M Hupa, D Yu Murzin, Catalytic pyrolysis of woody biomass in a fluidized bed reactor: Influence of the zeolite structure. Fuel, 2008.87(12): p. 2493-2501.
[64] Aho, A., N Kumar, K Eranen, T Salmi, M Hupa, D Murzin, Catalytic Pyrolysis of Biomass in a Fluidized Bed Reactor: Influence of the Acidity of H-Beta Zeolite. Process Safety and Environmental Protection, 2007.85(5): p. 473-480.
[65] Aho, A., N. Kumar, A.V. Lashkul, K. Eränen, M. Ziolek, P. Decyk, T. Salmi, B. Holmbom, M. Hupa, D. Yu.Murzin, Catalytic upgrading of woody biomass derived pyrolysis vapours over iron modified zeolites in a dual-fluidized bed reactor.Fuel.89(8): p. 1992-2000.
[66] Antonakou, E., A Lappas, M.H. Nilsen, A Bouzga, M. Stocker, Evaluation of various types of Al-MCM-41 materials as catalysts in biomass pyrolysis for the production of bio-fuels and chemicals. Ibid.2006. 85(14-15): p. 2202-2212.
[67] Iliopoulou, E.F., E.V. Antonakou, S.A. Karakoulia, I.A. Vasalos, A.A. Lappas, K.S. Triantafyllidis. Catalytic conversion of biomass pyrolysis products by mesoporous materials: Effect of steam stability and acidity of Al-MCM-41 catalysts. Chemical Engineering Journal, 2007.134(1-3): p. 51-57.
[68] Triantafyllidis, K.S., E Iliopoulou, E Antonakou, A Lappas, H Wang, T Pinnavaia. Hydrothermally stable mesoporous aluminosilicates (MSU-S) assembled from zeolite seeds as catalysts for biomass pyrolysis. Microporous and Mesoporous Materials, 2007.99(1-2): p. 132-139.
[69] Azeez, A.M., D Meier, J Odermatt, T Willner., Effects of zeolites on volatile products of beech wood using analytical pyrolysis. Journal of Analytical and Applied Pyrolysis, 2011.91(2): p. 296-302.
[70] Park, H.J., H.S. Heo, Jong-Ki Jeon, J Kim, R Ryoo, Kwang-Eun Jeong, Young-Kwon Park., Highly valuable chemicals production from catalytic upgrading of radiata pine sawdust-derived pyrolytic vapours over mesoporous MFI zeolites. Applied Catalysis B: Environmental, 2010.95(3-4): p. 365-373.
[71] Uzun, B.B. and N. Sarioglu, Rapid and catalytic pyrolysis of corn stalks. Fuel Processing Technology, 2009.90(5): p. 705-716.
[72] Pattiya, A., J.O. Titiloye, and A.V. Bridgwater, Fast pyrolysis of cassava rhizome in the presence of catalysts. Journal of Analytical and Applied Pyrolysis, 2008.81(1): p. 72-79.
[73] Kung, H. H., Transition metal oxides: Surface chemistry and catalysis. Elsevier, Delmon, B., Yates, J. T., (eds.), 1989.Vol. 40.
[74] Nokkosmäki, M.I., E.T Kuoppala, E.A Leppämäki, A.O.I Krause, A novel test method for cracking catalysts. Journal of Analytical and Applied Pyrolysis, 1998.44(2): p. 193-204.

[75] Lu, Q., Y Zhang, Z Tang, Wen-zhi Li, Xi-feng Zhu. Catalytic upgrading of biomass fast pyrolysis vapours with titania and zirconia/titania based catalysts. Fuel, 2010.89(8): p. 2096-2103.
[76] Pütün, E., Catalytic pyrolysis of biomass: Effects of pyrolysis temperature, sweeping gas flow rate and MgO catalyst. Energy, 2010.35(7): p. 2761-2766.
[77] Torri, C., M Reinikainen, C Lindfors, D Fabbri, A Oasmaa, E Kuoppala. Investigation on catalytic pyrolysis of pine sawdust: Catalyst screening by Py-GC-MIP-AED. Journal of Analytical and Applied Pyrolysis, 2010.88(1): p. 7-13.
[78] H.F. Rase, Handbook of Commercial Catalysts: Heterogeneous Catalysts, CRC Press, Boca Raton, FL, 2000
[79] Zabaniotou, A., O Ioannidou, E. Antonakou, A. Lappas., Experimental study of pyrolysis for potential energy, hydrogen and carbon material production from lignocellulosic biomass. International Journal of Hydrogen Energy, 2008.33(10): p. 2433-2444.
[80] Ates, F., A.E. Pütün, and E. Pütün, Pyrolysis of two different biomass samples in a fixed-bed reactor combined with two different catalysts. Fuel, 2006.85(12-13): p. 1851-1859.
[81] French, R., Czernik. S., Catalytic pyrolysis of biomass for biofuels production. Fuel Processing Technology, 2010.91 (1): p. 25-32
[82] Pütün, E., B.B. Uzun, and A.E. Pütün, Fixed-bed catalytic pyrolysis of cotton-seed cake: Effects of pyrolysis temperature, natural zeolite content and sweeping gas flow rate. Bioresource Technology, 2006. 97(5): p. 701-710.
[83] Ates, F., A.E. Pütün, and E. Pütün, Fixed bed pyrolysis of Euphorbia rigida with different catalysts. Energy Conversion and Management, 2005.46(3): p. 421-432.
[84] Adisak, P., Bio-oil production via fast pyrolysis of biomass residues from cassava plants in a fluidised-bed reactor. Bioresource Technology. 102(2): p. 1959-1967.
[85] Juutilainen, S.J., P.A. Simell, and A.O.I. Krause, Zirconia: Selective oxidation catalyst for removal of tar and ammonia from biomass gasification gas. Applied Catalysis B: Environmental, 2006.62(1-2): p. 86-92.
[86] Karimi, E., Briens, C., Berruti, F., Moloodi S., Tzanetakis T., Thomson M.J., Schlaf M., Red Mud as a Catalyst for the Upgrading of Hemp-Seed Pyrolysis Bio-oil. Energy &Fuels.2010.24(12): p. 6586-6600
[87] Rao, R., A. Dandekar, R.T.K. Baker, M.A. Vannice, Properties of Copper Chromite Catalysts in Hydrogenation Reactions. Journal of Catalysis, 1997.171(2): p. 406-419.
[88] M. G. Grønli,,G. Várhegyi, and C. D. Blasi, Thermogravimetric Analysis and Devolatilization Kinetics of Wood. Industrial & Engineering Chemistry Research200241 (17), 4201-4208
[89] Y. Wu, Z. Zhao, H. Li Fang HE., Low temperature pyrolysis characteristics of major components of biomass. Journal of Fuel Chemistry and Technology, 2009. 37(4):p. 427-432
[90] Nowakowski, D.J. and J.M. Jones, Uncatalysed and potassium-catalysed pyrolysis of the cell-wall constituents of biomass and their model compounds. Journal of Analytical and Applied Pyrolysis, 2008.83(1): p. 12-25.
[91] Available from http://radchem.nevada.edu/classes/chem455/lecture_22__thermal_methods.htm [cited 2011 5th September];
[92] Introduction to Mass Spectrometry. [cited 2011 14th September]; Available from http://www.chem.arizona.edu/massspec/intro_html/intro.html
[93] Coulson M, EC Project Bioenergy Chains Final Report, Aston University, ENK6-2001-00524.
[94] De Wild, P., Biomass pyrolysis for chemicals, PhD Thesis, Groninger University, July 2011
[95] Channiwala, S.A. and P.P. Parikh, A unified correlation for estimating HHV of solid, liquid and gaseous fuels. Fuel, 2002.81(8): p. 1051-1063.
[96] Lee KH, Kang BS, Park YK, Kim JS. Influence of reaction temperature, pre-treatment, and a char removal system on the production of bio-oil from rice straw by fast pyrolysis, using a fluidized bed. Energy & Fuels 2005; 19:2179-2184.
[97] Pattiya, A., Catalytic pyrolysis of agricultural residues for bio-oil production. PhD Thesis. November2007. Aston University
[98] Phyllis, database for biomass and waste. Energy research Centre of the Netherlands (ECN), 2005.
[99] Bridgeman, T.G., L I Darvell, J M Jones, P T Williams, R Fahmi, A V Bridgwater, T Barraclough, I Shield, N Yates, S C Thain, I S Donnison. Influence of particle size on the analytical and chemical properties of two energy crops. Fuel, 2007.86(1-2): p. 60-72.

[100] Corredor, D.Y., S. R. Bean, T. Schober, D. Wang. Effect of Decorticating Sorghum on Ethanol Production and Composition of DDGS. Cereal Chem, 2006.83(1): p. 17-21.
[101] Fahmi, R., The characterisation and optimisation of modified herbaceous grasses for identifying pyrolysis-oil quality traits. PhD Thesis. May 2007, Aston University: Birmingham.
[102] Ayhan, D., Calculation of higher heating values of biomass fuels. Fuel, 1997. 76(5): p. 431-434
[103] Peacocke, G., Ablative pyrolysis of biomass, in University of Aston in Birmingham. 1994.
[104] Mosier, N., C Wyman, B Dale, R Elander, Y Y Lee, M Holtzapple, M Ladisch. Features of promising technologies for pre-treatment of lignocellulosic biomass. Bioresource Technology, 2005. 96(6): p. 673-686.
[105] de Wild, P.J., H. den Uil, J.H. Reith, J.H.A. Kiel, H.J. Heeres, Biomass valorisation by staged degasification: A new pyrolysis-based thermochemical conversion option to produce value-added chemicals from lignocellulosic biomass. Journal of Analytical and Applied Pyrolysis, 2009.85(1-2): p. 124-133
[106] Rodríguez, J., M.J. Hernández-Coronado, M. Hernández, P. Bocchini, G.C. Galletti, M.E. Arias, Chemical characterization by pyrolysis/gas chromatography/mass spectrometry of acid-precipitable polymeric lignin (APPL) from wheat straw transformed by selected streptomyces strains. Analytica Chimica Acta, 1997.345(1-3): p. 121-129.
[107] Nonier, M.F., N. Vivas, N. Vivas de Gaulejac, C. Absalon, Ph. Soulié, E. Fouquet. Pyrolysis-gas chromatography/mass spectrometry of Quercus sp. wood: Application to structural elucidation of macromolecules and aromatic profiles of different species. Journal of Analytical and Applied Pyrolysis, 2006.75(2): p. 181-193
[108] Faix, O., et al., Gas chromatografic seperation and mass spectrometric characterization of polysaccharide derived products. Holz als Roh- und Werkstoff, 1991. 49: p. 213-219.
[109] Faix, O., D. Meir, and I. Fortmann, Gas chromatographic separation and mass spectrometric characterization of monomeric lignin derived products. Ibid.1990. 48: p. 281-285.
[110] Hernández, M., M J Hernández-Coronado, M D Montiel, J Rodríguez, M I Pérez, P Bocchini, G C Galletti, M E Arias, Pyrolysis/gas chromatography/mass spectrometry as a useful technique to evaluate the ligninolytic action of streptomycetes on wheat straw. Journal of Analytical and Applied Pyrolysis, 2001.58-59: p. 539-551.
[111] Kuroda, K.-i., A Nakagawa-izumi, B.B. Mazumder, Y Ohtani, K Sameshima. Evaluation of chemical composition of the core and bast lignins of variety Chinpi-3 kenaf (Hibiscus cannabinus L.) by pyrolysis-gas chromatography/mass spectrometry and cupric oxide oxidation. Industrial Crops and Products, 2005.22(3): p. 223-232.
[112] Boroson, M.L., JB. Howard, JP. Longwell, WA Peters, Product yields and kinetics from the vapour phase cracking of wood pyrolysis tars. AIChE Journal, 1989. 35(1): p. 120-128.
[113] James H. Gary and Glenn E. Handwerk (2001).Petroleum Refining: Technology and Economics (4th ed.). CRC Press
[114] James. G. Speight (2006). The Chemistry and Technology of Petroleum (4th ed.). CRC Press
[115] Reza Sadeghbeigi (2000).Fluid Catalytic Cracking Handbook (2nd ed.). Gulf Publishing.
[116] Sipilä, K., E Kuoppala, L Fagernäs, A Oasmaa., Characterization of biomass-based flash pyrolysis oils. Biomass and Bioenergy, 1998.14(2): p. 103-113.

12 APPENDIX - A

CHEMICAL IDENTIFICATION AND RELATIVELY PEAK AREA PERCENTAGES

Table 12-1: Chemical identification and relatively peak area percentages from pre-treatment of poplar by torrefaction and steam pre-treatment

ID	Compound name/synonyms	R/T	Formula	MW		Group	Fresh Poplar	Torrefied. Poplar	Steamed Poplar
1	Acetaldehyde/Acetic aldehyde/Ethanal	3.87	C_2H_4O	44	C	Aldehydes	0.46	0.35	N.D.
2	2-propenyidene-cyclobutene	4.22	C_7H_8	92	L	Hydrocarbons	N.D.	N.D.	0.57
3	2.5-dimethyl-furan	5.92	C_6H_8O	96	C	Furans	N.D.	N.D.	2.07
4	2.3 Butanedione/Butanedione/Diacetyl	6.65	$C_4H_6O_2$	86	C	Ketones	0.14	N.D.	N.D.
5	2-Methyl-Cyclopenten-1-one/2-Methyl-2-cyclopentenone	7.85	C_6H_8O	96	C	Ketones	N.D.	N.D.	1.03
6	Hydroxyacetaldehyde/Glycolaldehyde	8.08	$C_2H_4O_2$	60	C	Misc. Oxygenates	2.47	1.59	N.D.
7	5-methyl-2(3H)-Furanone	8.58	$C_5H_6O_2$	98	C	Furans	N.D.	N.D.	2.87
8	Acetic acid/Ethanoic acid	9.31	$C_2H_4O_2$	60	C	Acids	6.15	4.94	N.D.
9	Hydroxypropanone/1-Hydroxy-2-propanone/Acetone alcohol	10.80	$C_3H_6O_2$	74	C	Misc. Oxygenates	4.06	4.62	N.D.
10	3-methyl-phenol/m-Cresol/1-Hydroxy-3-methylbenzene	12.61	C_7H_8O	108	L	Phenols	N.D.	N.D.	2.40
11	2-methoxy-phenol/o-methoxy-phenol/o-Guaiacol	13.54	$C_7H_8O_2$	124	L	Guaiacols	N.D.	N.D.	3.31
12	Dimethyl phenol (2.3-; 2.4-; 2.5-)/Xylenols	14.28	$C_8H_{10}O$	122	L	Phenols	N.D.	N.D.	1.70
13	2(3H)-Furanone	14.96	$C_4H_4O_2$	84	C	Furans	N.D.	0.08	N.D.
14	1-Hydroxy-2-butanone	15.23	$C_4H_8O_2$	88	C	Misc. Oxygenates	0.22	0.40	N.D.
15	Dimethyl phenol (3.5, 3,4)/Xylenols	15.49	$C_8H_{10}O$	122	L	Phenols	N.D.	N.D.	1.17
16	3-Hydroxypropanal	15.50	$C_3H_6O_2$	74	C	Misc. Oxygenates	3.30	0.37	N.D.
17	3(2H)-Furanone	15.98	$C_4H_4O_2$	84	C	Furans	N.D.	0.13	N.D.
18	Butanedial/Succinaldehyde	17.59	$C_4H_6O_2$	86	C	Aldehydes	2.31	2.01	N.D.
19	2-Hydroxy-3-oxobutanal	17.72	$C_4H_6O_3$	102	C		1.03	0.95	N.D.
20	Furfural/furan-2-carboxaldehyde/fural/furfuraldehyde/2-furaldehyde/pyromucic aldehyde	18.40	$C_5H_4O_2$	96	C	Aldehyde	2.67	0.13	N.D.
21	4-Ethyl-2-methoxy-phenol/4-Ethyl-guaiacol	19.10	$C_9H_{12}O_2$	152	L	Guaiacols	N.D.	N.D.	4.36
22	5-Methyl-2(3H)-furanone/a-Angelica lactone/2.3-Dihydro-5-methyl-2-furanone	20.50	$C_5H_6O_2$	98	C	Furans/Lactones	0.17	N.D.	N.D.
23	2-Furanmethanol/2-Furfuryl alcohol	20.77	$C_5H_6O_2$	98	C	Furans	0.33	0.20	N.D.
24	1-Acetyloxy-2-propanone/1-Acetoxypropane-2-one/2-Oxopropyl acetate	21.11	$C_5H_8O_3$	116	C	Misc. Oxygenates	0.52	0.63	N.D.
25	2-Methyl-2-Cyclopenten-1-one	21.27	C_6H_8O	96	C	Ketones	0.19	0.23	N.D.
26	2-Ethyl-butanal/Tetrahydro-4-methyl-3-furanone	21.42	$C_6H_{12}O$	100	C	Aldehydes	0.54	0.72	N.D.
27	1-(2-Furanyl)ethanone/Acetylfuran/2-Acetylfuran/Furyl methyl ketone	22.50	$C_6H_6O_2$	110	C	Furans	0.45	0.09	N.D.
28	4-Cyclopentene-1.4-dione	22.70	$C_5H_4O_2$	96	C	Ketones	0.33	0.19	N.D.
29	1, 2, 4- Trimethoxybenzene/1, 2, 4- Trimethoxy-1 benzene	23.62	$C_9H_{12}O_3$	168	L	Syringols	N.D.	N.D.	3.61
30	2.3-Dihydro-5-methylfuran-2-one	24.29	$C_5H_6O_2$	98	C	Furans	3.09	0.08	N.D.

31	Dihydro-methyl-furanone	25.22					N.D.	1.00	N.D.
32	5-Methyl-2-furancarboxaldehyde/5-Methylfurfural/2-Formyl-5-methylfuran/2-Methyl-5-formylfuran	25.47	$C_6H_6O_2$	110	C	Furans	0.24	0.43	N.D.
33	3-Methyl-2-cyclo-penten-1-one	26.30	C_6H_8O	96	C	Ketones	0.30	0.39	N.D.
34	4-hydroxybutyric acid/4- hydroxy-butanoic acid	26.48	$C_4H_8O_3$	104	C	Acids	N.D.	0.39	N.D.
35	γ-Butyrolactone/4-butyrolactone/ 4-hydroxybutyric acid lactone/gamma-hydroxybutyric acid lactone	26.49	$C_4H_6O_2$	86			0.37	N.D.	N.D.
36	(5H)-furan-2-one/2(5H)-Furanone	27.05	$C_4H_4O_2$	84	C	Furans	2.58	2.77	N.D.
37	4-Propenyl-2.6-dimethoxyphenol(sis)/Methoxyeugenol (trans)	27.32	$C_{11}H_{14}O_3$	194	L	Guaiacols	N.D.	N.D.	2.48
38	2(5H)-FURANONE, 5-METHYL-	27.64	$C_5H_6O_2$	98	C	Furans	0.51	N.D.	N.D.
39	5-Methyl-2(5H)-Furanone/β-Angelica lactone	27.65	$C_5H_6O_2$	98	C	Furans	N.D.	0.58	N.D.
40	4-Hydroxy-5.6-dihydro-(2H)-pyran-2-one	28.14	$C_5H_6O_3$	114			1.71	0.93	N.D.
41	2-Hydroxy-1-methyl-1-cyclopentene-3-one/Maple lactone/2-Hydroxy-3-methyl-2-cyclopenten-1-one	29.18	$C_6H_8O_2$	112	C	Ketones	0.94	N.D.	2.32
42	2-Hydroxy-3-methyl-2-cyclopentene-one	29.30	$C_6H_8O_2$	112	C	Ketones	N.D.	1.95	N.D.
43	2-Hydroxy-1-methyl-1-cyclopentene-3-one/Maple lactone & 2.5-Dimethylcyclopentanone	29.31	$C_6H_8O_2$ & $C_7H_{12}O$	112	C	Ketones	1.51	0.08	N.D.
44	Anhydro-hexo-furanose: unknown	29.60					0.40	1.05	N.D.
45	4-Propenyl-2.6-dimethoxyphenol(trans)/Methoxyeugenol (trans)	29.68	$C_{11}H_{14}O_3$	194	L	Guaiacols	N.D.	N.D.	1.78
46	2-FURANONE, 2,5-DIHYDRO-3,5-DIMETHYL	29.80			C	Furans	N.D.	0.12	N.D.
47	Phenol	30.79			L	Phenols	5.03	3.27	6.92
48	2-Methoxyphenol/Guaiacol/Guaicol	31.53	$C_7H_8O_2$	124	L	Guaiacols	1.56	2.52	N.D.
49	overlapping spectra: unknown	32.37					N.D.	0.15	N.D.
50	Methyl 2-furoate/2-Furancarboxylic acid, methyl ester	32.87	$C_6H_6O_3$	126	C	Furans/Ester	0.20	0.27	N.D.
51	o-cresol/2-Methyl phenol	33.05	C_7H_8O	108	L	Phenols	0.34	0.61	N.D.
52	2-CYCLOPENTEN-1-ONE, 3-ETHYL-2-HYDROXY-	33.43			C	Ketones	N.D.	0.16	N.D.
53	3-Hydroxy-2-methyl-4H-pyran-4-one/Maltol	33.65	$C_6H_6O_3$	126	C	Misc. Oxygenates	0.35	N.D.	N.D.
54	4-METHYL-5H-FURAN-2-ONE/4-Methyl-2(5H)-furanone	34.63	$C_5H_6O_2$	98	C	Furans	N.D.	0.51	N.D.
55	p-Cresol/4-Methyl phenol	34.71	C_7H_8O	108	L	Phenols	0.13	N.D.	N.D.
56	2-Methoxy-3-methyl-phenol/	34.81			L	Guaiacols	0.21	N.D.	N.D.
57	p/m-Cresol/3/4-Methyl phenol	34.88	C_7H_8O	108	L	Phenols	N.D.	0.33	N.D.
58	2-Furanmethanol,tetrahydro-5-methyl-/Furfurylalcohol/Tetrahydro-5-methyl-2-furanmethanol	35.28	$C_6H_{12}O_2$	116	C	Furans	N.D.	1.02	N.D.
59	2-Methoxy-4-methyl phenol/Creosol/p-Methylguaiacol/4-Methylguaiacol	36.33	$C_8H_{10}O_2$	138	L	Guaiacols	1.48	3.08	2.91
60	anhydrosugar:unknown	36.61					1.16	N.D.	N.D.
61	Xylenols/Dimethyl phenol (2.3-; 2.4-; 2.5-)	36.85	$C_{10}H_{12}O_2$	164	L	Phenols	0.10	N.D.	N.D.
62	3.5-Dihydroxy-2-methyl-4H-pyran-4-one	37.16	$C_6H_6O_4$	142			0.23	N.D.	N.D.
63	benzoic acid/benzenecarboxylic acid/carboxybenzene	39.10	$C_7H_6O_2$	122	C	Carboxylic Acids	0.26	N.D.	N.D.
64	4-Ethyl-2-methoxyphenol/4-Ethyl guaiacol/4-Hydroxy-3-methoxy ethylbenzene/p-Ethylguaiacol	40.09	$C_9H_{12}O_2$	152	L	Guaiacols	0.20	N.D.	N.D.
65	1.4:3.6-Dianhydro-a-d-glucopyranose	41.74	$C_6H_8O_4$	144	C	Sugars	0.52	N.D.	N.D.

66	2-Methoxy-4-vinylphenol/4-Vinylguaiacol/p-Vinylguaiacol/4-Hydroxy-3-methoxystyrene	42.57	$C_9H_{10}O_2$	150	L	Guaiacols	0.76	1.21	N.D.
67	Eugenol/2-Methoxy-4-allylphenol/2-Methoxy-1-hydroxy-4-allylbenzene/Allylguaiacol	43.62	$C_{10}H_{12}O_2$	164	L	Guaiacols	0.57	N.D.	N.D.
68	4-propyl-guaiacol/2-methoxy-4-propylphenol	43.73	$C_{10}H_{14}O_2$	166	L	Guaiacols	0.12	N.D.	N.D.
69	5-(Hydroxymethyl)-2-Furancarboxaldehyde/5-(Hydroxymethyl)-2-furfural/HMF/5-(Hydroxymethyl)-2-furaldehyde	44.37	$C_6H_6O_3$	126	C	Furans	1.28	1.42	N.D.
70	1.2-Benzenediol/ Pyrocatechol/ o-Benzenediol	44.68	$C_6H_6O_2$	110			0.28	0.71	N.D.
71	2,6-Dimethoxy phenol/Syringol/1,3-Dimethoxy-2-hydroxybenzene/Pyrogallol dimethylether	44.91	$C_8H_{10}O_3$	154	L	Syringols	2.79	5.14	4.72
72	2-Hydroxy-butanedial/2-hydroxysuccin aldehyde	45.82	$C_4H_6O_3$	102			0.41	N.D.	N.D.
73	2-Methoxy-4-(1-propenyl)phenol/Isoeugenol,c&t/4-Propenylguaiacol/4-Hydroxy-3-methoxypropenylbenzene	45.95	$C_{10}H_{12}O_2$	164	L	Guaiacols	0.31	0.76	1.24
74	4-Methyl syringol/2,6-Dimethoxy-4-methylphenol	48.64	$C_9H_{12}O_3$	168	L	Syringols	1.61	3.39	N.D.
75	Vanillin/2-Methoxy-4-formylphenol/4-Hydroxy-3-methoxybenzaldehyde	49.04	$C_8H_8O_3$	152	L	Guaiacols	1.48	0.41	N.D.
76	Hydroquinone/1.4-Benzenediol/4-Hydroxyphenol/Dihydroxybenzene	49.24	$C_6H_6O_2$	110	L	Phenols	0.26	0.36	N.D.
77	4-hydroxybenzaldehyde/4-Formylphenol	49.71	$C_7H_6O_2$	122	L	Misc. Oxygenates	0.17	N.D.	N.D.
78	4-Methyl-1.2-benzenediol/4-methylcatechol/Homocatechol/Toluene-3.4-diol	50.82	$C_7H_8O_3$	124	L	Phenols	0.16	N.D.	N.D.
79	Homovanillin	51.32			L	Guaiacols	0.63	N.D.	N.D.
80	4-ethyl-Syringol	51.51	$C_{10}H_{14}O_3$	182	L	Syringols	0.22	0.56	N.D.
81	1-(4-Hydroxy-3-methoxyphenyl)ethanone/Acetoguaiacone	52.20	$C_9H_{10}O_3$	166	L	Guaiacols	0.88	0.28	N.D.
82	4-Vinyl-2.6-dimethoxyphenol/Syringol-4-vinyl	53.71			L	Syringols	0.60	0.60	N.D.
83	1-(4-hydroxy-3-methoxyphenyl)-2-Propanone/Guaiacylacetone/Vanillyl methyl ketone/4-Hydroxy-3-methoxyphenyl acetone	54.12	$C_{10}H_{12}O_3$	180	L	Guaiacols	0.66	0.34	N.D.
84	2.6-Dimethoxy-4-(2-propenyl)-Phenol	54.42	$C_{11}H_{14}O_3$	194	L	Guaiacols	N.D.	0.69	N.D.
85	trans-4-Propenyl-2.6-dimethoxyphenol/Methoxyeugenol	54.42	$C_{11}H_{14}O_3$	194	L	Guaiacols	0.97	1.15	N.D.
86	propioguaiacone/1-(4-Hydroxy-3-methoxyphenyl)propan-1-one	55.28	$C_{10}H_{12}O_3$	180	L	Guaiacols	0.12	N.D.	N.D.
87	4-((1E)-3-Hydroxy-1-propenyl)-2-methoxyphenol/Coniferol/Coniferyl alcohol	55.78	$C_{10}H_{12}O_3$	180	L	Guaiacols	0.28	N.D.	N.D.
88	4-Propenyl-2.6-dimethoxyphenol/Methoxyeugenol (sis)/4-propenyl syringol	56.30	$C_{11}H_{14}O_3$	194	L	Guaiacols	0.41	0.25	N.D.
89	1,6-Anhydro-b-D-glucopyranose/Levoglucosan	58.27	$C_6H_{12}O_5$	162	C	Sugars	10.06	9.53	8.57
90	trans-4-Propenyl-2.6-dimethoxyphenol/Methoxyeugenol (trans)	58.77	$C_{11}H_{14}O_3$	194	L	Guaiacols	1.38	N.D.	N.D.
91	4-Hydroxy-3.5-dimethoxybenzaldehyde/Syringaldehyde/Syringe aldehyde/Cedar aldehyde	59.59	$C_9H_{10}O_4$	182	L	Syringols	1.42	0.18	2.26
92	4-Hydroxy benzoic acid	60.27	$C_7H_6O_3$	138		Phenolic acids	1.31	N.D.	N.D.
93	Anhydrosugar: unknown	61.57					0.67	1.75	N.D.
94	1-(4-Hydroxy-3-dimethoxyphenyl)ethanone/Acetosyringone/3.5-dimethoxy-1-hydroxyacetophenone/Acetosyringon	61.94	$C_{10}H_{12}O_4$	196	L	Syringols	0.81	0.34	1.42
95	Syringyl acetone	63.37	$C_{11}H_{14}O_4$	210	L	Syringols	0.46	0.10	N.D.
96	propiosyringone/1-(4-hydroxy-3,5-dimethoxyphenyl)propan-1-one	64.41	$C_{11}H_{14}O_4$	210	L	Syringols	0.16	0.14	N.D.

Table 12-2: Chemical identification and relatively peak area percentages from pre-treatment of wheat straw by aquathermolysis

ID	Compound name/synonyms	R/T	Formula	MW		Group	270110H	270110A	Awheat straw
1	Hydroxyacetaldehyde/Glycolaldehyde	11.04	$C_2H_4O_2$	60.05	C	Misc. Oxygenates	N.D.	0.99	1.18
2	Acetic acid/Ethanoic acid	12.21	$C_2H_4O_2$	60.05	C	Acids	6.87	28.07	1.33
3	Propanoic acid/Propionic acid	13.69	$C_3H_6O_2$	74.00	C	Acids	N.D.	N.D.	0.11
4	Hydroxypropanone/1-Hydroxy-2-propanone/Acetone alcohol	14.00	$C_3H_6O_2$	74.08	C	Misc. Oxygenates	11.01	24.10	2.13
5	3-Hydroxy-2-butanone/2-Hydroxy-3-butanone	15.76	$C_4H_8O_2$	88.11	C	Misc. Oxygenates	0.16	0.45	0.20
6	3-Hydroxypropanal	16.58	$C_3H_6O_2$	74.08	C	Misc. Oxygenates	0.22	1.49	0.69
7	acetic anhydride/2-oxo-propanoic acid methyl ester	17.46	$C_4H_6O_3$	102.00	C	Acids	N.D.	N.D.	N.D.
8	1-Hydroxy-2-butanone	18.71	$C_4H_8O_2$	88.11	C	Misc. Oxygenates	1.20	1.46	0.13
9	Butanedial/Succinaldehyde	21.09	$C_4H_6O_2$	86.09	C	Aldehydes	0.98	1.89	0.45
10	Furfural/furan-2-carboxaldehyde/fural/furfuraldehyde/2-furaldehyde/pyromucic aldehyde	21.87	$C_5H_4O_2$	96.08	C	Aldehyde	4.78	3.31	1.21
11	2-Furanmethanol/2-Furfuryl alcohol	23.99	$C_5H_6O_2$	98.10	C	Furans	0.62	N.D.	0.22
12	2-Hydroxy-2-cyclopentene-1-one	24.06	$C_5H_6O_2$	98.00	C	Ketones	N.D.	N.D.	2.60
13	1-Acetyloxy-2-propanone/1-Acetoxypropane-2-one/2-Oxopropyl acetate	24.50	$C_5H_8O_3$	116.12	C	Misc. Oxygenates	1.93	1.95	0.12
14	2-Methyl-2-Cyclopenten-1-one	24.74	C_6H_8O	96.00	C	Ketones	1.06	0.56	0.11
15	2-Ethyl-butanal/Tetrahydro-4-methyl-3-furanone	24.94	$C_6H_{12}O$	100.16	C	Aldehydes	0.42	0.82	0.15
16	1-(2-Furanyl)ethanone/Acetylfuran/2-Acetylfuran/Furyl methyl ketone	25.51	$C_6H_6O_2$	110.11	C	Furans	0.38	N.D.	0.06
17	2.5-diethoxytetrahydro-furan	26.03	$C_8H_{16}O_3$	16N.D.	C	Furans	N.D.	0.60	N.D.
18	5-Methyl-2(3H)-Furanone/a-Angelica lactone2.3-Dihydro-5-methylfuran-2-one	27.37	$C_5H_6O_2$	98.10	C	Furans	0.60	0.92	N.D.
19	Propionic acid, Ethyl ester; Ethyl n-propionate; Propionic ether,	28.89	$C_5H_{10}O_2$	102.00	C	Acids	N.D.	0.16	N.D.
20	5-Methyl-2-furancarboxaldehyde/5-Methylfurfural/2-Formyl-5-methylfuran/2-Methyl-5-formylfuran	28.90	$C_6H_6O_2$	110.11	C	Furans	0.34	0.15	0.36
21	3-Methyl-2-Cyclopenten-1-one/3-Methyl-2-Cyclopentenone	29.69	C_6H_8O	96.13	C	Ketones	1.58	0.83	0.28
22	4-hydroxybutyric acid/4- hydroxy-butanoic acid	30.02	$C_4H_8O_3$	104.00	C	Acids	0.73	0.68	0.23
23	(5H)-furan-2-one/2(5H)-Furanone	30.50	$C_4H_4O_2$	84.07	C	Furans	0.96	1.21	0.42
24	5-Methyl-2(5H)-Furanone/β-Angelica lactone	31.15	$C_5H_6O_2$	98.10	C	Furans	0.67	0.42	N.D.
25	2-Hydroxy-1-methyl-1-cyclopentene-3-one/Maple lactone & 2.5-Dimethylcyclopentanone	32.33	$C_6H_8O_2$ & $C_7H_{12}O$	112.00	C	Ketones	4.13	2.73	1.02
26	4-METHYL-5H-FURAN-2-ONE/4-Methyl-2(5H)-furanone	32.68	$C_5H_6O_2$	98.00	C	Furans	0.42	0.34	N.D.
27	Phenol	33.86	C_6H_6O	94.11	L	Phenols	3.64	1.23	0.82
28	2-Methoxyphenol/Guaiacol/Guaicol	34.75	$C_7H_8O_2$	124.14	L	Guaiacols	4.35	1.61	0.69
29	2-Furanmethanol,tetrahydro-5-methyl-/Furfurylalcohol/Tetrahydro-5-methyl-2-furanmethanol	35.00	$C_6H_{12}O_2$	116.00	C	Furans	N.D.	N.D.	0.54
30	3-ETHYL-2-CYCLOPENTEN-1-ONE	35.15			C	Ketones	N.D.	0.11	N.D.
31	o-cresol/2-Methyl phenol	36.13	C_7H_8O	108.14	L	Phenols	1.65	0.57	0.46
32	3-Ethyl-2-Hydroxy-2-Cyclopenten-1-one/1.3-Ethyl-2-Hydroxy-2-Cyclopenten-1-one	36.51	$C_7H_{10}O_2$	126.00	C	Ketones	0.99	N.D.	N.D.
33	p,m-Cresol/3,4-Methyl phenol	37.75	C_7H_8O	108.14	L	Phenols	0.92	0.27	0.58
34	2-Methoxy-4-methyl phenol/Creosol/p-Methylguaiacol/4-Methylguaiacol	39.49	$C_8H_{10}O_2$	138.17	L	Guaiacols	1.19	0.26	0.66
35	Anhydrosugar: unknown	39.67			C	Sugars	N.D.	0.54	N.D.
36	Xylenols/Dimethyl phenol (2.3-; 2.4-; 2.5-)	39.89	$C_8H_{10}O$	122.17	L	Phenols	0.86	0.18	0.44
37	Ethyl phenol (2-; 3-; 4-;)	41.68	$C_8H_{10}O$	122.17	L	Phenols	1.21	0.19	0.57
38	4-Ethyl-2-methoxyphenol/4-Ethyl guaiacol/4-Hydroxy-3-methoxy ethylbenzene/p-Ethylguaiacol	43.19	$C_9H_{12}O_2$	152.19	L	Guaiacols	1.18	N.D.	N.D.

39	1,4:3,6-DIANHYDRO-.ALPHA.-D-GLUCOPYRANOSE	44.60	$C_6H_8O_4$	144.13	C	Sugars	N.D.	0.43	N.D.
40	4-Vinylphenol/4- ethenyl phenol/4- ethenylphenol/4- hydroxystyrene	45.31	C_8H_8O	12N.D.	L	Phenols	3.21	0.37	3.29
41	2-Methoxy-4-vinylphenol/4-Vinylguaiacol/p-Vinylguaiacol/4-Hydroxy-3-methoxystyrene	45.64	$C_9H_{10}O_2$	15N.D.	L	Guaiacols	3.91	0.32	N.D.
42	Eugenol/2-Methoxy-4-allylphenol/2-Methoxy-1-hydroxy-4-allybenzene/Allylguaiacol	46.65	$C_{10}H_{12}O_2$	164.20	L	Guaiacols	1.25	0.13	N.D.
43	2,6-Dimethoxy phenol/Syringol/1,3-Dimethoxy-2-hydroxybenzene/Pyrogallol dimethylether	47.81	$C_8H_{10}O_3$	154.17	L	Syringols	2.40	0.89	0.52
44	Vanillin/2-Methoxy-4-formylphenol/4-Hydroxy-3-methoxybenzaldehyde	48.87	$C_8H_8O_3$	152.15	L	Guaiacols	N.D.	N.D.	0.09
45	2-Methoxy-4-(1-propenyl)phenol/Isoeugenol,c&t/4-Propenylguaiacol/4-Hydroxy-3-methoxypropenylbenzene	48.91	$C_{10}H_{12}O_2$	164.20	L	Guaiacols	0.58	0.18	0.23
46	4-(2-propenyl)-phenoL/Chavicol/p-Chavicol/p-Allylphenol	50.07	$C_9H_{10}O$	134.00	L	Phenols	0.43	N.D.	N.D.
47	4-Methyl syringol/2,6-Dimethoxy-4-methylphenol	51.50	$C_9H_{12}O_3$	168.19	L	Syringols	0.49	0.10	0.40
48	Hydroquinone/1.4-Benzenediol/4-Hydroxyphenol/Dihydroxybenzene	52.04	$C_6H_6O_2$	110.11	L	Phenols	0.96	0.79	N.D.
49	4-hydroxybenzaldehyde/4-Formylphenol	52.64	$C_7H_6O_2$	122.12	L	Phenols	0.42	0.17	N.D.
50	4-Methyl-1.2-benzenediol/4-methylcatechol/Homocatechol/Toluene-3.4-diol	53.67	$C_7H_8O_3$	124.24	L	Phenols	0.70	0.42	N.D.
51	4-ethyl-Syringol	54.36	$C_{10}H_{14}O_3$	182.22	L	Syringols	0.35	N.D.	N.D.
52	1-(4-Hydroxy-3-methoxyphenyl)ethanone/Acetoguaiacone	55.12	$C_9H_{10}O_3$	166.18	L	Guaiacols	0.38	0.18	N.D.
53	4-Vinyl-2.6-dimethoxyphenol/Syringol-4-vinyl	56.55			L	Guaiacols	0.59	N.D.	0.31
54	1-(4-hydroxy-3-methoxyphenyl)-2-Propanone/Guaiacylacetone/Vanillyl methyl ketone/4-Hydroxy-3-methoxyphenyl acetone	57.05	$C_{10}H_{12}O_3$	180.20	L	Guaiacols	0.21	0.11	N.D.
55	trans-4-Propenyl-2.6-dimethoxyphenol/Methoxyeugenol	57.21	$C_{11}H_{14}O_3$	194.23	L	Guaiacols	0.73	N.D.	N.D.
56	4-Propenyl-2.6-dimethoxyphenol/Methoxyeugenol (sis)	59.10	$C_{11}H_{14}O_3$	194.23	L	Guaiacols	0.27	N.D.	N.D.
57	1,6-Anhydro-b-D-glucopyranose/Levoglucosan	60.25	$C_6H_{12}O_5$	162.14	C	Sugars	N.D.	2.00	56.18
58	trans-4-Propenyl-2.6-dimethoxyphenol/Methoxyeugenol (trans)	61.26	$C_{11}H_{14}O_3$	194.23	L	Guaiacols	0.54	0.13	N.D.
59	1,6-ANHYDRO-.BETA.-D-GLUCOFURANOSE	63.11	$C_6H_{12}O_5$	162.00	C	Sugars	N.D.	N.D.	0.64

Table 12-3: Chemical identification from catalytic fast pyrolysis of wheat straw

ID	Compound name/synonyms	R/T	Formula	MW	Group
1	Methylglyoxal/2-oxopropanal/pyruvaldehyde	1.74	$C_3H_4O_2$	72	Aldehydes/Ketones
2	2.3 Butanedione/Butanedione/Diacetyl	1.92	$C_4H_6O_2$	86.1	Ketones
3	2.5-Furandione, dihydro-3-methyllene-	2.04	C_2H_4O	112	Aldehydes
4	3-methyl-furan	2.35	C_5H_6O	82	Furans
5	2.5-dimethyl-furan	2.37	C_6H_8O	96	Furans
6	Acetic acid	2.75	$C_2H_4O_2$	60	Carboxylic acids
7	3-hydroxy-butanal	2.85	$C_4H_8O_2$	88	Aldehydes
8	Benzene/Benzol/Coal naphtha/Phenyl hydride	2.86	C_6H_6	78	Aromatic Hydrocarbons
9	1.2_propanediol, 2-acetate/2-Acetoxy-1-propanol	3.09	$C_5H_{10}O_3$	118	Misc. Oxygenates
10	3-Methyl-2-hexene	3.18	C_7H_{14}	98	Hydrocarbons
11	2H-Pyran-2-one/α-Pyrone/Coumain/2-Puranone	4.22	$C_5H_4O_2$	96	Esters
12	Toluene/methyl benzene	4.56	C_7H_8	92	Aromatic Hydrocarbons
13	Propylene Carbonate/1.3-Dioxolan-2-one, 4-methyl-/Carbonic acid, cyclic propylene ester	4.69	$C_4H_6O_3$	102	Esters
14	Hydroxypropanone/1-Hydroxy-2-propanone/Acetone alcohol	4.70	$C_3H_6O_2$	74.1	Misc. Oxygenates
15	Furfural/furan-2-carboxaldehyde/fural/furfuraldehyde/2-furaldehyde/pyromucic aldehyde	6.30	$C_5H_4O_2$	96.1	Aldehyde
16	Ethylbenzene	6.73	C_8H_{10}	106	Aromatic Hydrocarbons
17	o-Xylene/1.2-Dimethyl-Benzene	7.02	C_8H_{10}	106	Aromatic Hydrocarbons
18	3-Penten-2-one	7.04	C_5H_8O	84	Ketones
19	3-Furaldehyde/1.3-Furancarboxaldehyde	7.20	$C_5H_4O_2$	96	Furans
20	p-Xylene/1.2-Dimethyl-Benzene	7.64	C_8H_{10}	106	Aromatic Hydrocarbons
21	1.3.5.7-Cycloactatetraene	7.69	C_8H_8	104	Hydrocarbons
22	p-Xylene/1.4-Dimethyl-Benzene	7.73	C_8H_{10}	106	Aromatic Hydrocarbons
23	Styrene	7.79	C_8H_8	104	Aromatic Hydrocarbons
24	2-Methyl-2-Cyclopenten-1-one/2-Methyl-2-Cyclopentenone	8.24	C_6H_8O	96	Ketones
25	Benzene, 1-ethyl-4-methyl-/ Toluene, p-ethyl-/p-Ethylmethylbenzene	9.80	C_9H_{12}	120	Aromatic Hydrocarbons
26	3-Methyl-2-Cyclopenten-1-one/3-Methyl-2-Cyclopentenone	10.18	C_6H_8O	96	Ketones
27	Benzene, 1,2,3-trimethyl-/Hemimelitene	10.74	C_9H_{12}	120	Aromatic Hydrocarbons
28	3-Hydroxyphenylacetylene	10.97	C_8H_6O	118	Phenols
29	(5H)-furan-2-one/2(5H)-Furanone	11.07	$C_4H_4O_2$	84.1	Furans/Lactones
30	m-Cresol/3-Methyl phenol	11.35	C_7H_8O	108	Phenols
31	3.4-dihydro-2-methoxy-2H-pyran	11.37	$C_6H_{10}O_2$	114	
32	1-methyl-2-(1-methylethyl)-Benzene	11.79	$C_{10}H_{14}$	134	Aromatic Hydrocarbons
33	2-methyl-Benzofuran	11.85	C_9H_8O	132	Ethers
34	cis-β-Methylstyrene/cis-β-Propenylbenzene	12.02	C_9H_{10}	118	Aromatic Hydrocarbons
35	2-Hydroxy-3-methyl-2-cyclopenten-1-one/maple lactone	12.20	$C_6H_8O_2$	112	Ketones
36	Benzene, 1-propynyl-/Methylphenylacetylene	12.37	C_9H_8	116	Aromatic Hydrocarbons
37	3-Methyl-4-Penten-2-one	12.71	$C_6H_{10}O$	98	Ketones
38	Benzene, (2-methyl-2-propynyl)-	13.45	$C_{10}H_{12}$	132	Aromatic Hydrocarbons
39	2-methoxy-phenol/o-methoxy-phenol/o-Guaiacol	13.69	$C_7H_8O_2$	124	Guaiacols

40	2-methyl-phenol/o-Cresol	13.93	C_7H_8O	108	Phenols
41	Mequinol/4-methoxy phenol/p-Methoxyphenol/p-Guaiacol or 2-methoxy?????	14.01	$C_7H_8O_2$	124	Guaiacols
42	Benzofuran, 2-methyl-	14.33	C_9H_8O	132	Ethers
43	5-hydroxy-2.3-dimehtyl-2-Cyclopenten-1-one	14.85	$C_7H_{10}O$	110	Ketones
44	Benzene, 4-ethenyl-1.2-dimethyl-/Styrene, 3.4-dimethyl-	15.29	$C_{10}H_{12}$	132	Aromatic Hydrocarbons
45	5-Methyl-2-furancarboxaldehyde/5-Methylfurfural/2-Formyl-5-methylfuran/2-Methyl-5-formylfuran	15.60	$C_6H_6O_2$	110	Furans
46	Naphthalene, 1.2-dihydro-/Dialin	15.79	$C_{10}H_{10}$	130	Aromatic Hydrocarbons
47	2.5-Dihydroxybenzaldehyde	16.18	$C_7H_6O_3$	138	Syringols
48	Phenol	16.22	C_6H_6O	94.1	Phenols
49	Naphthalene	16.88	$C_{10}H_8$	128	Aromatic Hydrocarbons
50	2-methoxy-4-methyl-phenol/p-Cresol, 2-methoxy-/p-Creosol/p-Methylguaiacol	17.02	$C_8H_{10}O_2$	138	Guaiacols
51	1.2-Benzenediol/Pyrocatechol	17.28	$C_6H_6O_2$	110	Phenols
52	Hydroquinone	17.30	$C_6H_6O_2$	110	Phenols
53	2-Hydroxy-3-methyl-2-cyclopenten-1-one	17.31	$C_6H_8O_2$	112	Ketones
54	2.3-dimehtyl-2-Cyclopenten-1-one	17.58	$C_7H_{10}O$	110	Ketones
55	2-methyl-Benzaldehyde/o-Tolualdehyde	17.77	C_8H_8O	120	Aldehydes
56	2.3-Dihydro-benzofuran	18.29	C_8H_8O	120	Phenols
57	(1-Methylenebut-2-enyl)benzene	19.02	$C_{11}H_{12}$	144	Aromatic Hydrocarbons
58	p,m-Cresol/3,4-Methyl phenol	19.15	C_7H_8O	108	Phenols
59	4-Ethyl-2-methoxyphenol/4-Ethyl guaiacol/4-Hydroxy-3-methoxy ethylbenzene/p-Ethylguaiacol	19.40	$C_9H_{12}O_2$	152	Guaiacols
60	Mequinol/4-methoxy phenol/p-Methoxyphenol/p-Guaiacol	19.40	$C_7H_8O_2$	124	Guaiacols
61	1 H-Indene-1-one, 2.3-dihydro-/1-Indanone	19.52	C_9H_8O	132	Ketones
62	1.3-Dioxolane-4-methanol, 2.2 dimethyl-, (S)-	19.79	$C_6H_{12}O_3$	132	
63	1 H-Indene, 1-ethyidene	19.90	$C_{11}H_{10}$	142	Aromatic Hydrocarbons
64	3-Ethyl-2-Hydroxy-2-Cyclopenten-1-one/1.3-Ethyl-2-Hydroxy-2-Cyclopenten-1-one	20.38	$C_7H_{10}O_2$	126	Ketones
65	2-Methoxy-4-vinylphenol/4-Vinylguaiacol/p-Vinylguaiacol/4-Hydroxy-3-methoxystyrene	20.49	$C_9H_{10}O_2$	150	Guaiacols
66	2,6-Dimethoxy phenol/Syringol/1,3-Dimethoxy-2-hydroxybenzene/Pyrogallol dimethylether	21.55	$C_8H_{10}O_3$	154	Syringols
67	1.7-dimethyl-Naphthalene	22.85	$C_{12}H_{12}$	156	Aromatic Hydrocarbons
68	Vanillin/2-Methoxy-4-formylphenol/4-Hydroxy-3-methoxybenzaldehyde	23.14	$C_8H_8O_3$	152	Guaiacols
69	3.4-Anhydro-d-galactosan	23.69	$C_6H_8O_4$	144	Sugars
70	Benzoic acid, 4-Hydroxy-3-methoxy-/Vanillic acid	23.73	$C_8H_8O_4$	168	
71	1, 2, 4- Trimethoxybenzene/1, 2, 4- Trimethoxy-1 benzene	23.90	$C_9H_{12}O_3$	168	Syringols
72	2-Methoxy-4-(1-propenyl)phenol/Isoeugenol,c&t/4-Propenylguaiacol/4-Hydroxy-3-methoxypropenylbenzene	24.11	$C_{10}H_{12}O_2$	164	Guaiacols
73	3-methoxy-1.2-Benzenediol	24.53	$C_7H_8O_3$	140	Guaiacols
74	5-tert-Butylpyrogallol/ 1.5-tert-Butyl-1,2,3-Benzenetriol	25.84	$C_{10}H_{14}O_3$	182	Phenols
75	3.5-Dimethoxyacetophenone/1-(3.5-Dimethoxyphenyl)-ethanone	26.90	$C_{10}H_{12}O_3$	180	Syringols
76	2.6-Dimethoxy-4-(2-propenyl)-phenol	3N.D.	$C_{11}H_{14}O_3$	194	Syringols
77	6-Methoxy-3-methylbenzofuran	30.37	$C_{10}H_{10}O_2$	162	Furans
78	1-(4-Hydroxy-3-methoxyphenyl)ethanone/Acetoguaiacone	30.55	$C_9H_{10}O_3$	166	Guaiacols
79	1,6-Anhydro-b-D-glucopyranose/Levoglucosan	31.02	$C_6H_{12}O_5$	162	Sugars

80	1-(4-hydroxy-3-methoxyphenyl)-2-Propanone/Guaiacylacetone/Vanillyl methyl ketone/4-Hydroxy-3-methoxyphenyl acetone	31.50	$C_{10}H_{12}O_3$	180	Guaiacols
81	Desaspidinol/1-(2.6-Dihydroxy-4-methoxyphenyl)-1-butanone	31.53	$C_{11}H_{14}O_4$	210	
82	4-((1E0-3-Hydroxy-1-propenyl)-2-methoxyphenol	32.96	$C_{10}H_{12}O_3$	180	Guaiacols
83	trans-4-Propenyl-2.6-dimethoxyphenol/Methoxyeugenol	33.17	$C_{11}H_{14}O_3$	194	Guaiacols
84	4-Propenyl-2.6-dimethoxyphenol/Methoxyeugenol (sis)	34.34	$C_{11}H_{14}O_3$	194	Guaiacols
85	4-Hydroxy-3.5-dimethoxybenzaldehyde/Syringaldehyde/Syringe aldehyde/Cedar aldehyde	34.66	$C_9H_{10}O_4$	182	Syringols
86	4-Hydroxy-2-methoxycinnamaldehyde/2(E)-3-(4-Hydroxy-2-methoxyphenyl)-2-propanal	36.42	$C_{10}H_{10}O_3$	178	Guaiacols
87	1-(4-Hydroxy-3.5-dimethoxyphenyl)ethanone/Acetosyringone	36.94	$C_{10}H_{12}O_4$	196	Syringols
88	Acetylfuran/1-(2-furanyl)-ethanone	8.38	$C_6H_6O_2$	110	Furans
89	5-methyl-2(3H)-furanone/a-Angelica lactone	8.75	$C_5H_6O_2$	98	Furans

Table 12-4: Relatively peak area percentages of fast pyrolysis of wheat straw with various catalysts

ID	Straw 500	NiMo 500	Zirconia 500	Fe_3O_2 500	ZnO 500	CuCr 500	ZSM 500	TiO 500	FCC 500	Straw 600	Straw 700	CoMo 600	CoMo 700	ZSM 600	ZSM 700	Fe_3O_2 600	Fe_3O_2 700	CoMo 500	CoMo used 500	CoMo burn 500
1	N.D.	N.D.	N.D.	N.D.	N.D.	1.30	N.D.	N.D.	N.D.	0.96	1.97	4.59	N.D.	1.70	2.27	0.86	2.35	N.D.	1.90	2.98
2	0.74	1.20	N.D.	N.D.	N.D.	N.D.	2.31	2.17	1.97	0.78	1.17	N.D.	N.D.	N.D.	N.D.	0.66	1.07	1.36	2.12	1.10
3	3.91	11.98	1.97	3.78	7.92	10.67	N.D.	N.D.	5.52	5.81	10.82	25.37	23.40	4.63	6.23	5.26	12.78	12.20	11.43	25.62
4	N.D.	8.05	N.D.	N.D.	N.D.	N.D.	N.D.	N.D.	N.D.	N.D.	N.D.	10.75	10.64	1.67	2.83	1.96	3.72	5.55	7.59	10.11
5	N.D.	N.D.	1.01	N.D.	2.05	1.06	N.D.	0.38	2.67	0.47	0.63	1.56	1.35	N.D.	N.D.	0.48	0.95	0.53	1.36	1.35
6	13.96	10.66	6.05	14.02	22.74	42.23	9.42	9.43	15.38	13.50	19.92	16.89	15.88	1.85	6.88	11.91	21.23	21.69	12.08	21.17
7	N.D.	N.D.	N.D.	N.D.	N.D.	4.99	N.D.	N.D.	N.D.	N.D.	N.D.	N.D.	N.D.	N.D.	N.D.	N.D.	N.D.	N.D.	N.D.	4.10
8	N.D.	2.14	N.D.	N.D.	N.D.	N.D.	1.73	N.D.	N.D.	N.D.	N.D.	N.D.	6.27	6.29	5.88	N.D.	N.D.	N.D.	N.D.	N.D.
9	5.47	N.D.	2.89	2.27	5.33	N.D.	N.D.	3.41	4.44	4.02	6.17	4.75	N.D.	N.D.	N.D.	2.31	4.46	1.83	2.89	N.D.
10	N.D.	N.D.	N.D.	N.D.	N.D.	N.D.	N.D.	N.D.	N.D.	N.D.	N.D.	N.D.	1.91	N.D.	N.D.	N.D.	N.D.	N.D.	N.D.	N.D.
11	N.D.	N.D.	N.D.	N.D.	N.D.	N.D.	N.D.	N.D.	N.D.	N.D.	N.D.	N.D.	N.D.	N.D.	N.D.	N.D.	N.D.	0.55	N.D.	N.D.
12	N.D.	2.32	0.77	1.75	N.D.	0.66	3.34	N.D.	N.D.	1.22	1.49	3.68	3.66	13.60	13.88	0.92	2.67	N.D.	3.95	1.96
13	1.99	N.D.	1.56	1.86	N.D.	N.D.	N.D.	2.12	1.50	1.63	2.04	N.D.	N.D.	N.D.	N.D.	1.22	1.78	0.67	N.D.	N.D.
14	3.18	N.D.	1.23	1.48	N.D.	N.D.	N.D.	1.80	2.31	2.51	3.05	N.D.	N.D.	N.D.	N.D.	2.00	3.17	1.44	N.D.	N.D.
15	2.49	7.75	2.88	2.10	3.60	2.00	N.D.	1.91	3.08	1.75	3.04	1.39	1.53	N.D.	N.D.	3.11	1.32	4.75	2.26	2.06
16	N.D.	0.60	N.D.	N.D.	N.D.	N.D.	0.54	N.D.	N.D.	N.D.	N.D.	N.D.	N.D.	1.40	1.58	N.D.	0.25	N.D.	1.20	N.D.
17	N.D.	1.76	N.D.	N.D.	N.D.	N.D.	4.80	N.D.	N.D.	1.83	2.39	1.54	1.67	16.11	15.50	1.13	2.61	N.D.	2.49	1.51
18	0.42	N.D.	N.D.	N.D.	N.D.	N.D.	N.D.	N.D.	0.66	N.D.	N.D.	N.D.	N.D.	N.D.	N.D.	N.D.	N.D.	0.39	N.D.	N.D.
19	0.93	N.D.	1.03	N.D.	N.D.	N.D.	N.D.	1.05	N.D.	N.D.	N.D.	N.D.	N.D.	N.D.	N.D.	N.D.	N.D.	0.21	N.D.	N.D.
20	N.D.	N.D.	N.D.	N.D.	N.D.	N.D.	0.20	N.D.	N.D.	N.D.	N.D.	N.D.	N.D.	N.D.	N.D.	N.D.	N.D.	N.D.	N.D.	N.D.
21	N.D.	N.D.	N.D.	N.D.	N.D.	N.D.	N.D.	N.D.	N.D.	0.31	0.30	N.D.	N.D.	N.D.	N.D.	N.D.	N.D.	N.D.	N.D.	N.D.
22	N.D.	N.D.	N.D.	N.D.	N.D.	N.D.	N.D.	N.D.	N.D.	N.D.	N.D.	0.84	N.D.	0.67	1.03	N.D.	N.D.	N.D.	N.D.	N.D.
23	N.D.	1.27	0.70	0.40	N.D.	N.D.	N.D.	N.D.	N.D.	N.D.	N.D.	N.D.	0.86	N.D.	N.D.	0.31	0.38	N.D.	0.72	0.57
24	0.44	N.D.	0.49	0.41	N.D.	N.D.	0.13	0.37	0.52	0.46	0.72	0.41	0.55	N.D.	N.D.	0.49	0.66	1.09	1.19	1.12
25	N.D.	0.80	N.D.	N.D.	N.D.	N.D.	0.92	N.D.	N.D.	N.D.	N.D.	N.D.	N.D.	1.17	1.43	N.D.	N.D.	N.D.	0.41	N.D.
26	N.D.	1.71	0.69	N.D.	N.D.	N.D.	N.D.	N.D.	0.56	0.84	0.58	N.D.	N.D.	N.D.	N.D.	1.15	1.11	0.75	N.D.	N.D.
27	N.D.	N.D.	N.D.	N.D.	N.D.	N.D.	0.33	N.D.	N.D.	N.D.	N.D.	N.D.	N.D.	0.52	0.55	N.D.	N.D.	N.D.	N.D.	N.D.
28	N.D.	0.62	N.D.	N.D.	N.D.	N.D.	N.D.	N.D.	N.D.	N.D.	N.D.	N.D.	0.61	N.D.	N.D.	N.D.	N.D.	N.D.	0.89	N.D.
29	0.43	0.88	N.D.	N.D.	N.D.	N.D.	N.D.	0.39	0.75	N.D.	N.D.	N.D.	1.13	N.D.	N.D.	N.D.	N.D.	1.03	1.27	1.16
30	N.D.	N.D.	N.D.	N.D.	N.D.	N.D.	N.D.	N.D.	N.D.	N.D.	N.D.	N.D.	N.D.	N.D.	N.D.	N.D.	N.D.	1.53	N.D.	N.D.
31	1.74	N.D.	0.24	N.D.	N.D.	N.D.	N.D.	1.44	N.D.	0.36	0.33	N.D.	N.D.	N.D.	N.D.	N.D.	N.D.	N.D.	N.D.	N.D.
32	N.D.	N.D.	N.D.	N.D.	N.D.	N.D.	N.D.	N.D.	N.D.	N.D.	N.D.	N.D.	N.D.	N.D.	N.D.	N.D.	N.D.	N.D.	N.D.	0.34
33	N.D.	0.68	N.D.	N.D.	N.D.	N.D.	N.D.	N.D.	N.D.	N.D.	N.D.	N.D.	N.D.	N.D.	N.D.	N.D.	N.D.	0.41	N.D.	N.D.
34	N.D.	N.D.	N.D.	N.D.	N.D.	N.D.	0.46	N.D.	N.D.	N.D.	N.D.	N.D.	N.D.	0.75	0.98	N.D.	N.D.	N.D.	N.D.	N.D.
35	N.D.	N.D.	1.70	1.32	N.D.	N.D.	N.D.	N.D.	N.D.	1.32	2.03	N.D.	N.D.	N.D.	N.D.	1.26	1.29	N.D.	N.D.	N.D.
36	N.D.	N.D.	N.D.	N.D.	N.D.	N.D.	0.28	N.D.	N.D.	N.D.	N.D.	N.D.	N.D.	0.83	1.06	N.D.	N.D.	N.D.	N.D.	N.D.
37	1.68	N.D.	N.D.	N.D.	N.D.	N.D.	N.D.	1.11	1.63	N.D.	N.D.	N.D.	N.D.	N.D.	N.D.	N.D.	N.D.	1.42	N.D.	N.D.

38	N.D.	N.D.	N.D.	N.D.	N.D.	N.D.	0.43	N.D.	N.D.	N.D.	N.D.	N.D.	N.D.	0.32	0.32	N.D.	N.D.	N.D.	N.D.	N.D.
39	N.D.	N.D.	N.D.	N.D.	N.D.	N.D.	2.14	N.D.	N.D.	N.D.	N.D.	N.D.	N.D.	N.D.	N.D.	N.D.	N.D.	N.D.	N.D.	N.D.
40	0.31	N.D.	4.76	N.D.	N.D.	N.D.	N.D.	0.65	0.25	2.78	1.92	N.D.	N.D.	N.D.	N.D.	0.81	N.D.	N.D.	N.D.	N.D.
41	N.D.	N.D.	N.D.	N.D.	N.D.	N.D.	N.D.	N.D.	N.D.	N.D.	N.D.	N.D.	N.D.	N.D.	N.D.	N.D.	N.D.	N.D.	N.D.	N.D.
42	N.D.	N.D.	N.D.	N.D.	N.D.	N.D.	0.21	N.D.	N.D.	N.D.	N.D.	N.D.	N.D.	N.D.	N.D.	N.D.	N.D.	N.D.	N.D.	N.D.
43	N.D.	N.D.	N.D.	N.D.	N.D.	N.D.	N.D.	N.D.	N.D.	N.D.	0.61	N.D.	N.D.	N.D.	N.D.	N.D.	N.D.	N.D.	N.D.	N.D.
44	N.D.	N.D.	N.D.	N.D.	N.D.	N.D.	0.31	N.D.	N.D.	N.D.	N.D.	N.D.	N.D.	N.D.	N.D.	N.D.	N.D.	N.D.	N.D.	N.D.
45	0.63	1.51	N.D.	N.D.	N.D.	N.D.	N.D.	0.96	0.66	N.D.	N.D.	N.D.	N.D.	N.D.	N.D.	N.D.	N.D.	1.06	N.D.	N.D.
46	N.D.	N.D.	N.D.	N.D.	N.D.	N.D.	0.31	N.D.	N.D.	N.D.	N.D.	N.D.	N.D.	0.71	0.58	N.D.	N.D.	N.D.	N.D.	N.D.
47	N.D.	N.D.	N.D.	N.D.	N.D.	N.D.	0.35	0.59	N.D.	N.D.	N.D.	N.D.	N.D.	N.D.	N.D.	N.D.	N.D.	N.D.	N.D.	N.D.
48	0.30	N.D.	N.D.	N.D.	N.D.	N.D.	0.26	0.67	1.05	N.D.	N.D.	N.D.	1.35	N.D.	N.D.	N.D.	N.D.	1.11	N.D.	N.D.
49	N.D.	N.D.	N.D.	N.D.	N.D.	N.D.	N.D.	N.D.	N.D.	N.D.	N.D.	N.D.	N.D.	3.76	3.35	N.D.	N.D.	N.D.	N.D.	N.D.
50	1.43	0.53	1.14	0.70	N.D.	N.D.	N.D.	1.37	1.55	0.62	0.48	N.D.	N.D.	N.D.	N.D.	0.66	0.51	0.74	N.D.	N.D.
51	N.D.	N.D.	N.D.	N.D.	N.D.	N.D.	N.D.	1.13	N.D.	N.D.	N.D.	N.D.	N.D.	N.D.	N.D.	N.D.	N.D.	N.D.	N.D.	N.D.
52	N.D.	N.D.	N.D.	N.D.	N.D.	N.D.	0.32	N.D.	N.D.	N.D.	N.D.	N.D.	N.D.	N.D.	N.D.	N.D.	N.D.	N.D.	N.D.	N.D.
53	0.13	N.D.	N.D.	N.D.	N.D.	N.D.	0.88	1.40	1.31	N.D.	N.D.	N.D.	N.D.	N.D.	N.D.	N.D.	N.D.	1.17	N.D.	N.D.
54	2.04	N.D.	N.D.	N.D.	N.D.	N.D.	N.D.	0.30	0.43	0.94	N.D.	N.D.	N.D.	N.D.	N.D.	0.85	1.13	0.42	N.D.	N.D.
55	N.D.	N.D.	N.D.	N.D.	N.D.	N.D.	0.40	N.D.	N.D.	N.D.	N.D.	N.D.	N.D.	N.D.	N.D.	N.D.	N.D.	N.D.	N.D.	N.D.
56	2.19	N.D.	1.15	N.D.	N.D.	N.D.	N.D.	1.76	N.D.	0.93	N.D.	N.D.	N.D.	N.D.	N.D.	N.D.	0.27	N.D.	N.D.	N.D.
57	N.D.	N.D.	N.D.	N.D.	N.D.	N.D.	N.D.	N.D.	N.D.	N.D.	N.D.	N.D.	N.D.	0.48	0.30	N.D.	N.D.	N.D.	N.D.	N.D.
58	0.19	N.D.	N.D.	N.D.	N.D.	N.D.	N.D.	N.D.	N.D.	N.D.	N.D.	N.D.	N.D.	N.D.	N.D.	N.D.	N.D.	0.71	N.D.	N.D.
59	1.61	0.46	1.15	0.66	N.D.	N.D.	1.08	1.16	2.56	0.80	0.45	N.D.	N.D.	N.D.	N.D.	0.87	0.31	0.67	N.D.	N.D.
60	3.32	2.15	N.D.	2.38	1.03	1.31	N.D.	2.00	3.27	N.D.	2.40	N.D.	N.D.	0.20	0.55	2.49	0.54	3.01	1.11	N.D.
61	N.D.	N.D.	N.D.	N.D.	N.D.	N.D.	N.D.	0.48	N.D.	N.D.	N.D.	N.D.	N.D.	N.D.	N.D.	N.D.	N.D.	N.D.	N.D.	N.D.
62	3.35	N.D.	1.52	N.D.	N.D.	N.D.	N.D.	2.29	N.D.	N.D.	N.D.	N.D.	N.D.	N.D.	N.D.	N.D.	N.D.	0.67	N.D.	N.D.
63	N.D.	N.D.	N.D.	N.D.	N.D.	N.D.	0.90	N.D.	N.D.	N.D.	N.D.	N.D.	N.D.	7.22	5.01	N.D.	N.D.	N.D.	N.D.	N.D.
64	0.47	N.D.	N.D.	N.D.	N.D.	N.D.	0.37	0.72	0.60	N.D.	N.D.	N.D.	N.D.	N.D.	N.D.	0.68	N.D.	N.D.	N.D.	N.D.
65	7.81	0.52	8.90	9.52	9.20	2.58	3.36	4.16	1.32	9.05	8.12	N.D.	N.D.	2.85	3.05	7.98	6.74	1.12	0.81	N.D.
66	0.29	N.D.	4.08	4.30	N.D.	N.D.	2.61	3.46	2.85	2.96	1.74	N.D.	N.D.	0.89	N.D.	2.36	N.D.	0.41	0.17	N.D.
67	N.D.	N.D.	N.D.	N.D.	N.D.	N.D.	0.44	N.D.	N.D.	N.D.	N.D.	N.D.	N.D.	3.41	2.37	N.D.	N.D.	N.D.	N.D.	N.D.
68	2.88	N.D.	1.26	N.D.	N.D.	N.D.	0.63	1.69	0.83	N.D.	N.D.	N.D.	N.D.	N.D.	N.D.	N.D.	N.D.	0.35	N.D.	N.D.
69	N.D.	N.D.	N.D.	N.D.	N.D.	N.D.	N.D.	0.73	N.D.	N.D.	N.D.	N.D.	N.D.	N.D.	N.D.	N.D.	N.D.	N.D.	N.D.	N.D.
70	N.D.	N.D.	N.D.	N.D.	N.D.	N.D.	0.61	N.D.	N.D.	N.D.	N.D.	N.D.	N.D.	N.D.	N.D.	N.D.	N.D.	N.D.	N.D.	N.D.
71	0.71	N.D.	1.17	N.D.	N.D.	N.D.	N.D.	0.74	0.71	1.82	N.D.	N.D.	N.D.	N.D.	N.D.	0.63	N.D.	N.D.	N.D.	N.D.
72	1.45	N.D.	2.52	2.52	N.D.	N.D.	0.87	1.06	0.81	N.D.	1.03	N.D.	N.D.	0.64	1.00	1.80	N.D.	0.48	N.D.	N.D.
73	0.07	N.D.	N.D.	N.D.	N.D.	N.D.	0.72	0.72	1.04	N.D.	N.D.	N.D.	N.D.	N.D.	N.D.	N.D.	N.D.	N.D.	N.D.	N.D.
74	0.67	N.D.	0.55	0.55	N.D.	N.D.	0.90	0.85	0.89	N.D.	N.D.	N.D.	N.D.	N.D.	N.D.	N.D.	N.D.	N.D.	N.D.	N.D.
75	2.30	N.D.	4.63	4.77	1.36	1.17	N.D.	1.73	N.D.	2.44	2.44	N.D.	0.55	3.01	2.11	3.16	1.65	N.D.	N.D.	N.D.
76	N.D.	N.D.	1.93	1.73	1.85	0.31	0.29	N.D.	N.D.	0.18	1.39	N.D.	N.D.	1.13	0.64	1.28	0.54	N.D.	0.33	N.D.
77	0.16	N.D.	N.D.	N.D.	N.D.	N.D.	0.34	0.32	0.40	N.D.	N.D.	N.D.	N.D.	N.D.	N.D.	N.D.	N.D.	N.D.	N.D.	N.D.
78	0.17	N.D.	N.D.	N.D.	N.D.	N.D.	N.D.	0.48	N.D.	N.D.	N.D.	N.D.	N.D.	N.D.	N.D.	N.D.	N.D.	N.D.	N.D.	N.D.
79	2.77	N.D.	N.D.	N.D.	N.D.	N.D.	1.13	1.43	N.D.	N.D.	N.D.	N.D.	N.D.	N.D.	N.D.	N.D.	N.D.	N.D.	N.D.	N.D.
80	0.67	N.D.	N.D.	N.D.	N.D.	N.D.	N.D.	1.06	N.D.	N.D.	N.D.	N.D.	N.D.	N.D.	N.D.	N.D.	N.D.	N.D.	N.D.	N.D.

81	0.41	N.D.	N.D.	N.D.	N.D.	N.D.	0.59	0.73	0.35	0.17	N.D.	N.D.	N.D.	N.D.	N.D.	N.D.	N.D.	N.D.	N.D.	N.D.
82	0.12	N.D.	N.D.	N.D.	N.D.	N.D.	N.D.	0.38	N.D.	N.D.	N.D.	N.D.	N.D.	N.D.	N.D.	N.D.	N.D.	N.D.	N.D.	N.D.
83	0.32	N.D.	N.D.	N.D.	N.D.	N.D.	N.D.	0.43	N.D.	N.D.	N.D.	N.D.	N.D.	N.D.	N.D.	N.D.	N.D.	N.D.	N.D.	N.D.
84	0.14	N.D.	N.D.	N.D.	N.D.	N.D.	N.D.	N.D.	0.37	N.D.	N.D.	N.D.	N.D.	N.D.	N.D.	N.D.	N.D.	N.D.	N.D.	N.D.
85	0.21	N.D.	N.D.	N.D.	N.D.	N.D.	0.39	N.D.	N.D.	N.D.	N.D.	N.D.	N.D.	N.D.	N.D.	N.D.	N.D.	N.D.	N.D.	N.D.
86	1.35	N.D.	N.D.	N.D.	N.D.	N.D.	0.36	0.90	N.D.	N.D.	N.D.	N.D.	N.D.	N.D.	N.D.	N.D.	N.D.	N.D.	N.D.	N.D.
87	0.64	N.D.	N.D.	N.D.	N.D.	N.D.	0.70	0.65	0.46	N.D.	N.D.	N.D.	N.D.	N.D.	N.D.	N.D.	N.D.	N.D.	N.D.	N.D.
88	0.85	0.94	N.D.	N.D.	N.D.	N.D.	N.D.	0.78	1.39	N.D.	N.D.	N.D.	N.D.	N.D.	N.D.	N.D.	N.D.	1.92	N.D.	N.D.
89	2.99	N.D.	2.98	1.53	2.00	N.D.	0.72	2.48	2.40	1.30	2.27	N.D.	N.D.	N.D.	N.D.	1.50	0.82	1.72		

Table 12-5: Chemical identification and relatively peak area percentages from fast pyrolysis of aquathermolised wheat straw with catalysts

ID	Compound name/synonyms	R/T	Formula	MW	Group	Aqua'	Aqua' + CoMo	Aqua' + ZSM-5	Aqua' + NiMo	Aqua' + Fe_3O_2
1	2.5-Furandione, dihydro-3-methyllene-	2.029	C_2H_4O	112	Aldehydes	0.57	11.53	0.99	3.03	1.75
2	3-methyl-furan	2.45	C_5H_6O	82	Furans	1.00	11.39	0.86	5.60	1.49
3	Acetic acid	2.6	$C_2H_4O_2$	60	Carboxylic acids	0.53	N.D.	0.46	N.D.	1.44
4	Benzene/Benzol/Coal naphtha/Phenyl hydride	2.905	C_6H_6	78	Aromatic Hydrocarbons	N.D.	2.02	2.56	0.56	N.D.
5	3-Methyl-2-hexene	3.27	C_7H_{14}	98	Hydrocarbons	N.D.	0.80	N.D.	N.D.	N.D.
6	2.5-dimethyl-furan	3.418	C_6H_8O	96	Furans	N.D.	2.10	0.34	1.67	N.D.
7	Phenol	3.669	C_6H_6O	94.11	Phenols	N.D.	1.74	N.D.	1.12	N.D.
8	Toluene/methyl benzene	4.589	C_7H_8	92	Aromatic Hydrocarbons	0.30	2.58	6.65	1.52	N.D.
9	(5H)-furan-2-one/2(5H)-Furanone	5.47	$C_4H_4O_2$	84.07	Furans	0.50	1.96	0.39	1.47	N.D.
10	3-Furaldehyde	5.817	$C_5H_4O_2$	96.08	Aldehydes	N.D.	0.47	N.D.	N.D.	N.D.
11	3-Methyl phenol/m-cresol	6.034	C_7H_8O	108	Phenols	N.D.	0.74	N.D.	N.D.	N.D.
12	Furfural/furan-2-carboxaldehyde/fural/furfuraldehyde/2-furaldehyde/pyromucic aldehyde	6.52	$C_5H_4O_2$	96.08	Aldehydes	1.25	12.50	N.D.	6.13	1.39
13	Ethylbenzene	7.036	C_8H_{10}	106	Aromatic Hydrocarbons	N.D.	0.65	0.60	N.D.	N.D.
14	o-Xylene/1.2-Dimethyl-Benzene	7.138	C_8H_{10}	106	Aromatic Hydrocarbons	N.D.	1.16	7.03	N.D.	N.D.
15	Styrene	7.76	C_8H_8	104	Aromatic Hydrocarbons	0.27	1.16	N.D.	N.D.	N.D.
16	1.3.5.7-Cycloactatetraene	7.778	C_8H_8	104	Hydrocarbons	N.D.	N.D.	0.27	N.D.	N.D.
17	2.4-Heptadienal	7.919	$C_7H_{10}O$	110	Aldehydes	N.D.	N.D.	N.D.	2.38	N.D.

18	2-Methyl-2-Cyclopenten-1-one/2-Methyl-2-Cyclopentenone	8.236	C_6H_8O	96	Ketones	N.D.	2.48	N.D.	1.33	N.D.
19	Acetylfuran/1-(2-furanyl)-ethanone	8.436	$C_6H_6O_2$	110	Furans	N.D.	1.34	N.D.	1.32	N.D.
20	2-ethyl-5-methyl-furan	8.54	$C_7H_{10}O$	110	Furans	N.D.	1.30	N.D.	N.D.	N.D.
21	Benzene, 1-ethyl-4-methyl-/ Toluene, p-ethyl-/p-Ethylmethylbenzene	9.945	C_9H_{12}	120	Aromatic Hydrocarbons	N.D.	N.D.	0.43	N.D.	N.D.
22	5-Methyl-2-furancarboxaldehyde/5-Methylfurfural/2-Formyl-5-methylfuran/2-Methyl-5-formylfuran	10.037	$C_6H_6O_2$	110.11	Furans	N.D.	6.31	N.D.	N.D.	N.D.
23	Hydroquinone/1.4-Benzenediol	10.373	$C_6H_6O_2$	110	Phenols	N.D.	0.64	N.D.	4.18	N.D.
24	5-methyl-2(3H)-furanone/a-Angelica lactone	10.428	$C_5H_6O_2$	98	Furans	N.D.	N.D.	0.57	4.27	1.28
25	3-Hydroxyphenylacetylene	10.52	C_8H_6O	118	Phenols	N.D.	1.35	N.D.	N.D.	N.D.
26	2-Hydroxy-3-methyl-2-cyclopenten-1-one/maple lactone	12.171	$C_6H_8O_2$	112	Ketones	0.51	N.D.	0.40	2.68	0.77
27	Mequinol/4-methoxy phenol/p-Methoxyphenol/p-Guaiacol	13.9	$C_7H_8O_2$	124	Guaiacols	2.16	N.D.	3.05	1.59	1.88
28	2-Furanmethanol/2-Furfuryl alcohol	14.772	$C_5H_6O_2$	98.1	Furans	N.D.	N.D.	N.D.	2.46	1.04
29	Benzene, (1-methyl-2-butynyl)-	15.939	$C_{11}H_{12}$	144	Aromatic Hydrocarbons	N.D.	N.D.	0.18	N.D.	N.D.
30	Naphthalene/Albocarbon	16.878	$C_{11}H_{12}$	128	Aromatic Hydrocarbons	N.D.	N.D.	1.27	N.D.	N.D.
31	2-methoxy-4-methyl-phenol/p-Cresol, 2-methoxy-/p-Creosol/p-Methylguaiacol	17.016	$C_8H_{10}O_2$	138.17	Guaiacols	2.13	1.49	3.25	2.13	3.27
32	1.4:3.6-Dianhydro-a-glucopyranose	17.887	$C_6H_8O_4$	144	Sugars	N.D.	N.D.	1.05	1.96	N.D.
33	2.3-Dihydro-benzofuran	18.23	C_8H_8O	120	Phenols	1.31	N.D.	N.D.	N.D.	N.D.
34	4-Ethyl-2-methoxyphenol/4-Ethyl guaiacol/4-Hydroxy-3-methoxy ethylbenzene/p-Ethylguaiacol	19.4	$C_9H_{12}O_2$	152.19	Guaiacols	1.87	N.D.	1.41	0.77	0.75
35	1 H-Indene, 1-ethyidene	20.2	$C_{11}H_{10}$	142	Aromatic Hydrocarbons	N.D.	N.D.	1.21	N.D.	N.D.
36	2-Methoxy-4-vinylphenol/4-Vinylguaiacol/p-Vinylguaiacol/4-Hydroxy-3-methoxystyrene	20.48	$C_9H_{10}O_2$	150.18	Guaiacols	5.29	N.D.	6.74	0.72	4.94
37	2,6-Dimethoxy phenol/Syringol/1,3-Dimethoxy-2-hydroxybenzene/Pyrogallol dimethylether	21.54	$C_8H_{10}O_3$	154.17	Syringols	3.46	N.D.	2.82	N.D.	1.89
38	1.7-dimethyl-Naphthalene	22.995	$C_{12}H_{12}$	156	Aromatic Hydrocarbons	N.D.	N.D.	1.68	N.D.	N.D.
39	1, 2, 4- Trimethoxybenzene/1, 2, 4- Trimethoxy-1 benzene	23.9	$C_9H_{12}O_3$	168	Syringols	3.39	N.D.	3.56	1.14	2.11
40	2-Methoxy-4-(1-propenyl)phenol/Isoeugenol,c&t/4-Propenylguaiacol/4-Hydroxy-3-methoxypropenylbenzene	24.11	$C_{10}H_{12}O_2$	164.2	Guaiacols	1.28	N.D.	N.D.	N.D.	N.D.
41	5-tert-Butylpyrogallol/ 1.5-tert-Butyl-1,2,3-	25.83	$C_{10}H_{14}O_3$	182	Phenols	0.36	N.D.	0.69	N.D.	N.D.

	Benzenetriol									
42	a-D-Glucopyranose, 4-O-β-D-galactopyranosyl-	26.835	$C_{12}H_{22}O_{11}$	342	Sugars	N.D.	N.D.	27.63	N.D.	29.87
43	3.5-Dimethoxyacetophenone/1-(3.5-Dimethoxyphenyl)-ethanone	26.9	$C_{10}H_{12}O_3$	180	Syringols	N.D.	N.D.	3.27	1.25	N.D.
44	1,6-Anhydro-b-D-glucopyranose/Levoglucosan	27.8	$C_6H_{12}O_5$	162.14	Sugars	32.93	N.D.	N.D.	N.D.	N.D.
45	2.6-Dimethoxy-4-(2-propenyl)-phenol	30.04	$C_{11}H_{14}O_3$	194	Syringols	1.57	N.D.	1.61	N.D.	1.70
46	1-(4-Hydroxy-3.5-dimethoxyphenyl)ethanone/Acetosyringone	30.87	$C_9H_{10}O_3$	166.18	Syringols	0.81	N.D.	1.74	N.D.	N.D.

Table 12-6: Chemical identification and relatively peak area percentages from laboratory fast pyrolysis of wheat straw with CoMo

ID	Compound name/synonyms	R/T	Formula	MW	Group	280211C	8311C
1	Toluene/methyl benzene	4.22	C_7H_8	92	Aromatic Hydrocarbons	0.50	0.00
2	(5H)-furan-2-one/2(5H)-Furanone	4.84	$C_4H_4O_2$	84.07	Furans/Lactones	5.03	3.61
3	3-methyl-furan	5.93	C_5H_6O	82	Furans	4.08	7.55
4	Furfural/furan-2-carboxaldehyde/fural/furfuraldehyde/2-furaldehyde/pyromucic aldehyde	6.08	$C_5H_4O_2$	96.08	Aldehyde	3.20	1.10
5	2.5-dimethyl-furan	6.87	C_6H_8O	96	Furans	1.23	0.81
6	2-Methyl-2-Cyclopenten-1-one/2-Methyl-2-Cyclopentenone	8.00	C_6H_8O	96	Ketones	9.87	8.24
7	1.2.3-trimethyl-cyclopentene	8.11	C_8H_{14}	110	Hydrocarbons	0.00	0.44
8	Cyclopropene, 1-butyl-2-ethyl-	8.92	C_9H_{16}	124	Hydrocarbons	0.82	0.64
9	3-Methyl-2-Cyclopenten-1-one/3-Methyl-2-Cyclopentenone	10.02	C_6H_8O	96	Ketones	0.54	2.00
10	Phenol	10.42	C_6H_6O	94.11	Phenols	29.16	30.88
11	2.3-dimehtyl-2-Cyclopenten-1-one	12.10	$C_7H_{10}O$	110	Ketones	1.52	1.55
12	2-methyl-phenol/o-Cresol	12.69	C_7H_8O	108	Phenols	10.30	9.57
13	p,m-Cresol/3,4-Methyl phenol	13.45	C_7H_8O	108.14	Phenols	12.97	21.73
14	2.3-dimethyl-phenol	14.28	$C_8H_{10}O$	122	Phenols	3.13	0.63
15	2-ethyl-phenol	15.62	$C_8H_{10}O$	122	Phenols	2.81	1.83
16	3-ethyl-phenol	16.35	$C_8H_{10}O$	122	Phenols	2.00	1.63
17	2-Methoxy-4-(1-propenyl)phenol/Isoeugenol,c&t/4-Propenylguaiacol/4-Hydroxy-3-methoxypropenylbenzene	21.54	$C_{10}H_{12}O_2$	164.2	Guaiacols	1.34	0.00

Table 12-7: The effect of catalysts on pyrolysis products. Cells highlighted in yellow show a significant variation from wheat straw with no catalysts at 500°C

	Straw 500	NM 500	ZrO 500	Fe 500	ZnO 500	CuCr 500	ZSM 500	TiO 500	FCC 500	Straw 600	Straw 700	CoMo 600	CoMo 700	ZSM 600	ZSM 700	Fe 600	Fe 700	CoMo 500	CoMo used	CoMo regen
Aldehyde	6.40	19.73	4.85	5.88	11.52	18.96	0.40	1.91	8.60	8.51	15.83	31.35	24.94	6.32	8.50	9.22	16.44	16.95	15.59	34.76
Carboxylic acids	13.96	10.66	6.05	14.02	22.74	42.23	9.42	9.43	15.38	13.50	19.92	16.89	15.88	1.85	6.88	11.91	21.23	21.69	12.08	21.17
Ethers	1.99	0.68	1.56	1.86	N.D.	N.D.	0.21	2.12	1.50	1.63	2.04	N.D.	N.D.	N.D.	N.D.	1.22	1.78	1.62	N.D.	N.D.
Furans	5.99	11.38	5.02	1.53	4.05	1.06	1.06	6.36	8.26	1.76	2.90	12.30	13.11	1.67	2.83	3.93	5.49	12.02	10.22	12.62
Guaiacols	21.33	3.67	16.89	17.50	12.08	4.20	9.45	15.41	11.74	10.65	13.86	N.D.	N.D.	4.82	5.24	15.08	8.63	6.36	2.25	N.D.
Ketones	5.91	2.91	2.87	1.73	N.D.	N.D.	3.69	6.55	7.69	4.33	5.11	0.41	0.55	N.D.	N.D.	5.09	5.27	6.60	3.31	2.23
Misc. Oxygenates	8.65	N.D.	4.11	3.75	5.33	N.D.	N.D.	5.22	6.76	6.53	9.22	4.75	N.D.	N.D.	N.D.	4.30	7.63	3.27	2.89	N.D.
Phenols	3.66	0.62	6.46	0.55	N.D.	N.D.	1.48	5.06	2.19	3.71	1.92	N.D.	1.96	N.D.	N.D.	0.81	0.27	3.35	0.89	N.D.
Sugars	2.77	N.D.	N.D.	N.D.	N.D.	N.D.	1.13	2.17	N.D.	N.D.	N.D.	N.D.	N.D.	N.D.	N.D.	N.D.	N.D.	N.D.	N.D.	N.D.
Syringols	4.15	N.D.	9.89	9.08	1.36	1.17	0.41	3.70	6.58	4.01	7.23	4.17	N.D.	0.55	3.89	2.11	6.16	1.65	0.17	N.D.
TOTAL																				
Aromatic Hydro-carbons	N.D.	8.89	1.47	2.15	N.D.	0.66	14.99	N.D.	N.D.	3.04	3.88	6.07	12.46	57.22	53.81	2.36	5.92	N.D.	8.77	4.37
Hydro-carbons	N.D.	N.D.	N.D.	N.D.	N.D.	N.D.	N.D.	N.D.	N.D.	0.31	0.30	N.D.	1.91	N.D.	N.D.	N.D.	N.D.	N.D.	N.D.	N.D.
TOTAL																				

13 APPENDIX - B

CHROMATOGRAMS

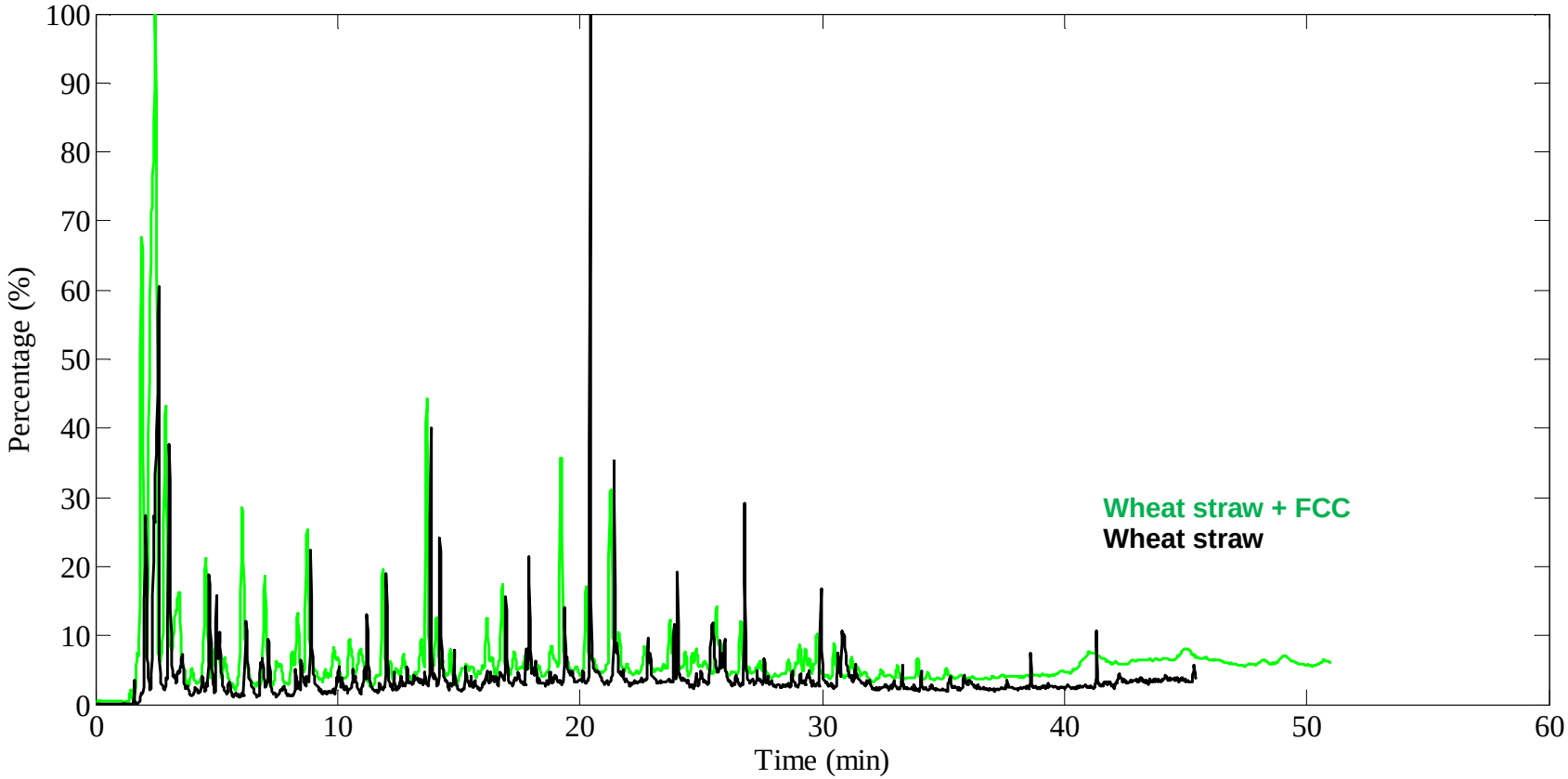

Figure 13-1: Chromatograms obtained from Py-GC/MS for wheat straw with FCC catalyst at 500C

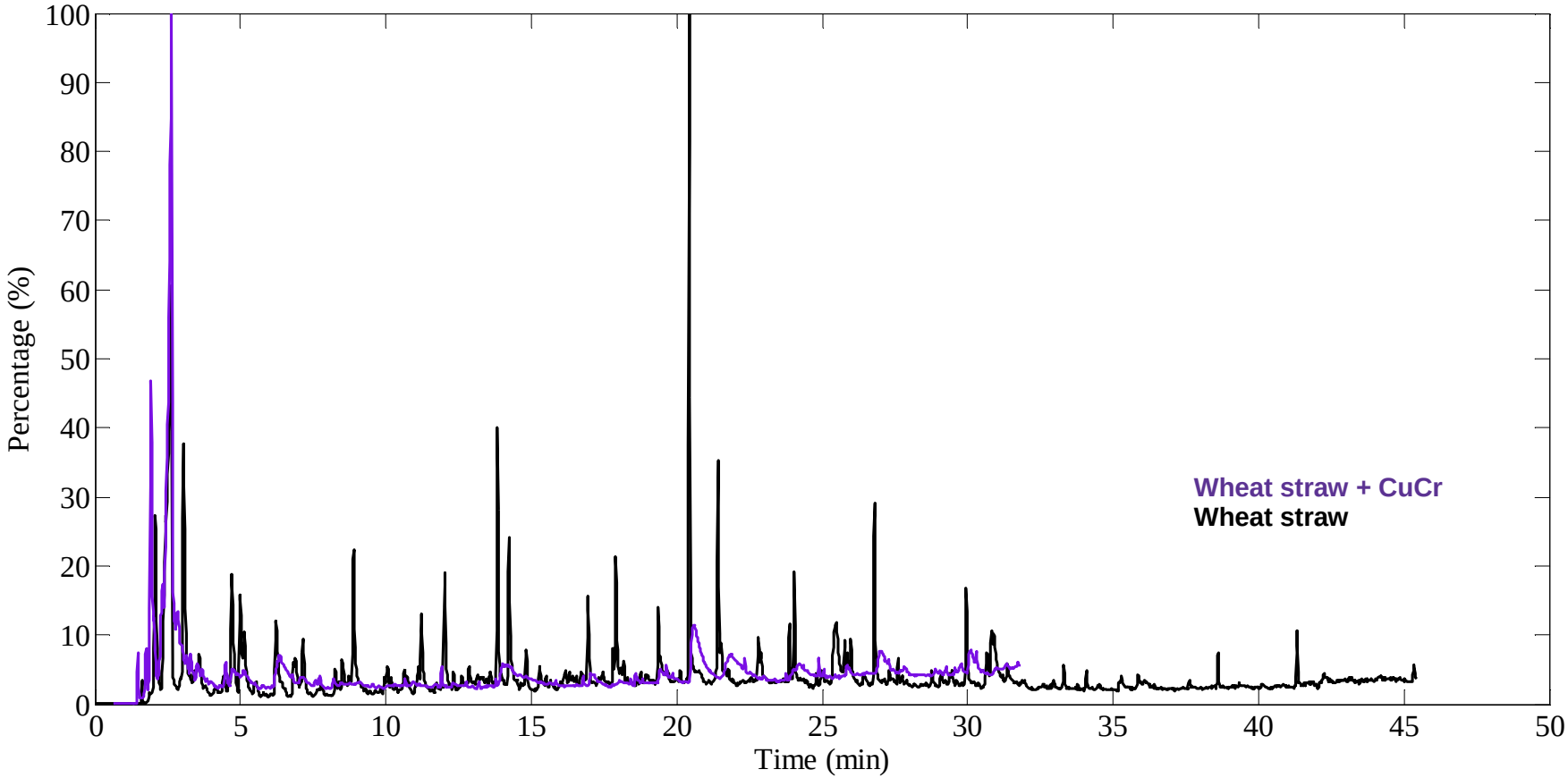

Figure 13-2: Chromatograms obtained from Py-GC/MS for wheat straw with Cu-Cr catalyst at 500C

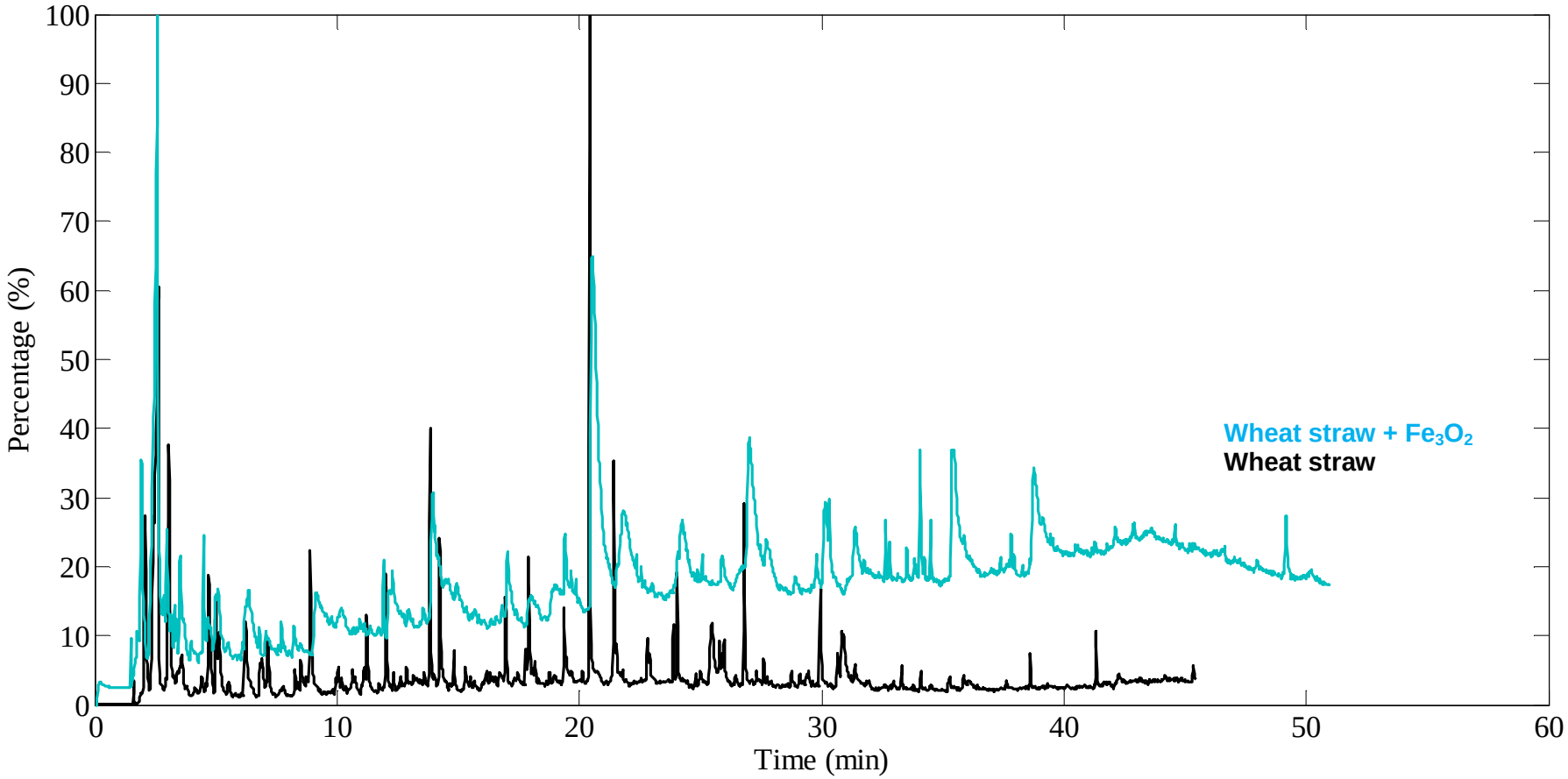

Figure 13-3: Chromatograms obtained from Py-GC/MS for wheat straw with Fe_3O_2 catalyst at 500C

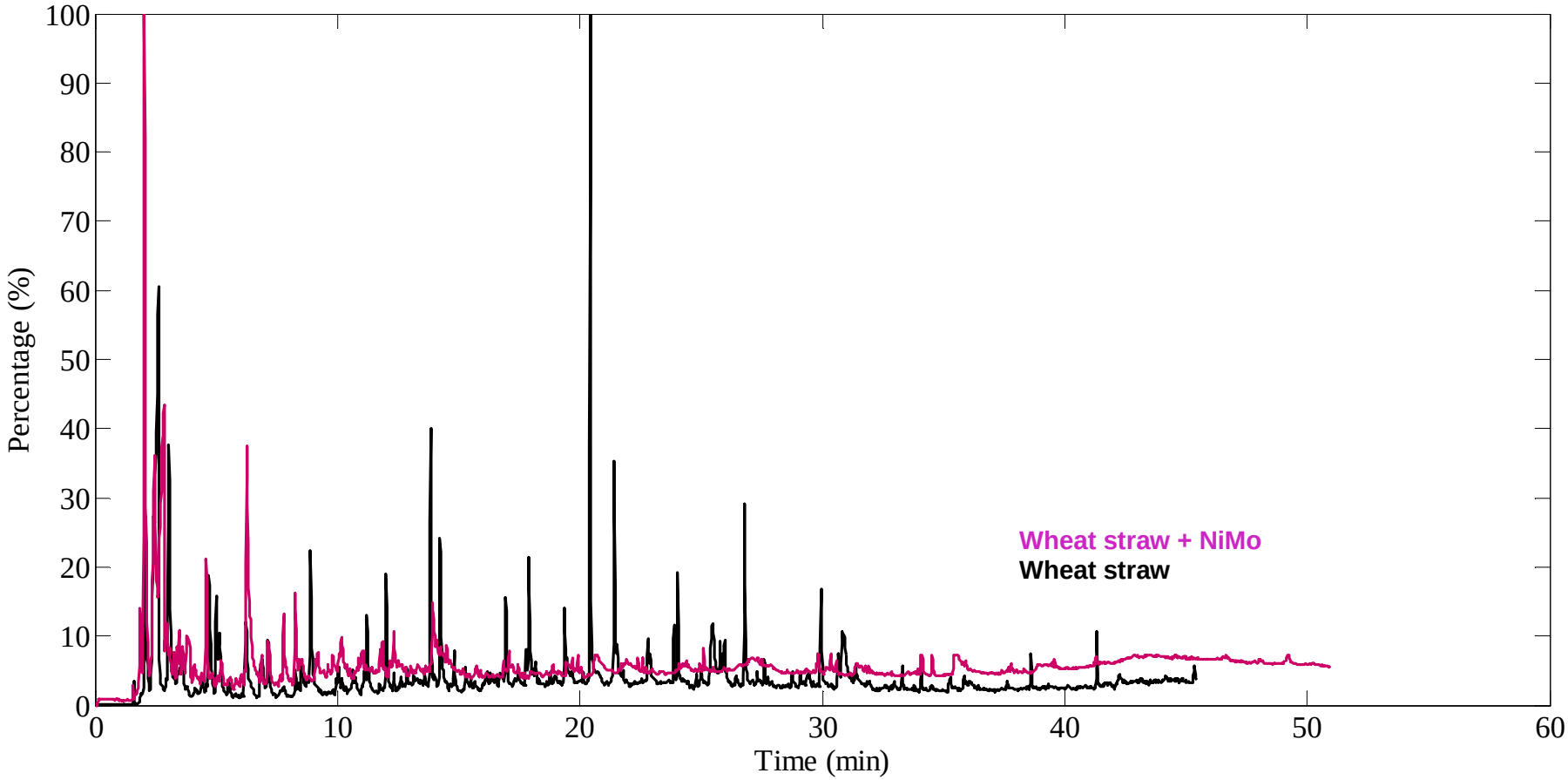

Figure 13-4: Chromatograms obtained from Py-GC/MS for wheat straw with NiMo catalyst at 500C

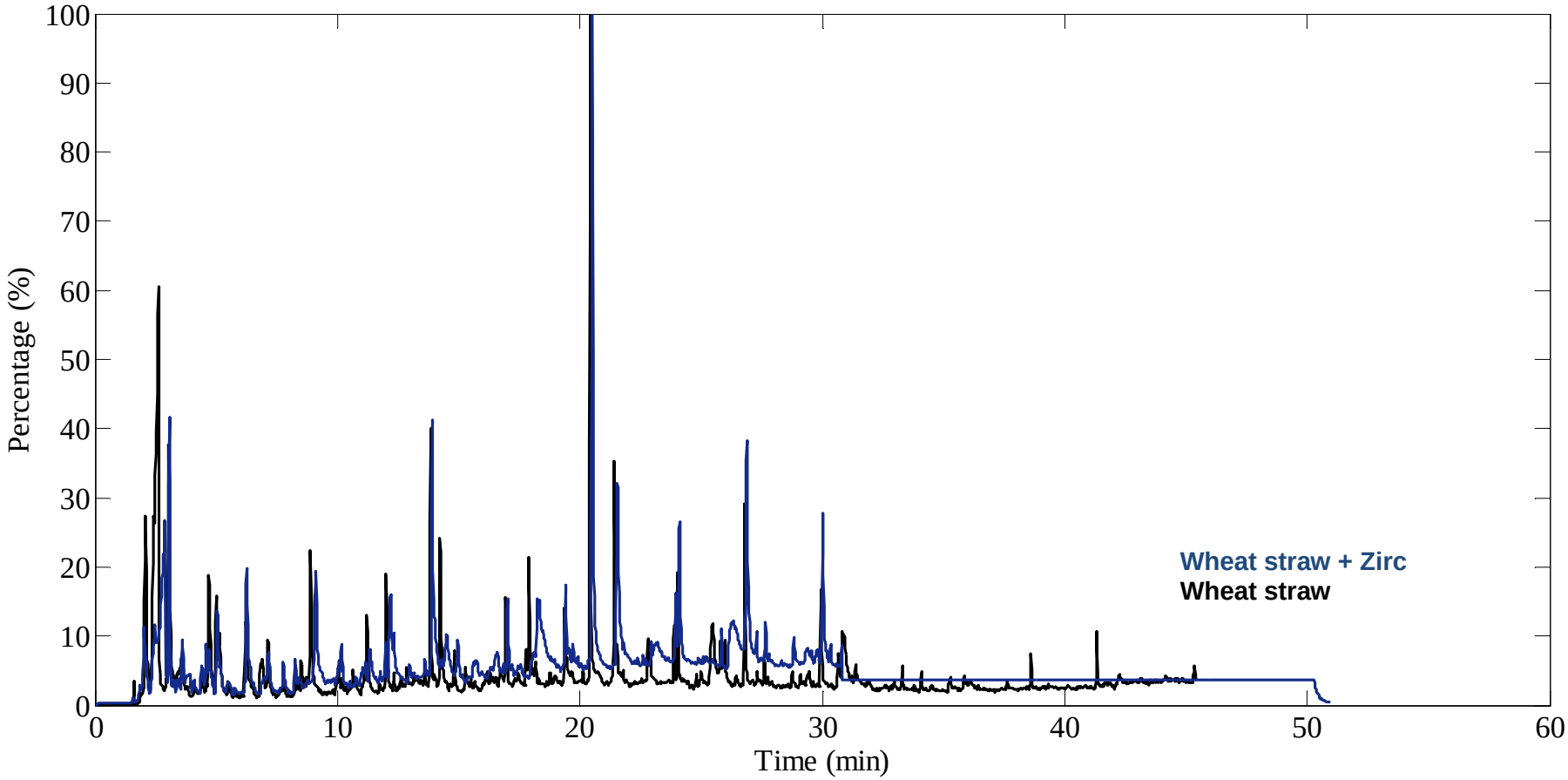

Figure 13-5: Chromatograms obtained from Py-GC/MS for wheat straw with Zirconia catalyst at 500C

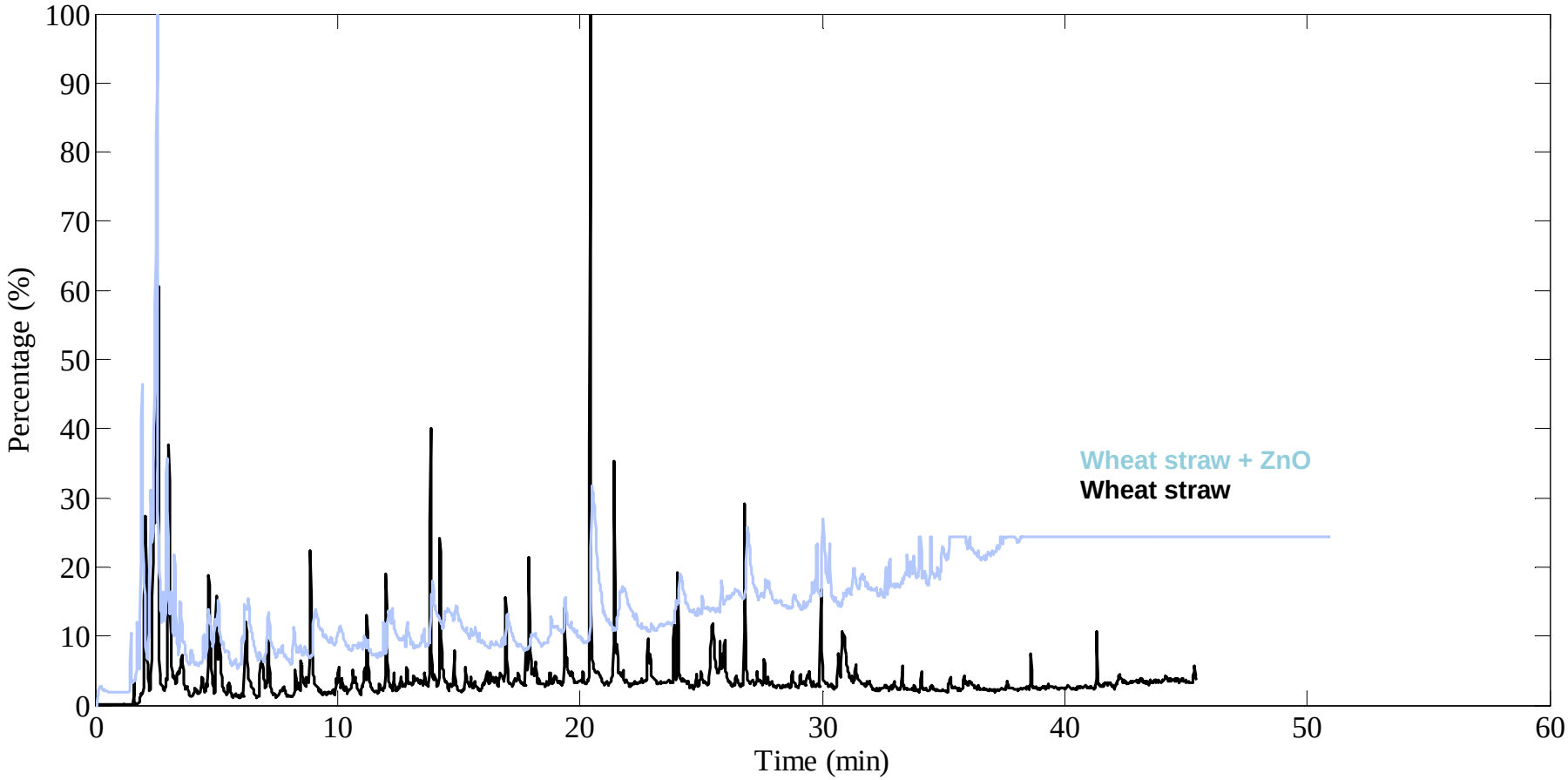

Figure 13-6: Chromatograms obtained from Py-GC/MS for wheat straw with ZnO catalyst at 500C

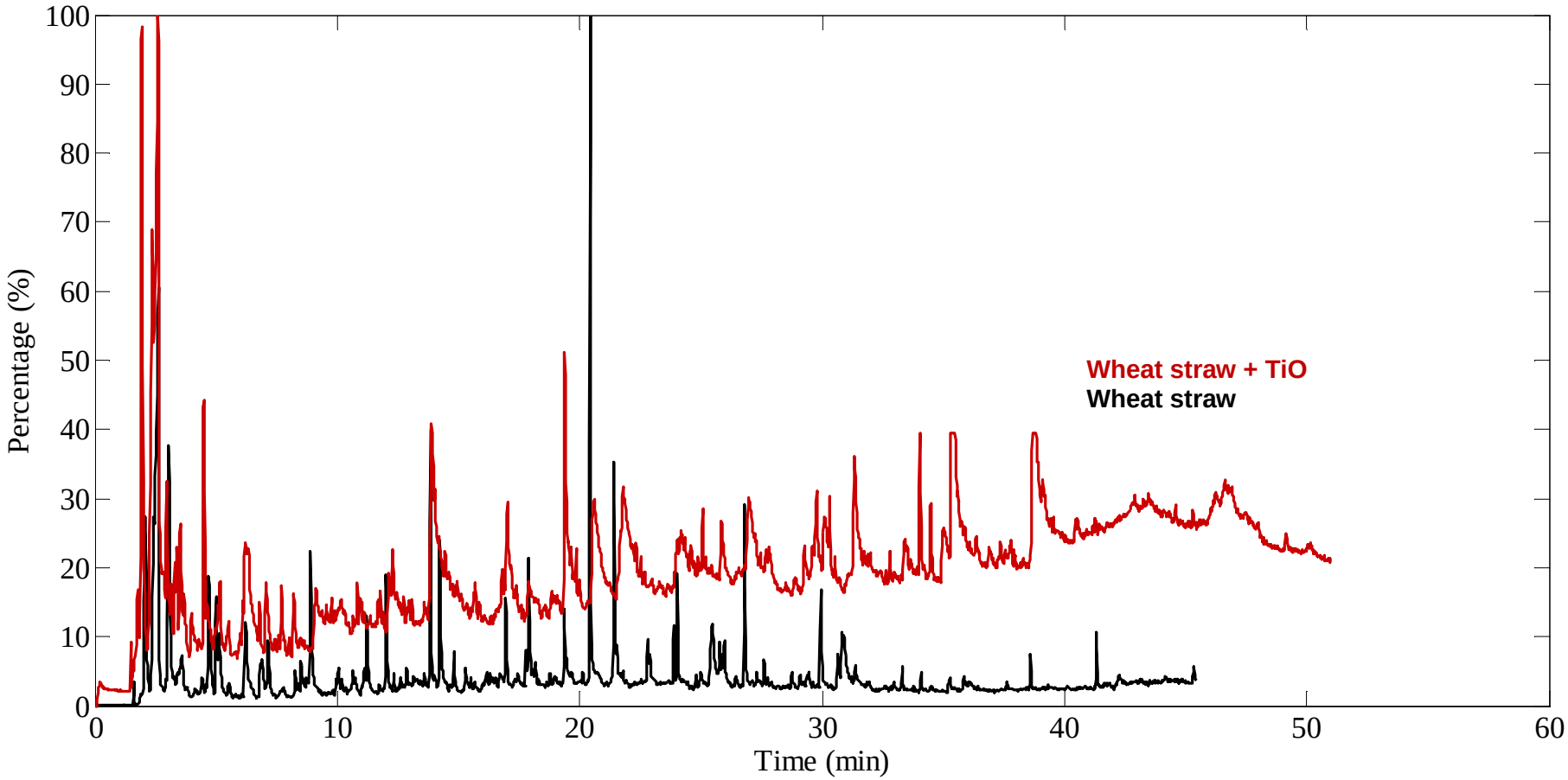

Figure 13-7: Chromatograms obtained from Py-GC/MS for wheat straw with TiO catalyst at 500C

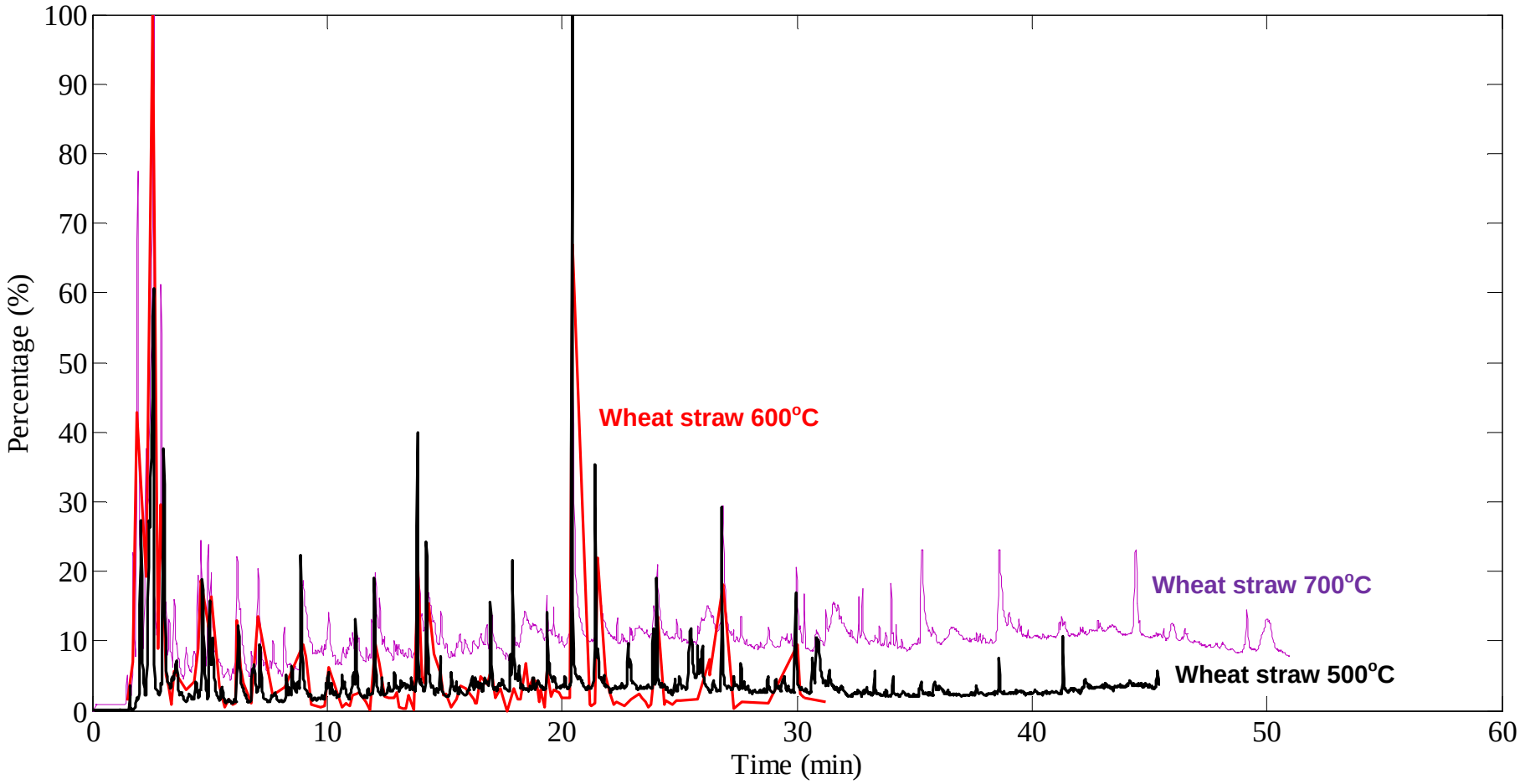

Figure 13-8: Chromatograms obtained from Py-GC/MS for wheat straw at 500C, 600C and 700C

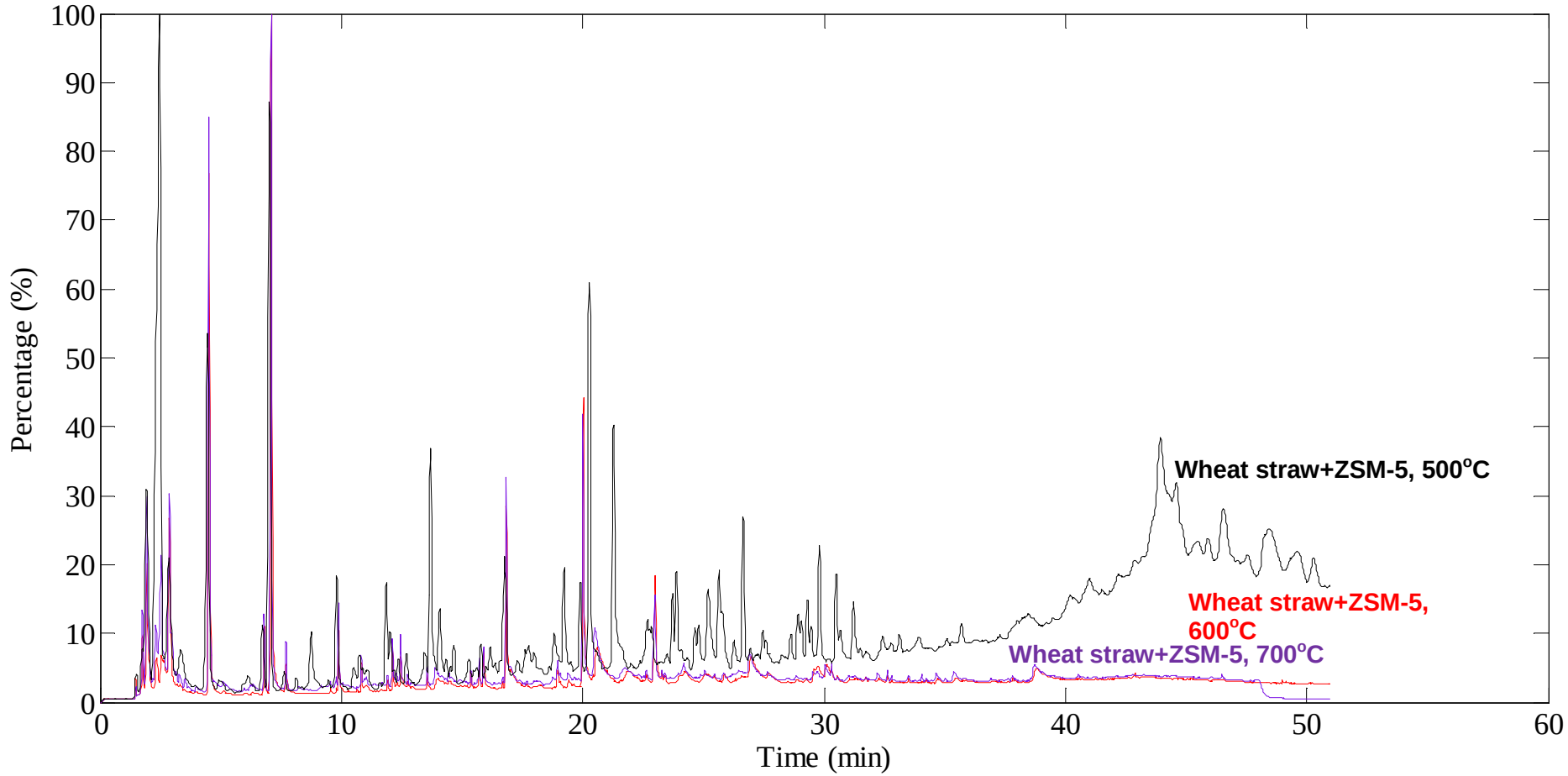

Figure 13-9: Chromatograms obtained from Py-GC/MS for wheat straw with H-ZSM-5 catalyst at 500C, 600C and 700C

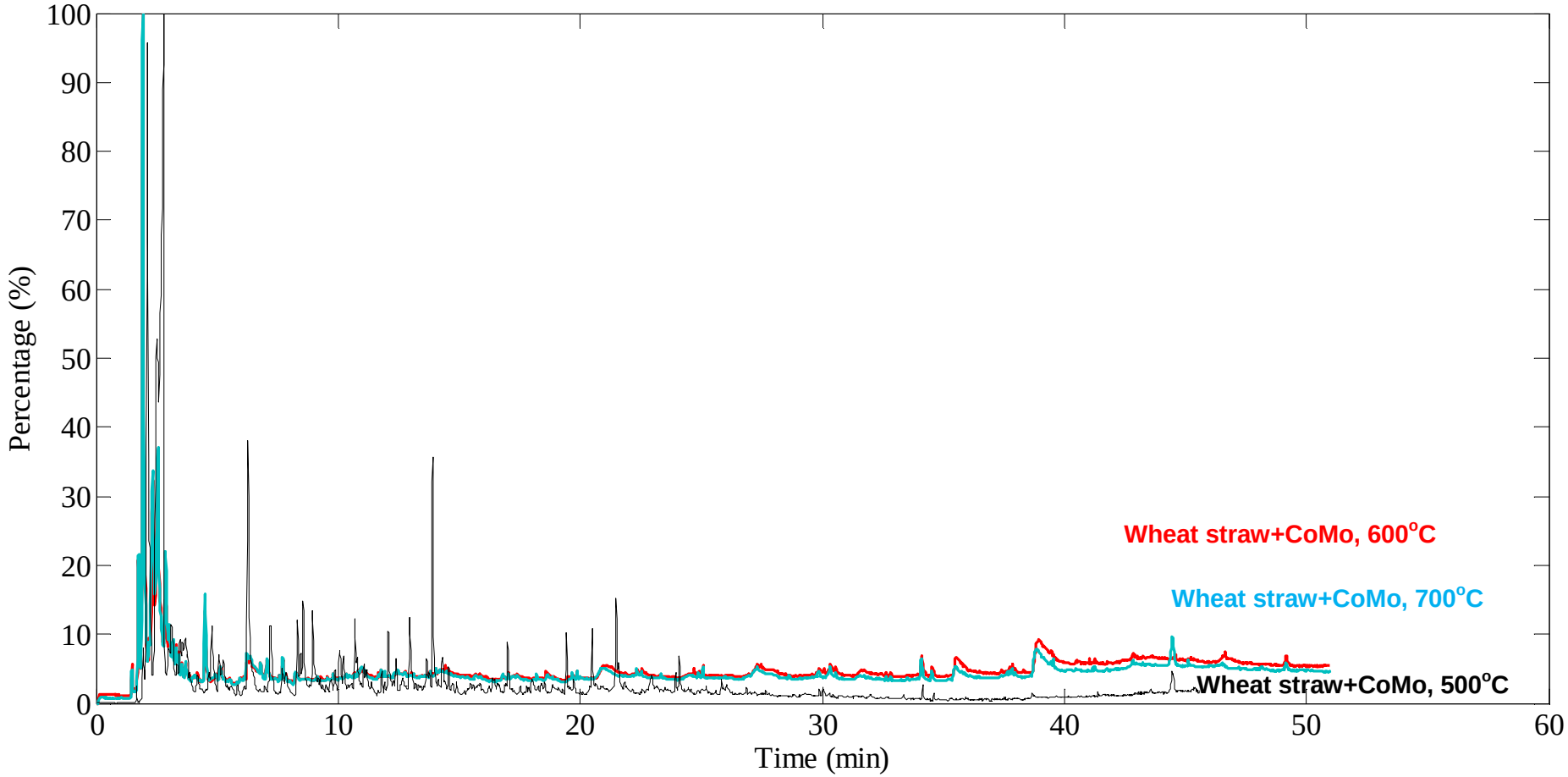

Figure 13-10: Chromatograms obtained from Py-GC/MS for wheat straw with CoMo catalyst at 500C, 600C and 700C

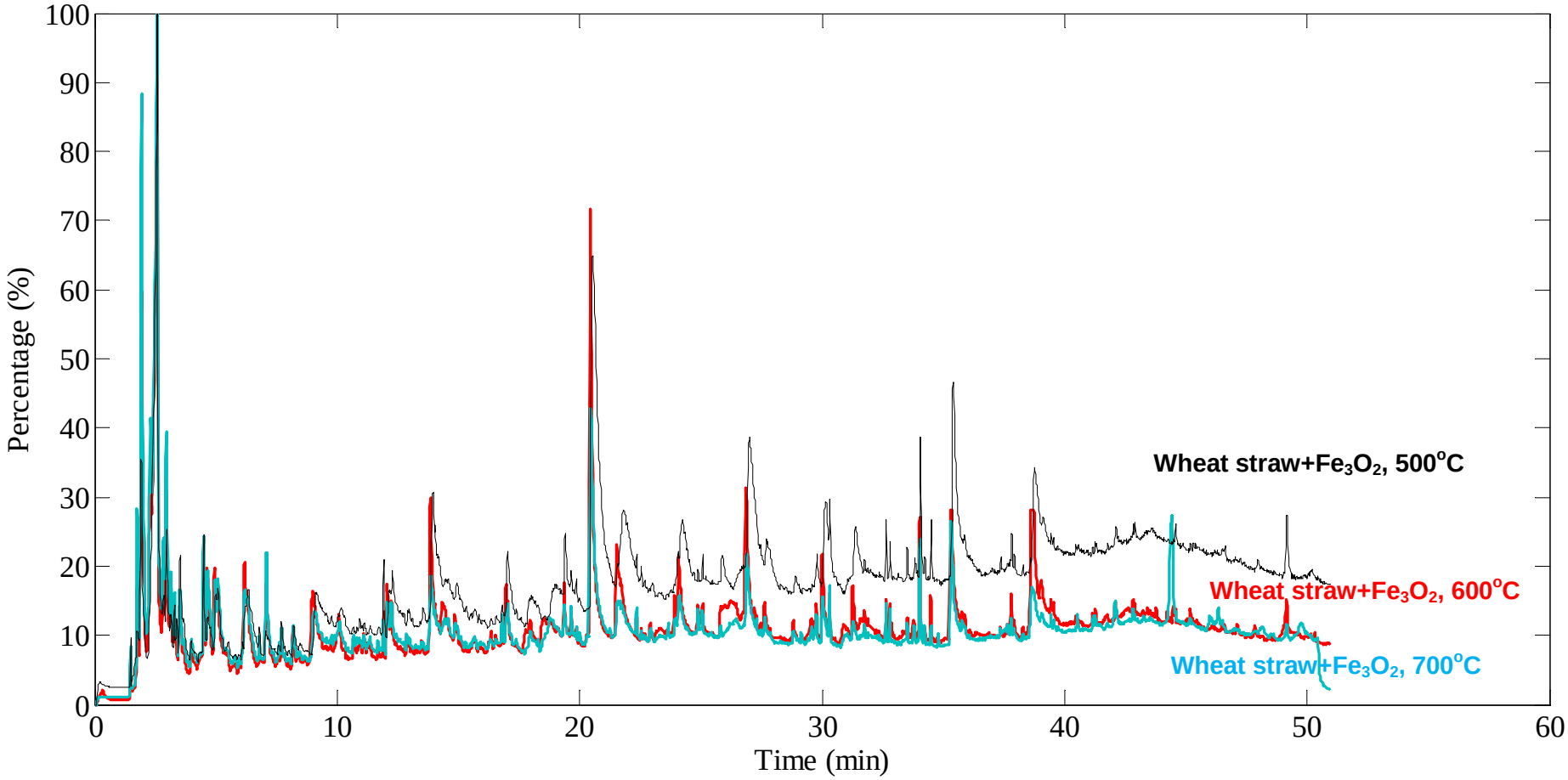

Figure 13-11: Chromatograms obtained from Py-GC/MS for wheat straw with Fe_3O_2 catalyst at 500C, 600C and 700C

14 APPENDIX - C

DESIGN DRAWINGS OF THE SECONDARY CATALYTIC FIXED BED REACTOR

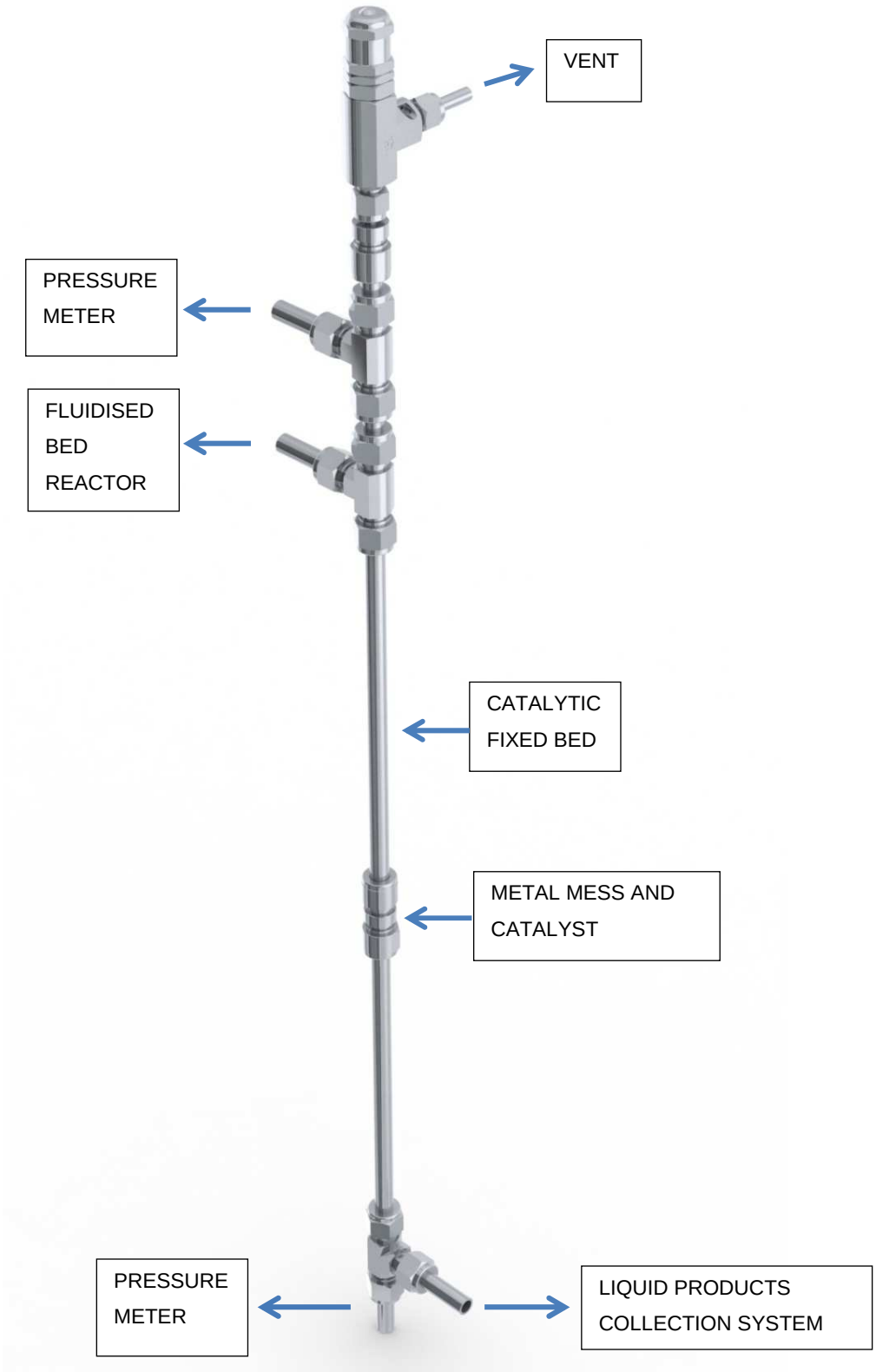

Figure 14-1: Image of the secondary catalytic fixed bed reactor by SolidWorks